Intercellular signalling, cell fate and cell shape in the *Drosophila* pupal wing

Aidan Maartens

Submitted in partial fulfilment of the requirements
for the degree of Doctor of Philosophy at the
University of Sussex

April 2012

I hereby declare that this thesis has not been and will not be submitted in whole or in part to another University for the award of any other degree.

Aidan Maartens

UNIVERSITY OF SUSSEX

Aidan Maartens, DPhil Biology

Intercellular signalling, cell fate and cell shape in Drosophila pupal wing development

Summary

The morphogenesis of tissues in animal development is orchestrated by intercellular signalling and executed by cell behaviours such as changes to shape. Understanding the link between signalling and cell shape changes is a key task of developmental biology. This work addresses this problem using the development of the pupal wing of *Drosophila melanogaster*. The pupal wing is a bilayered epithelium which is patterned into vein and intervein domains, and which secretes the cuticle of the adult wing. I first address the cellular basis of pupal wing development, and show that the process comprises a series of dynamic cell shape changes involving alterations to the apical and basolateral surfaces of the cells. Using temporally controlled mis-expression, I then investigate the role of intercellular signalling in these shape changes, and define the competence of cells in the wing to respond to ectopic signals. The dimensions of signalling in the pupal wing are then investigated, and I show that while BMP ligands can travel between the layers to promote vein development, such signalling is not a prerequisite for cellular differentiation. Within the plane of the epithelium, the BMP ligand Dpp can only induce signalling at a short range, potentially due to the upregulation of receptor levels in receiving cells. Finally, attention is turned to the means by which cell signalling controls cell shape changes, specifically in the crossveins. I identify the RhoGAP Cv-c as a downstream target of BMP signalling which acts to inhibit a novel RhoGTPase function in intervein development. This provides an example of how signalling pathways can enact cell shape changes, via the transcriptional regulation of RhoGAPs.

Acknowledgements

To those who aided my work. I firstly thank my supervisor, Rob, for getting me into this work, teaching me how to do science, persistent encouragement, and laboriously reading through earlier drafts of this thesis. Past members of the Ray Lab, in particular Andy, Christina, Shona, Cornelia, and the three young guns (James, Javi and Rob), were always helpful and fun to work with. I thank Dave Randall for help with SEM, Roger Phillips for help with the confocal, and Sarah Newbury for help with brightfield. The various members of the 4C corridor in the Couso and Alonso labs provided an unending source of expertise, support and more than welcome criticism. My secondary supervisor, Claudio Alonso, was always available for additional enthusiastic assistance. I thank the support and technical staff in the JMS building, in particular Dan Young, for providing the necessary conditions for research. Finally, I need to acknowledge the unsung heroes of the operation, the flies, through whom we glimpse the secrets of life.

To those who kept me fed and housed. The Nuffield Foundation funded an undergraduate summer scholarship that got me in to all of this. The Medical Research Council generously funded the 3 years of research of the DPhil. Finally, the British Society of Developmental Biology funded my attendance of two Spring conferences that strongly influenced some of the ideas presented here.

To those who kept me sane. Miriam, for putting up with and supporting a flypusher, particularly in the final months, the felines (Cleo and Juno), comforting if themselves slightly insane, my friends, both in JMS (holler at you Emile, John, Richard) and outside in the real world, for giving me other things to think about and do in these three years, and my brothers and parents for support, love and finance.

Table of Contents

List of Figures

* Page number that follows the Figure

List of Tables

* Page number that follows the Table

Abbreviations

ACV	Anterior crossvein
AJ	Adherens junction
AP	Anterior-posterior
APF	After puparium formation
BMP	Bone morphogenetic protein
Cad-GFP	*Drosophila* E-Cadherin-GFP
ECM	Extracellular matrix
EGFR	Epidermal growth factor receptor
HSPG	Heparan sulfate proteoglycan
LOF	Loss of function
Myo-II	Non-muscle Myosin-II
PCV	Posterior crossvein
RhoGAP	RhoGTPase activating protein
RhoGEF	RhoGTPase guanine nucleotide exchange factor
WPP	White prepupae

Chapter 1

Introduction

'*In the study of development we are interested not only in the final state to which the system arrives, but also in the course by which it gets there.' C.H. Waddington, 1957, p26*

One of the most remarkable aspects of development is morphogenesis, the emergence of ordered form in developing tissues. An initially simple group of cells - often in the form of a single layer of interconnected cells, an epithelium - is transformed into a complex three dimensional structure in a number of hours. The incredible diversity of morphogenetic events in animal development, from limb budding to lung branching to gut coiling, are underlain by a common set of cellular mechanisms, which include migration (Aman and Piotrowski, 2010), cell rearrangements (Hardin and Walston, 2004), ordered cell division (Lecuit and Le Goff, 2007), apoptosis (Domingos and Steller, 2007), and changes to cell shape (Sawyer et al., 2010). Elements of this 'morphogenetic alphabet' (Larsen and McLaughlin, 1987) will seldom be used in isolation; rather, different behaviours are co-ordinated across groups of cells within the tissue to achieve morphogenesis. Elucidating the means by which these morphogenetic processes are achieved, as well as how they are controlled in time and in space, is a fundamental question in current biology.

In the system studied in this thesis, the 'final state' is the adult wing of the fruit fly, *Drosophila melanogaster*. The course by which the system gets there involves an intricate series of morphogenetic events in the epithelium that secretes the wing cuticle, and extensive communication between its constituent cells. This intercellular communication utilises conserved signalling pathways and results in the allocation of the two primary cell fates in the epithelium, vein and intervein. The simplicity of the resulting cuticle pattern, comprised of pigmented vein channels and transparent intervein sectors, has made wing development a model system for epithelial patterning (Garcia-Bellido and de Celis, 1992; de Celis, 2003; Blair, 2007). The work presented here addresses the relationship between cellular patterning and morphogenesis in the pupal stage.

I. Epithelial morphogenesis in development

Features of Epithelia

Epithelia are sheets of interconnected cells with shared polarity that form the basis of much of the animal body plan. The apical surface of the epithelium faces either the external environment or, as in the case of epithelia that form the tubular networks of respiratory systems, the lumenal space, whereas the basal surface faces the interstitial spaces of the body and makes contact with the basal lamina (Fig. 1.1; Schock and Perrimon, 2002; Lubarsky and Krasnow, 2003). Whereas simple epithelia consist of a single layer of cells, stratified epithelia consist of multiple layers, some of which have detached from the basal lamina (Wright and Alison, 1984). Epithelia are further classified on the basis of the shape of their constituent cells: squamous epithelia are composed of flat, thin cells, cuboidal epithelia are composed of cells as tall as they are wide, and columnar epithelia are composed of tall, thin cells.

Cells within epithelia are linked by apical adherens junctions (AJs). AJs form links between adjacent cells that are based on homophilic interactions between the extracellular domains of E-Cadherin (E-Cad) (Fig. 1.1; Gumbiner, 1996). The cytoplasmic tail of E-Cad interacts with a number of proteins that interact with the Actin cytoskeleton (Gumbiner, 2005); thus AJs form a link between the cytoskeletons of adjacent cells. AJs are integral to the formation and maintenance of the apical-basal polarity which defines epithelia (Tepass and Tanentzapf, 2001). In invertebrates, epithelial cells are also connected by Septate Junctions, which lie basal to the AJs and form a barrier to trans-epithelial diffusion, as tight junctions do in vertebrates (Fig. 1.1; Tepass and Tanentzapf, 2001).

As well as cell-cell junctions, epithelia are characterised by basal junctions (BJs; Tepass and Tanentzapf, 2001), which link cells to the extracellular matrix (ECM, Fig. 1.1). The ECM is a meshwork of proteins that serves a variety of structural and signalling functions during development, including maintenance of tissue integrity and the binding of extracellular signalling molecules (Hynes, 2009; Rozario and DeSimone, 2010). The cell-ECM link is mediated by Integrins, the extracellular domains of which bind ECM components such as Laminin, and the intracellular domains of which mediate a connection to the Actin cytoskeleton (Brown et al., 2000; Delon and Brown, 2007). Thus, whereas AJs connect the cytoskeletons of adjacent cells, BJs connect the cytoskeleton to the ECM. In invertebrate epidermal epithelia, an

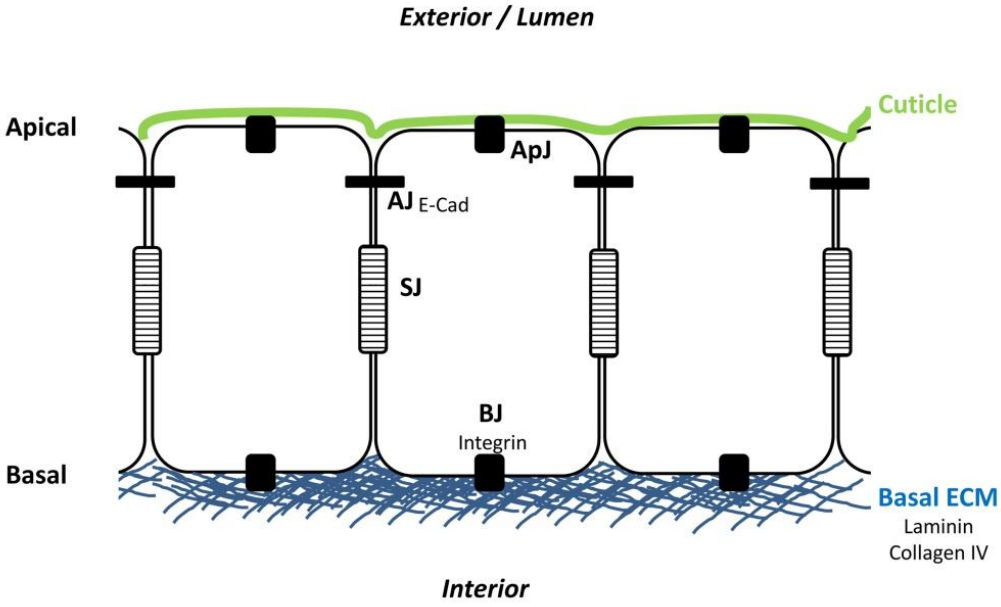

Figure 1.1. Epithelial architecture and cell junctions. Diagram of a simple columnar epithelium of the insect epidermis. ApJ = apical junction. AJ = adherens junction. BJ = basal junction. SJ = Septate junction. In the insect epidermis, cuticle (green) is secreted apically.

additional but less well understood cell-ECM junction mediates a connection to the apically secreted cuticle (Fig. 1.1; Tepass and Tanentzapf, 2001; Brown, 2011).

Epithelial morphogenesis and cell shape

The structural features of epithelia provide robustness in maintaining strong links between constituent cells and to the ECM, but also allow for substantial plasticity during development (Lecuit and Lenne, 2007). The basis of this plasticity is the dynamic nature of the junctions, particularly in the case of AJs which are continuously assembled and reassembled in developing tissues (Baum and Georgiou, 2011). Thus, whereas the breakdown of AJs underlies the epithelial-to-mesenchymal transition seen in embryonic development and tumorigenesis (Cano et al., 2000), AJ dynamics can drive morphogenetic events, as seen in the cell intercalation that occurs during germband elongation in *Drosophila* embryogenesis (Bertet et al., 2004; Levayer et al., 2011). The combination of robustness and plasticity means that epithelia can undergo dramatic morphogenetic transformations while remaining a laterally coherent sheet of cells.

A key component of the 'morphogenetic alphabet' utilised in development is changes to cell shape (Larsen and McLaughlin, 1987). Shape is described as the geometric features of the cell aside from size, position and orientation (Klingenberg, 2010). Within epithelia, cells can be spindle-like, columnar, cuboidal, or extremely flattened (Wright and Alison, 1984). Furthermore, certain morphogenetic transformations involve switching between these cell states, as is seen in flattening or columnarisation (Fristrom, 1988; Schock and Perrimon, 2002). In other cases, localised cell shape changes can change the topology of the epithelium. One of the best described examples of this phenomenon is in the bending of the epithelium inwards at points of invagination or furrows. Invaginations instigate gastrulation, as the mesoderm and endoderm are internalised within the blastula (Gilbert, 2006). They are also utilised in later developmental processes such as in *Drosophila* trachea formation (Brodu and Casanova, 2006) and vertebrate lens development (Plageman et al., 2011). Two cell shape changes commonly accompany this process: apical constriction and alterations to apical-basal length. Apical constriction involves a reduction in the cell's apical surface area, often accompanied by concomitant expansion of the basolateral surface and the formation of bottle- or wedge-shaped cells (Llimargas and Casanova, 2010; Sawyer et al., 2010). Invaginating cells also alter their apical-basal lengths, in a context-specific manner: in *Xenopus*, constricting bottle cells

elongate as they ingress (Lee and Harland, 2007), whereas in ascidian endoderm invagination, apical constriction is followed by apical-basal shortening (Sherrard et al., 2010). These shape changes are restricted to particular cells, yet have dramatic effects on the entire sheet, showing how restricted morphogenetic behaviours can alter epithelial topology.

The shape of a cell is determined by the interplay between internally and externally generated forces (Paluch and Heisenberg, 2009). Accordingly, changes to shape are caused by particular alterations to these forces. External forces are transmitted to the cell via its regions of contact with neighbouring cells or the ECM. For example, AJs can transmit tension across the apical domain of the epithelium (Rauzi and Lenne, 2011), and increases or decreases in tension along certain axes of the tissue can promote polarised cell shape changes (Butler et al., 2009; Solon et al., 2009). Internal forces can be generated by the cytoskeleton, in particular by the Actin cytoskeleton. For example, the polymerization of Actin monomers into filaments drives the membrane protrusions of filopodia (Ridley, 2011), and networks of antiparallel Actin filaments can be acted upon by the motor protein Myosin (in epithelia, non-muscle Myosin-II (Myo-II)) to produce contractile tension (Pollard and Cooper, 2009; Kasza and Zallen, 2011). This latter type of internally generated force plays a key role in apical constriction: networks of Myo-II and Actin accumulate at the apical cortex during *Drosophila* ventral furrow formation (Martin et al., 2009), dorsal closure (David et al., 2010), and tracheal invagination (Brodu and Casanova, 2006), as well as in vertebrate lens pit formation (Plageman et al., 2011) and neural tube closure (Haigo et al., 2003; Hildebrand, 2005). The contractile force generated by Myo-II on Actin is transmitted to the AJs, and as a result they are pulled inward (Dawes-Hoang et al., 2005), leading to a reduction in apical surface area.

Considering the fundamental role of the cytoskeleton in cell shape, and hence in morphogenesis, cytoskeletal dynamics must be spatially controlled within the cell. Key regulators of the cytoskeleton are the Rho family of small GTPases. RhoGTPases shuttle between inactive, cytosolic GDP-bound states, and active, membrane-associated GTP-bound states which affect a variety of cellular processes via binding to effector proteins (Jaffe and Hall, 2005). A common output of GTP-bound RhoGTPase signalling is the Actin cytoskeleton. For example, in a well-characterised pathway, GTP-bound RhoA (Rho1 in *Drosophila*) binds the effector Rho Kinase (Rok), relieving auto-inhibition and allowing Rok to activate Myo-II, which promotes the contractility of Actin filaments as discussed above. RhoA/Rok/Myo-II/Actin forms a ‘contraction cassette’ that is used in the cleavage furrow during cytokinesis (Piekny et al., 2005), during cell migration (Ridley et al., 2003) and in apical constriction in numerous developmental contexts (Dawes-Hoang et al., 2005; Escudero et al., 2007; Plageman et al.,

2011). The regulation of cytoskeletal dynamics by localised RhoGTPase activity is a common feature of morphogenesis during development (Schock and Perrimon, 2002).

II. The *Drosophila* wing: tissue morphogenesis

The adult wing

Epithelial morphogenesis creates many of the structures of the animal body. The development of the *Drosophila* wing offers numerous opportunities to address how this process occurs. The external appendages of insects consist of cuticle secreted by the epidermis, but whereas the rest of the integument is a single layer of cuticle, the wing is formed of two tightly adhered cuticle sheets. As well as providing the means for flight, the wings function in the production of species-specific courtship songs (Waldron, 1964) and in both mechanosensory and chemosensory perception (Stocker, 1994). Although not adorned with eyespots or other types of elaborate pigmentation, the cuticle of the *Drosophila melanogaster* wing can reflect a dazzling array of colour patterns by thin film interference (Shevtsova et al., 2011).

The most obvious pattern on the *Drosophila* wing blade is the stripes of the veins, darkly pigmented channels running through the transparent 'intervein' cuticle. The wing veins, which are not homologous with vertebrate veins, are ectodermally derived cuticular structures which provide structural support for the wing membrane during flight, as well as acting as channels for hemolymph, axons of sensory neurons and trachea (Comstock and Needham, 1899; Arnold, 1964; Wootton, 1992; Murray et al., 1995). In comparison to the ancestral insect wing, the wings of *Drosophila* (like those of other higher Diptera) show a reduced pattern of venation (Stark et al., 1999). The *Drosophila* pattern is composed of two classes of vein: the longitudinal veins (L1-L5), which run along the proximal-distal axis of the wing, and the crossveins, anterior (ACV) and posterior (PCV), which run perpendicular to it (Fig. 1.2). Each vein is composed of dorsal and ventral components, but these are differentially articulated, protruding from one surface and remaining flat on the other (Schatz, 1951; Garcia-Bellido and Santamaria, 1972). The simplicity of the vein/intervein pattern has contributed to its widespread use as a trait in developmental and genetic analyses over the past century (Bridges, 1920; Waddington, 1957; Garcia-Bellido, 1977).

Wing development

The wing is formed of cuticle secreted by an epithelium. Wing development involves the creation of a unique tissue architecture – an epithelial bilayer – to secrete the bilayer of cuticle

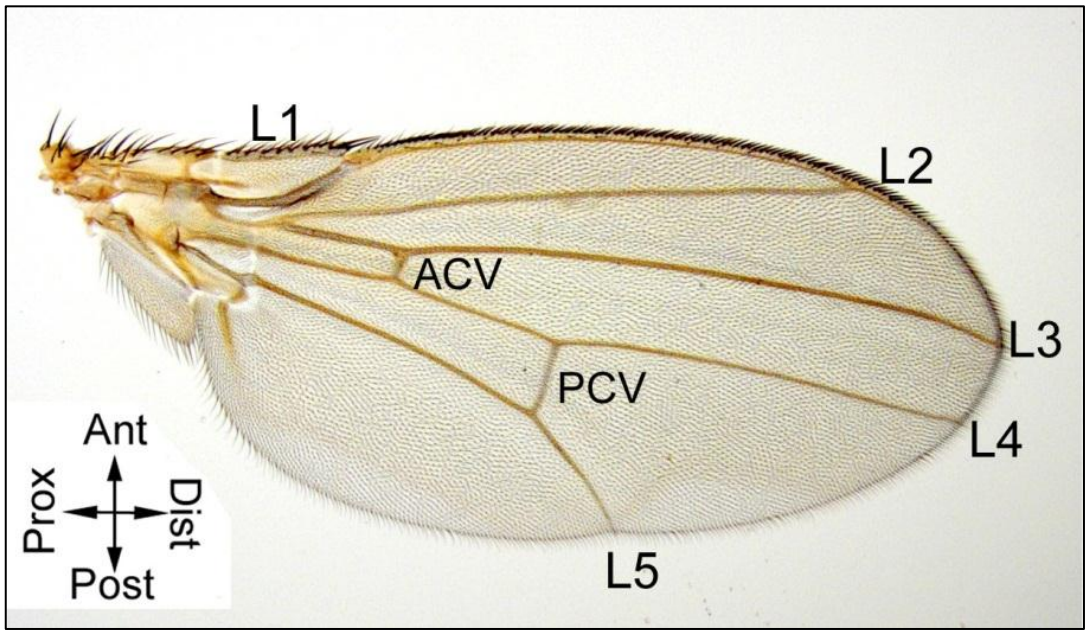

Figure 1.2. The adult wing of *Drosophila melanogaster*. Veins are labelled where they reach the margin. Compass shows wing axes: Ant = anterior, Post = posterior, Prox = proximal, Dist = distal.

that forms the adult wing. The process of wing development begins in the embryo. At the intersection of two stripes of gene expression, one of the segment polarity gene *wingless* and one of the BMP ligand *decapentaplegic*, a small group of cells in the dorsal epidermis is specified as presumptive wing and leg cells (Cohen et al., 1993). The presumptive wing cells then separate and migrate dorsally, and invaginate to give rise to a sack of cells called the wing imaginal disc. The wing disc, which remains attached to the hypodermis by a thin stalk, rapidly proliferates during the larval instars to comprise some 30,000 cells at the end of larval development (Martín et al., 2009). It is composed of two layers: the columnar layer which gives rise to the notum and the hinge and blade of the wing, and the squamous layer (also known as the peripodial epithelium) which does not contribute to the adult wing structures but plays key roles in disc eversion and the fusion of the left and right wing discs in the notum (Fig. 1.3; Fristrom and Fristrom, 1993). Because the disc arises from an invagination of the epidermis, the apical surfaces of both layers face the disc lumen, and hence each other (Pallavi and Shashidhara, 2005). The wing pouch at the centre of the columnar layer gives rise to the adult wing blade, but at this stage there are no morphological distinctions which reflect the vein/intervein pattern.

At the end of the third instar, the larva becomes stationary and forms the white prepupae (WPP). The wing discs, which had been developing internally within the larvae, then evaginate to lie outside of the body wall (Waddington, 1941). This process involves an initial apposition of the peripodial epithelium to the larval epidermis, followed by its subsequent disintegration, migration and apoptosis to allow the everting columnar epithelium through (Pastor-Pareja et al., 2004; Aldaz et al., 2010). This transforms the wing pouch, a monolayer epithelium (Fig. 1.3), into the prepupal wing, composed of dorsal and ventral layers[*] (Fig 1.4). As a result the apical surfaces of the epithelium shift from facing the lumen to facing externally.

Following eversion, the upper (dorsal) and lower (ventral) layers come together with their basal surfaces in apposition, forming a bilayer. The bilayer then elongates and expands in surface area owing to the flattening of the cells (Waddington, 1941). In this prepupal stage, rudiments of the presumptive veins are visible as broad channels between the apposed layers, although not fully representative of the adult vein pattern (Fig. 1.4; Waddington, 1941). This prepupal apposition is temporary, and at the beginning of the pupal phase, at around 12h after puparium formation (APF), an influx of hemolymph causes the two layers to separate, forming

[*] A note on the terminology used in this thesis: the pupal wing epithelium is composed of dorsal and ventral *layers*, each of which has apical and basal *surfaces*. The adult wing has dorsal and ventral cuticle *surfaces*.

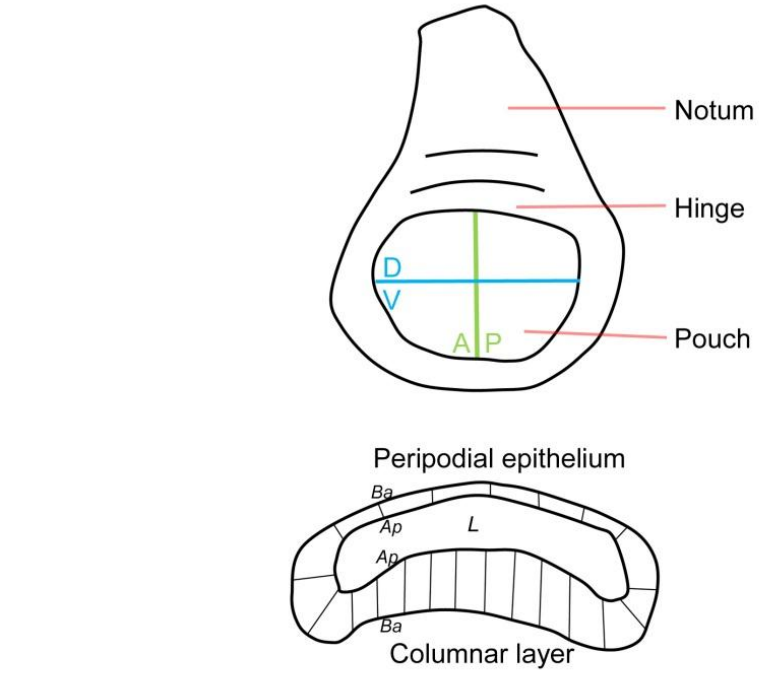

Figure 1.3. The wing disc. Top: wing disc with component parts of the columnar layer labelled. Green line: anterior-posterior compartment boundary of the pouch. Blue line: dorsal-ventral compartment boundary of the pouch. Bottom shows cross-section taken along the DV axis, showing overlying peripodial epithelium. Ap = Apical, Ba = Basal, L = Lumen. Adapted from Widmann and Dahmann (2009).

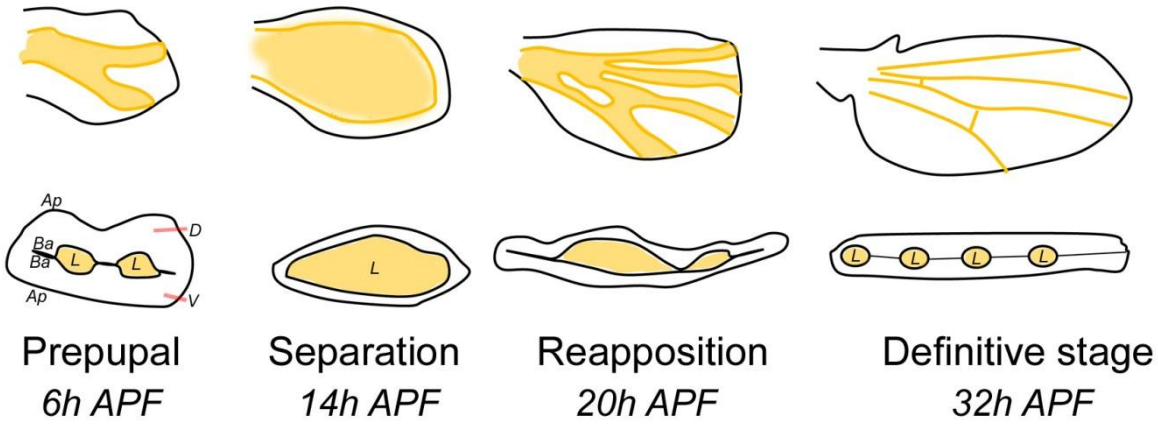

Figure 1.4. Wing morphogenesis between 0-32h APF. Top panels: morphology of the wing epithelium at set stages. Peach regions detail the extent of dorsal-ventral separation. Bottom panels: cross sections taken along the anterior-posterior axis of the wing. Ap = Apical, Ba = Basal, D = Dorsal, V = Ventral, L = Lumen. Adapted from Waddington, (1941), Fristrom, et al. (1993) and Blair (2007).

a cavity between them (Fig. 1.4). During the following ~6h of dorsal-ventral separation, the basal connections established in the previous stage appear to be lost in fixed sections (Waddington, 1941; Fristrom et al., 1993). The process of apposition followed by separation is also seen in the wings of other insects, for example the moth *Manduca sexta*. Interestingly, cells of the separated stage *Manduca* wing always retain connections to opposite cells via thin projections (Nardi and Ujhelyi, 2001), raising the possibility that connections are similarly maintained in the *Drosophila* separated wing but lost in the process of fixing or mounting.

The next stage of wing development involves the reapposition of the dorsal and ventral layers, a process initiated at around 16-18h APF by the extension of basal processes across the cavity to meet those extending from cells of the opposite layer (Waddington, 1941; Fristrom et al., 1993; Murray et al., 1995). The re-establishment of basal contacts occurs first around the periphery of the wing and then moves in to the centre. As this progresses, projections are also sent from 'intervein bands' in the middle of the wing (Fristrom et al., 1994). The veins emerge as regions of the wing which do not send out basal processes and do not appose, forming a network of vein lumens which is seen in the adult pattern (Fig. 1.4). Vein development is thus characterised by the persistence of dorsal-ventral separation, while intervein development is characterised by dorsal-ventral apposition. Following reapposition, the vein and intervein domains refine and the epithelium (which is columnar) becomes more regular. This culminates in the wing of ~32h APF which appears like the adult wing in pattern and proportion, and has been referred to as the 'definitive stage' (Fig. 1.4; Waddington, 1941).

The definitive stage wing appears as replica of the adult wing, but is less than half its size (Fristrom et al., 1993). The following stage of pupal wing development accordingly involves the achievement of the adult size, as the wing expands in surface area. As with prepupal expansion, this process is driven by the flattening of the cells (Waddington, 1941). Because the pupal cuticle in which the wing is loosely contained does not similarly expand, the wing folds extensively inside it. Folding coincides with the secretion of the adult cuticle from the apical surface of the cells, and as a result the folded tissue is sandwiched between the two cuticle layers.

The final stage of wing development is wing maturation, the process of expanding the folded wing after eclosion of the adult. This expansion is aided by hemolymph pressure and stroking of the wings by the hindlegs. Once the wing has expanded, the intervein epithelium degenerates and cells exit the wing via the hinge (Johnson and Milner, 1987). Clearing the wing of intervein cells requires the activity of the wing hearts of the scutellum, which promote the

flow of hemolymph through the wing after expansion; in their absence the persistence of cells between the cuticle layers prevents cuticle bonding, resulting in flightlessness (Togel et al., 2008). The only living cells remaining in the adult wing are those lining the veins, which include remnant epithelial cells of the veins as well as sensory neurons and trachea (Comstock and Needham, 1899; Johnson and Milner, 1987; Stocker, 1994). After cell clearing, the two cuticle surfaces come together and strongly adhere, and the cuticle tans. Once the wing is tanned, the fly is ready to fly.

Basal and apical features of the pupal wing

A defining feature of the pupal wing is the basal apposition of the two epithelial layers (Fig. 1.4), which is mediated by Integrins. Loss of Integrin function leads to the formation of blisters in the adult wing, which derive from the separation of the dorsal and ventral layers during pupal development (Brabant et al., 1996). Integrins are transmembrane heterodimers composed of α and β subunits that can promote adhesion between cell layers by binding to a common ECM which lies between them (Brown et al., 2000). In the developing wing, a common β subunit, β-PS (encoded by *myospheroid* (*mys*)), forms heterodimers with one of two α subunits, α-PS1 (encoded by *multiple edematous wings* (*mew*)) and α-PS2 (encoded by *inflated* (*if*)). The α subunits show a restricted and complementary pattern of expression in the wing: *mew* expression is largely restricted to dorsal cells, whereas *if* expression is largely restricted to ventral cells (Brower et al., 1984). This expression pattern reflects their restricted functional requirements, as determined by clonal analysis: *mew* is only required in dorsal cells (Brower et al., 1995), and *if* only in ventral cells (Brabant and Brower, 1993). In contrast, the common β-PS subunit, *mys*, is required in both dorsal and ventral cells (Brower and Jaffe, 1989). Thus, α-PS1:β-PS heterodimers function in the dorsal layer, and α-PS2:β-PS heterodimers function in the ventral layer.

ECM components in the wing show dynamic patterns of distribution through its morphogenesis. During prepupal apposition, a thin layer of Type IV Collagen and Laminin-containing ECM lines the basal surfaces of apposing cells (Murray et al., 1995), and in these regions basal junctions based on β-Integrin are formed (Fristrom et al., 1993). During the separation of the dorsal and ventral layers, the lumen is filled with ECM components as well as hemolymph, and during reapposition (when intervein cells re-form basal junctions), ECM components are transiently seen in a thin layer on the basal surfaces of intervein cells (Murray

et al., 1995), where β-Integrin is also localised (Fristrom et al., 1993). As reapposition progresses, ECM components are restricted to the vein lumen and spaces between the lateral surfaces of intervein cells (Fristrom et al., 1993; Murray et al., 1995). Thus, after reapposition ECM components are excluded from the regions where Integrins are found, i.e. on the basal surfaces of the cells. This raises the issue of what is the ligand for Integrins following reapposition. Interfering with Laminin function in the wing causes wing blistering (Martin et al., 1999; Urbano et al., 2009), which might suggest that a temporary interaction at the beginning of reapposition is necessary for the formation of basal junctions. Alternatively, other ECM components could mediate this function.

In basal profile, veins emerge as ECM-lined lumens in between the sectors of basally apposing intervein. Studies of the apical surface of the epithelium have also revealed the emergence of distinct apical cell morphologies in these two cell types. At the point of reapposition, apical constriction is seen in tracts of cells overlying the lumen, and is accompanied by apical enrichment of Actin (Fristrom et al., 1994) and the AJ component E-Cad (O'Keefe et al., 2007) . At the same time as vein cells are constricting, intervein cells progressively relax to assemble into a near-regular hexagonal array, an active process driven by the recycling of E-Cad at the AJs (Classen et al., 2005). Interestingly, during this period there is marked basal enrichment of E-Cad in intervein cells (O'Keefe et al., 2007), the function of which has yet to be established.

III. The *Drosophila* wing: cell signalling

Signal transduction pathways

A key aspect of wing development is the allocation of vein and intervein fates in the epithelium. Wing development offers an example of epithelial patterning that is characteristic of metazoan development: an initially uniform field of cells is segregated into discrete subtypes that subsequently execute discrete developmental programs. In the wing this process is achieved by intercellular communication mediated by highly conserved signal transduction pathways. In particular, cell fate specification involves the BMP, EGFR and Notch pathways (the *Drosophila* components of these pathways are shown in Table 1.1). These pathways are used reiteratively through development in the specification of diverse cell types, and pathway cross-talk has emerged as a key means by which context-specific cellular responses can be achieved (Shilo, 2005; Vivekanand and Rebay, 2006). Cross-talk also characterises fate specification in the wing. The primary, but not sole, output of signalling pathway activity is changes to the transcription of target genes (Barolo and Posakony, 2002).

The BMPs are members of the TGF-β superfamily, and BMP ligands function as dimers that signal through two types of serine/threonine kinase receptor (Type I and Type II). Activated receptors phosphorylate the Smad protein, which along with a co-Smad shuttles to the nucleus and influences the transcription of target genes (Fig. 1.5; Massague and Chen, 2000). BMPs control a multitude of processes during development, for example the dorsal-ventral patterning of the early embryo, a role conserved between vertebrates and invertebrates (Ross et al., 2001). A key feature of BMP signalling is its regulation at the level of extracellular regulation of the ligands. For example, in *Drosophila*, ligands are transported from lateral to dorsal-most regions of the embryo in a complex with the Short Gastrulation (Sog) and Twisted Gastrulation (Tsg) proteins (reviewed in O'Connor et al., 2006). Cleavage of this complex by the metalloprotease Tolloid (Tld) then releases the ligands to promote pathway activity (Shimmi et al., 2005b). As well as Smad-dependent pathways, ligand-bound receptors can also signal independently of Smad via a variety of intracellular factors (Moustakas and Heldin, 2005).

Ligands of the EGFR pathway signal as monomers, and some require intramembrane cleavage by the Rhomboid (Rho) protease in sending cells to produce the active ligand (Urban et al., 2001). All EGFR ligands signal through a single receptor tyrosine kinase (Egfr) which acts as a dimer to activate the RAS/MAPK intracellular cascade. Phosphorylated MAPK leads to changes

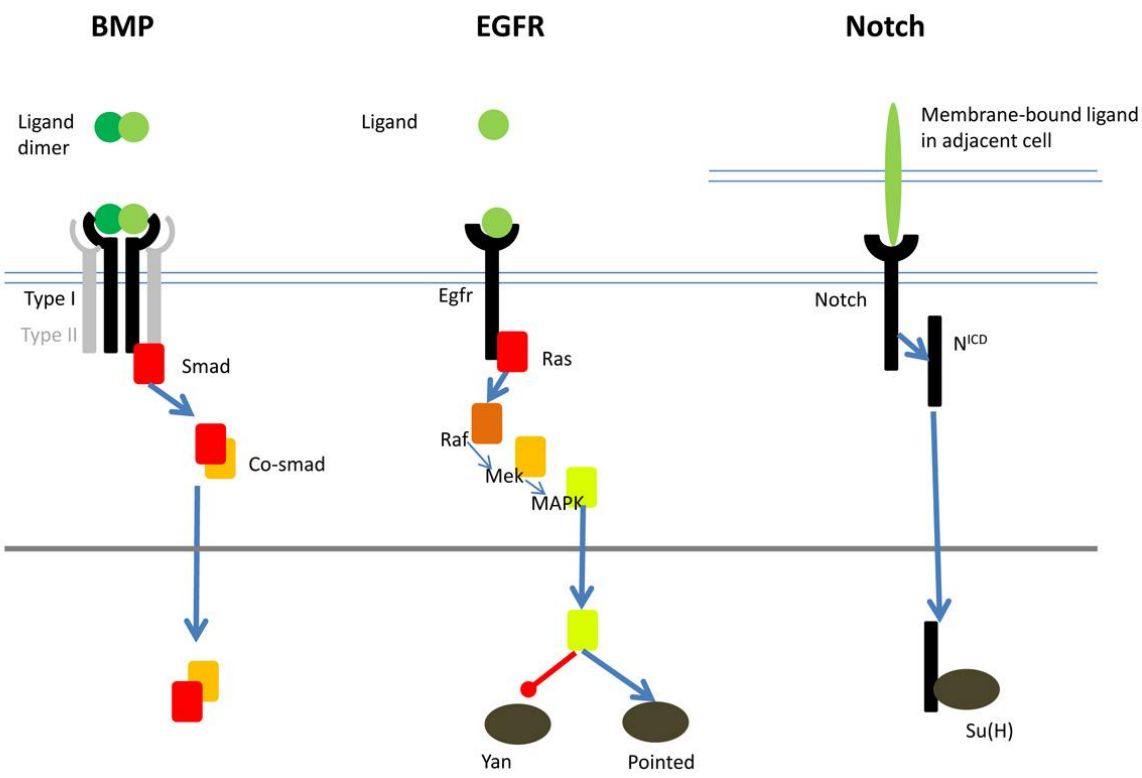

Figure 1.5. Architecture of the BMP, EGFR and Notch signalling pathways. Primary components of the pathways (ligands, receptors and intracellular transduction machinery) are shown. Blue lines show cell membranes, grey line shows nuclear envelope. Compiled from information in Massagué & Chen (2000), Shilo (2005), and Bray (2005).

	BMP	EGFR	Notch
Ligand	Decapentaplegic (*dpp*) Glass bottom boat (*gbb*) Screw (*scw*)	Vein (*vn*) Spitz (*Spi*) Keren (*Ker*) Gurken (*Gur*)	Delta (*Dl*) Serrate (*Ser*)
Receptor	**Type I** Thickveins (*tkv*) Saxophone (*sax*) **Type II** Punt (*pnt*)	Epidermal Growth Factor Receptor (*Egfr*)	Notch (*N*)
Intracellular transduction & Transcriptional Regulation	**Smad** Mothers against dpp (*Mad*) **Co-Smad** Medea (*Med*)	RAS/MAPK cascade Pointed (*pnt*) Anterior open (*aon*)	Notch intracellular domain (N^{ICD}) Suppressor of Hairless (*Su*(*H*))

Table 1.1. *Drosophila* components of BMP/EGFR/Notch signalling pathways.

in gene transcription by affecting two related ETS-family transcription factors, Yan (encoded by *anterior open* (*aon*)) and Pointed (Fig. 1.5). Yan, and which acts as a transcriptional repressor, is inhibited by phosphorylated MAPK, whereas Pointed, which acts as a transcriptional activator, is activated (Fig. 1.5; Shilo, 2005). There are four EGFR ligands in *Drosophila*: Spitz, Gurken, Keren and Vein, the latter of which does not require cleavage by Rhomboid for activation. Spitz is the primary ligand in development, and is broadly expressed; its pattern of activity is thus defined by the expression pattern of *rho* (Shilo, 2005). Like BMP signalling, the EGFR pathway has multiple roles during development, for example in *Drosophila* eggshell patterning and eye development.

In contrast to the BMP and EGFR pathways, ligands of the Notch pathway, Delta and Serrate, are membrane bound, and bind to the single receptor of the pathway (Notch) on adjacent cells (Fig. 1.6). Notch is subsequently cleaved to release the intracellular domain, which in co-operation with the Suppressor of Hairless (Su(H)) co-factor promotes transcription of target genes via the E(Spl) complex (Fig. 1.5; Bray, 2006). Juxtacrine Notch signalling is often involved in establishing cell fate distinctions between adjacent cells. This is seen in the process of lateral inhibition, where signalling in an initially equipotent field of cells specifies certain cells for a primary fate (e.g. neural) and others for a secondary fate (e.g. epidermal). Primary cells express high levels of the *Delta* (*Dl*) ligand, which activates the Notch pathway in surrounding cells, thus promoting the secondary fate (Cornell and Eisen, 2005). This pattern is reinforced by Notch activity inhibiting *Dl* expression in secondary cells, and Dl inhibiting Notch receptor activity in primary cells (del Álamo et al., 2011).

Vein patterning in the disc

The differentiation of vein and intervein cell subtypes in the pupal wing is preceded by the patterning of the larval wing disc into vein and intervein domains by intercellular signalling using the pathways described above. The creation of these domains is itself dependent on the earlier separation of the disc into exclusive non-intermingling compartments which respect the two planar axes of the tissue: anterior-posterior and dorsal-ventral (see Fig. 1.3). Compartments are defined by the expression of 'selector' genes: dorsal cells are defined by *apterous* expression, and ventral cells by its absence, while posterior cells are defined by *engrailed* and *invected* expression, and anterior cells by their absence (Blair, 2003).

As well as serving to separate cell populations, compartment boundaries serve a crucial function in organising signalling centres which direct long range patterning across the tissue (Brook et al., 1996). Signalling across the anterior-posterior (AP) compartment boundary is responsible for the formation of morphogen gradients that position the longitudinal veins on the AP axis. *engrailed* expression in cells of the posterior compartment induces expression of *hedgehog* (*hh*), which diffuses a short distance anterior to this (Basler and Struhl, 1994). Hh induces *dpp* expression in a stripe of cells anterior to the AP compartment boundary (Masucci et al., 1990). Dpp, along with another BMP ligand Gbb (Bangi and Wharton, 2006), then forms a long range gradient across the wing from this localised source of expression.

As a morphogen, Dpp acts from a localised source to direct patterning and growth over the whole disc via graded pathway activation (Affolter and Basler, 2007). The response of a given cell in the wing is dependent on the level of Dpp signalling it receives. The production of this signalling gradient is dependent on the regulation of Dpp diffusion at multiple levels. Dpp is seen in the extracellular domain away from its expression domain (Entchev et al., 2000; Teleman and Cohen, 2000), consistent with the diffusion of the ligand from the source. This process is not however wholly passive: diffusion is blocked in cells which lack the cell surface heparin sulphate proteoglycan (HSPG) Dally (Belenkaya et al., 2004). HSPGs, which can bind the ligand and thus restrict it to the cell surface, also play a key role in the formation of the Wingless (Han et al., 2005) and Hedgehog (Han et al., 2004) gradients. Another factor that influences Dpp diffusion is the receptor Tkv. *tkv* expression is inverse to pathway activation, such that high levels are seen in the most anterior and posterior regions, and these higher levels have been proposed to limit the diffusion of Dpp by binding and thus trapping the ligand (Lecuit and Cohen, 1998). Consistent with this model, ectopic expression of Tkv narrows the range of pathway activity, suggesting that increased receptor levels trap more of the ligand (Tanimoto et al., 2000). Where Tkv levels are lower, in more medial regions, it functions to transduce Dpp signals to promote proliferation and patterning (Nellen et al., 1996). Thus the Tkv receptor can both negatively and positively affect Dpp signalling.

The Dpp and Hh morphogens position the veins via the activation of downstream target genes. Hh is responsible for the positioning of L3 and L4, whereas Dpp is responsible for positioning L2 and L5 (de Celis, 2003; Crozatier et al., 2004). Although each longitudinal vein is positioned by a specific mechanism, the end result is the same: induction of *rho* expression (Sturtevant et al., 1993), and thus activation of the EGFR pathway (Guichard et al., 1999). For example, Dpp induces *spalt major* expression in a broad domain in the centre of the wing, which activates the *Knirps* and *Knirps-related* transcription factors in a stripe anterior to this domain. These

transcription factors in turn lead to the induction of *rho* expression in the L2 primordia (Lunde et al., 1998; Lunde et al., 2003). A general picture has arisen whereby the morphogens position the veins at the boundaries of the expression domains of their downstream transcriptional targets (Biehs et al., 1998). By the late third instar, this patterning culminates in the expression of *rho* in a pattern prefiguring that of the adult longitudinal veins: in four stripes along the AP axis of the wing which cross the margin and are symmetrical between dorsal and ventral compartments (Fig. 1.6 A; Sturtevant et al., 1993). *rho* is both necessary and sufficient to promote vein development in the larval stages, as indicated by gain-of-function and loss-of-function experiments (Sturtevant et al., 1993; Guichard et al., 1999), showing that this expression pattern reflects a functional role in vein specification.

Intervein domains lack *rho* and express *DSRF* (the *Drosophila* homologue of the *Serum Response Factor*, also known as *blistered*) in the sectors between these four vein stripes (Fig. 1.6; Montagne et al., 1996). Like *rho,* expression of *DSRF* is responsive to the Dpp and Hh gradients: its expression in the middle of the wing is controlled by Hh, and in the lateral sections of the wing by Dpp (Nussbaumer et al., 2000). It is excluded from the vein territories by *rho*-mediated repression (Roch et al., 1998), and in its absence, intervein domains are lost at the expense of vein domains. Following the establishment of the vein domains, they are maintained by continued EGFR pathway activity. A consequence of this activity is the expression of the Notch ligand *Dl* in the veins, which leads to the restriction of expression of the receptor *N* to the interveins, where it antagonises vein development (Fehon et al., 1991; de Celis et al., 1997; Biehs et al., 1998). Thus the Notch and EGFR pathways play exclusive and antagonistic roles in larval vein/intervein development. The outcome of these signalling events is the partitioning of the late third instar wing pouch into distinct vein and intervein gene expression domains (Fig. 1.6 A).

Vein patterning in the pupal wing

Vein/intervein signalling is elaborated in the pupal wing. *DSRF* is still expressed in intervein regions (Roch et al., 1998), where it is required for the formation of basal contacts between dorsal and ventral intervein cells (Fristrom et al., 1994). EGFR pathway activity in the veins is maintained (Sturtevant et al., 1993; Guichard et al., 1999), and induces expression of *dpp* in the vein primordia (Yu et al., 1996; de Celis, 1997). Dpp, signalling through the receptor Tkv (Ray and Wharton, 2001), activates the BMP pathway in the veins. The combined activity of

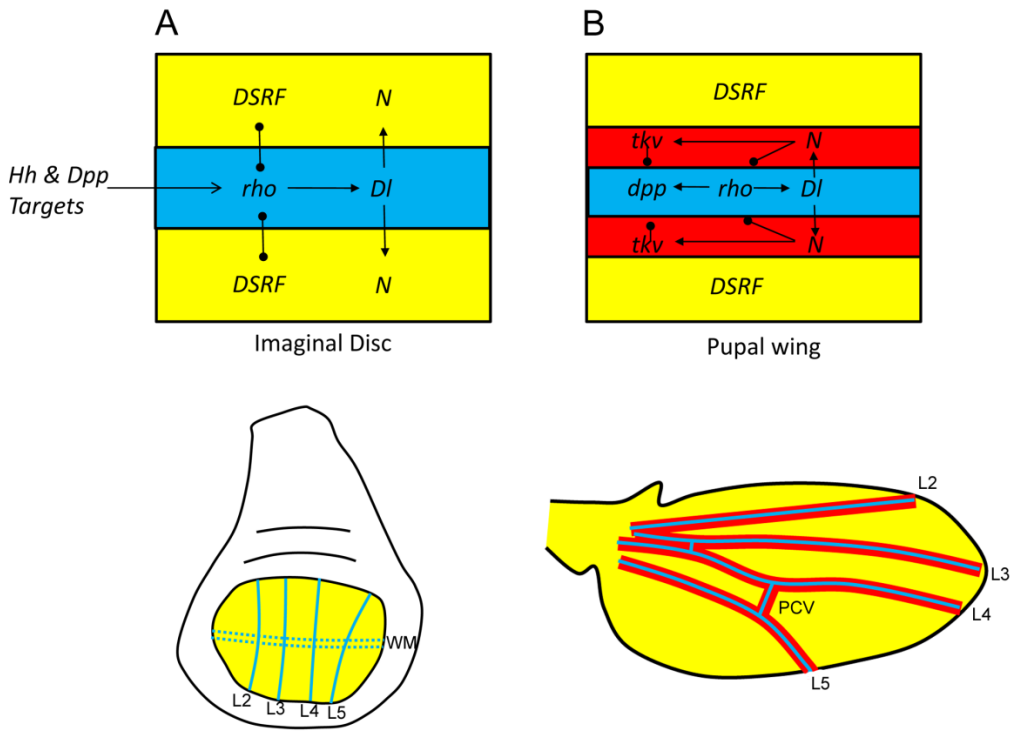

Figure 1.6. Vein/intervein gene expression domains in the disc and the pupal wing. (A) Wing disc. (B) Pupal wing after reapposition. Top panels: gene expression domains and signalling relationships. Arrows: pointed ends depict positive interactions, rounded ends depict inhibitory interactions. Bottom panels: expression domains mapped onto the wing. Blue = vein, yellow = intervein, red = pupal provein. WM = wing margin (cells which express *rho*).

the BMP and EGFR pathways in pupal development is required for continued vein development (Yu et al., 1996; Guichard et al., 1999), and they form a positive feedback loop such that ectopic activation of one pathway leads to the activation of the other (Yan et al., 2009b).

Dl is also expressed in pupal vein cells, and activates the Notch pathway in the intervein cells adjacent to the veins, which are termed the 'provein' (de Celis et al., 1997). Heightened Notch pathway activity in the provein leads to high levels of expression of the *N* receptor, and in addition the antagonism of the EGFR pathway by transcriptional suppression of *rho* (de Celis et al., 1997). Proveins also show heightened expression of the BMP receptor *tkv* (de Celis, 1997). Both Tkv and N antagonise vein development: reducing their function leads to the broadening of the domains of BMP and EGFR activity, leading to the differentiation of thicker vein cuticle (Lindsley and Zimm, 1992; de Celis, 1997; de Celis et al., 1997). As a result of this signalling, the pupal wing is divided into vein, intervein and provein gene expression domains (Fig. 1.6 B).

Tkv plays a dual role in the pupal wing: it at once transduces Dpp signals in vein cells to promote continued vein development, while at the same time antagonising vein development in the provein cells. These two functions are presumably controlled by distinct activity thresholds: whereas weaker *tkv* alleles give rise to thickened veins, stronger heteroallelic combinations lead to vein loss (Terracol and Lengyel, 1994; de Celis, 1997). How then does heightened Tkv expression in the provein regions antagonise vein development? pMad is not seen in the provein (Conley et al., 2000), so this affect is not mediated by transcriptional suppression. Rather, Tkv may act to 'trap' Dpp from the veins, preventing its diffusion by binding it while at the same time not transducing the signal (Sotillos and de Celis, 2005). As discussed above, a similar function has been proposed for Tkv in the disc (Lecuit and Cohen, 1998; Tanimoto et al., 2000). The question remains as to how Tkv can bind the ligand without activating downstream signalling.

Crossvein development

The crossveins are specified by a distinct mechanism to that of the longitudinal veins, although they do eventually show the same pattern of vein (e.g. *Dl*, *rho*, *dpp*) and provein (e.g. *N*) gene expression domains. A diverse group of genes that do not play an essential role in longitudinal vein development are involved in crossvein development. Alleles of some of these genes lead specifically to crossvein loss, and they have been hence called 'crossveinless' genes. The recent

characterisation ‘crossveinless’ genes, some of which were originally isolated in the early decades of the previous century (Lindsley and Zimm, 1992), has revealed a complex signalling network, involving the regulation of intercellular signalling at multiple levels to promote vein development specifically in the crossveins.

In contrast to the longitudinal veins, there is no pre-patterning of crossvein territories in the wing disc. Initial evidence for this came from clonal studies. Clones generated in the larval period tend to border longitudinal veins rather than cross them, suggesting that the veins create a clonal restriction (albeit one not as strong as those of the compartment boundaries) which limits proliferating intervein cells to discrete sectors (Bryant, 1970; Gonzales-Gaitain et al., 1994). In contrast, clones freely cross the crossveins, showing that if crossveins do form clonal restrictions, they are formed after the larval stages. Later work showed that the larval patterning network does not include crossveins: expression of *rho* in the disc is restricted to the longitudinal veins, and *DSRF* is expressed throughout the intervein regions where the ACV and PCV form (Sturtevant et al., 1993; Montagne et al., 1996).

The crossveins are specified in the pupal wing, coincident with reapposition. Whereas markers of EGFR pathway activity such as *rho* first define the longitudinal veins (Sturtevant et al., 1993), the first vein-specific marker seen in the crossveins is phosphorylated Mad (pMad), a readout of BMP pathway activity (Tanimoto et al., 2000). Between 18-22h APF, as reapposition commences, pMad accumulates in a broad band of cells in the region of the presumptive PCV (Conley et al., 2000). This accumulation coincides with the down-regulation of *DSRF* expression, which is initially expressed uniformly throughout the L4-5 intervein (Roch et al., 1998; Conley et al., 2000). PCV development thus involves the specification of vein fate in cells previously specified as intervein. As phosphorylated MAPK is absent in this early period (Ralston and Blair, 2005), the induction is independent of EGFR pathway activity. pMad accumulation and *DSRF* repression is then refined and strengthened by 26h APF, to give rise to a thin stripe that corresponds to the presumptive PCV. Following this period, general vein markers are expressed, including those signifying activation of the EGFR pathway (*aos*, *rho*, pMAPK), and *Dl* (Conley et al., 2000; Ralston and Blair, 2005). PCV development thus involves two steps: an initial specification and refinement step controlled by BMP signalling that is independent of EGFR, and a consolidation step where the canonical pupal vein signalling network is established.

Extracellular Regulation of BMP signalling: Cv and Cv-2

Characterisation of two 'crossveinless' genes revealed the importance of extracellular regulation of BMP ligands in PCV development. Extracellular modulators such as Tsg and Sog/Chordin limit the availability of BMP ligands to the receptors, as well as acting to transport ligands in numerous developmental contexts in vertebrates and invertebrates (Balemans and Van Hul, 2002). *crossveinless* (*cv*), the original allele of which was isolated almost a century ago (Bridges, 1920), is required for BMP pathway activity and the maintenance of dorsal-ventral separation in the PCV following apposition (Waddington, 1941; Shimmi et al., 2005a). *cv* encodes a secreted protein with homology to Tsg (Vilmos et al., 2005). As PCV loss phenotypes also result from loss of Sog and the Tolloid related protease Tolkin (Finelli et al., 1995; Serpe et al., 2005), this has led to the suggestion that a Cv-Sog-ligand complex, analogous to the Tsg-Sog-ligand complex in the embryo, is involved in PCV patterning (O'Connor et al., 2006; Fritsch et al., 2010). Because *dpp* is expressed in the longitudinal veins at the time of PCV specification (Yu et al., 1996), it is proposed to be transported from L4 and L5 into the PCV region by a Cv-Sog complex, which is then cleaved by Tok to release the ligand and promote signalling (O'Connor et al., 2006).

A second 'crossveinless' gene, *crossveinless-2* (*cv-2*), encodes a secreted protein that acts at a short range in the PCV to promote pathway activation (Conley et al., 2000; Serpe et al., 2008). Based on its ability to bind to cell surface HSPGs, BMP ligands and the Tkv receptor in vitro, Cv-2 appears to act at the cell surface to present ligands to receptors (Serpe et al., 2008). *cv-2* expression is activated by the initial BMP signal that specifies the PCV, so it acts as a positive feedback factor to enhance the signal (Serpe et al., 2008). Recently, another extracellular HSPG-binding protein, Larval Translucida (Ltl), has been implicated in PCV development. Loss of Ltl causes moderate expansion of the PCV, and hence it is proposed to function as a signalling antagonist (Szuperak et al., 2011). Like *cv-2*, *ltl* is activated downstream of the initial BMP signal. Considering this, these two secreted proteins appear to form a feedback mechanism to refine and enhance pathway activation in the PCV.

Crossveinless genes not encoding BMP components

The above examples demonstrate the importance of the extracellular environment of BMP ligands for PCV development, but the characterisation of two other 'crossveinless' genes revealed neither secreted proteins, nor members of the BMP pathway. *detached* (*det*) alleles

display partial loss of the PCV, resulting in a 'detached' island of vein material between L4 and L5 (Lindsley and Zimm, 1992). *det* was shown to be an allele of *Dystrophin* (*Dys*; (Christoforou et al., 2008). The loss of *Dystroglycan* (*Dg*) gave the same phenotype showing that, as elsewhere (Ehmsen et al., 2002), Dg and Dys function together. The basis of the 'detached' phenotype is the failure to maintain pMad accumulation at the junctions with the longitudinal veins (Christoforou et al., 2008). As a result, vein development is restricted to a detached fragment in the middle of the L4-L5 intervein.

The final characterised 'crossveinless' gene is *crossveinless-c* (*cv-c*). Hypomorphic alleles of *cv-c* retain a small fragment of vein between L4 and L5 (Lindsley and Zimm, 1992), similar to *det*. *cv-c* is required for a number of developmental events in the embryo: head involution, invagination of the posterior spiracles and trachea, dorsal closure, midgut constriction, and remodelling of the Malpighian tubules (MpTs) (Denholm et al., 2005). All of these processes involve tissue morphogenesis driven by changes to cell shape and arrangement. Cv-c appears to enact these changes via regulation of the cytoskeleton: the apical accumulation of Actin and Myo-II seen in both elongating MpTs and apically constricting tracheal placode cells is lost in *cv-c* mutants (Denholm et al., 2005; Brodu and Casanova, 2006), and as a result the morphogenesis fails.

The role of *cv-c* in PCV development is not clear, but its characterisation as a RhoGAP (Denholm et al., 2005) suggests that some aspect of RhoGTPase regulation is involved. RhoGTPases shuttle between active and inactive states. This shuttling is regulated by three classes of protein: the RhoGEFs, which catalyse the exchange of GDP for GTP, thus promoting the active state (Schmidt and Hall, 2002); the RhoGDIs, which bind GDP-bound Rho and restrict it to the cytosol (Garcia-Mata et al., 2011); and the RhoGAPs, which catalyse the intrinsic GTPase potential, thus promoting the inactive state (Bernards and Settleman, 2004). As Cv-c is a RhoGAP, this would imply that negative regulation of some aspect of RhoGTPase activity is required for PCV development. Although RhoGTPases have not yet been implicated in the crossvein patterning network (see above), it is of note that weak hypomorphic mutants of *Cdc42* show an extra-crossvein phenotype (Genova et al., 2000). Clarifying the role of *cv-c* in crossvein development will go some way to addressing this issue.

IV. Missing pieces in pupal wing development

Cellular basis of wing formation

Whereas the patterning of the wing disc into vein and interveins has been extensively characterised, the relationship between signalling and cellular differentiation in the pupal wing has received less attention (de Celis, 2003). To understand this relationship we first require a description of the morphological changes that occur in the pupal wing. Although well described on a tissue level (Fig. 1.4; Waddington, 1941; Fristrom et al., 1993), several aspects of the process of wing morphogenesis remain to be described on a cellular level, particularly with regards to vein/intervein differentiation. For example, although it is known that vein cells apically constrict following reapposition (Fristrom et al., 1994), the sequence of apical constriction following this point has not been defined, and it is not known whether all veins show a similar pattern of apical constriction. Furthermore, the relationship between apical constriction and overall cell morphology is unclear. In other systems, apical constriction leads to formation of bottle- or wedge-shaped cells (Sweeton et al., 1991; Lee and Harland, 2007), but the three dimensional shape of vein cells is not known. This is particularly pertinent when we ask how cells form the vein lumen: is it a case of differential adhesion, such that the non-adherence of vein cells forms the lumen (Hogan and Kolodziej, 2002), or is constriction on the apical-basal axis key (Fristrom et al., 1994; O'Keefe et al., 2007)? Finally, how cellular differentiation relates to the secretion of the adult wing cuticle is not known. As the adult cuticle is the 'final state to which the system arrives,' uncovering the cellular history of its construction is key to an understanding of wing development. Understanding this aspect of wing development will add to our understanding of how cellular behaviours underlie the formation of the structures of the animal body. Furthermore, it will form a platform for investigations into how intercellular signalling influences cell shape during wing development.

Spatial and temporal features of intercellular signalling

Although the outline of the pupal signalling network is fairly well described, several aspects of cell signalling in the pupal wing are still poorly understood. The first issue arises when we consider the tissue's architecture. Figure 1.6 B depicts a two dimensional signalling network, with communication occurring within the plane of the epithelium; however, the pupal wing is

a bilayer, with basal layers in apposition (Fig. 1.4). Signalling between the two component layers, which we term 'interplanar' signalling, has indeed been implicated in vein development. For example, clonal analysis has shown that the differentiation of vein in mutant clones can promote vein-like cuticle in the opposite surface (Garcia-Bellido and de Celis, 1992; Milan et al., 1997). Furthermore, certain vein-loss mutants lead to non-autonomous loss of vein structures in the opposite, wild type surface (Garcia-Bellido, 1977), while other vein loss mutants only lead to vein loss when mutant in both surfaces (de Celis, 1997; Ray and Wharton, 2001). All these studies suggest that interplanar signals are able to promote vein development in the opposite layer. However, both the endogenous function and mechanism of this interplanar signalling are still unclear. Interactions between epithelial layers are characteristic of development in both vertebrates and invertebrates (Gurdon, 1987; Bienz, 1997), as interplanar signals allow one layer to influence the behaviour of another. Pupal wing development presents an opportunity to investigate this phenomenon, particularly with regard to how such signalling contributes to cellular differentiation within each layer. It is also of interest to determine the relationship between interplanar signalling and 'intraplanar' signalling, within the plane of the epithelium.

A second issue involves the relationship between cell signalling, cell fate and cellular differentiation. Although vein/intervein domains are established in the disc, this is not associated with any cell shape changes, which only occur after apposition in the pupal wing. Pathway activity is thus latent with respect to cell shape changes in the stages preceding differentiation. Furthermore studies have suggested that although cell fate remains quite plastic up until differentiation, signalling after this point does not play a role in vein differentiation (Yu et al., 1996; Huppert et al., 1997; Guichard et al., 1999). Characterising the relationship between cell specification, determination and differentiation is necessary for a general understanding of the process. It will allow us to define the temporal features of cell signalling in the wing, and to link these to both the shape changes and spatial aspects of signalling discussed above.

Link between signalling and cell shape

A key missing piece of wing development is the means by which pathway activity is translated into the cell shape changes that occur after reapposition. In a simplistic but helpful portrayal of development we can define the process as patterning, the differential acquisition of cell fates, followed by differentiation, the transformation of these fates into the appropriate

morphological changes by way of some of the mechanisms discussed above. According to such a formulation, certain genes give the instructions, and others carry them out. It has been variously noted we know a lot more about the former class than the latter (Pradel and White, 1998; Schock and Perrimon, 2002; Lovegrove et al., 2006; Bataille et al., 2010; Ghabrial et al., 2011). These latter genes have been termed 'morphogenesis' (Ghabrial et al., 2011) or 'realisator' (Garcia-Bellido, 1975) genes, as they act to "specify at a cellular level characteristics that are central in morphogenetic processes" (Pradel and White, 1998: 418).

Where developmental realisators have been identified, a common output is the Actin cytoskeleton. For example, apical constriction and invagination characterise the formation of the ventral furrow in the mesoderm of *Drosophila*. This process is dependent on the mesoderm patterning gene *twist* inducing expression of *folded gastrulation* (*fog;* Costa et al., 1994). The Fog protein is then apically localised (Dawes-Hoang et al., 2005) where it controls the enrichment of both AJs and RhoGEF-2 (Kolsch et al., 2007). RhoGEF-2 in turn concentrates Rho1 activity apically, leading to activation of Myo-II and Actin-mediated apical constriction. *fog* thus 'realises' *twi*-directed furrow formation by modulating the dynamics of the cytoskeleton.

How then do vein/intervein signalling pathways direct cellular differentiation in the wing? The primary output of signal transduction pathways are changes in gene expression (Barolo and Posakony, 2002), so we can seek realisators in the transcriptional output of the pathways. Early PCV development offers an opportunity to study a process controlled exclusively by BMP pathway activity (Ralston and Blair, 2005). However, all of the known targets of BMP signalling in this process appear to act on the patterning level, acting either to inhibit intervein fate or to produce or enhance the BMP signal. The question remains as to how pathway activity leads to the morphogenesis of the vein, for example in terms of apical constriction of vein cells or the formation of the vein lumen. Such factors are also lacking in the longitudinal veins (in stark comparison to the multitude of genes identified to act at the patterning level (de Celis, 2003)), and indeed in the intervein, where the expression of *DSRF* promotes intervein development via currently unknown targets (Montagne et al., 1996; Roch et al., 1998). An understanding of this developmental process requires identification of some of the realisators that mediate cell shape changes downstream of fate determining signals.

V. Aims and outcomes

As documented above, multiple aspects of pupal wing development are currently poorly understood, and this thesis investigates these issues using a variety of imaging and genetic techniques. In doing so we address general questions in developmental biology: how cells co-operatively form tissue structures, the mechanics of intercellular signalling in tissue, the role of communication between epithelial layers, and the means by which signalling pathways enact cell shape changes.

We begin by characterising the wild type process. In Chapter 3, the cellular basis of pupal wing development is addressed using various imaging techniques, with a particular focus on how cells form the structures of the vein. Numerous novel cell behaviours involving sometimes dramatic alterations to cell shape are documented, which are co-ordinated across cell types to create supra-cellular structures that form the vein lumen and act as a template for the adult cuticle. With these cell shape changes in mind, we next turn our attention to their spatiotemporal control by signalling pathways. In Chapter 4, we use temporally controlled ectopic expression to probe the responses of cells to up-regulating pathway activity at defined times during pupal development. This allows us to define the phenocritical period of pupal signalling, showing that after reapposition has completed, cells are determined and cannot adopt alternate fates. In Chapter 5 we turn to the spatial aspects of intercellular signalling in the wing, first addressing the role that interplanar signalling plays in vein/intervein development. We show that BMP ligands can signal between the layers, but also that cell differentiation can occur autonomously when impeded in the opposing layer. We then show that the BMP ligand Dpp acts at a short range within the plane of the epithelium, and propose that its range is restricted by the induction of *tkv* expression. Finally, we turn to the question of how signalling influences cell shape, and in Chapter 6 identify Cv-c as a key realisator of BMP-mediated cell shape changes during PCV development. Cv-c functions to inhibit a function for Rho1 in promoting intervein development. We define both the effector Rok and *DSRF* as outputs of Rho1 in this process.

The work presented in this thesis provides multiple insights into the relationship between cell signalling and cell shape changes in the context of a model developing epithelium. The relevance of these findings to other developmental contexts is elaborated in the Discussion.

Chapter 2

Materials & Methods

I. Fly husbandry, stocks and crosses

Flies were cultured on standard yeast cornmeal glucose medium, and raised at 25˚C unless otherwise indicated. The *cv-c*^{M62} allele was a gift of Barry Denholm (University of Cambridge), *Cdc42*^{1} a gift of Rick Fehon (University of Chicago), *Rho1*^{72R} a gift of David Strutt (University of Sheffield), *Ubi-DECad-GFP* a gift of Nick Brown (University of Cambridge), *sqh-mCherry, sGMCA* a gift of Nicole Gorfinkel (University of Cambridge), *ap-Gal4, TubGal80*^{ts} a gift of Bruce Edgar (ZMBH, Heidelberg), *UAS-N*^{ECD} a gift of Jose Inyaki Pueyo (University of Sussex), *UAS-Dad* a gift of Tetsuya Tabata (University of Tokyo), and the *UAS-cv-c-GFP* lines a gift of Tadashi Uemura (Kyoto University). All other stocks were obtained from the Bloomington Stock Centre, Vienna *Drosophila* RNAi Centre (VDRC), or the FlyTrap project at Yale. A complete list of all fly stocks used and generated in this thesis is shown in Tables A.1 and A.2 in the Appendix.

Generation of recombinant stocks

Recombinant stocks with two or more transposons or alleles were generated for mis-expression, genetic interaction, dorsal rescue and mutant analysis experiments. As transposons carry the *w*$^{+}$ marker, crosses were carried out in a *w*^{1118} background. For insertions on the same chromosome (e.g. *Ubi-DECad-GFP* and *UAS-Mad-dsRNA*), a recombinant chromosome was generated by crossing *w/Y ; Insertion-A* males to *w/w ; Insertion-B* females, and crossing the resulting *w/w ; Insertion-A/Insertion-B* females to *w/Y ; If/CyO* males. Individual *w/Y ; Insertion-A, Insertion-B/CyO* recombinant males were selected by the presence of 2x *w+* markers and backcrossed to *w ; If/CyO* females to generate stocks. Typically, 5 to 10 stock lines were established and subsequently tested. For insertions on different chromosomes (e.g. *Ubi-DECad-GFP* and *UAS-dpp*), both were crossed independently to *w ; If/CyO ; MKRS/TM6b* females to generate *w/Y ; Insertion-A/If ; +/Tb* males and *w/w ; +/CyO ; Insertion-B/TM6b* females, which were crossed. *w ; Insertion-A/CyO ; Insertion-B/TM6b*

progeny were selected by the presence of 2x *w+* markers, and used to generate a stock which was subsequently tested.

Clonal analysis

To assess the requirements of genes in the two layers of the pupal wing, loss of function clones were generated with the FLP-FRT technique (Xu and Rubin, 1993) and Minute alleles used to increase clone size (Morata and Ripoll, 1975). For *cv-2* and *gbb* clones, *y w/Y ; FRT-G13 M(2)53* males were crossed to *w hs-FLP; Adv/CyO* females, and *w hs-FLP/Y ; FRT-G13 M(2)53/CyO* males crossed to *y w ; FRT-G13 sha cv-2^{K74}* or *y w ; FRT-G13 sha gbb^{D20}* females. Bottles were brooded every 24h, progeny aged for 24h, heat shocked for 2h in a 37ºC waterbath and returned to 25ºC until eclosion. Wings from Cy+ females were dissected and screened for clones, detected by the *sha* marker. *Dg^{O86}* clones were previously generated in the lab by the same method. For *cv-c* clones, the Minute technique was not feasible due to the dominant crossvein phenotypes associated with the parent *FRT82B RpS3* stock. *+/Y ; ; FRT-82B Ubi-GFP* males were crossed to *y w hs-FLP; ; Dr/TM3 Sb*, and *y w hs-FLP/Y ; ; FRT-82B, Ubi-GFP/TM3 Sb* males crossed to *FRT-82B, cv-c^{M62}/TM3 Ser, GFP* females. Bottles were heat shocked as above, GFP+ white prepupae (WPP) collected, and aged for 24 to 32h. Pupae were fixed, wings dissected, and Serrate+ wings selected and stained for antibodies as detailed below. As the clones were marked with GFP, Cad-GFP could not be used to assess cell shape, and Phalloidin was used to label Actin.

To generate clones of cells expressing target genes, the FLPout technique was used (Struhl and Basler, 1993). *UAS-X* males were crossed to *w hs-FLP ; UAS-myr-mRFP ; Act>CD2>Gal4* virgins, and 40 minute heat shocks were induced in L1-L2 larvae (for larger clones), in wall crawling L3 larvae (for smaller clones), or in 16-24h APF pupae (for single cell labelling). Pupae were aged to between 24h and 32h APF, fixed, and wings dissected and either mounted directly in Aquapolymount (Polysciences) or immunostained as detailed below. To analyse apical cell shape in clones, *UAS* transgenes were recombined with the *Ubi-DECad-GFP* insertion as detailed above. To assess phenotypes in the adult wings, pupae were allowed to develop until eclosion.

Limiting gene expression to the dorsal epithelium

To assess the requirements of genes between the dorsal and ventral layers, *ap-Gal4* was used to limit gene expression to the dorsal epithelium in otherwise mutant animals. In the case of *cv*, *w/Y ; ap-Gal4, UAS-GFP/CyO* males were crossed to *Sp Bl L/CyO* females, and *+/Y ; ap-Gal4, UAS-GFP/Sp Bl L* males crossed to *w cv^{43} ; UAS-cv*. Males of the genotype *w cv^{43}/Y ; UAS-cv/ap-Gal4, UAS-GFP* were selected and compared to *w cv^{43}/Y ; UAS-cv/Sp Bl L* controls. For *cv-2*, *w/Y ; cv-2^{K74} , ap-Gal4, UAS-GFP/CyO* males were crossed to *w/w ; cv-2^{K61}, UAS-cv-2/CyO* females and *w/w ; cv-2^{K74} , ap-Gal4, UAS-GFP/cv-2^{K61}, UAS-cv-2* progeny selected and analysed. For controls, *w/Y ; cv-2^{K74}/CyO* males were crossed to *cv-2^{K61}, UAS-cv-2/CyO* females and Cy- progeny selected. For *cv-c*, *w/Y ; ap-Gal4/CyO ; cv-c^{1}* males were crossed to *w ; If/CyO ; MKRS/TM6b* females and *w/Y ; ap-Gal4/If ; cv-c^{1}*/MKRS males selected and crossed to *w ; ; cv-c^{M62}, UAS-cv-c/TM6b* females. *w ; ap-Gal4/+ ; cv-c^{M62}, UAS-cv-c/cv-c^{1}* were selected and compared to *w ; If/+ ; cv-c^{M62}, UAS-cv-c/cv-c^{1}* controls.

Gal4 and Gal4/Gal80^{ts} crosses

To express genes under the control of the Gal4/UAS system (Brand and Perrimon, 1993), Gal4 lines (Table 2.1) were crossed to the appropriate UAS line and progeny raised at 25ºC unless otherwise indicated. To temporally restrict mis-expression in pupal development, Gal4/Gal80ts lines (Table 2.2; McGuire et al., 2003) were crossed the appropriate UAS line, left to mate in a vial at 25ºC for 24 hours, and transferred to a bottle at 18ºC which was brooded every 3 days. For dorsal expression experiments, *UAS-X* males were crossed to *w ; ap-Gal4/CyO, GFP ; Tub-Gal80^{ts}* females and progeny raised at 18ºC until the WPP stage, at which point GFP- pupae were selected and transferred to apple juice plates, and staged for defined time periods before shifting to 29ºC until eclosion. Cy- adults were selected and wings analysed. Variation was limited within each experiment, and the most representative wing chosen for the Figure. To induce brief periods of ubiquitous expression of a target gene, *UAS-X* males were crossed to *w ; Act-5C-Gal4/CyO, GFP ; Tub-Gal80^{ts}* females and progeny raised at 18ºC until the WPP stage, at which point GFP- pupae were selected and staged for defined time periods, shifted to 29ºC for 8h, and returned to 18ºC until eclosion. Cy- adults were selected and wings analysed. In certain cases bottles with progeny at various stages of development were shifted to 29ºC, either until eclosion or for brief periods, and adult wings analysed. In our hands, as in others (Bainbridge and Bownes, 1981; Classen et al., 2005; Yan et al., 2009a), development at 18ºC takes twice as long as that at 25ºC, allowing for calibration of relative developmental stages at which expression was induced.

Gal4 line	Expression pattern
A9	Wing disc and pupal wing, stronger in the dorsal compartment
Actin 5C (Act5C)	Ubiquitous. *In pupal wings higher in vein cells*
apterous (ap)	Dorsal compartment. *Dorsal expression maintained in the pupal stage*
blistered (bs)	*In pupal wing seen at a low level across the wing*
dpp-blk	Stripe of cells anterior to the AP boundary (source of Dpp morphogen gradient in the disc)
engrailed (en)	Posterior compartment. *Expression pattern maintained in pupal development, as assessed with Gal80^{ts}*
MS1096	Wing disc, stronger in the dorsal surface
spalt-major (sal)	Domain of cells in the centre of the wing, anterior margin at L2, posterior margin between L4 and L5. *Expression pattern maintained, though weak, in pupal wing as assessed with Gal80^{ts}*
Tubulin (Tub)	Ubiquitous, strong

Table 2.1. Gal4 lines used in this study. Italics show additional information arising from this study.

Gal4/Gal80^{ts} line	Expression pattern in the pupal wing	Source
A9-Gal4 ; ; Tub-Gal80^{ts}	General expression in the wing	Generated in this study
w ; Act5C-Gal4 / CyO, GFP ; Tub-Gal80^{ts}	Ubiquitous expression	Generated in this study
w ap-Gal4 / CyO, GFP ; Tub-Gal80^{ts}	Dorsal expression	Bruce Edgar (ZMBH, Heidelberg)
w ; en-Gal4 / (CyO, GFP) ; Tub-Gal80^{ts} / (TM6b, Tb)	Posterior compartment expression	Generated in this study
w ; sal-Gal4 / (CyO, GFP) ; Tub-Gal80^{ts} / (TM6b, Tb)	Expression in the middle of the wing	Generated in this study

Table 2.2. Gal4/Gal80^{ts} lines used in this study.

Genetic interactions with *cv-c*

To test for genetic interaction between *Rho1* and *cv-c*, *w/Y ; $Rho1^{72R}$/CyO ; cv-c^{M62}/TM6b* males were crossed to *w ; If/CyO ; MKRS/TM6b* females, and *w/Y ; $Rho1^{72R}$/If ; cv-c^{M62}/MKRS* males crossed with *y w ; ; cv-c^{1}*. Control (*w ; If/+ ; cv-c^{M62}/cv-c^{1}*) and experimental (*w ; $Rho1^{72R}$/+ ; cv-c^{M62}/cv-c^{1}*) wings were scored for the presence of PCV material as described in Christoforou, et al (2008), with the following phenotypic classes: complete PCV, gap (a gap between the PCV and L4 or L5), detached (no connections between the PCV and the longitudinal veins), point (a small point of venation remains), crossveinless (no PCV material). This presents a phenotypic series, from weakest (complete) to strongest (crossveinless). To test for genetic interaction between *Cdc42* and *cv-c, w/Y ; ; Df(3R)Exel6267/TM6b* males were crossed to *y w $Fur2^{R4}$ /FM7h*, and *FM7h/Y ; ; Df(3R)Exel6267/ +* males crossed with *y w $Cdc42^{1}$/FM6,* and *y w $Cdc42^{1}$/FM7h ; ; Df(3R)Exel6267/+* females crossed to *y w/Y ; ; cv-c^{1}* males. Control (*y w/FM7h ; ; Df(3R)Exel6267/cv-c^{1}*) and experimental (*$Cdc42^{1}$/y w ; ; Df(3R)Exel6267/cv-c^{1}*) wings were scored for PCV phenotypes as described above.

II. Imaging

Brightfield

Adult wings were dissected in Ethanol and allowed to dry on a glass slide, and mounted in DPX (Fisher). Images were taken on a Zeiss Axiophot microscope, and further processed using Adobe Photoshop Elements to crop and alter brightness, contrast and resolution.

Scanning electron microscopy

For scanning electron microscopy (SEM), adult flies were collected just after eclosion, and either processed directly or allowed to mature in empty vials until the wings were fully expanded and tanned. Wings were dissected from the body and washed twice for 15 minutes to overnight with absolute Ethanol (Fisher) and then for 15 minutes in Hexamethyldisilazane (HMDS, Sigma). Wings were rinsed with HMDS and laid out on a glass slide, allowed to dry

completely, and then mounted on aluminium stubs covered with a graphite disk (EM Sciences) or conductive carbon cement (PLANO). Alternatively, wings were dissected from newly eclosed animals and mounted directly without processing. Samples were sputter coated with gold, and imaged on a LEO S420 Stereoscan electron microscope.

Confocal microscopy

Autofluorescence of the adult wing cuticle was imaged in mutants bearing the *yellow* mutation, which produces the highest emission intensity (R. Ray, pers. comm.). For this technique, wings were mounted in Aquapolymount (Polysciences) or DPX (Fisher), and were imaged with a Zeiss NLO confocal microscope using 488nm excitation and a 560nm long-pass filter.

For pupal wings, pupae were immersed in PBS (Phosphate buffered saline) droplets, dissected from their pupal cases and killed by puncturing the head, and fixed in 4% Paraformaldehyde (Sigma) in PBS at 4˚C overnight. Pupae were then washed 3 x 5 minutes in PBTx (1X PBS + 0.1% Triton X-100), and transferred to PBTx droplets on Sylgard plates. The pupal cuticle was removed, and wings dissected from the thorax at the hinge. In certain conditions, such as in a *Ubi-DECad-GFP* background, no staining was necessary and wings mounted directly by transferring with forceps to an Aquapolymount (Polysciences) droplet on a glass slide, and gently laying a coverslip on top. For antibody staining, fixed wings were transferred to Eppendorf tubes and blocked in PBTx + 1% NGS (Normal goat serum) + 0.1% BSA (Bovine serum albumin) for 2 hours at room temperature. Block was removed, 35µl primary antibody added, and wings incubated overnight on a gentle rotator at 4˚C. Primary antibody was removed and wings washed 3 x 5 minutes in PBTx + 0.1% BSA, and 35µl secondary antibody added. Wings were incubated for 2h at room temperature, before washing 3 x 5 minutes in PBTx + 0.1% BSA. To detect Actin, wings were incubated with 35µl Alexa-647 conjugated Phalloidin (Molecular Probes, 1:400) for 30m at room temperature, before washing 3 x 5 minutes in PBTx. Wings were then transferred to clean PBTx droplets, and mounted in Aquapolymount as above. Mounted wings were imaged on a Zeiss NLO confocal microscope, using 40x and 60x objectives. Confocal stacks were analysed with Zeiss LSM Image Browser software. The dorsal layer was identified by the campaniform sensilla on the apical surface of L3. Further image processing was carried out using Adobe Photoshop Elements.

Primary antibodies used: α-DSRF (Active Motif; 1:1000), α-β-galactosidase (ICN/Cappel; 1:1000), α-Rho1 (DSHB, P1D9; 1:20). Secondary antibodies used: Alexa-488 goat α-mouse, Alexa-546 goat α-mouse, Alexa-488 goat α-rabbit, and Alexa-546 goat α-rabbit (all Molecular Probes, 1:1000), Cy5 α-mouse (1:50, gift of JP Couso, University of Sussex). Due to the inefficacy of the α-pMad antibody, α-DSRF was used as a read out of BMP pathway activity. *DSRF* repression has been previously shown to be a direct response to BMP signalling in the pupal wing (Conley et al., 2000).

III. Image analysis

Semi-automated apical cell area measurement

For apical cell area measurements, *w ; Ubi-DECad-GFP* males were crossed to Oregon R females, and female progeny of the genotype *w/+ ; Ubi-DECad-GFP/+* were collected as WPP, aged to between 16h and 32h APF at 2h time intervals, and fixed, dissected and mounted as detailed above. Dissecting prior to 16h was prohibited by the attachment of the pupal cuticle to the wing epithelium. 3-4 wings from each time point were imaged. In 16h and 18h APF wings, the campaniform sensilla that form prior to apposition were used as landmarks for the three wing regions analysed. The L3 region was centred on the most distal sensillum on this vein. We adopted a semi-automated approach based on the Cell Profiler program (Carpenter et al., 2006; available at www.cellprofiler.org). Cropped images were processed in a custom pipeline in which individual cells are identified, outlined and their apical area measured by pixel number in the enclosed region. Measurements were converted to μm^2, exported into Microsoft Excel and manually curated, and the pipeline re-run with altered stringency to obtain measurements that were incorrectly outlined in the first run. New measurements were added to the Excel file, and the final set processed into histograms in Excel.

Apical area measurement in FLPout clones

To assess the effect of ectopic gene expression on apical cell area, single apical sections from confocal stacks were used. Clone cells were identified by the myr-mRFP marker, and their first row neighbours (those sharing a junction with a clone cell) and second row neighbours (those

sharing a junction with a first row cell) identified. For each clone, average apical area was calculated for each of these classes by measuring total area of the class and dividing by number of constituent cells. As apical cell area varies in intervein regions across the wing (from ~8μm^2 to ~30μm^2 in the same wing), and indeed between wings, control cells were picked from a similar clone-free region of the intervein of the same wing. Measurements were taken manually using the Zeiss LSM Image Browser software. Because of the wide variation in cell size across the wing, we calculated the effect of clones by comparing average size of each of the classes to the average size of internal control cells. Thus, ratios of clone : control, first row neighbour : control and second row neighbour : control were calculated for each clone, and averaged over all the clones for the experimental condition. The standard deviation of these average ratios was calculated using the STDEV function in Microsoft Excel.

3D reconstructions

To label single cells with GFP, we aimed to administer heat shocks after the final mitosis in the pupal wing, which occurs around 20-22h APF (Schubiger and Palka, 1987). To obtain a readily detectable GFP signal, animals need to be aged for 8h after heat shock. *w/Y ; UAS-GFP* males were crossed to to *w hs-FLP ; UAS-myr-mRFP ; Act>CD2>Gal4* females, and WPP were collected from the progeny, which were aged for 16, 18, 20, 22 and 24h, heat shocked in vials for 40 minutes in a 37ºC waterbath, transferred to agar plates and aged for a further 8 hours before fixing at 24, 26, 28, 30 and 32h APF respectively. Wings were dissected, stained with Phalloidin and mounted as above. Actin was used to identify the position of marked cells within the wing. Confocal stacks were cropped around the labelled cell, and three dimensional projections generated using the LSM Image Browser software.

Chapter 3

Dynamic cell shape changes during pupal wing development

I. Chapter Overview

The *Drosophila* wing is a widely used model system for investigating how cell signalling patterns epithelia, yet the cell shape changes that underlie formation of the structures of the pupal wing, in particular the wing veins, have not been thoroughly described. Here, we have employed a variety of imaging techniques to investigate these changes. We find that wing development involves a dynamic series of cell shape changes that are co-ordinated to give rise to the structures of the pupal epithelium and adult cuticle. These changes are underpinned by remodelling of both the apical and basolateral membranes, and are capable of influencing the shapes of nearby cells. Overall, cell shape is remarkably plastic throughout pupal wing development. This work adds to our understanding of the cellular basis of wing formation, and provides a platform for investigations into the signals that control it.

II. Introduction

Tissue morphogenesis creates complex structures from initially simple arrangements of cells. Collective cell behaviours, such as migration, rearrangement, and changes in shape are essential for its correct execution. Cell shape changes derive from the interplay between intrinsic factors, such as the cytoskeleton, and extrinsic factors, such as the constitution of the surrounding extracellular matrix (ECM) (Paluch and Heisenberg, 2009). For instance, in migrating cells, cytoskeletal remodelling drives the formation of lamellipodia and filopodia, which in turn are stabilised by adherence to the ECM via focal adhesions that form 'traction sites' for movement (Ridley et al., 2003). In *Drosophila* imaginal discs, maintenance of the columnar cell shape depends both on regulation of the cytoskeleton by RhoGTPases (Widmann and Dahmann, 2009), and on the constricting force provided by the Collagen-rich basement membrane that ensheathes the disc (Pastor-Pareja and Xu, 2011). Using such mechanisms, cells can generate a remarkable array of morphologies suited to their function (consider a Purkinje neuron, compared to a ciliated epithelial cell, compared to a phagocyte).

In the context of epithelia, localized cell shape changes drive morphogenesis in numerous developmental contexts (Lecuit and Lenne, 2007). Cell shape changes such as apical constriction, apical-basal elongation, and cell flattening all play important roles in epithelial morphogenesis (Fristrom, 1988; Schock and Perrimon, 2002). The *Drosophila* wing is a particularly amenable model system for studying epithelial morphogenesis. The adult wing is largely composed of cuticle that is secreted by an epithelial bilayer during pupal development, which is primarily composed of two cell types, intervein and vein. Intervein cells give rise to the expanses of tightly-apposed transparent cuticle, and vein cells give rise to pigmented channels that act as conduits for hemolymph and provide structural support during flight (Wootton, 1992).

As is true for many developmental systems, our knowledge of the patterning of the wing far exceeds our understanding of how patterning mechanisms are translated into the differentiation of cellular phenotypes (de Celis, 2003; Lovegrove et al., 2006; Ghabrial et al., 2011). Although wing morphogenesis at the tissue level has been well described (Waddington, 1941; Fristrom et al., 1993), the cell shape changes that accompany pupal wing development have not been addressed in detail. Furthermore, it is not clear how cellular morphologies in the pupal wing correspond to the cuticular structures of the adult. Here, we address the cell

shape changes that underlie the formation of the pupal and adult wing. We document dynamic and unexpected patterns of cellular morphogenesis, involving the reshaping of apical and basolateral membranes to produce striking cellular morphologies that create the distinctive architecture of the wing.

III. Results

Vein morphology in the adult wing

We first set out to characterise the final state to which the developmental system arrives, the adult wing. It has long been noted that veins have a distinct morphology on the two surfaces of the adult wing (Schatz, 1951; Garcia-Bellido and Santamaria, 1972). Using light microscopy, the longitudinal veins appear asymmetric, protruding from one surface and being flat on the other, and this articulation has a stereotyped pattern: L2, the PCV, and proximal L4 protrude from the ventral surface, whereas L3, distal L4, and L5 protrude from the dorsal surface (Fig. 3.1 A). When visualised with scanning electron microscopy (SEM), the distinct structure of the veins on both surfaces of the wing is evident. The protruding surface is formed of an arch of cuticle, 2-3 trichomes wide, raised from the surface of the surrounding intervein (Fig. 3.1 B, D). In contrast, the flat surface is almost indistinguishable from the surrounding intervein (Fig. 3.1 C), but when viewed at an angle it appears as a low ridge, typically one trichome wide, that is flanked by shallow furrows (Fig. 3.1 E). To visualize the veins in cross-section, we took advantage of the autofluorescence of the cuticle and generated 3D reconstructions with confocal microscopy. The longitudinal vein lumen appears as a semi-circular channel with the arched surface forming the rounded side and hence making up a greater part of the perimeter (Fig. 3.1 I, I'). This structure forces the surrounding intervein to adopt an oblique angle, and as the longitudinal veins in the proximal wing alternate between being arched ventrally and dorsally (Fig. 3.1), the wing blade assumes a 'corrugated' topology (Fig. 3.1 J, J'), similar to what has been described for other insects (Wootton, 1992).

In contrast to the longitudinal veins, the crossveins show a unique morphology that is not arched or flat. The ventral surface of the PCV is composed of a series of ridges rising up towards base of the trichomes producing an irregular surface (Fig. 3.1 F). This creates an 'annulated' morphology, as has been described for the crossveins in other insects (Wootton, 1992). The distinction between the two vein morphologies is clearly seen where the arched surface of L4 and the annulated surface of the PCV meet (Fig. 3.1 H). Unlike the longitudinal veins, which show distinct arched and flat surfaces, the two surfaces of the crossveins both appear annulated. However, the ventral surface is more pronounced than the dorsal surface (Fig. 3.1 H, G) consistent with claim that the vein is ventrally articulated (Garcia-Bellido, 1977). Confocal projections also reveal the distinct PCV morphology (Fig. 3.1 K). In sagittal section, the

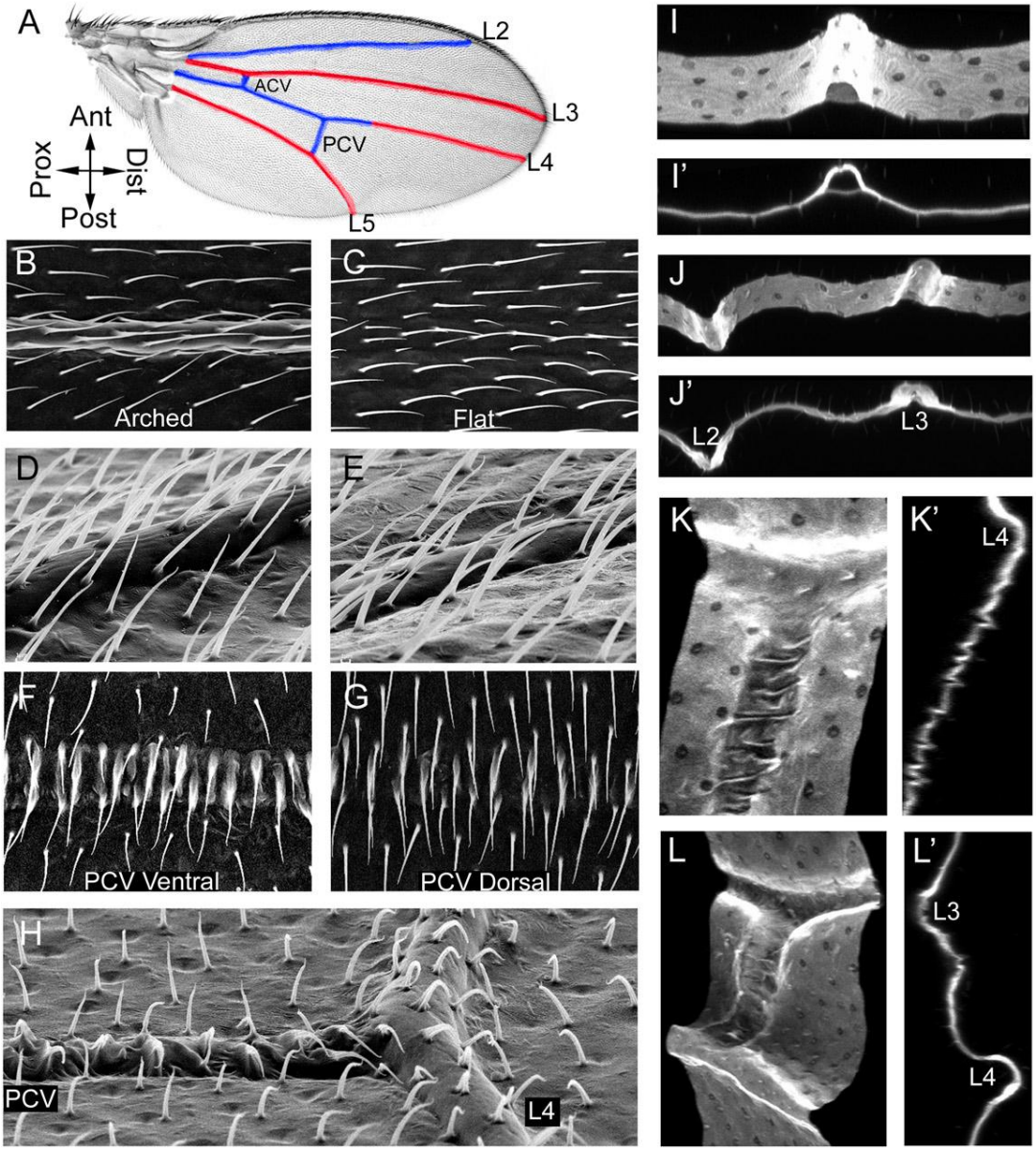

Figure 3.1. The structure of the adult wing veins. (A) Adult wing showing longitudinal veins and crossveins, with ventrally arching veins false coloured blue, and dorsally arching veins false coloured red. (B-H) SEM and (I-M) confocal images of adult wings. SEM images show the trichomes that are secreted by every cell of the pupal wing and appear white. (B) Ventral L2, showing the arched surface. (C) Dorsal L2, showing the flat surface. (D) Ventral L4, viewed at an angle, showing the arched surface. (E) Ventral L5, viewed at an angle, showing the flat surface. (F) PCV ventral, rotated 90º**.** (G) PCV dorsal, rotated 90º. (H) PCV junction with L4 viewed from distal end of wing. (I) Angled confocal surface projection of ventral L2 (ventral up), and the same image in cross-section (I'). (J) Angled surface projection of L2 and L3 (dorsal up), and the same image in cross-section showing corrugated pattern formed by alternate arching (J'). (K) Angled surface projection of the junction of the PCV and L4, (K') sagittal section through the PCV. (L) Angled surface projection of the ACV, (L') sagittal section through the ACV. Images D, E and H courtesy of Rob Ray.

PCV exhibits a ruffled profile, reflecting the ridges seen with SEM (arrows in Fig. 3.1 K'), and the ACV displays a similar morphology (Figs. 3.1 L-L''). The morphological distinction between longitudinal and crossveins presumably reflects the different mechanisms that pattern them in the pupal wing (O'Connor et al., 2006; see also Chapter 6), and has potential relevance for their structural roles in the wing (Wootton, 1992).

Pupal wing development between apposition and the definitive stage

We next sought to address how the cuticular structures of the veins are created. The pupal wing that secretes the cuticle is a bilayer epithelium, with the basal surfaces of each layer in apposition and the apical surfaces facing outward. Preliminary to studies of pupal vein morphology, we first looked at tissue level changes in the apical and basal profiles of wings of flies bearing the *Ubi-DECad-GFP* insertion (Oda and Tsukita, 2001), in which *Drosophila* E-Cadherin tagged with GFP (Cad-GFP) is ubiquitously expressed. At 16h after puparium formation (APF), the dorsal and ventral layers are separated, and apically the epithelium is disordered and veins cannot be distinguished (Fig. 3.2). Apposition starts at ~18h APF, and veins emerge as constricting bands of cells which show an apical enrichment of Cad-GFP, mirroring the endogenous enrichment (O'Keefe et al., 2007). These bands of constriction then refine over the following 14 hours, coincident with the expansion of sectors of apposition, such that by the definitive stage (32h APF), the veins are clearly distinct from the surrounding intervein. The wing is composed of constricted stripes of vein cells overlying the vein lumens, and sectors of apically relaxed and basally apposed intervein between them (Fig. 3.2). Shortly after this stage (beginning at ~36h APF) wing folding begins and the adult cuticle is secreted, after which Cad-GFP cannot be used to image cell morphology.

The time course shown in Fig. 3.2 allows for calibration of developmental stages to specific time points: separation (16h APF), reapposition (18-22h APF), refinement (24-30h APF), the definitive stage (32h APF), and wing folding (36h+ APF). This is useful considering the timing of these stages varies between laboratories: for example, in one report, apposition and refinement take place at later time points, such that the 40-44h wing appears similar to our 32h APF wing (Urbano et al., 2009). Such differences may be influenced by genetic background (e.g. our wild type wing is in fact *w/+ ; Ubi-DECad-GFP/+*), and differing laboratory conditions (e.g. if animals were raised at room temperature, rather than 25ºC as in this work).

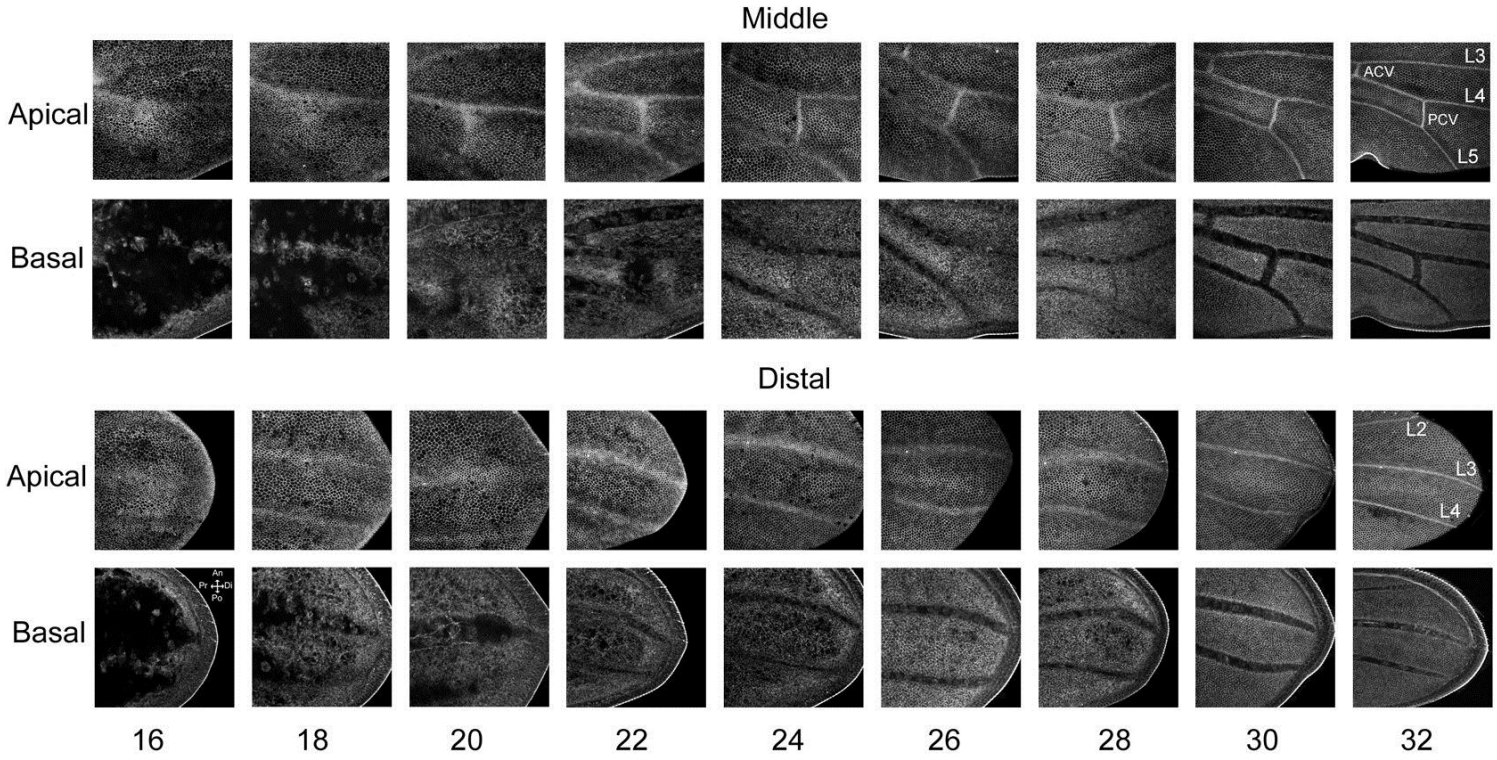

Figure 3.2. The process of vein/intervein differentiation following reapposition. Apical and basal sections in middle and distal portions of wings of the genotype *w/+ ; Ubi-DECad-GFP/+* from 16-32h APF. Cad-GFP labels apical adherens junctions and basal apposition. Age as h APF shown below images. Initial apical disorder and basal separation is followed by progressive apposition and constricting vein bands, which then refine by the definitive stage (32h APF), in which veins are labelled. Compass abbreviations: An=Anterior, Po=Posterior, Pr=Proximal, Di=Distal.

Cell arrangement in the pupal wing veins foreshadows adult cuticle morphology

Considering the distinctive cuticular morphology of veins in the adult wing, both between the dorsal and ventral surfaces and between vein types, it was of interest to determine if these distinctions are evident earlier in development. Because vein morphology is most refined at the definitive stage (32h APF), we first addressed cell shape at this point, using Cad-GFP to label apical cell outlines. At this stage, there is a distinctive arrangement of cells in the side of the vein that will give rise to the arched cuticle compared to that which gives rise to the flat cuticle. This difference is most apparent in L3, where the presumptive arched surface (dorsal) is formed of a band of trapezoidal and diamond-shaped central cells, one to two cells wide, flanked by a row of smaller and thinner diamond-shaped cells (Fig. 3.3 A). In contrast, the presumptive flat surface (ventral) is formed of a single row of trapezoidal cells flanked by smaller, diamond-shaped cells (Fig. 3.3 A'). Similar distinctions in arched/flat morphology are observed in L2 (Fig. 3.3 B, B') and L5 (Fig. 3.3 D, D'), and to a lesser extent in L4 (Fig. 3.3 C, C'). Therefore, the presumptive arched surface of the vein is generally broader and composed of more cells than the presumptive flat surface. Additionally, veins on both the arched and flat surfaces are composed of two cell types: larger central cells, and smaller and thinner flanking cells.

As in the adult, the crossveins adopt a distinct morphology in the pupal wing. PCV cells are smaller (see also below), more compact, and form more irregular polygonal shapes (Fig. 3.3 E). Although the ventral surface appears broader than the dorsal (Fig. 3.3 E'), both surfaces adopt the same morphology. Therefore, the morphological differences seen in the adult wing vein, both in terms of the arched/flat asymmetry of the longitudinal veins and the distinctive crossvein morphology, are foreshadowed by the apical shapes adopted by vein cells at the definitive stage.

Apical constriction and the achievement of the definitive stage morphology

It has previously been demonstrated that vein cells are apically constricted compared to intervein cells (Fristrom et al., 1994; Classen et al., 2005; O'Keefe et al., 2007). However, as we have shown above, not all vein cells constrict to the same extent, with flanking cells appearing smaller than central cells. To determine how these distinctions arise, we performed a quantitative analysis of apical cell area during the period between reapposition and the definitive stage (see Methods). For this experiment we assessed three regions of the wing: the

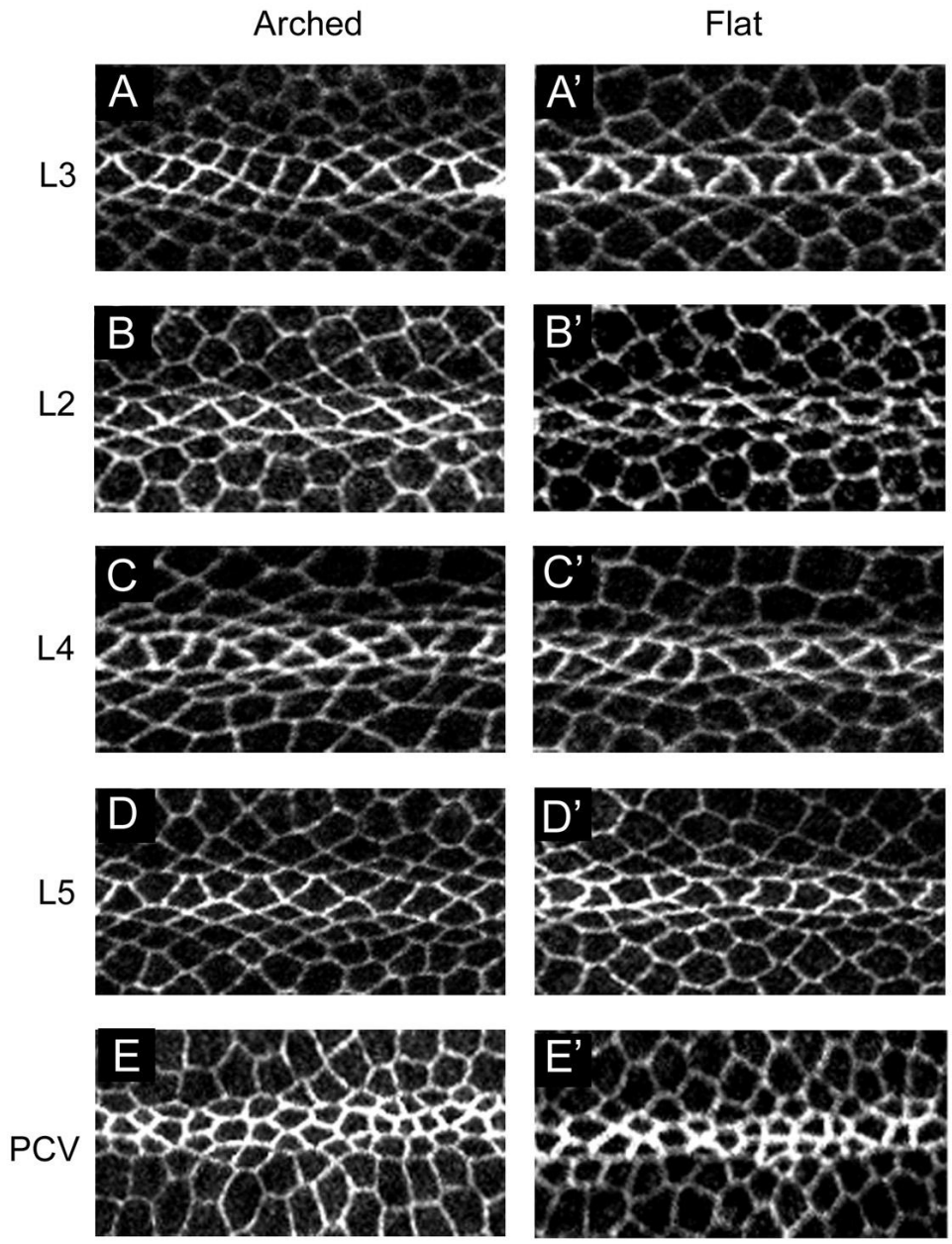

Figure 3.3. Apical morphology of vein cells in the definitive stage pupal wing. Single sub-apical sections of veins in 32h APF wings from females of the genotype *w/+ ; Ubi-DECad-GFP/+*. (A) L3 dorsal. (A') L3 ventral. (B) L2 ventral. (B') L2 dorsal. (C) L4 ventral. (C') L4 dorsal. (D) L5 dorsal. (D') L5 ventral. (E) PCV ventral. (E') PCV dorsal. The PCV has been rotated 90º for comparison with the longitudinal veins.

dorsal surface of L3 (Fig. 3.4 A), the ventral surface of L3 (Fig. 3.4 B), and the ventral surface of the posterior crossvein (Fig. 3.5). The regions were chosen to compare development between arched and flat surfaces of the longitudinal veins, and between the longitudinal veins and crossveins. The analysed regions were focussed on the developing vein, and included adjacent intervein regions.

At 16h APF, apical cell surface areas across the wing are quite variable, ranging from 7 to 35μ^2 (Fig. 3.4 A-B, 3.5 A), with a small class of cells (around 10% of the total) with apical surface areas in excess of 35μ^2 that we infer are undergoing mitosis. Between 16-20h APF, these larger cells are lost with the completion of the final round of mitosis (Schubiger and Palka, 1987), and there is a general reduction in apical cell surface area, so that the range narrows to between ~4 and ~25μ^2 (Fig. 3.4 A-B, 3.5 A). As discussed above, the presumptive veins first appear during this period as apically constricting bands of cells. Between 20-24h APF, the epithelium relaxes and the range of apical cell areas broadens slightly. By this stage, more cells are incorporated into the presumptive arched surface of L3 than into the presumptive flat surface (compare 24h time point in Fig. 3 A with 3 B). This foreshadows the pattern seen at 32h APF (Fig. 3.2) and in the adult cuticle (Fig. 3.1), showing that the vein achieves an asymmetric morphology by incorporating a different number of cells into the two layers of the vein. Between 24-28h APF, there is a progressive refinement of vein and intervein territories, which produces a bimodal distribution of apical surface areas composed of smaller vein cells (~4-~9.5μ^2) and larger intervein cells (~9.5-~22μ^2) (Fig. 3.4 A-B, 3.5 A).

In the interval between 28-32h APF, cells in longitudinal veins and crossveins show distinct behaviours. In the dorsal surface of L3, the bimodal distribution seen at 28h APF is lost by 32h APF (Fig. 3.4 A). This change is as a result of the relaxation of central vein cells, such that their apical surface areas overlap with those of the intervein cells adjacent to the vein (yellow and orange cells in Fig. 3.4 C). This relaxation is specific to the central cells, so the smallest cells of the vein are the flanking cells (red cells in Fig. 3.4 C), and is also seen on the ventral surface (Fig. 3.4 D). Therefore, vein development involves an initial apical constriction in all vein cells followed by the subsequent relaxation of central cells between 28-32h APF. This phenomenon is intriguing considering differences in constriction do not reflect known distinctions in the expression of vein patterning genes (Sotillos and de Celis, 2005; Blair, 2007).

In contrast to the longitudinal veins, constriction of presumptive PCV cells is not followed by any relaxation. Instead, the distinction between vein and intervein populations is enhanced by 32h APF, producing a clear bimodal distribution (vein: ~3-~10μ^2; intervein: ~10-~24μ^2; Fig. 3.5.

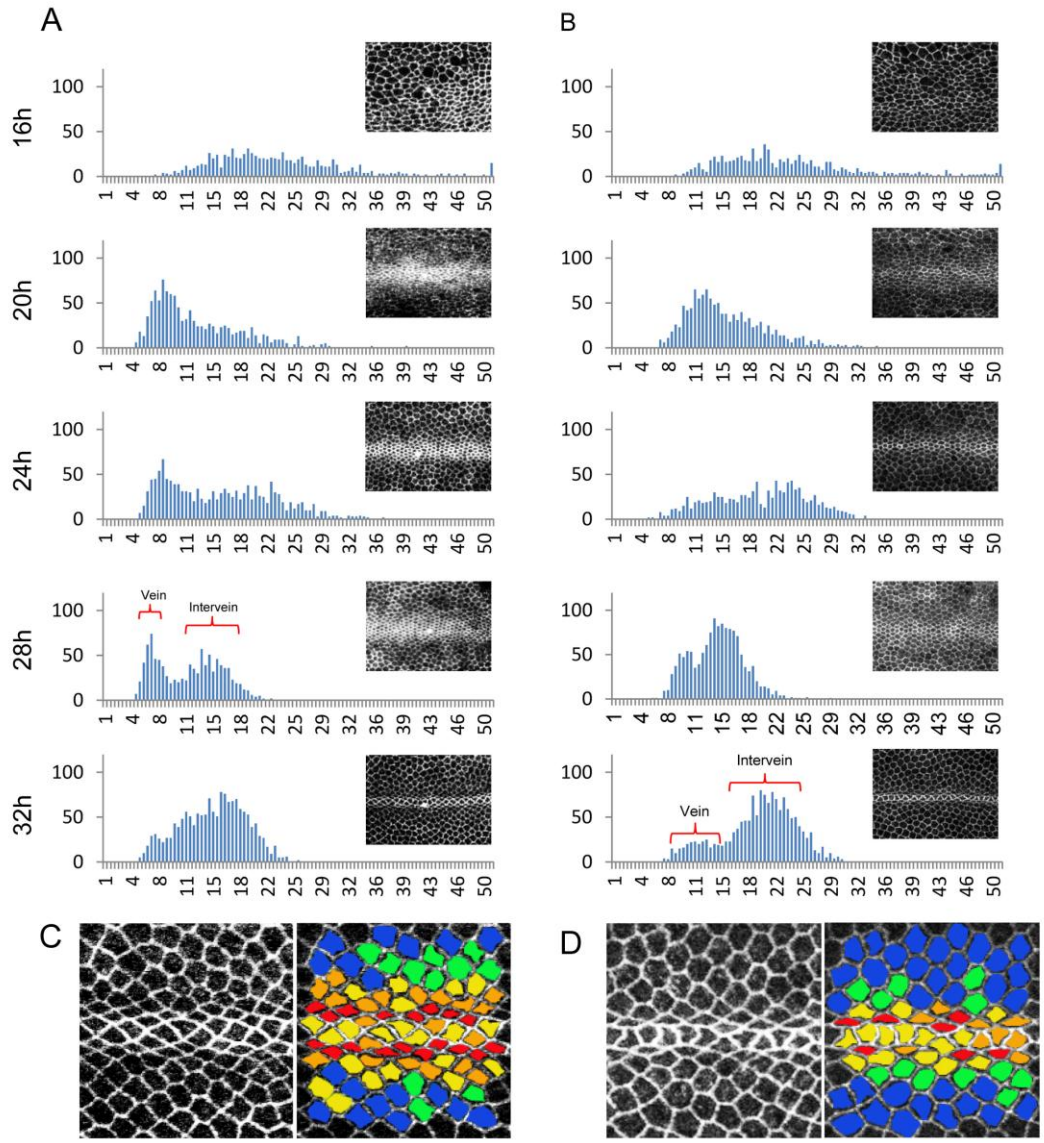

Figure 3.4. Apical cell area changes in L3. (A-B) Histograms derived from Cell Profiler measurements (3-4 wings and ~1000 cell measurements per time point) showing estimated apical cell areas in the vein and surrounding intervein at 16, 20, 24, 28 and 32h APF. Y axis indicates number of cells in each area class. X axis indicates apical area, demarcated in 0.5µm^2 intervals. Images above graphs show representative wings for each time point. Red brackets indicate vein and intervein populations. (A) L3 dorsal. (B) L3 ventral. (C-D) Apical vein sections of L3 dorsal (C) and ventral (D) at 32h APF, with cells manually colour coded according to estimated apical cell area derived from Cell Profiler measurements, as follows: <9µm^2 = red; 9-11.5µm^2 = orange; 11.5-14µm^2 = yellow; 14-16.5µm^2=green; >16.5µm^2 = blue.

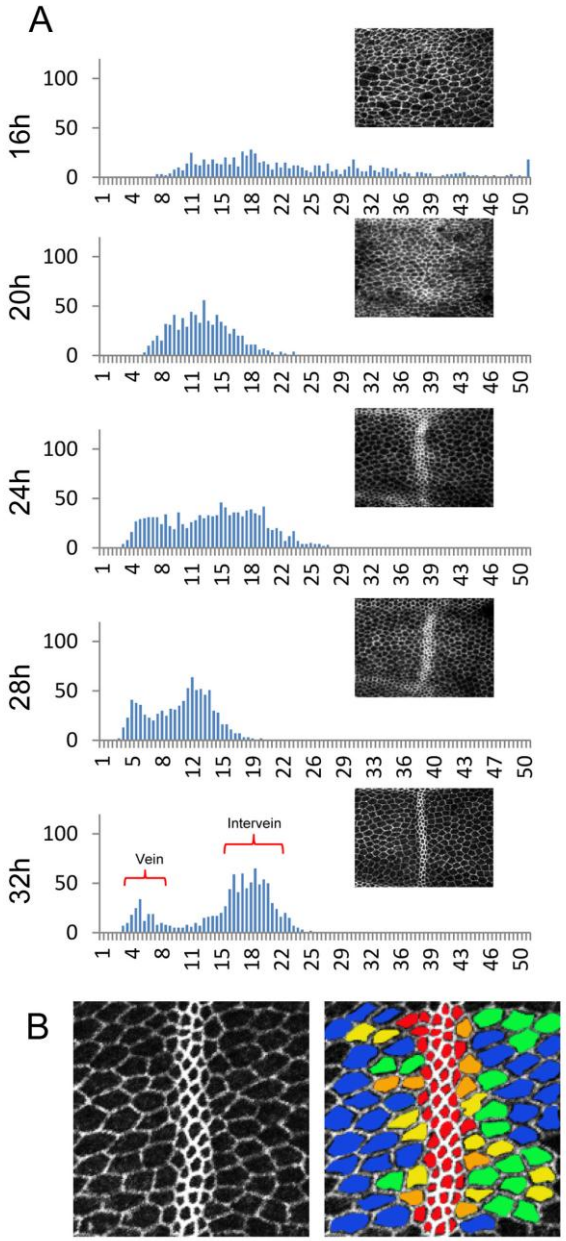

Figure 3.5. Apical area changes in the PCV. (A) Histograms derived from Cell Profiler measurements (3-4 wings and ~1000 cell measurements per time point) showing estimated apical cell areas in the PCV and surrounding intervein at 16, 20, 24, 28 and 32h APF. Y axis indicates number of cells in each area class. X axis indicates apical area, demarcated in 0.5μ^2 intervals. Images above graphs show representative wings for each time point. Red brackets indicate vein and intervein populations. (B) Apical vein sections of PCV at 32h APF with cells colour coded according to estimated apical cell area as follows: <9μm^2 = red; 9-11.5μm^2 = orange; 11.5-14μm^2 = yellow; 14-16.5μm^2 = green; >16.5μm^2 = blue.

A). In contrast to the longitudinal veins, cells in the middle of the crossvein are as small as those on the edges (red in Fig. 3.5 D). Indeed, cells of the PCV have the smallest apical areas of the wing (compare Fig. 3.5 A to Fig. 3.4 A). Crossveins thus follow a different differentiation pathway from longitudinal veins, culminating in distinct morphology both at the definitive stage and in the adult wing.

Taken together, these results show that apical constriction in the wing is not a uniform process: different patterns of constriction and relaxation result in the morphology of the central and flanking vein cells, and in distinctive morphologies of longitudinal veins and crossveins.

Further characterisation of intercellular gaps in the intervein

Given the distinct apical morphologies of vein and intervein cells, we next turned our attention to their three-dimensional (3D) morphology. We used FLP-out clones to label individual cells of the pupal wing with cytoplasmic GFP, and determined 3D shape with confocal microscopy (see Methods). In the period of refinement following reapposition, between 24 and 28h APF, intervein cells typically appear in pairs. This is consistent with the observation that the final mitosis of wing cells occurs later in intervein cells as compared to vein cells (Schubiger and Palka, 1987); most intervein cells had divided after the administration of the heat shock. When not in proximity to the veins or margin, intervein cells have a columnar morphology, with the central part of the cell narrower than the apical or basal surfaces (Fig. 3.7 A). This central narrowing leads to gaps between the lateral surfaces of adjacent cells (arrow in Fig. 3.7 A), which have been previously noted and give the wing a ‘spongy’ appearance after reapposition (Waddington, 1941).

To further analyse these intercellular gaps, we expressed GFP throughout the dorsal epithelium and analysed sections progressively from apical to basal. In apical sections GFP is continuous across the sheet (Fig. 3.6 A), but in sections 1.5µm basally the gaps appear as continuous stripes lacking GFP between multiple cells (Fig. 3.6 A’). These stripes are oriented along the proximal-distal axis of the wing (arrow in Fig. 3.6 A’) or, where in proximity to the veins, towards them (arrowhead in Fig. 3.6 A’). The nuclei appear more basally (Fig. 3.6 A’’), and at the basal surface GFP is seen continuously across the sheet (Fig. 3.6 A’’; Fig. 3.6 B).

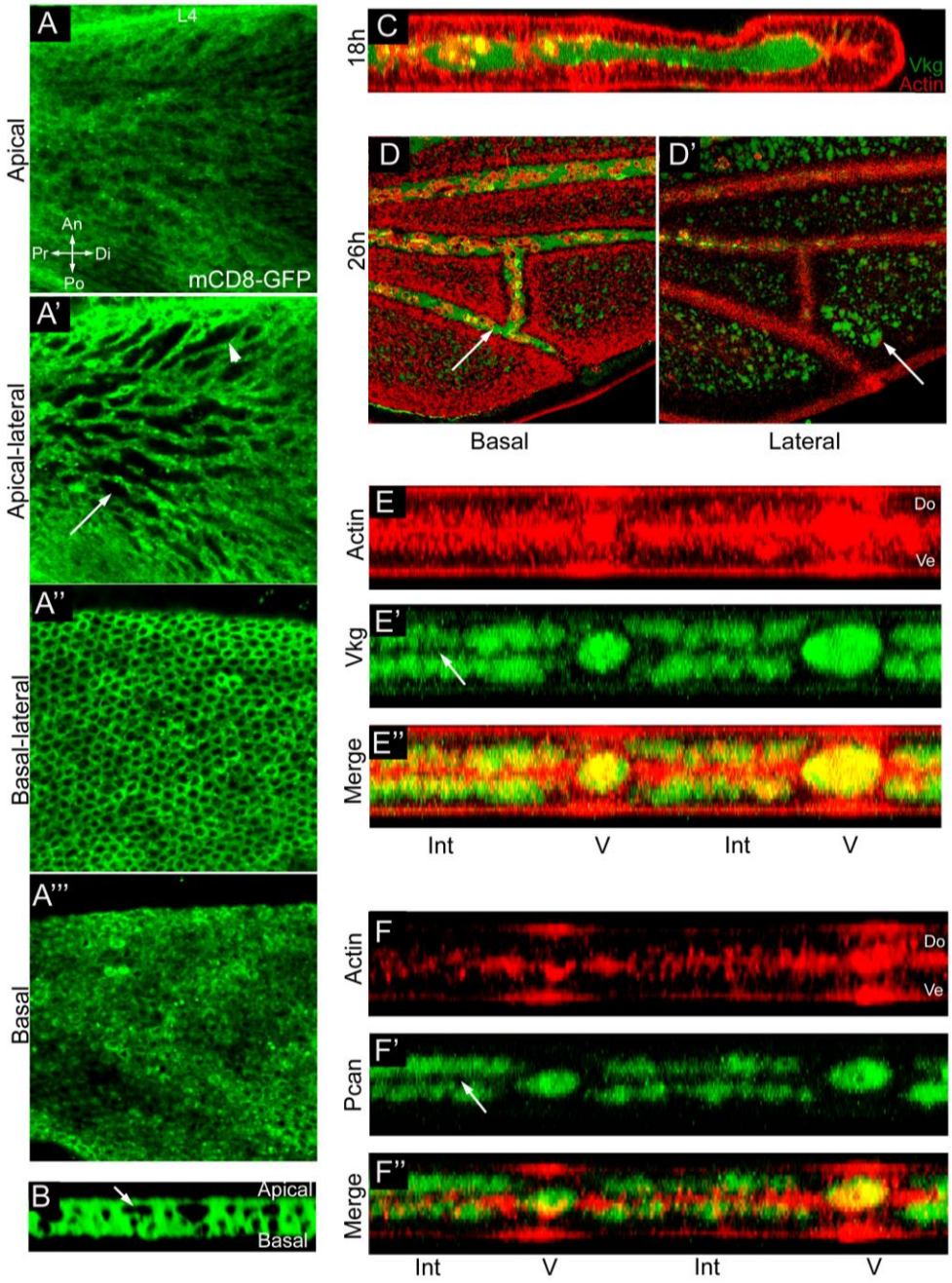

Figure 3.6. Gaps between the lateral surfaces of intervein cells and ECM distribution. (A-A'''). Single sections from apical to basal in the dorsal layer in *apGal4, TubGal80^{ts} >UAS-mCD8GFP,* raised at 18ºC and shifted to 29ºC at WPP stage and imaged at 32hAPF. Focussed on the L4-5 intervein region distal to the PCV. Arrow in A' shows the gaps appearing as stripes running proximal-distally. Arrowhead in A' shows stripes running towards L4. Gaps in A'' are nuclei. (B) Z section showing the lateral gaps (arrow). (C) Viking-GFP (green) in Z section of an 18h APF wing, stained with Phalloidin to detect Actin (red). Vkg-GFP fills the lumen between the layers. (D) Vkg-GFP in a 26h APF wing, basal section showing its localisation in the vein lumen (arrow), and absence from intervein apposition. (D') Lateral section, with Vkg-GFP seen in intervein sectors. (E-E'') Z section of 26h APF wing showing differential Vkg-GFP enrichment: in the lumen of veins, and in the lateral gaps between intervein cells. E' shows absence from regions of intervein basal apposition. (F-F'') Perlecan-GFP in the 26h pupal wing, arrow in F' shows lack of enrichment in intervein basal surfaces. Abbreviations: Int=Intervein, V=Vein, An=Anterior, Po=Posterior, Pr=Proximal, Di=Distal, Do=Dorsal, Ve=Ventral.

Previous reports have shown that after reapposition the ECM components Laminin and the Type IV Collagen Cg25C are enriched in these intercellular gaps, as well as being enriched in the lumen of the veins (Fristrom et al., 1993; Murray et al., 1995; Urbano et al., 2009). However, it is not known whether other ECM components display similar localisation. We utilised tagged ECM components from a GFP protein trap library (Morin et al., 2001), specifically the other Type IV Collagen in *Drosophila*, Viking (Yasothornsrikul et al., 1997), and the heparin sulphate proteoglycan Perlecan (Voigt et al., 2002). We find that both components show the same distribution as those previously described. Before apposition, Vkg-GFP fills the lumen between the dorsal and ventral layers and is not seen associated with the apical or lateral surfaces of the cells (Fig. 3.6 C). Once reapposition completes, Vkg-GFP is limited to two regions: the lumen of the veins (arrow in Fig. 3.6 D), and in the gaps between intervein cells as seen in lateral sections (Fig. 3.7 D'). These two localisations are highlighted in Z sections (Fig. 3.6 E-E''). Notably, Vkg-GFP is absent from the points of basal apposition between wing cells (arrow in Fig. 3.6 E'). Pcan-GFP shows same localisation as Vkg (Fig. 3.6 F-F''). Thus all ECM components so far tested display the same localisation in the pupal wing after reapposition: in the vein lumen, and between the lateral surfaces of intervein cells.

A composite of central and flanking vein cells creates the lumen

We next addressed the morphology of vein cells. We observe two types of vein cell that, given their relative positions in the developing vein, correspond to the central and flanking types that we have described above. Central vein cells take on the shape of an inverted "Y", with small apical surfaces that broaden along the anterior-posterior axis and then split into two fine projections that straddle the vein lumen (Fig. 3.7 C, C'). As a result, the basal surface of the cell forms an arch which forms the 'ceiling' of the lumen, and the tips of the projections make contact with cells in the other cell layer (Fig. 3.7 C''). Flanking cells do not straddle the lumen, and thus lie on one side of the vein. These cells assume a more uniform columnar shape (Fig. 3.7 D, D'), and the apical surface is shifted with respect to the basal surface, so that the cell appears to lean towards the vein midline. Compared to the thin projections sent by central vein cells, flanking cells make broader contacts with cells in the opposite layer (Fig. 3.7 D''), and thus contribute more to the lateral surface of the lumen than the thin projections of the central cells. This shows that the veins are composed of two distinct cell types, and that both of these subtypes make contact with the opposite layer. The lumen is formed by the combination of the two morphologies in either layer.

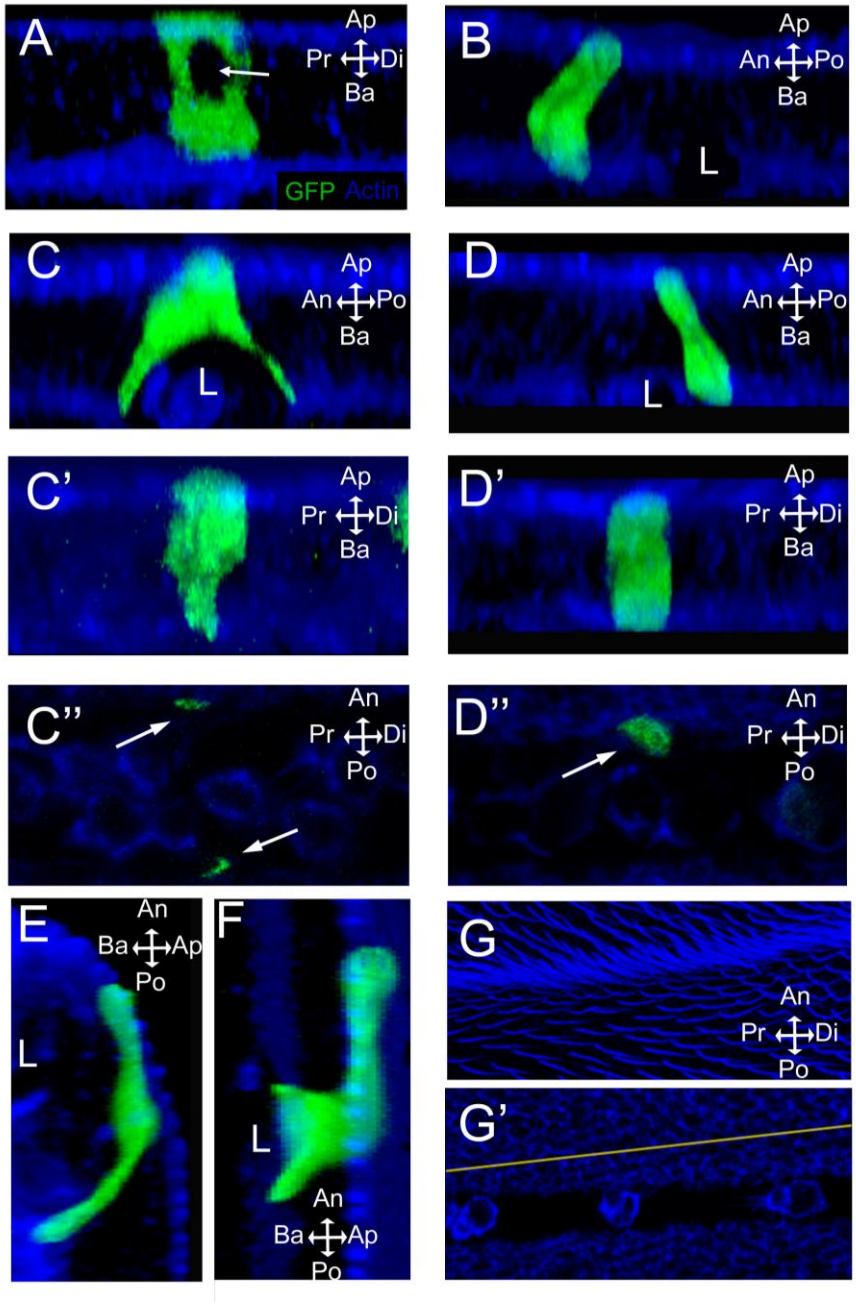

Figure 3.7. Cell morphology in three dimensions following reapposition. 3D reconstructions of single cells expressing cytoplasmic GFP (green) in wings stained with Phalloidin (blue). Vein cells are shown either 'vein-on' (looking down the lumen, anterior to the left), or 'side-on' (with proximal to the left). (A) Intervein pair showing gap between lateral surfaces of the cells (arrow). (B) Intervein pair near the vein (lumen marked with 'L') showing leaning morphology. (C) Central vein cell viewed vein-on, (C') viewed side-on, (C'') basal section showing the ends of the basal projections (arrows). (D) Flanking vein cell viewed vein-on, (D') viewed side-on (D''), basal section showing apposition on one side of the lumen (arrow). (E) Intervein cell adjacent to the anterior margin showing elongation in anterior direction. (F) L2 central vein cell showing the anterior shift of cell apex. (G) Apical section of L2 vein showing apical Actin enrichment in vein cells, (G') basal section showing lumen more posterior to the apical surface (apical position shown by yellow line overlay). Number of 3D reconstructions performed and analysed = 93. Abbreviations: Ap=apical, Ba=Basal, An=Anterior, Po=Posterior, Pr=Proximal, Di=Distal, L=Lumen.

Notably, despite the distinct apical morphologies of presumptive arched and flat surfaces of the vein (Fig. 3.3), central and flanking cells adopt the same 3D morphologies in the two layers. This implies that these two cell shapes must be arranged differently to produce a continuous lumen. Furthermore, the epithelium as a whole is flat, so the arched/flat morphology seen in the adult cuticle is not produced by cell shape changes in the period following apposition. Rather, they must arise later in development.

Apical and basal domains of the cell often do not align

As we have described above, the apical and basal surfaces of flanking vein cells are not in alignment, so that the cells appear to lean toward the vein. This morphology is also observed in intervein cells in close proximity to the veins, as their apical surfaces are displaced toward the vein (Fig. 3.7 B). This suggests that the force from the apical constriction of vein cells pulls the adjacent apices towards it, while apposition creates an 'anchor' that holds the basal portion of the cell in place. This effect is particularly striking in intervein cells near the anterior margin. Due to the fold in the epithelium at the margin, the apical surfaces of the cells are displaced anterior to the point of basal apposition, and as a result the cells elongate in this direction such that the majority of the cell body lies perpendicular to the apical-basal axis of the epithelium (Fig. 3.7 E). The margin also effects the morphology of nearby L2 vein cells, the apices of which are correspondingly shifted anteriorly (Fig. 3.7 F), such that the apical surface of the vein does not overlie the vein lumen (Fig. 3.7 G & G'). Similar effects are seen in cells in proximity to the posterior margin. Thus, apical-basal orientation of cells is not uniform across the wing blade, but influenced by proximity to veins, and to the margin.

In addition to the apical displacements seen in cells adjacent to the veins or margin, there is a wing-wide cell shape change that occurs as the wing reaches the definitive stage. Between 28 and 32h APF, the apical surfaces of all cells are displaced distally relative to the cell body. On a tissue level, this displacement is only apparent in the PCV (as it runs perpendicular to the axis of the shift), where the constricted apices are seen distal to the lumen (Fig. 3.8 A-A''). Single cell labelling reveals the cellular basis of the effect. The apical surfaces of central vein cells are shifted distally, and linked to the bulk of the cell by a slender cytoplasmic connection, creating remarkable cell shapes (Fig. 3.8 B-B', E). The apical surfaces of flanking vein cells, which are already displaced towards the vein (Fig. 3.8 C), now shift their apices distally (Fig. 3.8 C'). This shift is perpendicular to the initial angle and thus creates an 'r' shaped morphology when

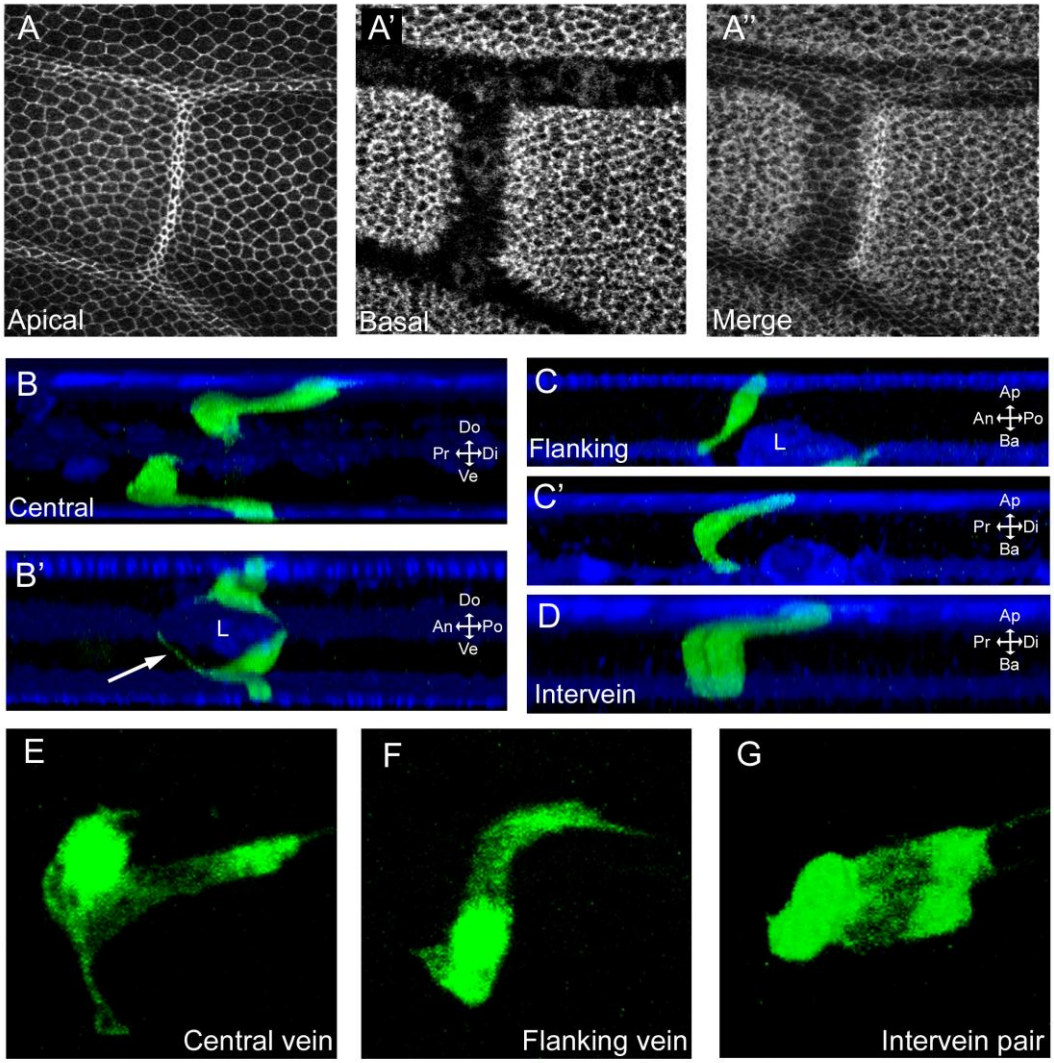

Figure 3.8. Distal shift of cell apices relative to the cell body. (A-A'') Cad-GFP in apical (A) or basal (A') sections of the PCV region in *Ubi-DECad-GFP/+* wings. (A'') Overlay of apical and basal showing the distal shift of the constricted apices relative to the lumen. (B-G) 3D reconstructions of single cells expressing cytoplasmic GFP (green) in 32h APF wings stained for Actin (blue). (B) Two central cells viewed side-on, showing distal shift of apical portions of the cells. (B') Same cells viewed vein-on, highlighting thinness of basal projections (arrow). (C) Flanking vein cell viewed vein-on, showing the leaning in towards centre of vein and basal apposition adjacent to lumen. (C') Same cell shown side-on, showing distal shift of cell apex. (D) Intervein pair shown side-on with similar distal shift. (E-G) Z stack projections of the three cell types viewed from above. Each cell terminates at its distal end with the trichome, secretion of which begins at around 28h APF. Number of 3D reconstructions performed and analysed = 88. Abbreviations: Ap=apical, Ba=Basal, An=Anterior, Po=Posterior, Pr=Proximal, Di=Distal, Do=Dorsal, Ve=Ventral.

viewed from above (Fig 3.8 F). Intervein cells also show distal displacements of the apical surface (pair shown in Fig. 3.8 D & G). This cell shape change is not an artefact of the fixing process, as it is also observed in unfixed wings. Furthermore, it is temporary: cells labelled some 6h later do not show it (see below).

Both the cause and function of this general displacement are unclear, but as it is seen in every cell, it must reflect a wing-wide process unrelated to the differentiation of a particular cell type. Additionally, whether it reflects a shift of the cell apices distally, or the cell bodies proximally, remains to be determined. Because it affects all cells in the wing, it could potentially arise from a force transmitted across the wing, providing a pulling force from either end of the wing. Indeed, it has recently been shown that forces from the contraction of the hinge region after reapposition promote cell elongation and rearrangement across the wing blade (Aigouy et al., 2010). A similar phenomenon may thus occur as the wing reaches the definitive stage.

Labelling the other constituent cell types of the wing

Single-cell labelling also revealed two of the cell types of the wing that are not part of the wing epithelium: neurons and trachea, both of which reside within the vein lumen. Thin axons of neurons snake through the lumen of L3 (Fig. 3.9 A) where they project from the dorsal sensilla (Murray et al., 1984). In Z section a thin axon is seen underneath the basal arching of the central vein cell, which itself is neighboured by a flanking cell (Fig. 3.9 B-B'). Labelling also revealed substantially larger tracheal cells (Fig. 3.9 C), which were also detected by labelling all trachea with *btl-Gal4>UAS-GFP*. Trachea enter the wing from the hinge via the base of the radial veins, and project through the lumen of L2-5 (Fig. 3.9 D). Not all wings showed the same pattern of tracheal projections, for example trachea are often restricted to L3. The thickness of the trachea and the presence of small filopodia like protrusions projecting laterally are seen under higher magnification (Fig. 3.9 E).

Co-operative cell shape changes create a convoluted cuticle

While the pupal wing at the definitive stage appears identical to the adult wing in pattern and proportion, the cellular morphology of the veins does not yet reflect the arched and flat morphologies observed in the adult cuticle. To determine when this final morphology arises,

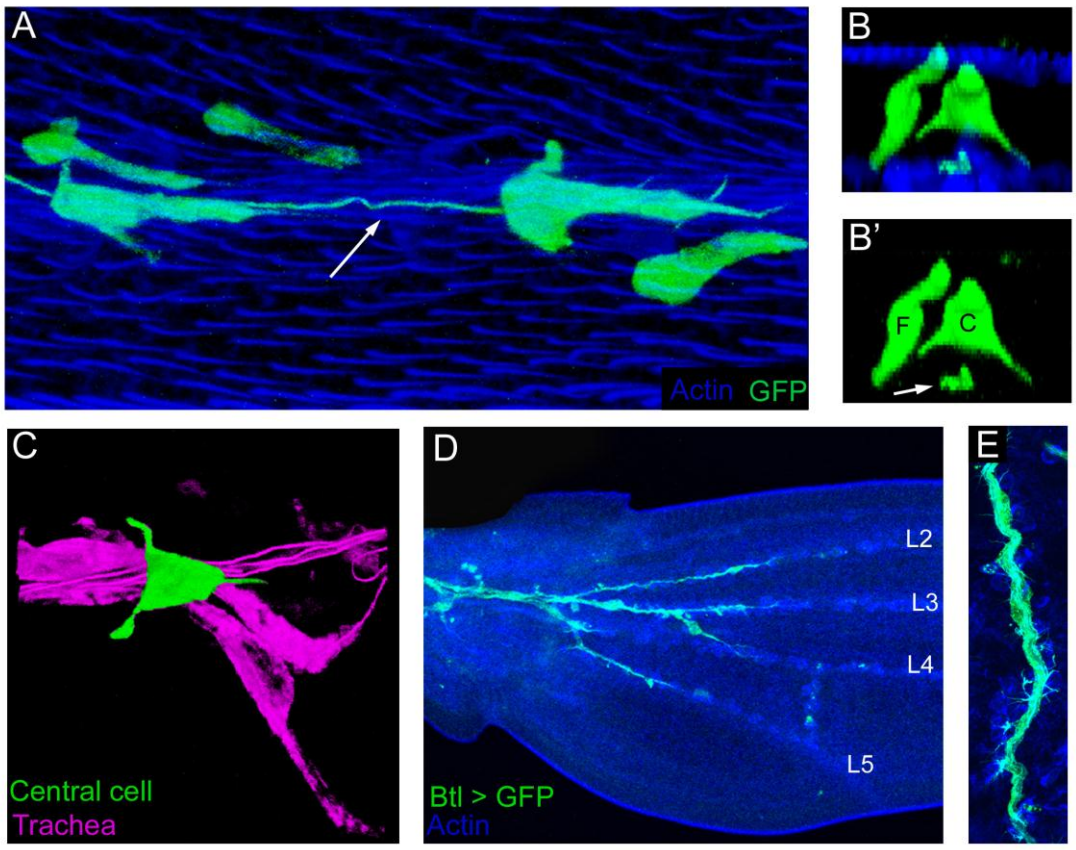

Figure 3.9. Additional cell types of the pupal wing. (A) Flanking and central vein cells in and around L3, showing the thin process of an axon within the vein lumen (arrow). (B-B') Z section showing central ('C') and flanking ('F') cell types, and the thinness of the axon process within the lumen (arrow). (C) Central vein cell (green) in proximal L3, arching over the lumen in which are seen trachea (false coloured pink). (D) Wing of *btl-Gal4 > UAS-GFP* at 26h APF stained for Actin (blue), showing trachea entering the wing from the hinge and extending along the lumen of L2-5. (E) Close up of proximal tracheal section, showing thin lateral extensions (arrow).

we investigated cell shape after the definitive stage. The second expansion of the wing is driven by cell flattening, and leads to folding of the epithelium within the confines of the pupal cuticle (Fristrom et al., 1993). The pattern of folding is invariant between wings, and the veins are situated at the peaks of the folds that form along the proximal-distal axis (Rob Ray, pers. comm.). This folding occurs with respect to the future arched/flat articulation of the adult wing veins, with the arched surfaces lying at the peaks of the folds and the flat surfaces lying in the troughs. Thus, the cellular distinction between the arched and flat surfaces that is evident at the definitive stage may play a role in directing the folding of the epithelium in the second expansion phase.

The morphology of the vein cuticle at this stage is striking. The veins appear as broad bands of alternating ridges and grooves that run perpendicular to the proximal-distal axis of the vein (Fig. 3.10 A). As a result, the cuticle is convoluted along this axis (Fig. 3.10 A'). This structure is determined by the shapes of the vein cells that secrete it. In apical sections, single vein cells are split into a central portion and proximal and distal arms (Fig. 3.10 B, C), while in more basal sections they spread out to form irregularly defined shapes (Fig. 3.10 B', C'). Two indentations in their apical surfaces separate the main bulk of the cell, which underlies one cuticle ridge, from thin proximal and distal arms, which extend to underlie the two adjacent ridges. As a result, the cells adopt a 'w' shape when viewed from the side (Fig. 3.10 B'', D), with each of the indentations forming part of one of the cuticular grooves. Each of the grooves will form from the coordinated morphogenesis of a group of central and flanking vein cells such that it runs across the width of the vein.

In addition to the apical remodelling, the basal morphology of vein cells also changes at this stage. Whereas in earlier stages, the arching of the central cell delineates the top of the lumen, central cells in the folded wing assume a relatively flat basal surface (Fig. 3.10 B'''). Flanking cells are also flat basally, and produce sheet-like projections from the basal surface that extend towards the centre of the vein, and which will underlie the adjacent central cells (arrows in Fig. 3.10 C', D'). Thus, the elaborate cellular architecture that formed the lumen after apposition is a transient structure that is lost when the wing undergoes expansion and folding.

The intervein cuticle at this stage appears as a field of interdigitated, stellate plates in apical sections (Fig. 3.10 A, E), which are formed by apical cytoplasmic projections called hair pedestals (Mitchell et al., 1983; Fig. 3.10 E'). The apical remodelling that gives rise to these projections results in a highly folded cuticle, just as vein cell remodelling creates a convoluted cuticle. Interestingly, single cell labelling reveals that each cell does not contribute exclusively

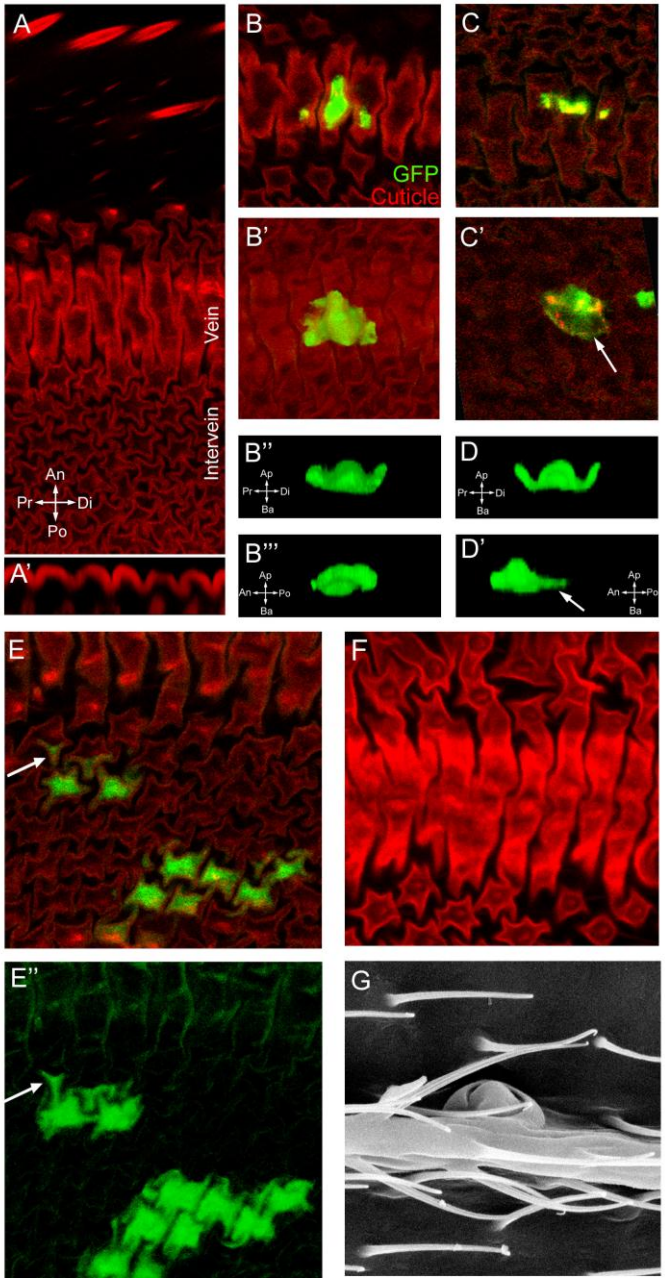

Figure 3.10. Cell and cuticle morphology in the folded wing. (A-F) GFP-expressing clones in wings between 60-76h APF, showing cytoplasmic GFP (green) and cuticle autofluorescence (red). (A) Cuticle autofluorescence of vein and intervein regions showing distinct cuticular subtypes as labelled. (B-B''') Central vein cell: apical section (B), basal section (B'), side-on (B''), showing proximal and distal arms, vein-on (B'''), showing the loss of basal arching. (C-C') Flanking vein cell: apical section (C), basal section (C'), showing sheet-like projection (arrow). (D-D') Flanking cell: side-on (D), showing proximal and distal arms, vein-on (D'), showing the sheet-like projection posteriorly towards centre of vein. (E) Intervein cells in apical section, (E') basal section, arrows show projections into neighbouring protrusions. (F) Cuticle autofluorescence in wings from a newly eclosed adult prior to expansion, showing the L3 vein grooves and intervein pedestals. (G) SEM image of newly eclosed adult L3 immediately after expansion, also showing sensillum (image courtesy of Rob Ray). Compass abbreviations: An=Anterior, Po=Posterior, Pr=Proximal, Di=Distal, Ap=Apical, Ba=Basal.

to a single hair pedestal: labelled cells often send thin projections in to neighbouring pedestals (arrows in Fig. 3.10 E, E'). Thus, each individual pedestal, which forms a single cuticle plate, can be comprised of more than one cell.

Vein articulation arises during wing maturation

While the morphology of vein and intervein cells during the second expansion reflects another major morphogenetic transition, the grooves produced by vein cells during this stage once again do not reflect the final vein morphology seen in the adult wing. Indeed, when the wings of newly eclosed flies are analysed, the morphology of the cuticle is the same as it was at the end of the second expansion (Fig. 3.10 F). It is only immediately after the wing has flattened that the arched/flat morphology is seen (Fig. 3.10 G). Thus, vein articulation is not achieved by vein cells adopting an arched or a flat morphology, but rather by the behaviour of the cuticle as it is expanded by the influx of hemolymph during wing maturation. The eventual articulation thus results from the broader expanse of cuticle produced by the arched surface, which is presumably a result of the greater number of cells recruited into this surface of the vein earlier in development (Fig. 3.4).

IV. Summary

The insect wing is a simple appendage composed of a thin bilayer of adhered cuticle and the veins that channel through it, and its development involves an intricate series of morphogenetic events in the epithelium which secretes the cuticle. This work has documented the cell shape changes that occur within the developing epithelium following pupal reapposition. Apical constriction, the formation of basal arches, the distal displacement of cellular apices and the formation of grooves all highlight the plasticity of wing cells to adopt different morphologies while remaining a coherent epithelial sheet. The co-ordination of morphological changes across cell types creates the architecture of the veins, both in the formation of a lumen after apposition, and in the secretion of the adult cuticle by cells of the folded wing.

Vein cell differentiation involves apical constriction, a process which begins following pupal reapposition. In numerous developmental contexts, apical constriction accompanies the formation of invaginations in the tissue (Sawyer et al., 2010). However, in certain experimental conditions, invagination occurs in the absence of constriction (Llimargas and Casanova, 2010), and in vivo, apical constriction in the *Drosophila* eye is not accompanied by an invagination but rather an indentation, the morphogenetic furrow (Cagan, 2009). In the wing, constriction is accompanied neither by invaginations nor indentations, and the epithelium remains flat. Other cellular mechanisms, not active in the pupal wing, are thus required for these tissue level changes. Commonly, alterations to the apical-basal length of constricting cells accompany invaginations (Lee and Harland, 2007; Sherrard et al., 2010), and we have demonstrated that both vein and intervein cells span the apical-basal axis of the epithelium; the absence of changes to apical-basal length in constricting vein cells may thus be a contributory factor. The wing is a developmental system in which apical constriction is not associated with the formation of invaginations or ingressions, and thus presents an in vivo model in which constriction and invagination are uncoupled. In particular, identifying the mechanisms which counteract invagination in the wing will contribute to our understanding of the cellular basis of this fundamental process.

Apical constriction does however influence the morphology of nearby cells within the epithelium: we have shown that the apices of adjacent intervein cells are drawn toward the vein. This is consistent with the force generated by apical constriction being transmitted to

neighbouring cells via the AJs, and as a result drawing nearby cells toward the source of the force. As the basal surfaces of the cells are attached to the apposing surface via Integrin-based focal adhesions, they are 'locked in', and the displacement is only seen in the apical surface. This gives rise to the 'leaning' morphology that we observe in our single cell analysis. According to this model, apposition provides a basal anchor for cells in the epithelium, while the apical portions of the cells are much more plastic. These examples also show how wing development involves changes to cell morphology that are both active (apical constriction) and passive (leaning).

What controls apical constriction in vein cells? Both the BMP and EGFR pathways are required for vein development (Sotillos and de Celis, 2005), and loss of EGFR signalling has been shown to lead to the loss of vein constriction (O'Keefe et al., 2007), but the targets of these pathways that mediate constriction are not known. Constriction is instigated by apical contractions of Actin driven by Myo-II in numerous other systems (Sawyer et al., 2010), so the Actin cytoskeleton is a probable target. Indeed, pupal vein cells show apical enrichment of Actin (Fristrom et al., 1994). In Chapter 6, we address how signalling pathway activation might lead to cytoskeleton-based shape changes.

While we have shown that all vein cells undergo apical constriction, the constriction is not uniformly maintained, giving rise to larger central cells and constricted flanking cells. Thus two cell morphologies arise from different cell behaviours after an initially shared constriction. Distinct morphologies are also seen in 3D, with central cells forming basal arches and flanking cells leaning in towards the vein midline. This subdivision of vein cell types is surprising considering there is no indication of a distinction of the two cell types at the level of gene expression (Sotillos and de Celis, 2005; Blair, 2007). Potential mechanisms for the control of this phenomenon are investigated in the Discussion.

Single cell labelling has allowed us to determine the cellular architecture that creates the vein lumen (Fig. 3.11). The vault of one side of the lumen is created from a mosaic of the basolateral surfaces of the two cell types, with the top formed by central cells and lateral surfaces formed by a combination of flanking cells and thin central cell projections. This structure is adopted symmetrically in the opposing layer, and the basal connections between vein cells link the vault of one surface of the vein to vault of the other surface, creating the circular cross-section of the lumen. The continuity of the lumen between the dorsal and ventral layers is thus ensured by the formation of basal contacts between vein cells, and not for example by the basal surfaces of vein cells being less adhesive, as had been hypothesised

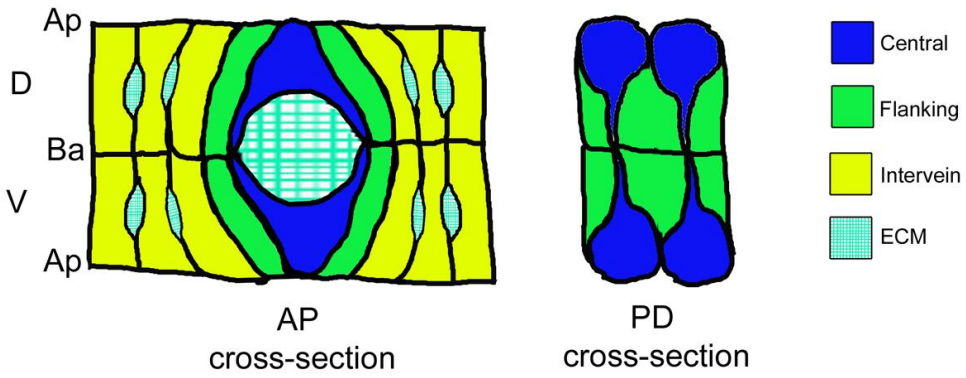

Figure 3.11. Cellular constitution of the veins. Diagram showing the constitution of the veins as revealed by single cell labelling. Cell types labelled as shown in key. Left: cross section is taken across the vein, viewed vein-on. Right, cross-section is taken along the vein midline, and cells viewed from the lumen. Ap=Apical, Ba=Basal, D=Dorsal, V=Ventral, AP=Anterior-posterior, PD=Proximal-distal

(Hogan and Kolodziej, 2002). The contact made between vein cells has implications for the signalling between dorsal and ventral layers that appears to be involved in vein development (Milan et al., 1997; see Chapter 5). Signalling based on cell-cell contact is increasingly seen to play an important role in development (Rorth, 2003; Roy et al., 2011), and the basal connections between vein cells raises the possibility that they could serve as signalling centres.

The final stage of pupal wing development involves an expansion of surface area driven by cell flattening, and the apical secretion of the adult cuticle. The apical surfaces of wing cells are remodelled at this stage: single-cell labelling reveals that vein cells adopt 'w' shapes that collectively form the series of parallel grooves that gives rise to the convoluted cuticle. Intervein cells form apical pedestals, and we have shown that each cell can contribute to more than one cuticular pedestal. In both vein and intervein, cuticular structures are formed from multiple cells acting in a co-ordinated fashion. Similarly, earlier in development the vein lumen is formed by an arrangement of different vein cell types connected between both layers. Higher order structures are formed by co-ordinated cell shape changes. An intriguing and open ended question is how these changes are co-ordinated between cells.

The veins of the adult wing blade are composed of an arched surface and a flat surface. Our studies show that this morphology is not achieved until after the expansion of the adult wing, as newly eclosed wings show the same ridged vein pattern seen in previous stages. How then is the articulation achieved? We have shown that the definitive stage veins are generally broader on their presumptive arched surface, and that this results from more cells being incorporated into the developing vein. This would lead to a greater area of cuticle being secreted from the presumptive arched surface. As the bonding of the cuticle is restricted to intervein regions, the vein surface with the greater area will, under the pressure of the influx of hemolymph, arch outwards. Cuticle hardening during wing maturation would then ensure that the structure persisted. According to this model, the final articulation of the adult longitudinal veins is dependent on the relative area of cuticle secreted by the veins earlier in development, and the arching itself is a passive response to hemolymph pressure during wing expansion.

Chapter 4

Investigating cell competence in the pupal wing

I. Chapter Overview

Intercellular signalling is a means by which cells can both co-ordinate their actions with other cells and indeed induce actions in others, allowing for the harmonisation of behaviours like shape changes across tissues. Three highly conserved signalling pathways are involved in the specification of vein/intervein fates in the wing: BMP, EGFR and Notch. Interactions between these pathways are essential to produce the wild type venation pattern. In this Chapter, we use temporally controlled mis-expression to address how cells respond to increases or decreases in signalling pathway activity during pupal development. We define the period during which cells are most sensitive to fate inducing signals, and the point after which cell fate is determined. These results allow us to place signalling events and the cell fate choices they control within the timeline of cellular and tissue morphogenesis.

II. Introduction

Cell competence to intercellular signalling in the pupal period

Development involves the progressive restriction of a cell's potential to give rise to multiple differentiated subtypes. As described in Chapter 3, the two primary cell subtypes in the *Drosophila* wing epithelium, vein and intervein, follow a distinct programme of cellular morphogenesis leading up to cuticle secretion. This differentiation is preceded by the patterning of the wing disc into vein and intervein domains, by a signalling network which is maintained and elaborated in the pupal wing (see Fig. 1.5).

Previously, the consequences of interfering with the BMP (Yu et al., 1996), EGFR (Guichard et al., 1999), or Notch (Shellenbarger and Mohler, 1978; Huppert et al., 1997) pathways specifically in pupal development have been addressed. These studies utilised either the heat shock (hsp70) promoter to induce brief pulses of expression of pathway components, or temperature sensitive alleles of receptors which were shifted to the restrictive period at defined points during pupal development. Interfering with signalling specifically in pupal development resulted in ectopic venation (BMP or EGFR activation, Notch inhibition) or vein loss (BMP or EGFR inhibition, Notch activation). These studies showed that although specification occurs in the disc, cells in the early pupal wing are still competent to respond to these pathways and to follow the alternative developmental program. Although the conditions of the experiments differed between reports, they revealed overlapping phenocritical periods for the three signalling pathways. The production of ectopic veins or vein loss was restricted to approximately the first 32h of pupal development, which corresponds to the period between disc eversion and the definitive stage (see Table 4.1). Cells were not competent to respond to ectopic signalling after that point, suggesting that cell fate was determined.

There are however certain limitations with the above studies. For example, heat shock mediated mis-expression must be limited to brief periods due to the lethality that results from prolonged time at the restrictive temperature (37ºC). Brief periods of mis-expression might not induce a response if cellular sensitivity to the signal is reduced, but not lost. Furthermore, in the case of the BMP pathway (on which a large part of the current work is focussed), only extracellular components of the pathway have been tested (Dpp and Sog; Yu et al., 1996). The failure of these extracellular molecules to affect cell identity may arise if changes to the extracellular environment preclude ligand-receptor interactions. If so, cells in later stages may

still be competent to respond to pathway activation. The use of cell autonomous pathway activators would address this issue. Finally, the fact that studies were carried out in numerous different conditions means it is difficult to compare phenocritical periods of the difficult experiments, especially when we consider the variation in timing of developmental stages reported between laboratories. On the basis of these issues, we tested the competence of cells to vein-promoting and vein-inhibiting signals through pupal development, using the same method to target each of the three pathways.

Using the Gal4/Gal80^{ts} system to investigate competence

In this Chapter the Gal4/Gal80^{ts} system is used to investigate the competence of cells in the developing pupal wing to ectopic signalling. The Gal4/UAS system allows for tissue specific expression of target genes (Brand and Perrimon, 1993), helping to define the role of a gene in defining cellular identity (Phelps and Brand, 1998). The addition of Gal80^{ts} to this setting allows for the activity of Gal4 to be temporally regulated by temperature (McGuire et al., 2003). At the permissive temperature (18ºC), Gal80^{ts} is functional and binds to Gal4, preventing its interaction with UAS sequences. At the restrictive temperature (29ºC), Gal80^{ts} is inactivated, thus relieving Gal4 inhibition. Gal4 is then able to bind UAS sequences, leading to gene expression. The expression of Gal4 itself is temperature sensitive (Duffy, 2002), so this system provides controlled induction of high levels of target gene expression, and the use of different Gal4 driver lines offers spatial, as well as temporal, control. In this Chapter, we use the Gal4Gal80^{ts} system to test the responses of cells at given points in pupal development to ectopic pathway activation, thus uncovering when cells are most sensitive to signalling, and when the competence to respond the signals is lost.

Using Gal4/Gal80^{ts}, mRNA of the target gene can be detected as soon as 30m after shifting to the restrictive temperature, and after 6h mRNA levels are comparable to that of flies lacking Gal80^{ts} (McGuire et al., 2003). To determine if such rapid induction occurs in the pupal wing, we investigated the expression of a GFP-tagged version of the BMP ligand Gbb (Gbb-GFP) in a time course experiment. GFP is not detected when animals are kept at 18ºC, but patchy low-level GFP expression is observed within 2h of the shift to 29ºC (Fig. 4.1). Within 4h of the shift, Gbb-GFP is detected at higher levels, particularly in the margin and the veins, and after 6h expression is seen across the wing (Fig. 4.1 A).

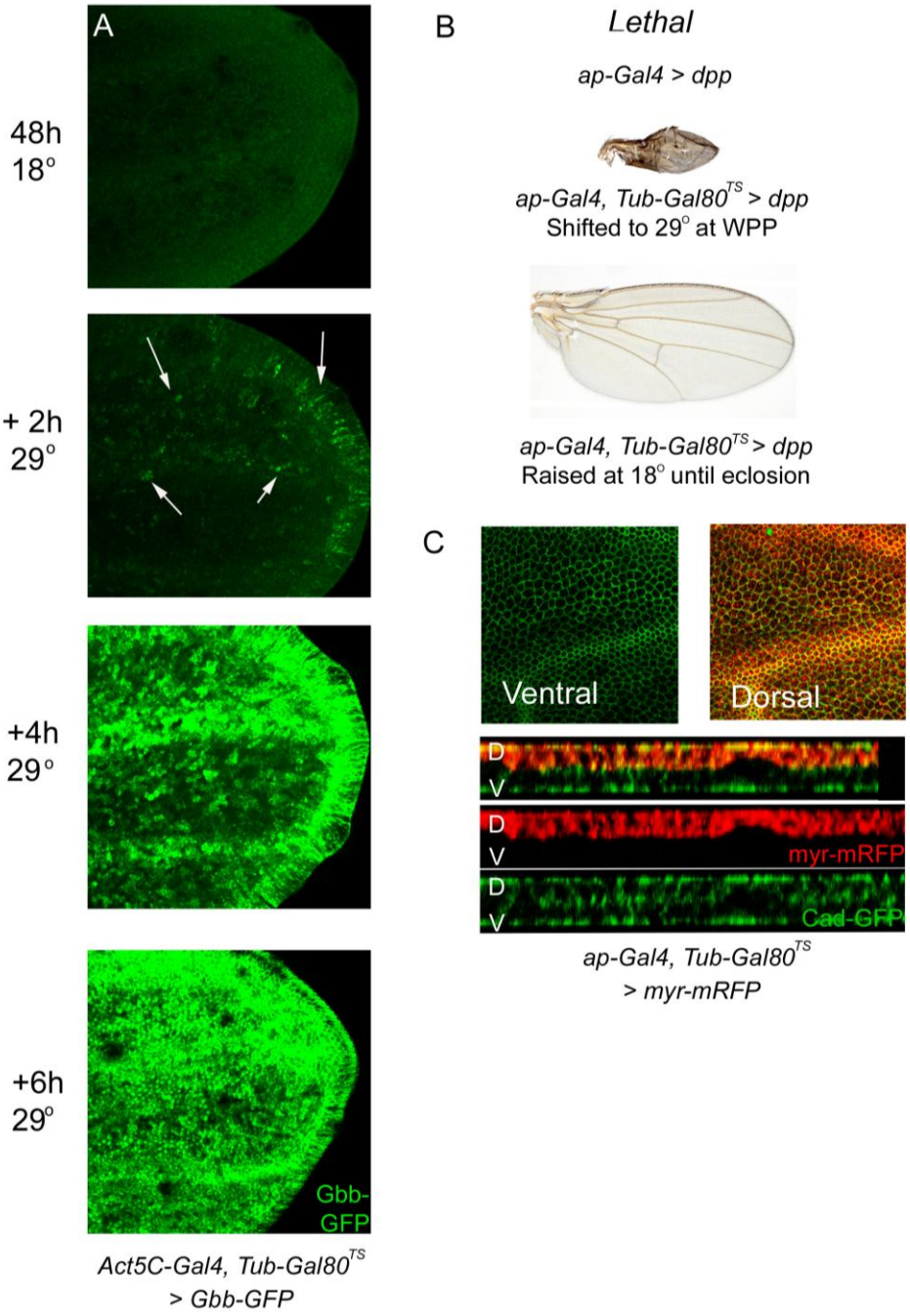

Figure 4.1. The Gal4/Gal80ts system. (A) Time course of wings from animals of the genotype *Act5C-Gal4, TubGal80^{ts} > UAS-Gbb-GFP* raised at 18ºC until 48hAPF. Top panel shows control raised at 18ºC, with a background level of signal from the wing tissue. Lower panels shows progressive emergence of GFP in wings 2h, 4h and 6h after shift to 29ºC (wings come from different animals). GFP is widespread by 4h after shift. (B) Top: *ap-Gal4 > UAS-dpp* is lethal at 25ºC. Middle: *ap-Gal4, TubGal80^{ts} > UAS dpp* animals were raised at 18ºC until the WPP stage, and shifted to 29ºC until eclosion. Eclosers show severely affected wings. Bottom: flies of the same genotype raised at 18ºC until eclosion show wild type wings. (C) Dorsal specificity of *ap-Gal4, Tub-Gal80^{ts}*. Animals of the genotype *ap-Gal4 / Ubi-DECad-GFP, UAS-myr-mRFP ; TubGal80^{ts}/ +* were raised at 18ºC until the WPP phase, shifted to 29ºC, and wings dissected 26h APF. Top panels show absence of the marker in the ventral apical surface. Lower panels show Z sections, in which the marker is exclusively confined to the dorsal epithelium.

To show that Gal80^{ts} effectively silences Gal4-mediated gene expression in the wing, we tested the effects of overexpressing the BMP ligand Dpp with the dorsal *ap-Gal4* driver. Without Gal80^{ts}, dorsal expression of Dpp is lethal. In contrast, with Gal80^{ts} there is no lethality when animals are raised at 18ºC (n=112 adults). Furthermore, adults displayed phenotypically normal wings (Fig. 4.1 B). This contrasts to the wings of animals which are shifted to the restrictive temperature at the beginning of pupal development, which are severely affected (Fig. 4.1 B, and see below). Thus Gal4/Gal80^{ts} allows for functional silencing at 18ºC and rapid induction of target gene expression after shifting up to 29ºC. When shifting back down to 18ºC, Gal80^{ts} is once again functional, and binds to and inhibits Gal4, halting ectopic expression. However, silencing of Gal4 activity is complicated by the perdurance of protein expressed during the period at the restrictive temperature. GFP protein perdurance has been shown to extend up to 12h after the shift down to 18ºC (McGuire et al., 2003), and as RNA and protein stability will vary between constructs, the degree of perdurance will vary between experiments. Thus, although shifting down stops de novo expression, residual protein can still function.

Experimental overview

To address cell competence to pathway activation using the Gal4/Gal80^{ts} system, gene expression is induced at specific points in pupal development, and the phenotypic consequences are observed in the adult wing. In these experiments we use the adult wing as a readout for events that happen at the cellular level, reasoning that induction of vein or intervein fate will result in the secretion of distinctive vein or intervein cuticle. Different UAS constructs are used allowing for multiple steps in the signalling pathways to be tested, and the effects of pathway activation are compared to those of pathway inhibition.

Two experimental conditions were employed. Firstly, we used *ap-Gal4, TubGal80^{ts}* to drive mis-expression of target genes in the dorsal layer of the pupal wing (Fig. 4.1 C). We tested the response to dorsal mis-expression at defined intervals during pupal development, by raising animals at 18ºC and shifting staged pupae to 29ºC until eclosion (Fig. 4.2, see Materials and Methods). This allows for assessment of the cumulative effect of mis-expression when induced at increasingly later time points, and reveals when cells no longer respond to the signal. Expression of *ap-Gal4* in later pupal stages is confirmed by the high levels of GFP seen in *ap-Gal4 > UAS-GFP* late stage pupae. In the second experimental condition, we used *Act-5C-Gal4*,

TubGal80^{ts} to drive ubiquitous gene expression (Fig. 4.1 A). In this condition, restricted periods of ubiquitous expression are induced by shifting staged pupae to 29ºC for 8hr, and then shifting back down to 18ºC for the rest of development (Fig. 4.2). This reveals the period during which cells are most sensitive to pathway activation or inhibition, and also avoids potential problems of cumulative phenotypes resulting from continued expression. As discussed above, the perdurance of protein from the 8hr period at 29ºC means that whilst expression is halted after the shift down, residual signalling may occur for a period afterwards.

While the first experimental condition defines when cells are no longer competent to vein-promoting or vein-inhibiting signalling, the second determines when cells are most sensitive to this signalling (i.e. the phenocritical period) (Fig. 4.2). In these experiments, animals are classified based on the time at 18ºC when they were shifted up (as hours after puparium formation (APF)). Because development at 18ºC takes twice as long as that at 25ºC (Bainbridge and Bownes, 1981), this timing can be equated to developmental stage by calibrating to the sequence of development at 25ºC (Table 4.1). Due to the rapid induction of target gene expression (Fig. 4.1 A), we expect only a short delay between shifting up and ectopic signalling.

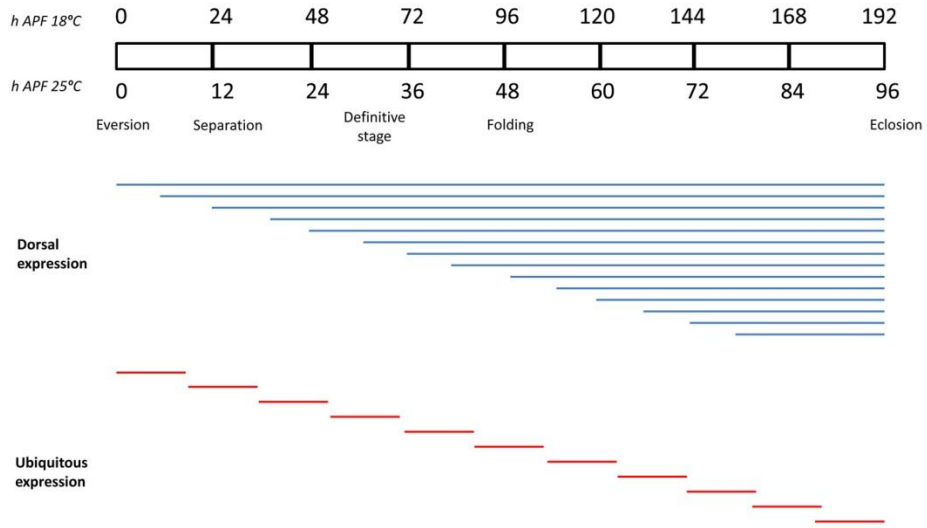

Figure 4.2. Two Gal4/Gal80^{ts} experimental conditions. Top shows timeline of pupal development, with hours at 18ºC shown above bar, hours at 25ºC shown below bar, and key stages in wing development shown below timeline. Lines show time spent at 29ºC. Blue lines show the dorsal expression experiment, in which *ap-Gal4, Tub-Gal80^{ts} > UAS-X* are raised at 18ºC until the WPP stage, aged for defined periods and shifted to 29ºC until eclosion. Expression is induced progressively later in development to define the time at which cells do not respond to the signal. Red lines show the restricted ubiquitous expression experiment, in which *Act5C-Gal4, Tub-Gal80^{ts} > UAS-X* are raised at 18ºC until the WPP stage, aged for defined periods and shifted to 29ºC for 8hr periods before shifting down to 18ºC again. This reveals the phenocritical period of ectopic expression.

	Stage	Hours after WPP formation, 25°C	Hours after WPP formation, 18°C
Prepupal	*Eversion*	0	0
	Apposition	4	8
	Expansion	6	12
Pupal	*Separation*	12	24
	Reapposition	18	36
	Refinement	24	48
	Definitive Stage	32	64
	Expansion and folding	36	72

Table 4.1. Developmental stages of pupal wing development at 25°C and 18°C. Hours indicate when stage begins.

III. Results

BMP ligands induce ectopic veins and blisters in early pupal development

We first assessed the response of cells to expression of the two BMP ligands involved in postembryonic development, Dpp and Gbb. Dorsal expression of *dpp* from the white prepupal stage (WPP) until eclosion results in lethality, with >90% of progeny failing to eclose from pupal cases (see Table A3 in the Appendix). The wings of escapers were dark, small and crumpled (Fig. 4.3 A). When newly eclosed, the wings are inflated and filled with fluid, which indicates that crumpling of the cuticle arises after the loss of this fluid from the wing. These phenotypes are similar to those observed when expressing *dpp* throughout wing development with other drivers (Haerry et al., 1998). When animals were shifted up at the separation stage (26, 28 and 32h APF), lethality was still high (Table A.3), and wings showed a similar phenotype (Fig. 4.3 B-D). When shifted at the reapposition stage (40, 46 and 48h APF) wings show a more moderate phenotype (Fig. 4.3 E-G). Wings are blistered and veins are broader than in wild type (e.g. Fig. 4.3 G), and the phenotype gets less severe with the later shifts. When animals were shifted at the refinement stage (52h APF) the wing appears relatively normal, with veins only slightly less refined as compared to wild type (Fig. 4.3 H). Animals shifted later than this point show a wild type venation pattern (Fig. 4.2 I, J). These results show that expression of *dpp* in the dorsal epithelium in the pupal wing induces ectopic venation and blistering, which are presumably correlated with the expansion of vein territories in the pupal wing epithelium (see Chapter 5). Importantly, these phenotypes are only observed when induced prior to the refinement stage, indicating that the competence of cells to ectopic Dpp is lost after this stage.

Considering the severe phenotypes and lethality resulting from the early stage shifts, we limited dorsal expression of *dpp* to restricted periods by shifting animals down to 18ºC after 12-20h at 29ºC. Animals shifted at the separation stage (24 and 28h APF) showed complete blistering of the surfaces (Fig. 4.4 A, B), whereas in animals shifted around the time of reapposition (32 and 36h APF), blistering was restricted to the centre of the wing overlying the PCV (Fig. 4.4 C, D). Animals shifted following reapposition (40h APF) did not show wing blisters, although the veins were broader (Fig. 4.4 E). Thus, blistering resulting from dorsal mis-expression of *dpp* is progressively restricted to the centre of the wing when expression is induced at later time points.

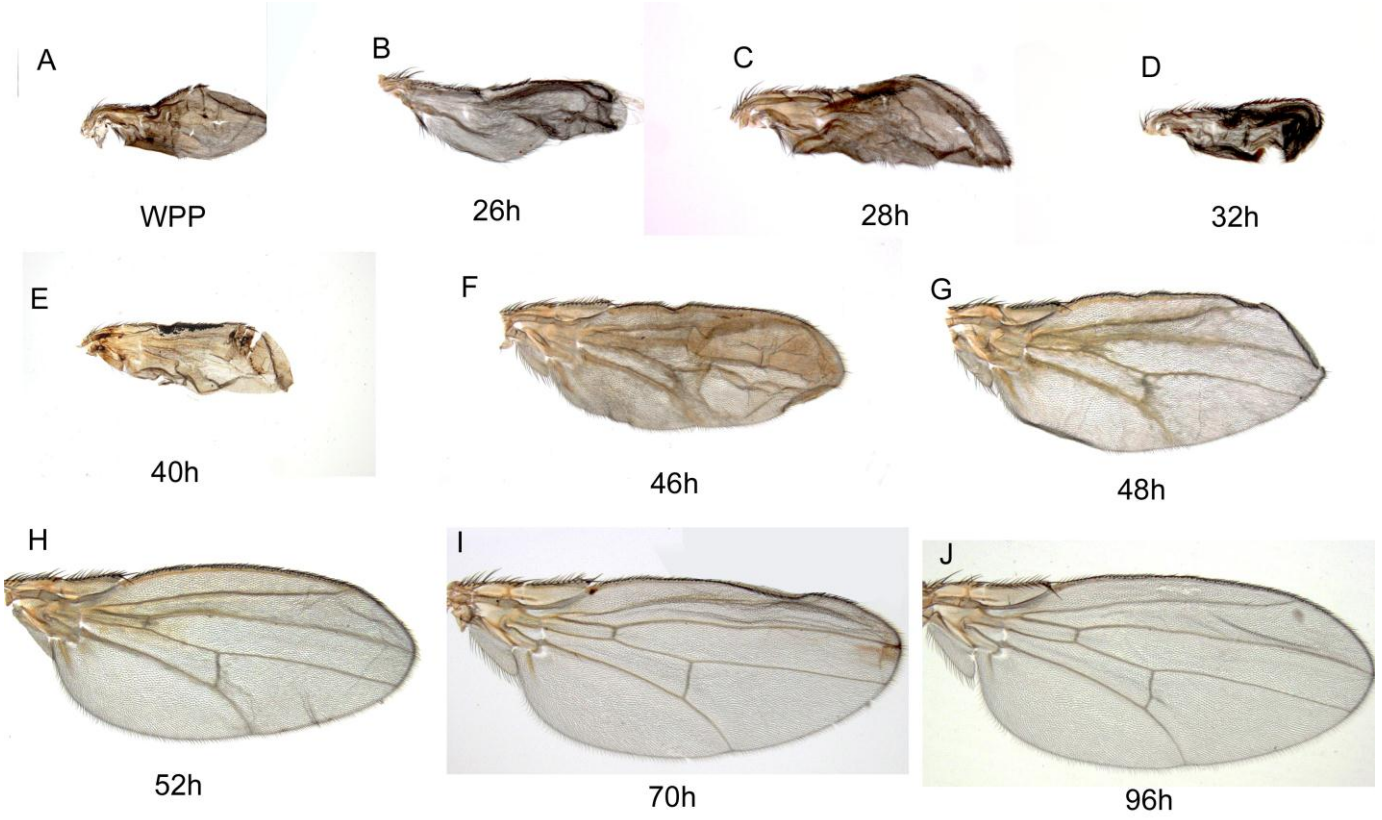

Figure 4.3. Dorsal expression of *dpp* induced progressively through pupal development. (A-J) *ap-Gal4, TubGal80^{ts} > UAS dpp* animals were raised at 18ºC until the WPP stage, then shifted to 29ºC at the hours indicated below the images until eclosion. As with all subsequent figures, typical wings from adult eclosers of each time-point are shown. As males showed same phenotypes as females, both male and female wings are shown.

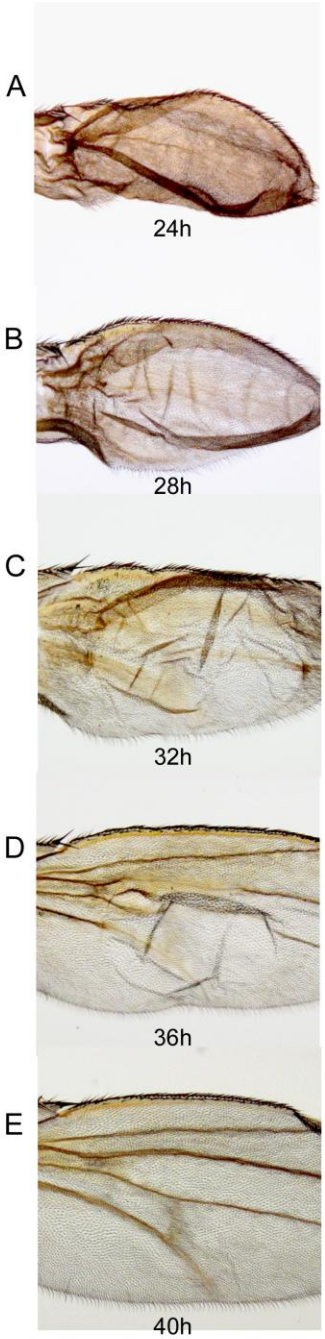

Figure 4.4. Limited dorsal expression of *dpp* and restriction of blistering to the centre of the wing. (A-E) *ap-Gal4, TubGal80^{ts} > UAS dpp* animals were raised at 18ºC until the WPP stage, and shifted to 29ºC at the hours indicated below the images for 12-20h, then shifted back to 18ºC until eclosion.

Dorsal expression of the other BMP ligand, *gbb*, from early pupal stages also resulted in lethality but at a lower level as compared to *dpp* (Table A.3). Shifting animals up at the WPP stage, the prepupal expansion and the separation stages (16, 20 and 22h APF) gave rise to wings that were blistered and darkened (Fig. 4.5 A, B, C), similar to the effects seen with *dpp* expression at the same stages. Animals shifted during separation (26, 30 and 32h APF) show a progressive reduction in severity of the phenotype, and a restriction of the region of blistering to the centre of the wing (Fig. 4.5 D-F). Outside of the blistered region, veins are broader as compared to wild type (Fig. 4.5 F). Shifting up at reapposition (40h APF) only resulted in mild vein broadening (Fig. 4.5 G), and shifting following this time had no effect on the wing (Fig. 4.5 H-I). Thus, the expression of Gbb in the dorsal epithelium led to ectopic phenotypes only when induced prior to reapposition.

Figures 4.4 and 4.5 show that BMP ligands induce the formation of wing blisters, which are progressively restricted to the middle of the wing in later shifts. Wing blistering commonly arises from a failure of basal apposition in the pupal wing (Fristrom et al., 1994; Brabant et al., 1996), but can also arise from the failure of epithelial adherence to the apical ECM (Bokel et al., 2005). In the following Chapter we will show that ectopic BMP signalling leads to a failure of basal apposition, suggesting this is the basis for the blisters in the adult wing. Interestingly, the progressive restriction of blisters to the centre of the wing parallels the endogenous sequence of reapposition in the wing, which begins at the margin and proceeds towards the centre of the wing such that the intervein around the PCV is the last region to appose (Waddington, 1941). The restriction of blistering therefore suggests that the ability of dorsally expressed BMP ligands to inhibit apposition depends on the state of apposition in the wing when the signals are produced. According to this model, apposition cannot be undone by the activation of the BMP pathway.

Ubiquitous Dpp expression reveals a phenocritical period

We next sought to define the phenocritical period for mis-expression of BMP ligands. We restricted ubiquitous expression using *Act5C-Gal4, Tub-Gal80^{ts}*, shifting staged pupae to 29ºC for 8hr periods before shifting down to 18ºC. The response to *dpp* was first tested. When shifted up at the WPP stage, wings showed slight deltas at the ends of L4 and L5 but were otherwise wild type (Fig. 4.6 A). When shifted up at the prepupal expansion stage (16 and 20hAPF), ectopic venation was observed around the distal tip of L2, between L3 and L4, and

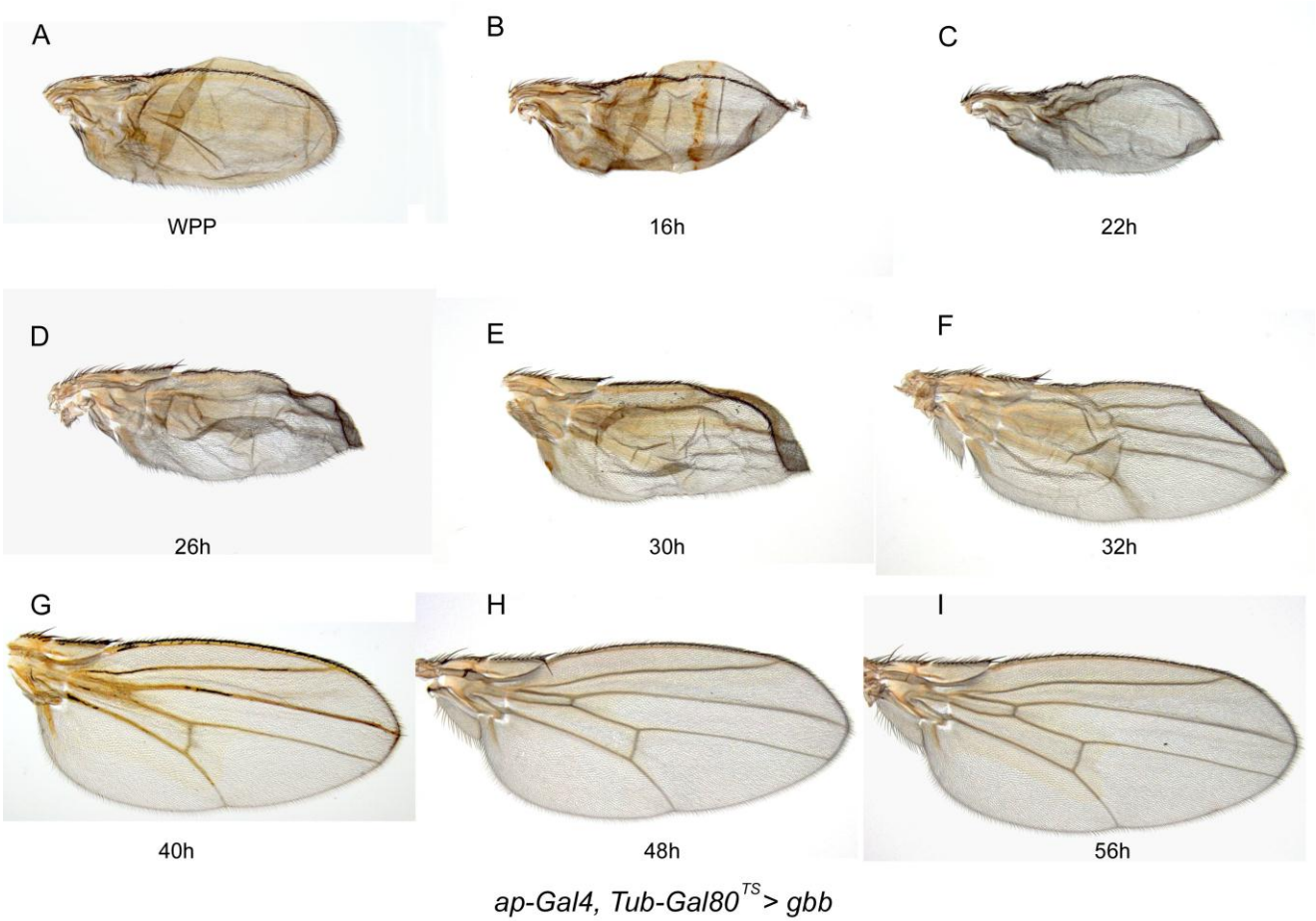

Figure 4.5. Dorsal expression of *gbb* induced progressively through pupal development. (A-I) *ap-Gal4, TubGal80^{ts} > UAS gbb* animals were raised at 18ºC until the WPP stage, then shifted to 29ºC at the hours indicated below the images until eclosion.

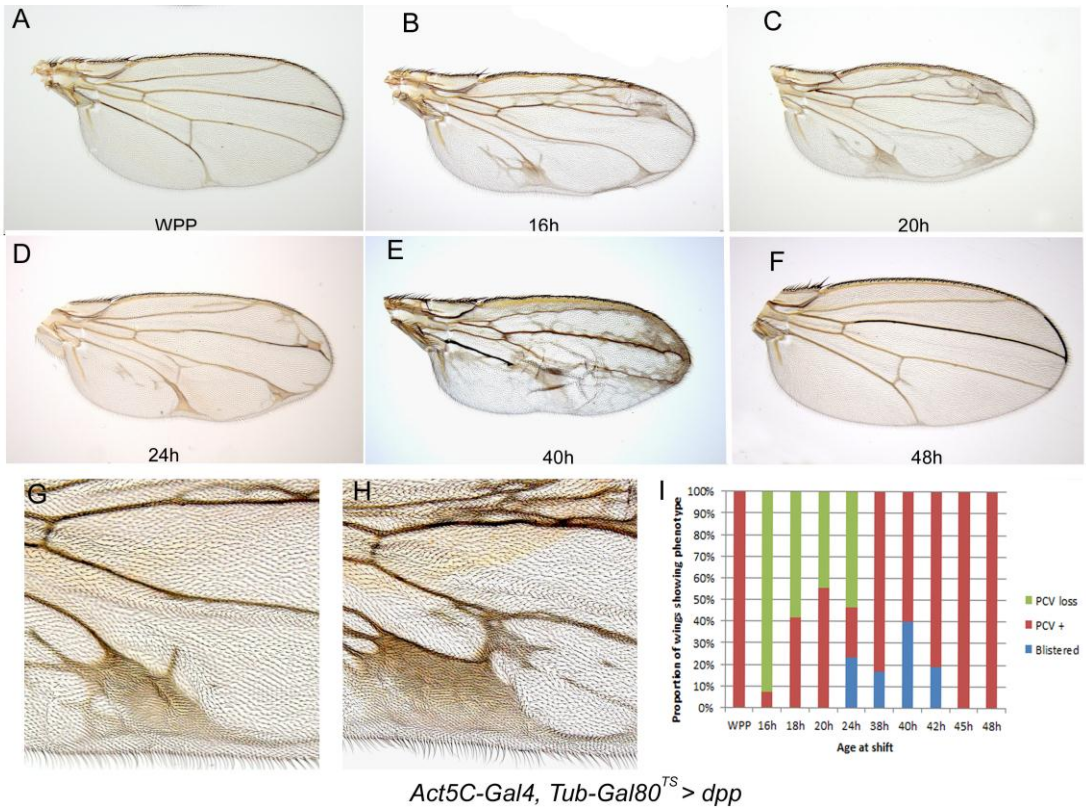

Figure 4.6. Restricted ubiquitous expression of *dpp* reveals the phenocritical period. (A-F) *Act5C-Gal4, TubGal80^{ts} > UAS dpp* animals were raised at 18ºC until the WPP stage, then shifted to 29ºC at the hours indicated below the images for 8h, and shifted back to 18ºC until eclosion. Shifts carried out during or after the refinement stage did not affect wing patterning aside from a spur coming off the PCV (F), a phenotype seen with variable penetrance in both parent stocks. (G, H) Close ups of the PCV region of animals shifted at 20h, showing loss of PCV (G) and expansion of PCV material (H). (I) Graph showing proportion of wings showing wild type PCV (red), PCV loss (green) or blistering (blue), in the classes as indicated on the X axis. PCV loss is limited to shifts induced between 16-24h APF. Blistering occurs in shifts induced between 24-38h APF.

around the distal tip of L5 (Fig. 4.6 B, C). Interestingly, expression in this period commonly led to loss of the PCV, even when L5 was much broader (Fig. 4.6 G, H; PCV loss seen in 51/86 wings scored in 16h, 18h, 20h and 24h shift classes). The PCV loss phenotype was restricted to shifts carried out between 16-24h APF (Fig. 4.6 I). These results suggest that widespread BMP activation can interfere with PCV specification (see Chapter Summary). When animals were shifted up at reapposition (38 and 40h APF), in addition to ectopic venation wings also showed blisters located in the middle of the wing (Fig. 4.6 E). Shifts carried out during or after the refinement stage (45h+ APF) did not affect wing patterning (Fig. 4.6 F). Hence, the phenocritical period for *dpp* mis-expression is between 16-42h APF, which corresponds to the stages of prepupal expansion, separation, and pupal reapposition.

In contrast to *dpp*, 8h periods of ubiquitous *gbb* expression in pupal development had no effect on the adult wing. This suggests that the threshold level for Gbb to induce BMP pathway activity is higher than that for Dpp, and brief periods of expression do not reach it. We will show in Chapter 5 how expression of *dpp* has more severe effects on a cellular level, which is consistent with the role of Dpp as the primary BMP ligand in wing development, and Gbb playing more of an accessory role (Ray and Wharton, 2001).

8h periods of *dpp* expression have defined the period of maximal sensitivity as corresponding to the period of separation and reapposition, which is consistent with the dorsal expression experiments. As discussed in Chapter 3, reapposition coincides with the first signs of cellular differentiation between vein and intervein cells, as vein cells constrict and form lumen, and basal contacts are re-formed in the intervein sectors. Our results thus suggest that these cellular changes precede the end of the phenocritical period. This would be consistent with the restriction of blisters to the centre of the wing following dorsal expression, as discussed above.

Cell autonomous BMP pathway activation shows the same phenocritical period

We have shown that BMP ligands do not promote vein phenotypes when expression is induced after reapposition. Two possibilities could account for the loss of phenotypes in later shifts: firstly, ligands induce pathway activity, but cells do not respond to it (i.e. their fate is determined); secondly, the cells are still competent, but the ligands cannot activate downstream signalling. The latter possibility could arise if changes to the extracellular environment prevent interactions between ligand and receptor. To distinguish between these possibilities we activated the pathway cell autonomously. If the cells cannot respond to the

autonomous activation of the pathway in later stages, we will see a similar phenotype as with the ligands. If however cells are still competent, the activated receptor will be able to induce phenotypes in later shifts.

We utilised an activated form of the receptor Tkv (*UAS-tkv^{QD}*) which constitutively activates the pathway (Nellen et al., 1996). As was the case with *dpp*, dorsal expression of *tkv^{QD}* was lethal when induced in early stages of pupal development (Table A.3). Rare escapers from the WPP shift class showed darkened wings which were highly folded and crumpled (Fig. 4.7 A). Later shifts showed the same pattern as *dpp*, namely a reduction in phenotype such that vein pattern was unaffected in wings shifted after 44h APF (Fig. 4.7 B-H). Thus, *tkv^{QD}* only leads to wing phenotypes when expression is induced prior to the refinement stage. To determine the phenocritical period for *tkv^{QD}* expression, 8hr periods of ubiquitous *tkv^{QD}* expression were induced. These shifts revealed a very similar phenocritical period for *tkv^{QD}* as was seen for *dpp*, with shifts induced in the prepupal expansion, separation and reapposition stages showing a severe blistering and darkening phenotype, while shifts induced prior the WPP stage or after reapposition showing only minor effects on the vein pattern (Fig. 4.8 A-H). Thus the phenocritical period for *tkv^{QD}* induced wing phenotypes is between 16-48h APF, which is notably similar to that of *dpp* (16-42h APF).

As cells show the same competence to cell autonomous pathway activators as to ligands, this indicates that after reapposition and the beginning of refinement, BMP pathway activation cannot alter cell fate in the wing. Cells are most sensitive to heightened BMP activity between separation and the completion of reapposition. This further highlights reapposition as a critical stage in the determination of cell fate.

Activating the EGFR pathway during pupal development

We next addressed whether the same temporal signalling sensitivity applied to the other pathway required for vein formation in the pupal wing, EGFR. It has been previously shown that wing venation is affected by both loss and gain of EGFR activity in early pupal development (Guichard et al., 1999). As in the aforementioned study, we here use ectopic expression of *rhomboid* (*rho*) to achieve EGFR pathway activation. We first induced dorsal expression of *rho* at set points in pupal development until eclosion. Expression in the early stages led to high levels of lethality (Table A.3 in the Appendix). Shifting animals during prepupal expansion (16h APF) led to wings that showed a phenotype similar to that following

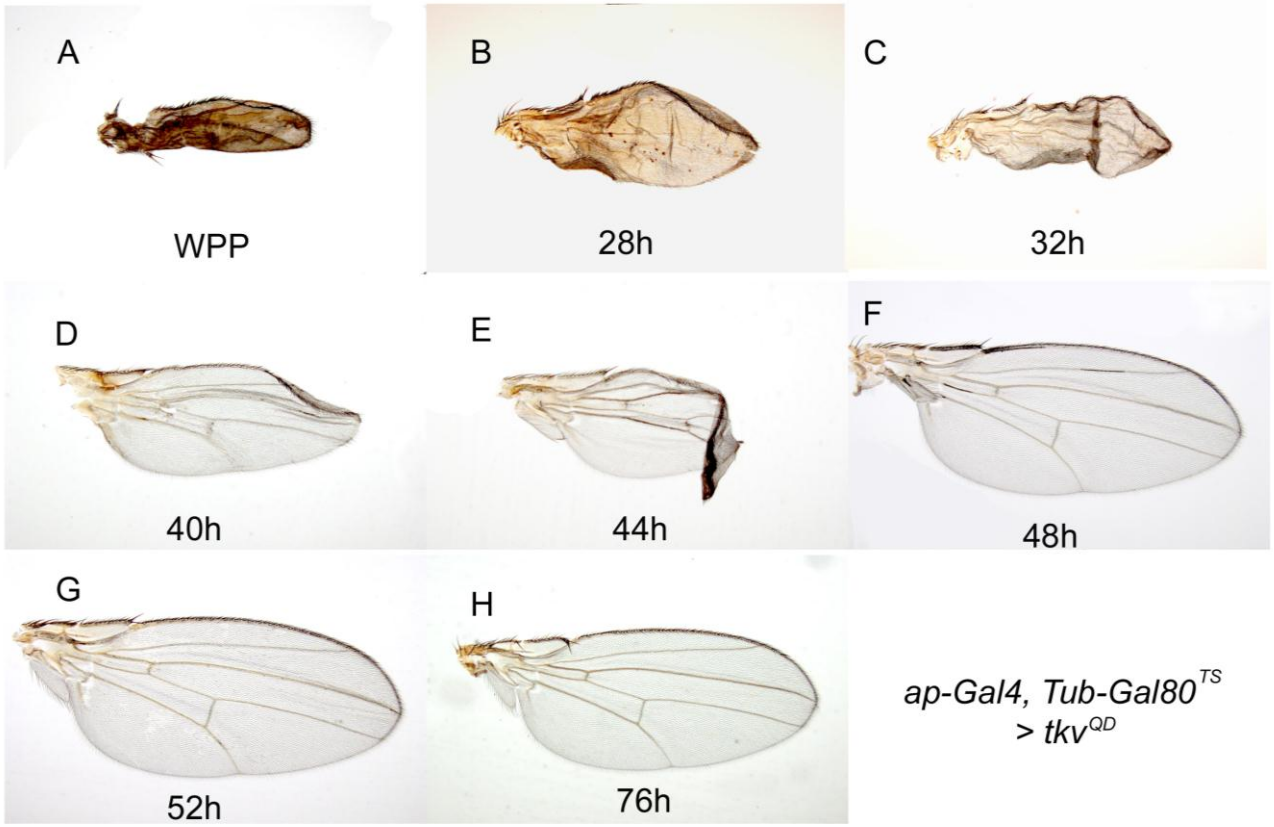

Figure 4.7. Dorsal expression of *tkv*^{QD} induced progressively through pupal development. (A-J) *ap-Gal4, TubGal80*^{ts} *> UAS tkv*^{QD} animals were raised at 18ºC until the WPP stage, and shifted to 29ºC at the hours indicated below the images until eclosion.

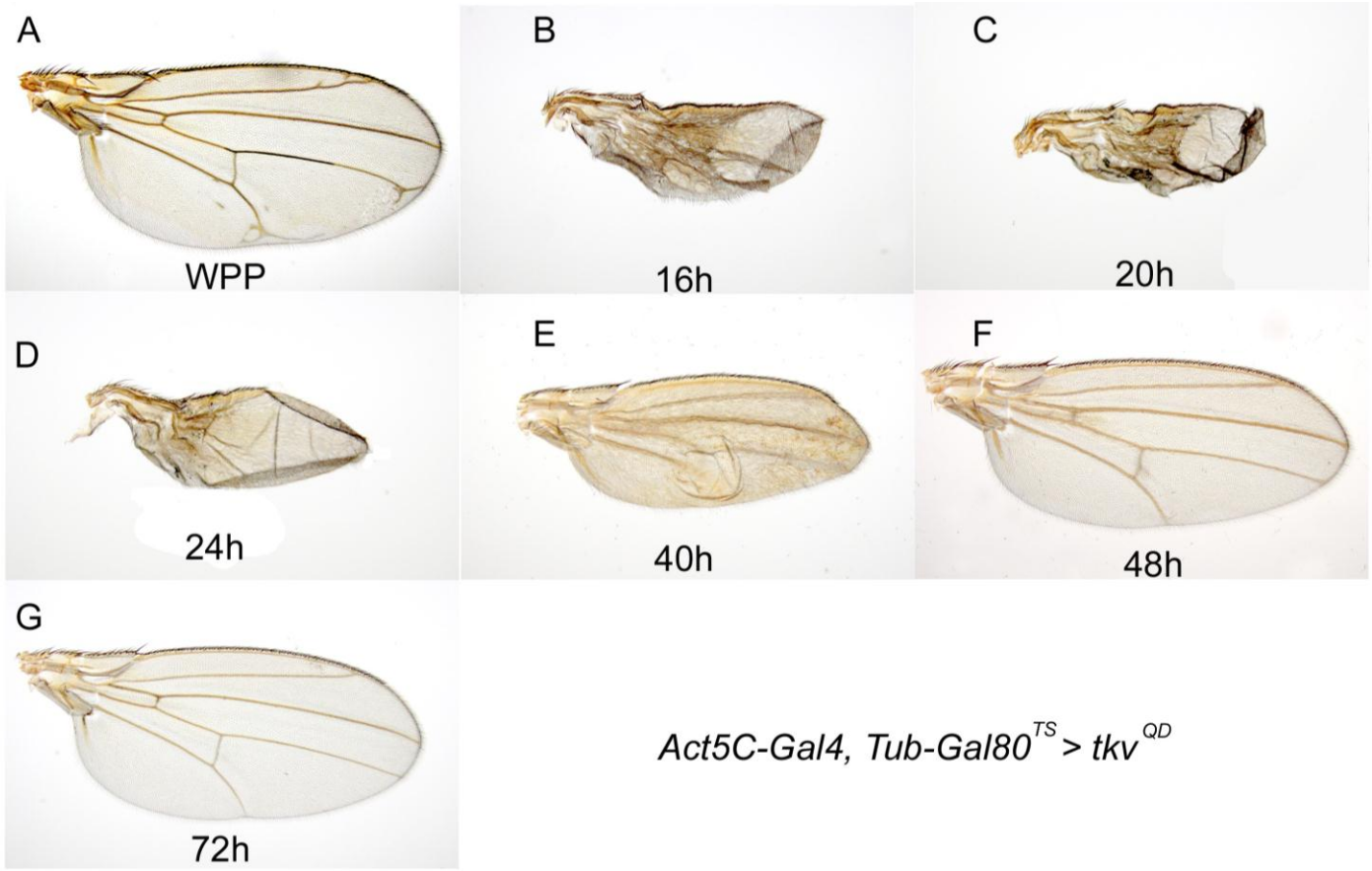

Figure 4.8. Restricted ubiquitous expression of *tkv*^{QD} reveals the phenocritical period. (A-G) *Act5C-Gal4, TubGal80*^{ts} > *UAS tkv*^{QD} animals were raised at 18ºC until the WPP stage, then shifted to 29ºC at the hours indicated below the images for 8h, and shifted back to 18ºC until eclosion.

BMP activation: wings were smaller, darker and crumpled (Fig. 4.9 A). Later shifts showed the same reduction in phenotype as was seen with dorsal BMP activation, although the point at which the wings showed a wild type venation and apposition phenotype (40h APF) was slightly earlier (Fig. 4.9 B-H). Thus, like the BMP components, dorsally expressed *rho* induces ectopic wing phenotypes when shifts are carried out prior to reapposition. To determine the phenocritical period of EGFR activation, 8hr periods of ubiquitous *rho* expression were induced. Phenotypes from such shifts were milder than those arising from dorsal expression, but still uncovered a phenocritical period. Shifts induced at the WPP stage produced wild type wings (Fig. 4.10 A), but in shifts carried out during prepupal expansion (16h, 20h, 24h APF) ectopic wing vein phenotypes were observed, with the most severe ectopic venation seen in the 24h APF class (Fig. 4.10 B-D). Ectopic vein material was clustered around the distal tips of the longitudinal veins (Figs. 4.10 G, H) or seen as stripes in the intervein between neighbouring veins (Fig. 4.10 D). Consistent with the dorsal mis-expression data, inducing 8h of ubiquitous expression after reapposition does not affect the wing (Fig. 4.10 E, F).

Thus, competence of pupal wing cells to ectopic EGFR pathway activation is the same as that for BMP pathway activity: expression induced after reapposition does not produce ectopic vein phenotypes. In combination with the above described results this suggests that once reapposition is complete and the domains refining, cells are unresponsive to vein-promoting signals. This indicates a shift from cell fate plasticity to fate determination.

Reductions in Notch activity during pupal development

We next addressed the effects of interfering with the third signalling pathway involved in pupal wing vein development, Notch. Loss of Notch leads to vein thickening, due to an expansion of expansion of BMP and EGFR pathway activity (de Celis et al., 1997; Sotillos and de Celis, 2005). Previous studies have suggested that the phenocritical period for Notch sensitivity is between reapposition and the definitive stage (Shellenbarger and Mohler, 1978; Huppert et al., 1997), and we here sought to determine whether similar sensitivity is revealed with the Gal4/Gal80^{ts} system. We expressed two targets to knockdown pathway activity: a line of *Notch RNAi* which is lethal with multiple drivers but gives typical Notch pathway phenotypes with weaker drivers (see Table A.4 in the Appendix), and the extracellular domain of Notch (N^{ECD}) which acts as dominant negative to reduce the efficiency of endogenous signalling (Rebay et al., 1993).

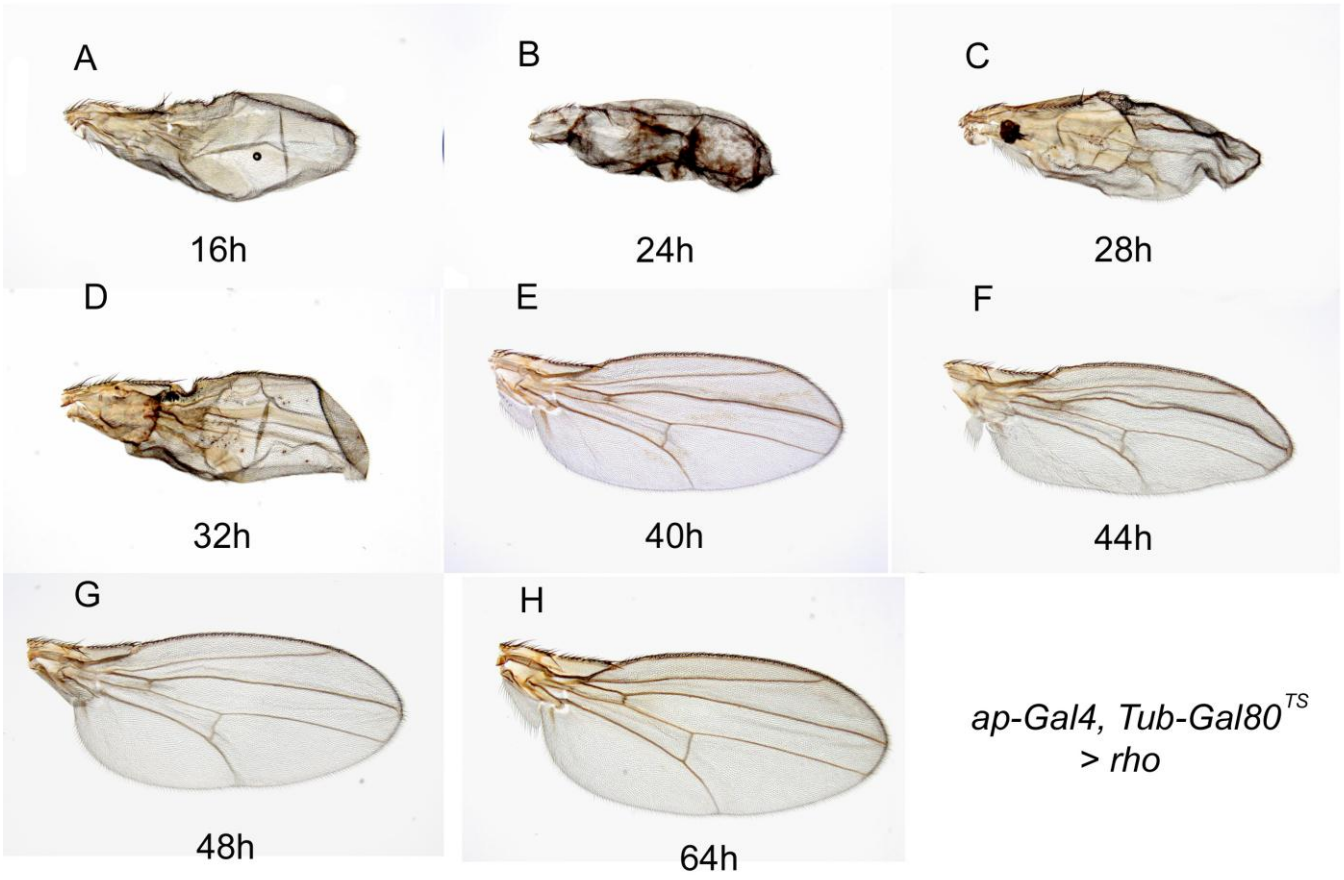

Figure 4.9. Dorsal expression of *rho* induced progressively through pupal development. (A-J) *ap-Gal4, TubGal80^{ts} > UAS rho* animals were raised at 18°C until the WPP stage, and shifted to 29°C at the hours indicated below the images until eclosion.

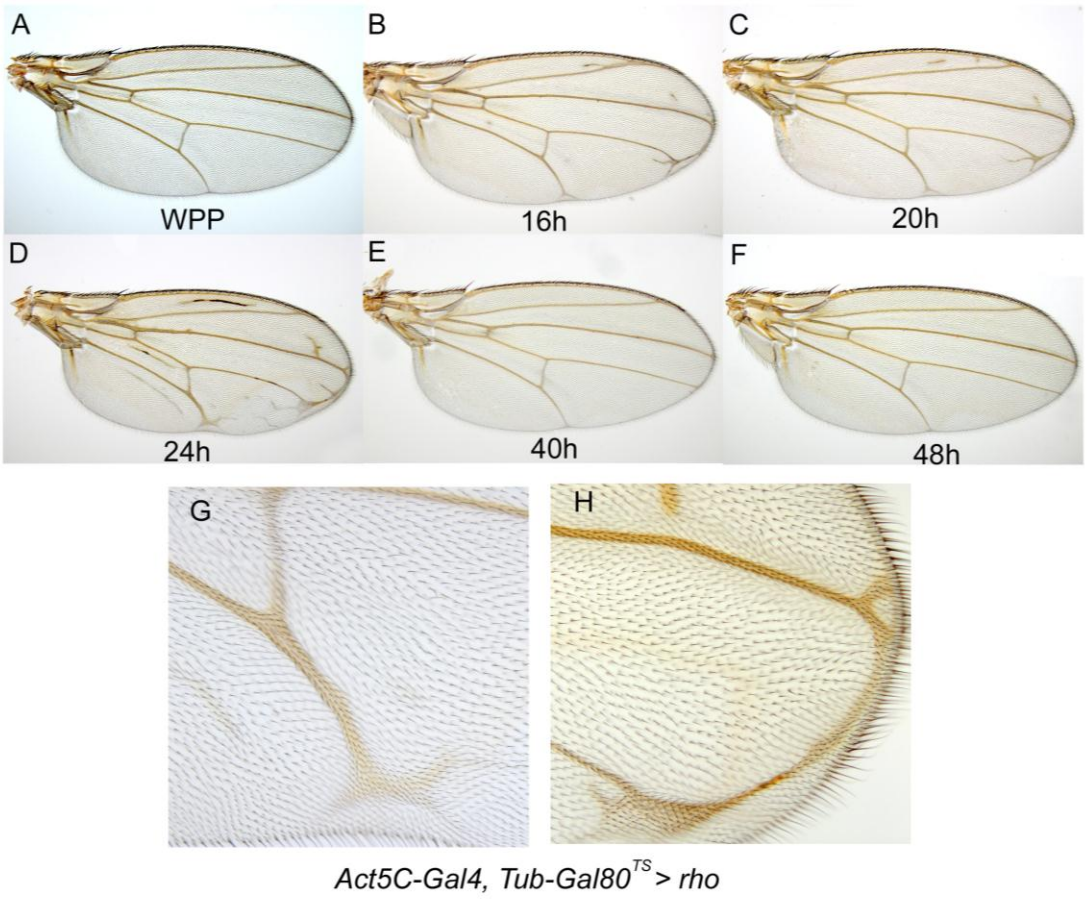

Figure 4.10. Restricted ubiquitous expression of *rho* reveals the phenocritical period. (A-F) *Act5C-Gal4, TubGal80^{ts} > UAS rho* animals were raised at 18ºC until the WPP stage, shifted up to 29ºC at the hours indicated below the images for 8h, and shifted back down to 18ºC until eclosion. (G-H) Closeups of distal L5 (G) and distal L3 and L4 (H) of wings from the 24h class, showing vein thickening, deltas and ectopic veins.

Ubiquitous expression of both constructs for 8h periods in pupal development led to the thickening of veins, but with slightly different temporal dynamics. When *N RNAi* animals were shifted from the WPP stage, vein thickening was seen (Fig. 4.11 A), whereas 8hr of N^{ECD} expression from the WPP stage did not affect vein width (Fig. 4.11 E, E'). This difference may reflect the perdurance of the transcribed *dsRNA* molecules which continue to evoke the RNAi response after animals had been shifted back down to the permissive temperature. When *N RNAi* or N^{ECD} animals were shifted at the prepupal expansion stage (16h and 24h APF), vein thickening was seen (Fig. 4.11 B, C, F-G'), which was more marked with the *RNAi* as compared to N^{ECD}. Additionally, these shifts also led to the formation of blisters between the wing layers, which are likely to result from an expansion of vein territories at the expense of intervein. Indeed, the Notch ligand *Dl*, which is required to establish the domains of Notch activation in the provein domains (de Celis et al., 1997), was recovered in a screen for wing blister mutants (Prout et al., 1997). When *N RNAi* or N^{ECD} animals were shifted at or after reapposition (40h+ APF), wings were not affected (Fig. 4.11 D, H, H').

Thus, cells show the same competence to inhibiting Notch pathway activity as they do for activating the BMP and EGFR pathways: shifts carried out after reapposition do not cause vein thickening. This finding is surprising given the maintenance of *N* expression in the proveins and *Dl* expression in the veins in the stages beyond this point (Huppert et al., 1997). Our data show that in the hours leading up to the definitive stage, although Notch/Delta signalling persists in the vein/provein domain, reducing Notch functionality to the extent that RNAi or N^{ECD} can does not lead to the loss of the proveins. To account for this discrepancy, we can consider that a key output of Notch signalling in the provein is repression of *rho* transcription and hence EGFR pathway activation (de Celis et al., 1997). Thus, in early stages the loss of Notch inhibition of EGFR signalling leads to broadened veins. However, cells across the intervein lose their sensitivity to heightened EGFR signalling after reapposition (Figs. 4.9, 4.10), so if *rho* expression is expanded into the provein when knocking down Notch function in later shifts, cells are not competent to respond to it. This functional intertwining would determine that the competence of cells to reductions in Notch signalling would be dependent on their competence to EGFR signalling.

Vein cells show the same temporal competence to intervein-promoting signals

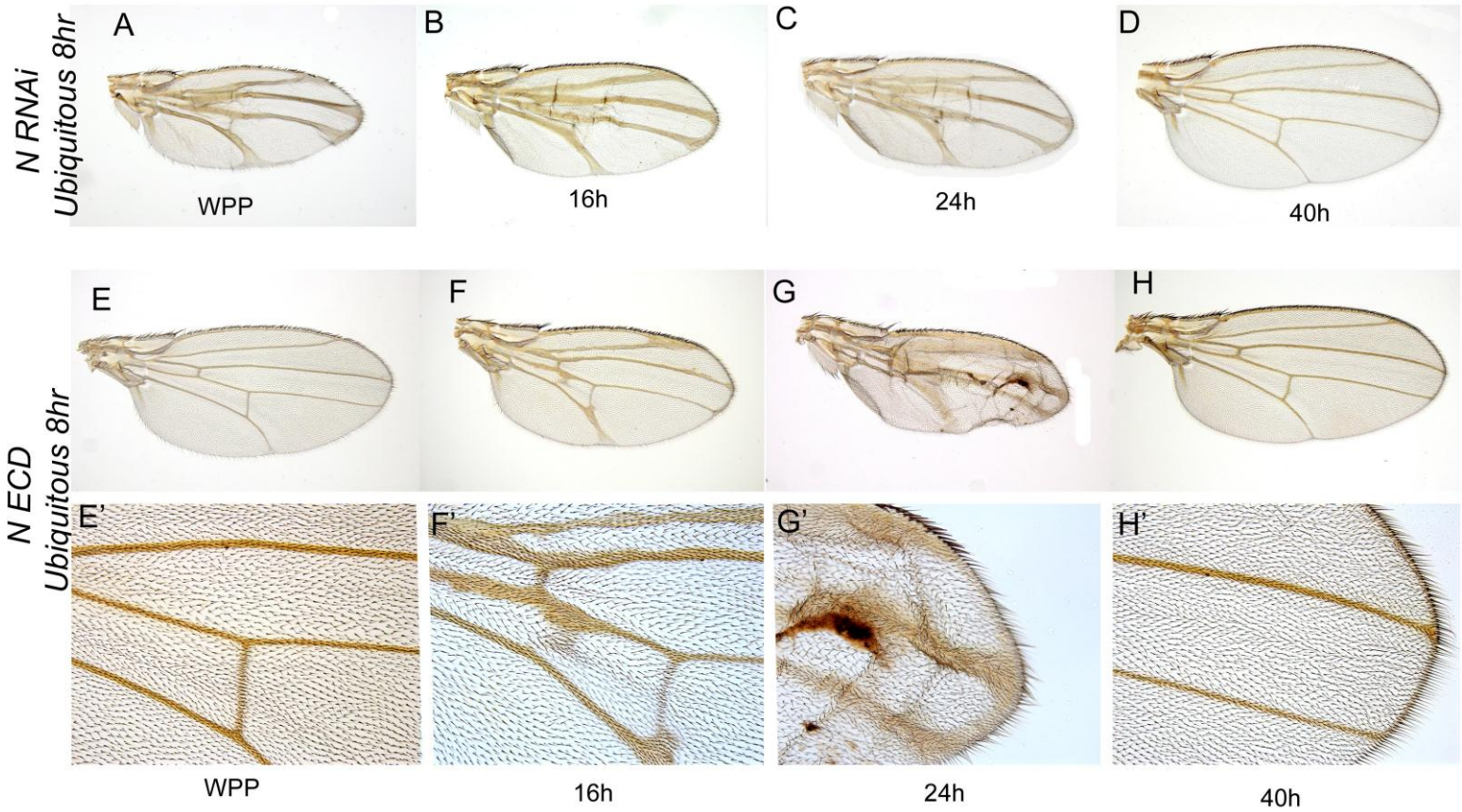

Figure 4.11. Knocking down Notch pathway functionality progressively through pupal development. (A-D) *Act5C-Gal4, TubGal80^{ts} > UAS-N-dsRNA* animals were raised at 18ºC until the WPP stage, then shifted to 29ºC at the hours indicated below the images for 8h, and shifted back to 18ºC until eclosion. (E-H) *Act5C-Gal4, TubGal80^{ts} > UAS N^{ECD}* animals were raised at 18ºC until the WPP stage, then shifted to 29ºC at the hours indicated below the images for 8h, and shifted back to 18ºC until eclosion. (E'-H') Close up of wing regions of each of the time-points, showing vein widening and blistering restricted to shifts induced 16-24h APF.

The above experiments test the competence of intervein-specified cells to vein-promoting signals, and we next addressed the competence of vein-specified cells to vein-inhibiting signals. It has been previously shown that overexpression of Sog leads to vein inhibition in a period overlapping that of Dpp induced vein promotion (Yu et al., 1996), but as with ligand overexpression this effect could be due to a reduction in the ability of extracellular Sog to function after apposition. We thus inhibited pathway activity by knocking down signal transduction downstream of the receptor, using Daughters against decapentaplegic (*Dad*), which inhibits the phosphorylation of the receptor-Smad Mad by ligand-bound BMP receptors (Tsuneizumi et al., 1997; Kamiya et al., 2008), and *dsRNA* targeting Mad itself.

We first induced expression of *Dad* in the dorsal epithelium at set points in pupal development until eclosion. When animals were shifted at the WPP stage, *Dad* expression gave rise to loss of vein pigmentation in the distal portions of L3 and L4 (Fig. 4.12 A), consistent with an inhibition of BMP pathway activity. In these wings, a faint stripe can be seen in these distal regions, which likely reflects the vein cuticle secreted by cells of the ventral layer, which are unaffected by dorsal knockdown (we will show in Chapter 5 how dorsal BMP knockdown results in dorsally autonomous vein loss). Shifts induced during prepupal expansion and separation (18, 24, 28 and 32h APF) had progressively less severe effects on vein structures, although in the 32h APF class veins were still patchy and did not reach the margin (Fig. 4.12 B-E). Expression during or after reapposition (40h+ APF) did not result in vein loss phenotypes (4.12 F-H).

When dorsal expression of *Mad dsRNA* was induced at the WPP stage, wings showed a similar loss or reduction in distal vein structures (Fig. 4.13 A), as well as folds in the wing particularly anterior to L3. This phenotype is progressively lost with later shifts, such that animals shifted at prepupal separation (16h APF) show patchy reductions in L4 (Fig. 4.13 B), and those shifted at the separation stage or later (24h+ APF) show normal veins (Fig. 4.13 C, D). The lack of a phenotype in the 24h APF shifts, which we would expect to lead to vein loss considering the above results, could arise from the inefficacy of the RNAi as compared to Dad.

To reduce EGFR signalling autonomously, we utilised *dsRNA* of the sole receptor of the pathway, *Egfr* (see Appendix A.4). Inducing *Egfr RNAi* in the dorsal epithelium throughout pupal development led to extremely curled wings, in which the effects on venation could not be analysed. Curling could occur if cell division was inhibited in the dorsal layer: *Egfr* mutant clones have been shown to be defective in proliferation (Diaz-Benjumea and Garcia-Bellido, 1990), and thus the final mitoses which occur in the pupal period (Schubiger and Palka, 1987) would rely on a basal level of Egfr function. To avoid problems associated with prolonged

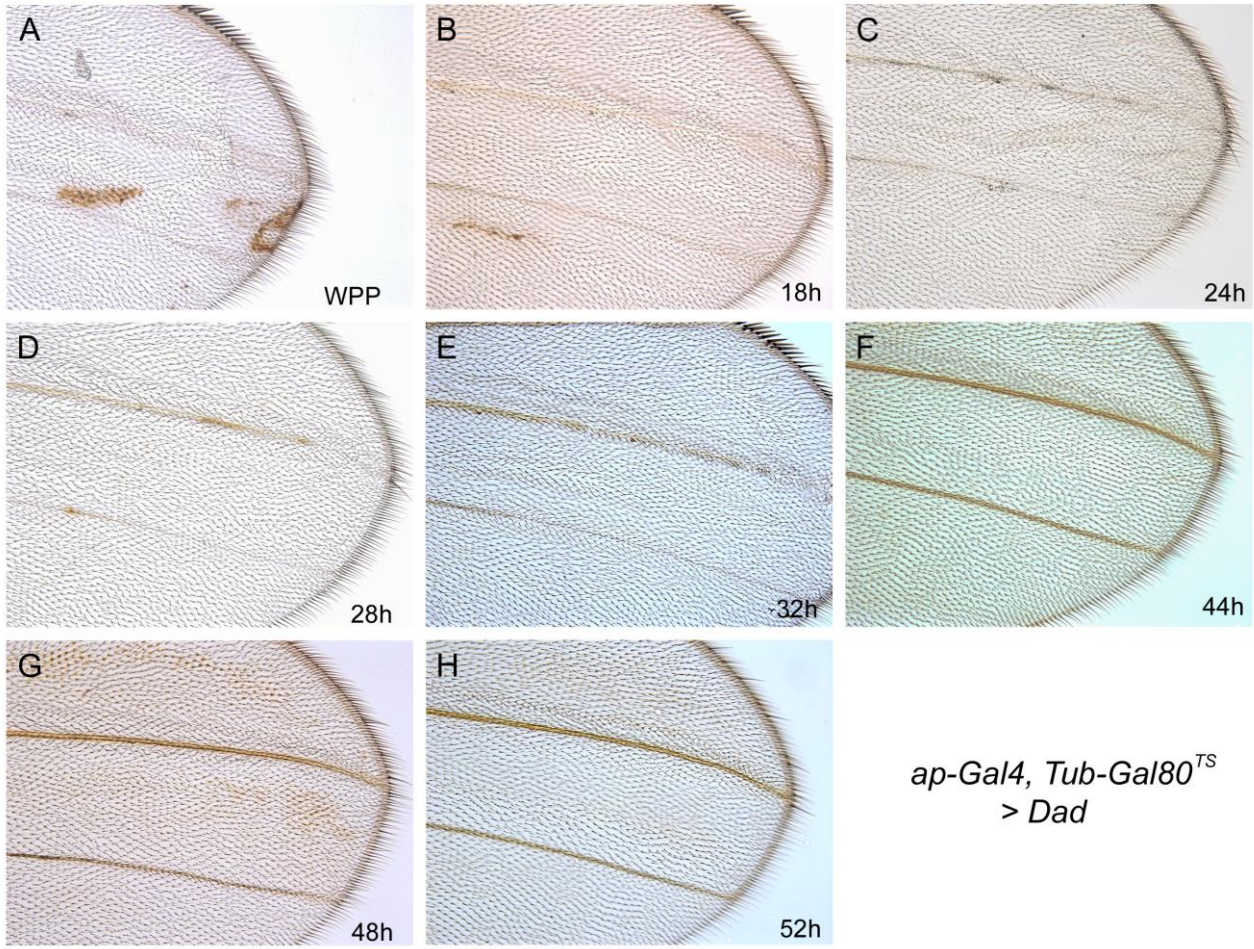

Figure 4.12. Dorsal expression of *Dad* induced progressively through pupal development. (A-H) *ap-Gal4, TubGal80^{ts} > UAS-Dad* animals were raised at 18ºC until the WPP stage, and shifted to 29ºC at the hours indicated in the images until eclosion

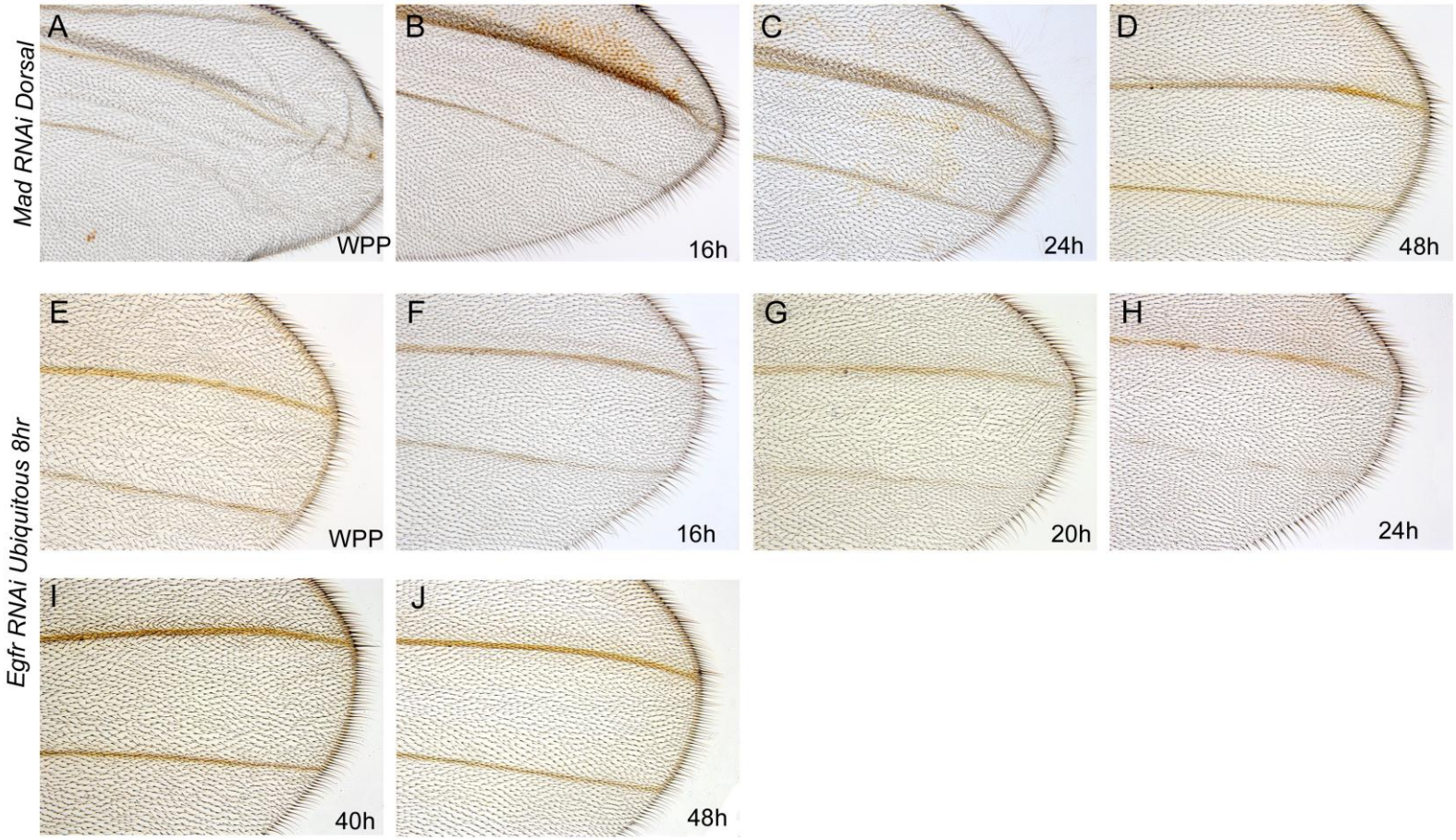

Figure 4.13. Effects of *Mad* and *Egfr RNAi* in pupal development. (A-D) *ap-Gal4, TubGal80^{ts} > UAS-Mad-dsRNA* animals were raised at 18ºC until the WPP stage, and shifted to 29ºC at the hours indicated in the images until eclosion. Vein loss is limited to shifts induced at or prior to 16h APF. (E-H) *Act5C-Gal4, TubGal80^{ts} > UAS-Egfr-dsRNA* animals were raised at 18ºC until the WPP stage, then shifted to 29ºC at the hours indicated below the images for 8h, and shifted back to 18ºC until eclosion. L4 loss is limited to shifts induced between 16-24h APF.

expression we drove expression ubiquitously for 8hr periods. The most sensitive region of the wing to reductions in *Egfr* function is distal L4, as has been previously described (Clifford and Schupbach, 1989). Animals shifted up at the WPP stage showed a slight patchiness in L4 (Fig. 4.13 E), which increased in severity in later shifts such that in animals shifted during separation (24h APF) the vein was almost entirely absent (Fig. 4.13 H). This vein loss phenotype was not observed after reapposition (40h+ APF; Fig. 4.13 I, J). Thus vein cells are most sensitive to reductions in EGFR pathway in shifts induced between 16h and 24h APF, revealing a similar period of sensitivity for reducing EGFR activity as for promoting it.

Overall, these results show that the transformation of vein into intervein, induced by blocking BMP or Egfr pathway signal transduction, is only seen when shifts are performed prior to the completion of reapposition. The adoption of an alternate developmental program in the pupal wing in response to ectopic signalling is thus limited to this early period. An implication of this result is that cell determination in the pupal wing follows reapposition.

IV. Summary

Cellular differentiation in the pupal wing cells is preceded by the establishment of plastic domains in the proliferating disc corresponding to the future pattern, which are conditionally specified to develop as either vein or intervein. These signalling domains are maintained and elaborated in the pupal wing. Using the Gal4/Gal80^{ts} system, we have described how cells are capable of switching fates up until just after the initiation of cellular differentiation. Once reapposition is complete and domains refine, cells are locked in to the particular program of differentiation and unable to adopt an alternate developmental program. This suggests that reapposition marks the point after which cells are determined.

Combining the results from multiple transgenes, we can assemble a phenocritical timeline of cellular sensitivity to vein/intervein promoting signals (Fig. 4.14). The timeline shows that the competence of cells to adopt an alternate developmental program in response to ectopic signalling lasts up until after the commencement of reapposition. As reapposition marks the beginning of cellular differentiation, this suggests that the early stages of differentiation in the pupal wing are reversible processes. For example, intervein differentiation involves the re-forming of basal contacts and the relaxation of the apical surface. When the BMP pathway is activated in these cells at this time point, they are competent to adopt the alternate program (i.e. vein), apically constricting and forming a basal lumen. Indeed, such plasticity is inherent in the notion of the 'provein': proveins are established in the pupal wing to limit the width of the veins, and we will show in Chapter 5 that knocking down the function of *N* or *tkv* in the provein leads to the widening of the domain of apical constriction. Thus, endogenous signalling at the start of cellular differentiation involves the inhibition of 'vein' behaviours in cells originally specified as such. Our results extend this plasticity to both vein and intervein cells throughout the pupal wing. Such plasticity may allow the wing to align the appropriate regions of differentiation between the dorsal and ventral layers, a possibility we will return to in the following Chapter.

After the completion of reapposition, however, the competence to respond to inductive signals is lost, and ectopic expression does not affect the vein pattern of the wing. We have shown how both ligands and cell autonomous pathway activators display this behaviour, demonstrating that changes to the extracellular environment which preclude ligand-receptor interactions are not the contributing factor. Rather, cells become refractory to pathway

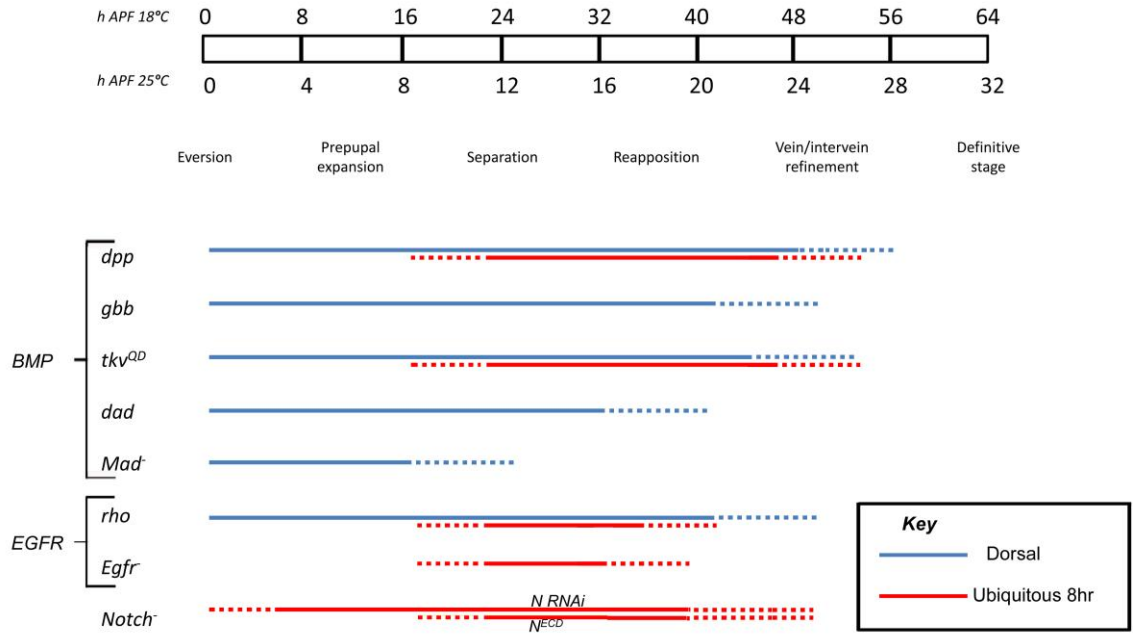

Figure 4.14. Phenocritical timeline for cellular responses to pathway activation/inhibition. Timeline at top shows developmental hours after WPP formation at 18ºC (upper) and 25ºC (lower) respectively. Developmental stages (see also Fig. 3.2) in wing development are shown below. For each gene, blue lines show the sensitivity to dorsal expression, and red lines show sensitivity to ubiquitous 8hr expression. Dotted lines indicate the expected delay between shifting up and signalling, and the probable perdurance after shifting down.

activity. An interesting feature of ligand expression was the progressive restriction of wing blisters to the centre of the wing. This pattern mimics that of apposition in the wild type wing, as the region of non-apposition is progressively restricted to a central cavity (Waddington, 1941). This parallel implies that the ability of BMP pathway activity to prevent apposition is defined by the extent of apposition in the wing; in apposed regions, intervein cells cannot switch to the vein development program in response to these signals.

As inferred from the adult cuticle, cells receiving vein-promoting or vein-inhibiting signals after the completion of reapposition do not carry out the necessary cellular morphogenesis (e.g. apical constriction or relaxation). This could arise due to a change in the regulation of target genes, i.e. a change in the transcriptional output of the pathway. For example, if a key 'realisator' gene becomes insensitive to the transcriptional output of the pathway, its activity would thus be muted. According to this model, if the output of the pathway shifts away from the realisators that control these cell shape changes, pathway activation will no longer be able to influence cell shape. Alternatively, once cellular differentiation reaches a certain point, it may not be able to be 'undone' by ectopic inductive signals. For example, once Integrin-based basal junctions are formed between the two layers, they might not be able to be broken down (or altered, to form a lumen) by heightened BMP/EGFR signalling. In terms of the apical surface, once the intervein cells have assembled into a regular hexagonal array (Classen et al., 2005), apical constriction may require a substantial increase in force produced by contracting Myo-II and Actin. The targets of BMP/EGFR activity would then not be able to induce the necessary increase in contraction, and thus pathway activity would have no effect. According to this model, the physical links between cells would be a mechanism for cell fate restriction in the wing. The output of the pathways would not change, but would lose their capacity to enact cell shape changes.

An important aspect of the timeline is its restricted time scale in relation to the whole of pupal development: the pre-pupal and pupal stages last around 96h, yet altering BMP/EGFR/Notch pathway activity only affects vein/intervein development within the first third of this period. As discussed in the previous Chapter, cells are not latent in this second third of pupal development, but instead undergo further morphogenesis, flattening and remodelling their apical surfaces. In the case of vein cells, BMP/EGFR pathway knockdown in later stages did not affect the morphology of the adult veins, so the cellular morphogenesis preceding cuticle deposition may not require the continued activity of these pathways. Similarly, intervein cells in these stages do not respond to heightened pathway activity by secreting a vein-like cuticle. The question thus arises as to which factors control the cell shape changes of the folded wing.

The secretion of a wild type intervein cuticle requires the *dusky* and *miniature* genes, which act to control the apical cell shape changes in the folded wing (Roch et al., 2003). However, the mechanism by which these genes achieve this apical remodelling is currently unclear. In the embryonic epidermis, multiple zona pellucida domain-containing proteins, including Dusky and Miniature, have been shown to co-operatively control cell-ECM links and Actin cell extensions (Fernandes et al., 2010). These proteins could thus form a similar role in the wing. They would act downstream of the vein/intervein patterning network, but not be dependent on their continued activities. The distinctive 'w' shapes of vein cells uncovered in the previous Chapter suggest that additional or alternate vein-specific factors or mechanisms would be involved in the vein cells.

Brief periods of ectopic expression allowed us to determine the lower limit of the phenocritical window: the earliest time at which we see an effect in target cells (Fig. 5.14). Our data show that during the first 8h of the prepupal period, as the disc everts and apposes, heightened BMP or EGFR signalling does not lead to ectopic venation in the adult wing. EGFR pathway activity is however maintained in vein domains from the disc to the pupal wing (Sturtevant et al., 1993), and *dpp* expression in some vein primordia can be seen in the prepupal wing (Ralston and Blair, 2005). Given these expression patterns, we might expect ectopic signalling in this early stage to promote vein fate, so the question arises as to why they do not. A possible explanation involves the loss of the vein-promoting signal following the shift down to the permissive temperature. If the signal is not maintained, cells which were induced as vein by heightened BMP/EGFR pathway activity would revert to an intervein identity once more. The maintenance of pathway activity until reapposition would thus be critical. If so, the first eight hours do not represent an 'incompetent' stage, but rather highlight the plasticity of cells to revert to their original developmental program if induction is not sustained.

Restricting ubiquitous expression to 8h periods also revealed the distinctive effects that different signalling components had on the wing. We showed that Dpp was able to promote ectopic venation in intervein regions while also inhibiting the formation of the posterior crossvein (PCV). The development of the PCV begins with a broad band of BMP pathway activity that is refined into a narrower, clearly defined stripe in the hours following apposition (Conley et al., 2000; see also Chapter 6). Sog and Cv-2 are extracellular modulators of BMP signalling which are required to enhance pathway activity during PCV development, and they too lead to PCV loss when overexpressed (Yu et al., 1996; Serpe et al., 2008). However, in these cases ligand sequestering by the excess protein is proposed to play a role (as both Cv-2 and Sog can bind BMP ligands), with PCV loss arising from the restriction of ligand availability

to the receptor and hence the loss of pathway activity. In the case of Dpp, mis-expression would *increase* ligand availability to the receptor, so another mechanism must be in play. PCV development involves creating a sharp distinction between high and low levels of BMP signalling, and a brief pulse of Dpp would be expected to increase pathway activity uniformly across the region, thus abolishing this distinction. As a result, the PCV would be lost. According to this model high levels of BMP signalling alone are not responsible for the development of this vein, but rather the restriction of high levels of signalling to a defined stripe of cells.

Chapter 5

Interplanar and intraplanar signalling

I. Chapter Overview

Having described the cellular morphogenesis that underlies pupal wing development, and the competence of cells to vein/intervein inducing signals, we next sought to probe the spatial dynamics of signalling in the pupal wing. This Chapter investigates the function of signals both between and within the two layers of the wing in the differentiation of cellular phenotypes. We term the former type of signalling 'interplanar,' and the latter type of signalling 'intraplanar'. Interplanar signalling is poorly understood, and is here addressed with a combination of Gal4/Gal80^{ts} controlled mis-expression, clonal analysis, and rescue experiments. Intraplanar signalling is addressed by means of FLPout clones to test the influence that ectopic expression of BMP components has in intervein cells and their neighbours.

II. Introduction

Wing morphogenesis involves the transformation of a monolayer into a bilayer, with basal surfaces in apposition. The bilayer is a symmetrical structure, with the dorsal and ventral components of the veins aligning to form the vein lumen, which lie in between the sectors of intervein. This architecture provides cells of the pupal wing with both adjacent and opposite neighbours (see Fig. 3.11). As a result, cells can signal both to adjacent cells within the same layer, which we here term 'intraplanar' signalling, and to cells of the opposite layer, which we here term 'interplanar' signalling. The ability of BMP signals to operate in each of these dimensions is the focus of this Chapter.

Intercellular signalling controls cell fate in the wing. In the pupal wing, EGFR and BMP activity defines vein domains, and increasing the activity of either pathway leads to the differentiation of ectopic venation (Yu et al., 1996; Guichard et al., 1999). Vein cells also express the Notch ligand *Dl*, which activates the Notch pathway (leading to heightened expression of the *N* receptor) in bands of intervein cells adjacent to the veins. These 'provein' cells also show high levels of expression of the BMP receptor *tkv.* Both N and Tkv function to antagonise vein development, and as a result play a key role in the regulation of vein width. Intervein cells are defined by expression of *DSRF*, which is repressed by BMP and EGFR signalling in the veins and thus limited to the interveins. This signalling network creates domains of gene expression corresponding to the vein and intervein fates (see Fig. 1.5).

Interplanar signalling between the dorsal and ventral layers of the wing has previously been shown to play a role in vein development. For example, clones mutant for genes which cause ectopic venation can lead to the differentiation of ectopic vein cuticle in the opposite surface (Garcia-Bellido and de Celis, 1992; Milan et al., 1997). In other cases, clones mutant for vein loss alleles were reported to cause dominant loss of veins in the opposite surface. For example, when clones of *veinlet* (a hypomorphic allele of *rho*) covered the dorsal surface of L2, they led to vein loss, whereas ventral clones did not (Garcia-Bellido, 1977). A similar phenotype was reported for loss of function *rho* alleles (Guichard et al., 1999). In these cases the genetic constitution of the dorsal cells appeared to determine the differentiation of the ventral cells. This led to the proposal that although the veins are independently specified in the wing disc, the differentiation of vein structures in the ventral layer requires a specific signal from the dorsal veins (Garcia-Bellido, 1977; Garcia-Bellido and de Celis, 1992). In the case of

the PCV, clones of the *cv* gene showed a similar behaviour: whereas 6/11 dorsal clones led to vein loss, 0/12 ventral clones affected the vein (Garcia-Bellido, 1977). As *cv* has since been since been characterised as encoding an extracellular modulator of BMP signalling (Shimmi et al., 2005a; Vilmos et al., 2005), BMP signals have emerged as a candidate for mediators of this interplanar induction specifically in the crossveins (Marcus, 2001).

However, several lines of evidence run contrary to the model of directional interplanar induction. Ventral clones of ectopic venation mutations can induce vein differentiation in the dorsal surface (Milan et al., 1997), suggesting ventral cells have the capacity to signal to dorsal cells as well. Vein-like structures (as determined by darker cuticle pigmentation and increased hair density) can also develop when transplanting ventral fragments of pre-eversion discs into metamorphosing hosts (Milan et al., 1997). In such cases dorsal-ventral apposition is precluded, yet ventral vein structures still appear able to differentiate. Furthermore, when dorsal identity is lost in *ap* mutants, expression of factors downstream of *ap* creates wings of 'double ventral' identity, showing the ventral arching pattern on both surfaces (O'Keefe and Thomas, 2001). These wings differentiate ventral vein structures in the absence of any dorsally derived inductive signal. In terms of the inductive signals themselves, it has further been shown that clones mutant for BMP ligands only lead to vein loss when covering *both* surfaces of the vein (de Celis, 1997; Ray and Wharton, 2001). This would suggest that ligand expression in *either* dorsal or ventral layer is sufficient to promote vein development in both layers. The discord between these reports and the interplanar induction model led to a reappraisal of the role of interplanar signalling in vein development.

In the other dimension of signalling, intraplanar signalling, pupal wing development involves a shift in the range of BMP ligands. Dpp forms a long range gradient in the disc that promotes growth and patterning (Affolter and Basler, 2007). However, in the pupal wing *dpp* expression is limited to the regions of pathway activation, the veins (Yu et al., 1996; Conley et al., 2000; Ray and Wharton, 2001). A potential limit to the range of Dpp in the pupal wing is the heightened expression of *tkv* in the provein regions that may act as a barrier to diffusion, trapping the ligand without transducing the signal (Sotillos and de Celis, 2005). It is not known whether ectopic Dpp or Gbb is capable of inducing signalling in a paracrine fashion in the intervein, and if so at what range. To address the range of signalling in the wing, in this Chapter we generate clones of cells in the intervein expressing these components, and assess the effect on the fate and differentiation of neighbouring cells. These also allow us to address the relationship between intraplanar and interplanar signalling, by assessing the behaviour of cells in the opposing layer.

III. Results

Investigating the interplanar requirements of PCV patterning genes

To investigate the interplanar requirements of PCV patterning genes, we specifically reduce gene function in one layer, leaving the other wild type. This is achieved by three methods. Firstly, clonal analysis allows for the generation of patches of homozygous mutant tissue in otherwise heterozygous animals (Xu and Rubin, 1993). We compare the phenotypic consequences of clones that cover either the dorsal or the ventral layer only ('single sided') with those that cover both ('double sided'). Secondly, in 'dorsal rescue' experiments we utilise the Gal4/UAS system (Brand and Perrimon, 1993) to drive expression of the wild type gene in the dorsal compartment in otherwise homozygous mutant animals. Thirdly, to determine the effect of providing the wild type gene product exclusively in the ventral layer, we drive the expression of *dsRNA* in the dorsal layer to knockdown gene function only in dorsal cells ('dorsal knockdown').

The results of such experiments allow us to distinguish between alternate models of interplanar signalling. If signals from one layer are required to promote vein development in the opposite layer, as would be the case if directional interplanar induction occurred, loss of gene function in one layer only will result in loss of vein in both layers. Alternatively, if vein development proceeds autonomously in either layer, loss of gene function in one layer will only affect vein structures in that layer. Finally, if loss of function from one layer is compensated by the function of the gene in the opposite layer, only loss of function in *both* dorsal and ventral layers will lead to vein loss. The phenotypic outcomes of these experiments can therefore reveal the role that interplanar signalling plays in vein development.

Extracellular BMP components can function from either layer to promote PCV development

cv clones were reported to lead to the loss of the PCV when they covered the dorsal surface (Garcia-Bellido, 1977). However, clones of ligands of the same pathway (*dpp* and *gbb*) were not (de Celis, 1997; Ray and Wharton, 2001). Considering this inconsistency, we reappraised the role of interplanar BMP signalling in PCV development. It was previously shown that *gbb*

could function from either layer to promote vein development (Ray and Wharton, 2001), and we sought to confirm this result by generating clones of a different, molecularly defined loss of function (LOF) allele, gbb^{D20}. Out of a total of 81 clones analysed, 11 completely covered both dorsal and ventral surfaces of the PCV region, and all led to complete vein loss (Fig. 5.1 A). In contrast, clones which covered the dorsal (Fig. 5.1 B) or ventral (Fig. 5.1 C) surfaces only did not lead to vein loss (dorsal: 5/5 clones; ventral: 8/8 clones). Thus, as was previously described, *gbb* function is only required in one layer of the pupal wing to suffice for its function. Loss of *gbb* from one layer is compensated by its presence in the opposite layer.

To re-evaluate the role of *cv*, we first performed a dorsal rescue experiment, asking whether dorsally expressed *cv* could rescue the mutant phenotype. We generated males hemizygous for a *cv* null allele in which expression of wild type *cv* was driven in dorsal cells by *ap-Gal4.* Control animals, which lack Gal4 and hence in which *UAS-cv* is silent, show loss of the PCV as assessed both by light microscopy (Fig. 5.1 D) and SEM (Fig. 5.1 F). However, when *cv* is expressed in the dorsal layer with *ap-Gal4*, wings show complete rescue of the PCV (Fig. 5.1 E; complete PCV in 50/50 wings). When the ventral surface of the adult wing is viewed with SEM, the wild type vein morphology is observed (Fig. 5.1 G, compare to Fig. 3.1 F). The ventral layer, which is mutant for *cv*, secretes a wild type cuticle as a result of the expression of *cv* in the dorsal layer.

We next used RNAi to knock down *cv* function. Expression of *cv dsRNA* (VDRC# 9727) with the wing general *A9-Gal4* driver led to variable loss of the PCV (Fig. 5.1 H) particularly in males (as *A9* is an X-linked insertion), as well as ectopic venation around the distal tip of L5. When expression levels are increased by raising animals at 29ºC, all males completely lack the PCV and the majority of females show partial PCV loss (see Table A.5 in the Appendix). In contrast, driving *dsRNA* in the dorsal layer using *ap-Gal4* does not lead to the loss of the PCV, even at 29ºC (Fig. 5.1 I). The same result was observed when using a different *dsRNA* insertion (VDRC #9729, Table A.5). Thus, in contrast to knockdown of *cv* in both dorsal and ventral layers, knockdown of *cv* function in the dorsal layer does not affect PCV development; wild type *cv* function in the ventral layer suffices for function. In conjunction with the dorsal rescue experiment, this shows that *cv* is only required in one layer of the pupal wing for PCV development.

crossveinless-2 (*cv*-2) is another extracellular modulator of BMP signalling required for pathway activation in the PCV (Conley et al., 2000; Serpe et al., 2008), the interplanar requirements of which have not yet been addressed. We first performed a dorsal rescue

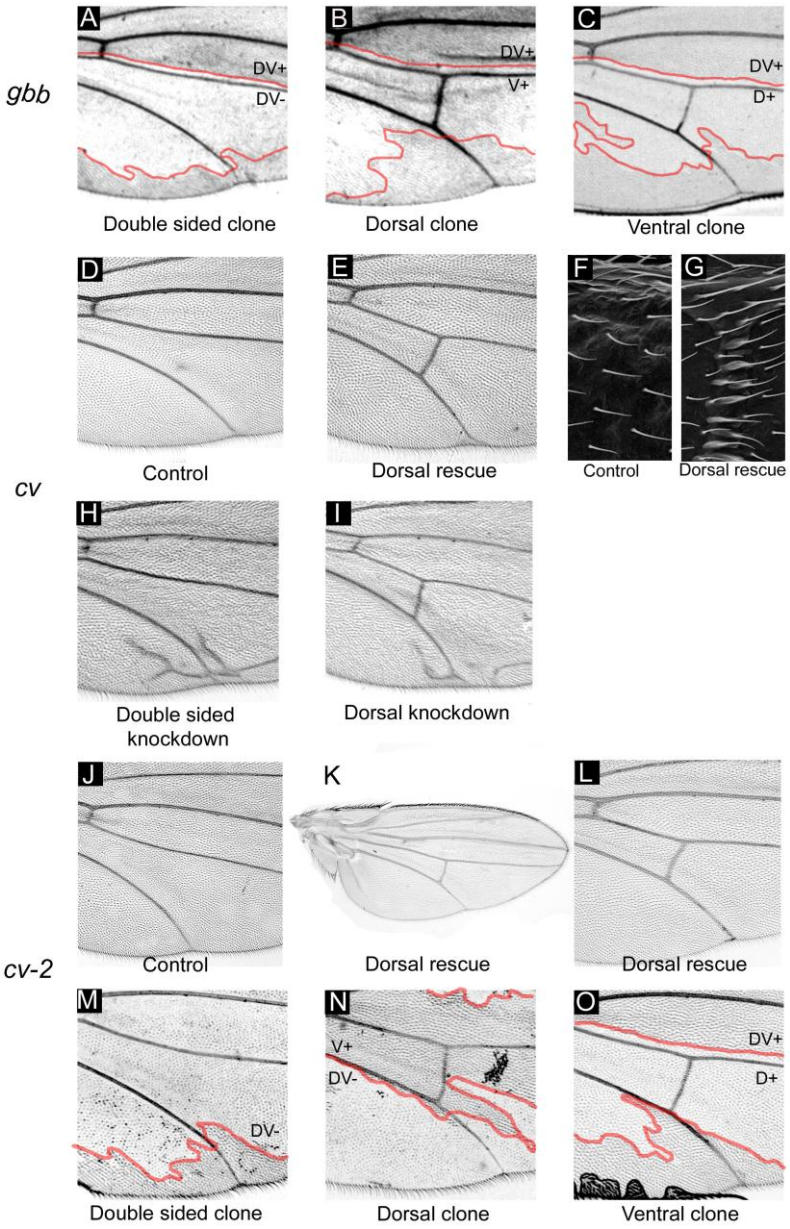

Figure 5.1. Extracellular BMP components can signal from either layer in PCV development. (A-C) The effects of *gbb*^{D20} clones, marked with *shavenoid*, on the PCV. Clones are outlined in red, and the genetic constitution of the territories on either surface is indicated (DV+ = wild type both surfaces; D+ = ventral clone, V+ = dorsal clone, DV- = double-sided clone). Loss from both layers leads to PCV loss (A), whereas single-sided dorsal (B) or ventral (C) clones have no effect. (D-G) *cv* dorsal rescue experiment. (D) Control *cv*^{43}*/Y ; UAS-cv/Sp Bl L* males show PCV loss. (E) Dorsal expression of *cv* in *cv*^{43}*/Y ; UAS-cv/ap-Gal4* males leads to PCV rescue, showing that dorsal expression of *cv* is sufficient for function. (F, G) SEM images of the PCV at its junction with L4, from wings of the genotypes in D and E respectively, showing full rescue of PCV annulation when *cv* is dorsally expressed. (H-I) *cv* dorsal knockdown experiment. (H) *A9-GaL4 > UAS-cv dsRNA* flies lack the PCV. (I) Dorsal *RNAi* in *ap-GaL4 > UAS-cv dsRNA* does not affect the PCV. (J-L) *cv-2* dorsal rescue experiment. (J) Control *cv-2*^{K61}*/cv-2*^{K74}*, UAS-cv-2* flies show PCV loss. (K) Dorsal expression of *cv-2* in *cv-2*^{K61}*, ap-Gal4/cv-2*^{K74}*, UAS-cv-2* flies leads to altered wing shape, but wild type PCV. (L) At 18ºC, PCV rescue is still complete. (M-O) The effects of *cv-2* ^{K74} clones, marked with *shavenoid*, on the PCV, marked as indicated above for *gbb* clones. Loss from both layers leads to PCV loss (N), whereas single sided dorsal (O) or ventral (P) clones have no effect.

experiment. Control flies (null for *cv-2* and carrying the *UAS-cv-2* insertion but not Gal4) display a completely penetrant PCV loss phenotype (Fig. 5.1 J), with variable expressivity related to sex (small vein remnants seen in 16/19 male wings, and 3/31 female wings). In contrast to *cv*, ectopic expression of *cv-2* produced dominant phenotypes: wings were smaller and almond-shaped (Fig. 5.1 K). The reduction in size and shape of the wing may derive from ectopic Cv-2 interfering with BMP signalling in the larval wing disc, as it has been shown that high levels of Cv-2 and its vertebrate orthologue can antagonise BMP signalling, presumably by binding ligands (Binnerts et al., 2004; Ambrosio et al., 2008; Serpe et al., 2008). Regardless of the effect on overall wing morphology, dorsal expression of *cv-2* rescued PCV loss, both at 25ºC (Fig. 5.1 K; 17/19 wings showed a complete PCV, 2/19 showed a small gap between the PCV and L4), and at 18ºC, at which temperature the dominant phenotypes were less severe (Fig. 5.1 L; 45/48 wings showed a complete PCV; 3/48 showed a slight gap between the PCV and L4). Thus, dorsal expression of *cv-2* is sufficient for its function.

Dorsal knockdown experiments were not possible, as the one available *cv-2 dsRNA* line (VDRC #2938) gave no phenotype even when driven ubiquitously throughout development, so LOF clones were generated. In 78 clones analysed, vein loss was only observed in double-sided clones (Fig. 5.1 M). As with *gbb, cv-2* clones covering the entire dorsal (Fig. 5.1 N, n=5) or ventral (Fig. 5.1 O, n=8) surface did not lead to vein loss. In the course of these experiments, it was reported that single-sided *cv-2* clones do not affect pMad accumulation in the PCV (Serpe et al., 2008), which corroborates our data. In sum, *cv-2* expression is only required in one layer of the pupal wing for PCV development.

These results show that all tested members of the BMP extracellular signalling cassette show the same behaviour: wild type function in one layer is sufficient, and it does not matter which layer is wild type. This is inconsistent with the dorsal to ventral induction model (as ventrally secreted proteins are also capable of rescue). Considering this behaviour, we can propose two alternate underlying mechanisms. First, proteins secreted from the wild type layer are able to promote signalling in the opposite layer, potentially by diffusing across the lumen or via the regions of basal contact identified in Chapter 3. According to this 'direct' mechanism, interplanar signals directly induce vein development in the mutant layer. The second potential mechanism is that the promotion of vein development in the wild type layer indirectly leads to the adoption of the vein program in the opposite layer. This may arise if, for instance, intervein development in the pupal wing is critically dependent on the re-formation of basal contacts with the opposite layer at reapposition; the failure to form these contacts would switch cells

onto the vein program. Experiments designed to test direct versus indirect signalling are described below.

Dg and *Dys* can function from either layer to promote PCV development

We next addressed the interplanar requirements of other crossvein patterning genes. As described in Chapter 1, *Dystroglycan* (*Dg*) and *Dystrophin* (*Dys*) are required for the maintenance of BMP signalling in junctions of the PCV with L4 and L5. *Dg/Dys* mutants show variable PCV loss phenotypes, most commonly leaving a detached fragment of venation between L4 and L5 (Christoforou et al., 2008). As Dg is a transmembrane protein, and Dys a cytoplasmic protein, it was of interest to see how these non-secreted proteins behaved in similar tests for interplanar function.

To address the interplanar requirements for Dys, we utilised two *dsRNA* lines: one which targets Exon 4 (Dys Ex4 RNAi), hence targeting the long isoforms, and one which targets all isoforms (Dys COOH RNAi; van der Plas et al., 2007). When crossed to a variety of drivers, each shows variable crossvein loss (Table A.7; Fig. 5.2 D, E). Ubiquitous expression with *Act5C-Gal4* led to variable PCV loss phenotypes in 93.91% of wings with Ex4 RNAi (7/115 wild type, 64/115 gapped, 42/115 detached, 2/115 point) and 100% of wings with COOH RNAi (118/357 detached, 236/357 point, 3/357 crossveinless) of wings scored (Fig. 5.2 A). Similarly, when crossed to *sal-Gal4*, both lines lead to loss of the PCV specifically within the *sal* domain, in 61% of wings with Ex4 RNAi (n=110) and 100% with COOH RNAi (n=133) of wings scored (Fig. 5.2 B). However, when *RNAi* is induced dorsally with *ap-Gal4*, wings were wild type in 100% (Ex4 RNAi, n=109) and 99.29% (COOH RNAi, 422/425 wild type, 2/425 gapped, 1/425 detached) of cases (Fig. 5.2 C-E). Thus, whereas knockdown of *Dys* function in both layers leads to PCV loss, dorsal knockdown does not affect PCV development.

To test the interplanar requirements of *Dg*, Dg^{O86} clones were analysed. In 32 clones analysed which overlapped the PCV, vein loss was only observed when clones were double sided (Fig. 5.2 F). These double-sided clones recapitulate the null *Dg* phenotype in leaving a detached fragment of vein between L4 and L5 (Christoforou et al., 2008). Where the entire dorsal (n=4) or ventral (n=2) surface was mutant, the PCV was wild type (Fig. 5.2 G, H). Thus, like *Dys*, *Dg* can function in either layer alone to promote PCV development.

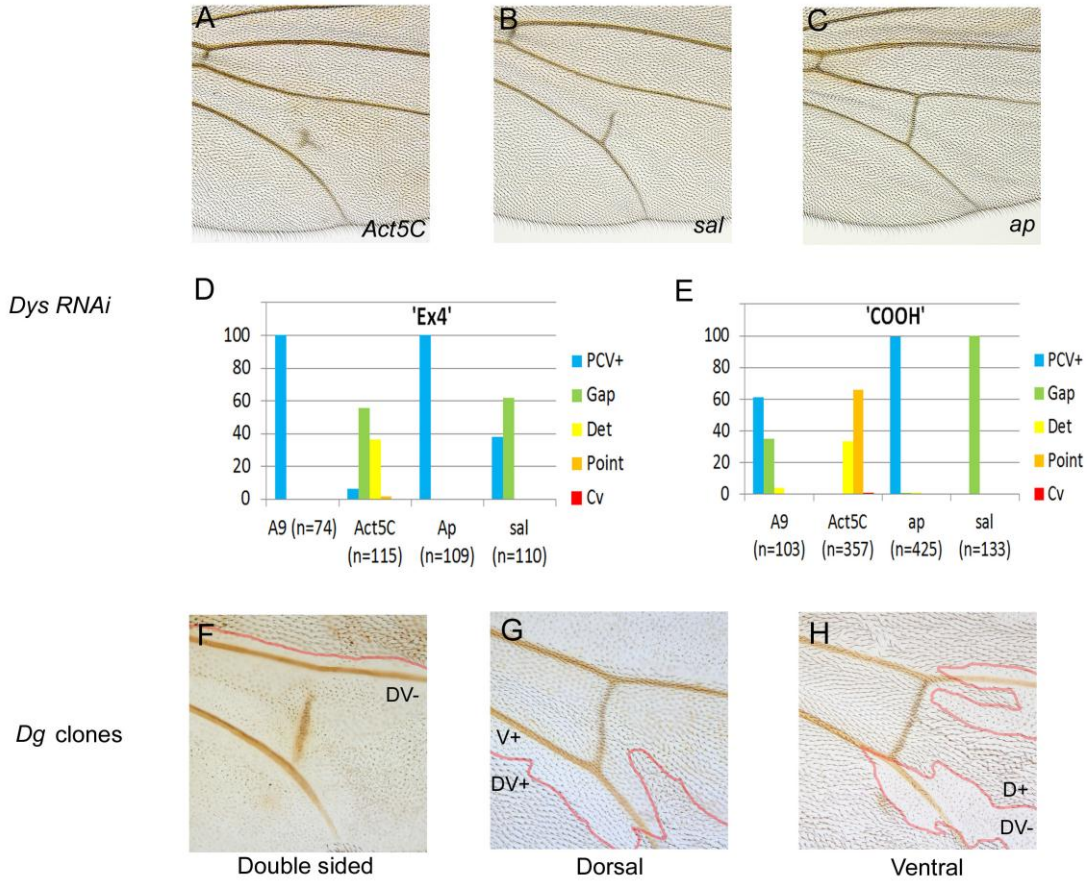

Figure 5.2. *Dys* and *Dg* can function from either layer. (A-E) Phenotypic effects of driving *Dys dsRNA* with various drivers. Two lines were utilised: COOH, which targets all transcripts, and 'Ex4', which targets the long isoforms (van der Plas, et al. 2007). (A) 'COOH' RNAi driven ubiquitously with *Act-5C-Gal4* leads to substantial PCV loss. (B) 'COOH' RNAi driven in the middle of the wing with *sal-Gal4* leads to autonomous PCV loss within the *sal* domain. (C) 'COOH' RNAi driven dorsally with *ap-Gal4* does not lead to vein loss. (D-E) Distribution of phenotypes, as shown as a percentage of total wings scored, for the two RNAi lines with the various drivers tested (drivers and n numbers indicated on X axis). Phenotypes are classed as in Christoforou, et al (2008), and colour coded in order of severity: wild type (blue), gap between L4/5 and the PCV (green), detached island of venation (yellow), small point of vein (orange), crossveinless (red). Note that for both RNAi lines, dorsal expression does not lead to PCV loss. (F-G) The effects of Dg^{086} clones, marked with *shavenoid*, on the PCV. Clones are outlined in red, and the genetic constitution of the territories on either surface is indicated (DV+ = wild type both surfaces; D+ = ventral clone, V+ = dorsal clone, DV- = double-sided clone). Loss from both layers leads to the detached phenotype typical of null alleles (F), whereas single sided dorsal (G) or ventral (H) clones do not lead to vein loss.

How then can the transmembrane Dg/Dys complex function in one layer to compensate for their loss in the opposite layer? To account for this behaviour, we can consider the fact that the output of Dg/Dys in the PCV is the maintenance of BMP signalling. Genetic interactions suggest that Dg/Dys antagonises Notch activity (Christoforou et al., 2008), and this antagonism would in turn lead to a reduction in *tkv* expression, relieving the block to Dpp diffusion. Dpp diffusing from the adjacent longitudinal veins thus promotes pathway activity to complete the PCV. In the absence of Dg/Dys, Notch activity is still high, and provein suppression of vein development continues. As a result, vein development is restricted to the middle of the intervein in a detached fragment. Considering this model, if Dg/Dys is lost from one layer, Dpp in the wild type layer would diffuse within the epithelium to connect the PCV to the adjoining longitudinal veins. Extracellular BMP proteins can promote signalling in the opposite tissue (Fig. 5.1; de Celis, 1997; Ray and Wharton, 2001), so Dpp may also able to promote signalling in the provein region of the opposite *Dg/Dys* mutant tissue. According to this model Dpp from the same source promotes venation in both the intraplanar and interplanar dimensions, and Dpp is therefore the 'interplanar output' of Dg/Dys function in the wing.

Domineering interplanar non-autonomy of *cv-c*

The final crossvein patterning gene tested was *cv-c. cv-c* has been characterised as a RhoGAP (Denholm et al., 2005), and hypomorphs display a variable PCV loss phenotype (Lindsley and Zimm, 1992), but its role in PCV development is not known, and the focus of the following Chapter. Here, we address the interplanar requirements of *cv-c* in PCV development. We first attempted a dorsal rescue experiment, but the lethality and dominant phenotypes that arise from dorsal expression of *cv-c* made this unfeasible (see Table A.8 in the Appendix). We then performed dorsal knockdown, using a *dsRNA* line which has previously been shown to phenocopy *cv-c* mutants (Denholm et al., 2005; see also Chapter 6). As a control, RNAi was induced in both layers. *en-Gal4* drives expression throughout posterior compartment, and such wings show loss of most of the PCV (Fig. 5.3 A). Similarly, when driven in the middle of the wing with *sal-Gal4*, we observe loss of the PCV autonomously within the *sal* domain (Fig. 5.3 B). Thus, knocking down *cv-c* function in both layers of the pupal wing leads to autonomous loss of vein material. Dorsal knockdown with *ap-Gal4* was partially lethal, with the Gal4>RNAi class eclosing at 73.82% of the control balancer class (n=1248 flies scored). Of these animals, only 4/293 wings showed a wild type PCV. The rest showed three principal phenotypes: partial PCV loss, most commonly seen as gaps between the PCV and L4 (Fig. 5.3 C; 89/293 wings

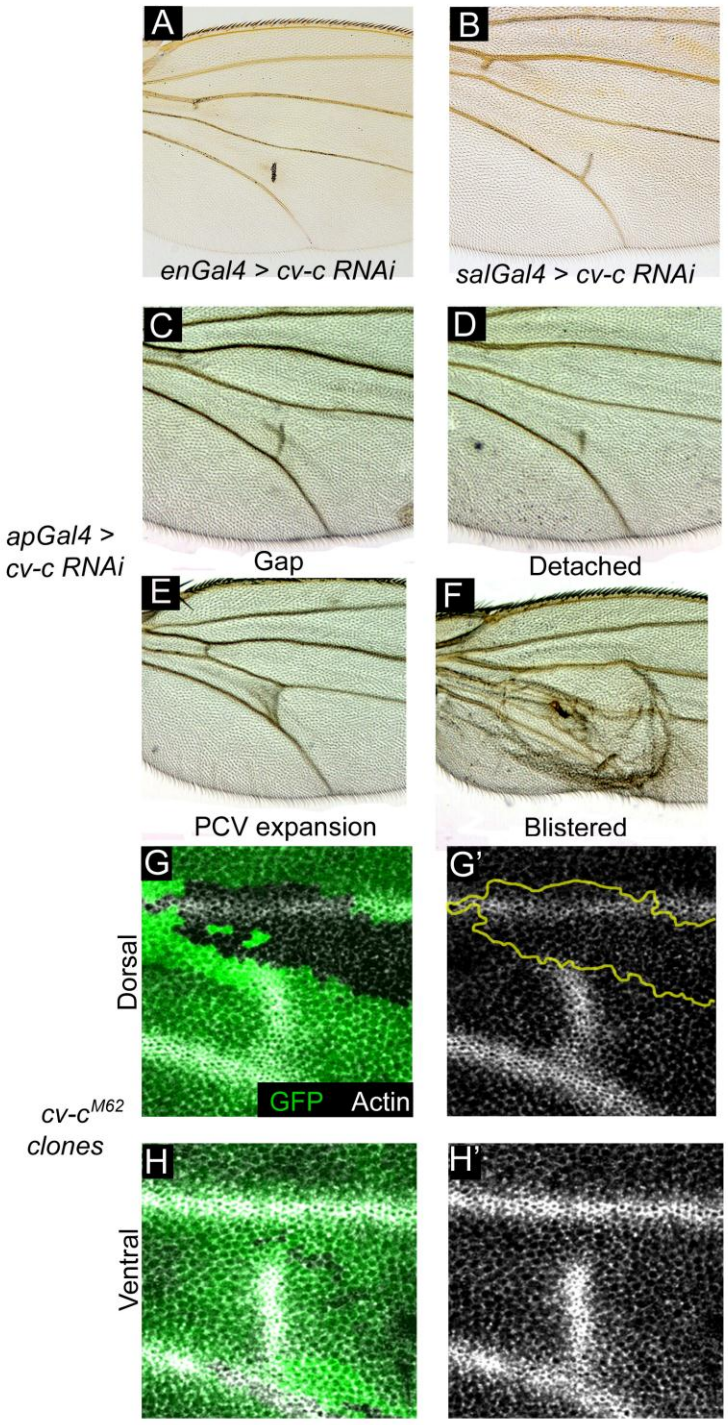

Figure 5.3. Domineering interplanar non-autonomy of *cv-c.* (A-F) Wing phenotypes resulting from *cv-c RNAi.* (A) *RNAi* in the posterior compartment driven by *en-Gal4* leads to a detached phenotype. (B) *RNAi* driven in the middle of the wing with *sal-Gal4* leads to autonomous vein loss within the *sal-Gal4* domain. (C-F) *RNAi* driven in the dorsal compartment with *ap-Gal4* leads to gaps in the PCV (C), a detached phenotype (D), the expansion of PCV material (E) and wing blistering (F) (proportions and n numbers in the text). (G-H') *cv-c*^{M62} clones, marked by the absence of GFP (green), in the pupal wing, and stained for Actin (white). A clone covering the anterior half of the dorsal layer of the PCV (G, clone outline shown in yellow in G') leads to loss of apical enrichment of Actin in both dorsal (G') and ventral (H') layers, even though the ventral layer does not show any clones (H).

scored) or as a detached island of venation (Fig. 5.3 D; 44/293); the broadening and loss of definition of the PCV territory (Fig. 5.3 E; 98/293); and blistering between the wing surfaces (Fig. 5.3 F; 58/293). The cause of the ectopic blistering is unclear, but is unlikely to reflect a role for Cv-c in maintaining apposition (see Chapter 6). In terms of the gap and detached phenotypes, loss of Cv-c function in one layer can lead to the loss of PCV both autonomously within that layer, and also dominantly inhibits PCV development in wild type cells of the opposite layer.

To address whether this behaviour was seen in both directions, we generated LOF *cv-c* clones and observed the effects in the pupal wing. To assess vein development we stained for Actin, which is apically enriched in vein cells (Fristrom et al., 1994). Clones only led to defects in Actin localisation when covering the crossveins. Seven clones were recovered which covered segments of the PCV, all of which led to the loss of apical enrichment of Actin. Importantly, this loss was seen both autonomously within the bounds of the clone (Fig 5.3 G, G'), and non-autonomously in the opposite, wild type layer (Fig. 5.3 H, H'). This effect was seen for both dorsal clones (n=4) and ventral clones (n=3), showing that *cv-c* loss from either layer leads to the non-autonomous inhibition of vein development in the opposite layer. The clones are further described in Chapter 6.

cv-c is thus unique amongst crossvein patterning genes in that it displays domineering non-autonomy. Wild type tissue in one layer cannot compensate for loss of *cv-c* in the opposite layer, and indeed the wild type tissue itself cannot develop as vein in the absence of *cv-c* function in the opposite layer. We will describe in Chapter 6 how Cv-c is a RhoGAP that acts to inhibit the activity of Rho1 and its effector Rok specifically in the PCV region. Importantly, Rok shows the same domineering non-autonomous inhibition of vein development when hyperactivated in one layer. Because its targets show the same behaviour, we can propose that Cv-c loss in one layer leads to Rho1/Rok hyperactivation, which in turn inhibits vein development in the opposite layer. How Rho1/Rok does this is unclear, but it may involve promoting the extension of basal processes typical of intervein cells, which could be capable of dominantly inducing the adoption of intervein fate in the opposite layer (see Chapter Summary).

Consequences of inhibiting BMP signal transduction in one layer

In the previous experiments, vein development is promoted in both layers by signalling molecules from one layer. We next addressed the consequences of inhibiting the transduction of BMP signals in one layer, by affecting cell autonomous components of the pathway. We performed dorsal knockdown experiments using *dsRNA* for the receptor *tkv* and the receptor-Smad *Mad*. Expression of these constructs throughout development with *ap-Gal4* is lethal or produces small and dark wings in which vein phenotypes could not be distinguished (Table A.6). We therefore used *Gal80^{ts}* to limit expression to the pupal period, and assessed the effects on cell shape (using Cad-GFP) and cell fate (by analysing *DSRF* expression) in the pupal wing. As described in Chapter 3, ubiquitously expressed Cad-GFP shows the same localisation as endogenous Cadherin, namely showing enrichment at the apical adherens junctions (O'Keefe et al., 2007), and we have also found it to be a useful marker of apposition in basal sections. *DSRF* is expressed in intervein cells where it is required for intervein development (Montagne et al., 1996), and is repressed in vein cells by the activity of EGFR and BMP pathway activity (Roch et al., 1998; Conley et al., 2000), so it is used as a marker for intervein fate in the wing.

When induced ubiquitously during pupal development with *Act5C-Gal4*, *Mad RNAi* leads to the loss of well-defined stripes of apically constricted vein cells in both dorsal (Fig. 5.4 A) and ventral (Fig. 5.4 A'') layers (compare with Figure 5.4 B). In particular, apical constriction in the PCV region is entirely absent (arrow in Fig. 5.4 A). In basal sections we observe the loss of the vein lumen in the distal portions of L4 and L5, and in the PCV (Fig. 5.4 A'). We next expressed *Mad dsRNA* in the dorsal layer. This leads to a reduction of apical constriction throughout the dorsal layer (Fig. 5.4 C), and loss of the PCV and distal L4 and L5 as assessed with *DSRF* (Fig. 5.4 C''). However, the ventral layer develops normally: apical constriction in all veins is seen (Fig. 5.4 D), as well as a wild type pattern of *DSRF* expression (Fig. 5.4 D'). Thus, *Mad RNAi* in the dorsal layer leads to autonomous vein loss. In these wings, dorsal cells are unable to transduce any potential rescuing signal from the opposite layer, and are thus 'deaf' to interplanar signals from the wild type, ventral layer. However, ventral vein differentiation is unaffected.

Dorsal expression of *tkv dsRNA* shows similarities and differences to *Mad dsRNA*. In the dorsal layer, the stripes of apical constriction and heightened Cad-GFP from the veins are reduced, particularly in distal sections of the wing (Fig. 5.5 A). Furthermore, *DSRF* expression is expanded into these domains (Fig. 5.5 A'), showing that they have adopted intervein fate. In contrast, the ventral layer shows constricted stripes of vein cells (Fig. 5.5 B) that repress *DSRF* (Fig. 5.5 B'). In Z section, the autonomous expansion of *DSRF* expression into the vein territories of the dorsal layer is clearly evident (arrows in Fig. 5.5 C'). Although vein

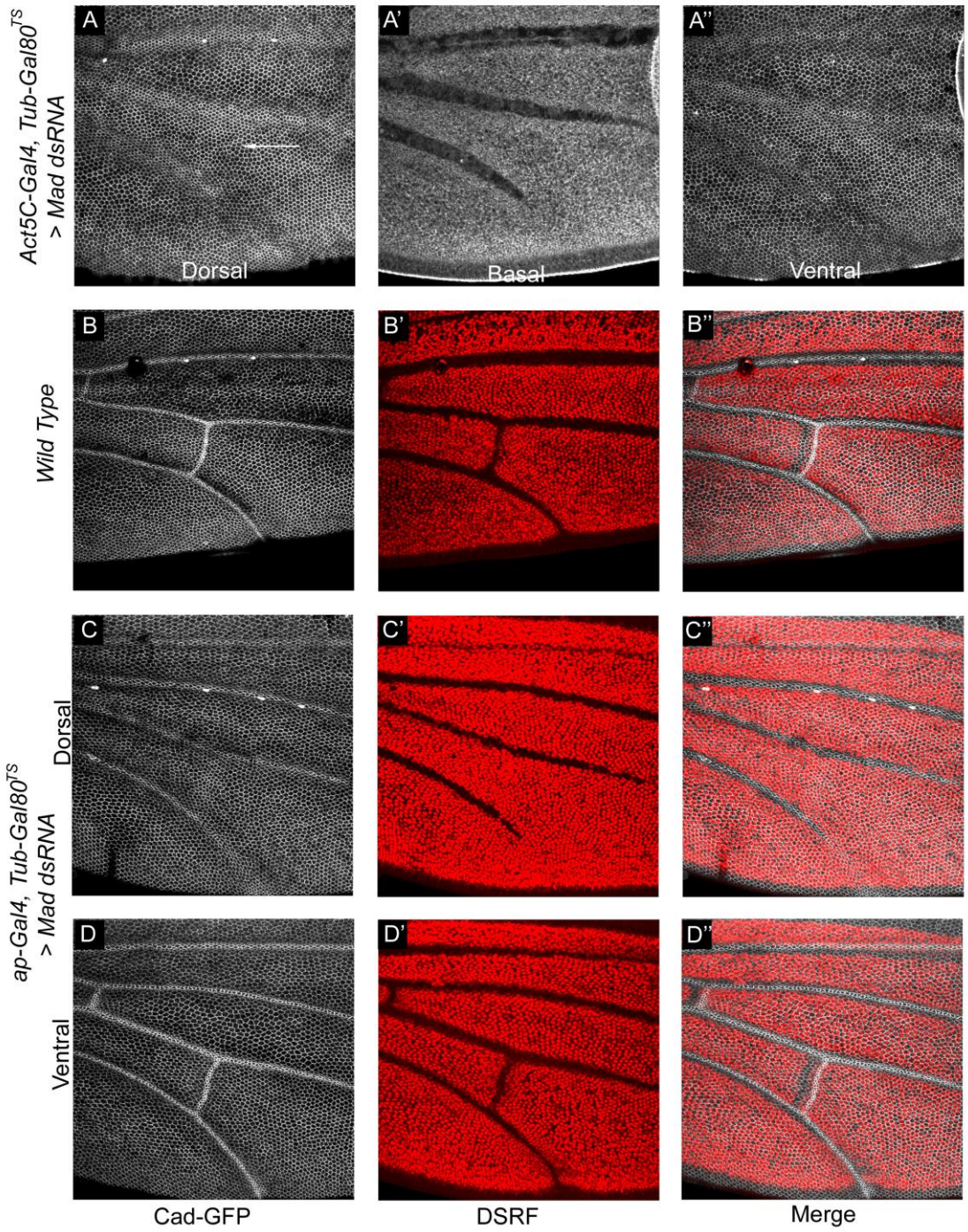

Figure 5.4. Dorsal expression of *Mad dsRNA* causes autonomous vein loss. (A-A'') Vein loss in animals of the genotype *Act5C-Gal4/Ubi-DECad-GFP, UAS-Mad-dsRNA ; TubGal80^{ts}/+* raised at 18ºC until the WPP stage, and shifted to 29ºC until dissection at 32h APF. Vein loss is seen as a loss of constriction apically, in the dorsal (A) and ventral (A'') layers, as well as a loss of lumen in basal sections (A'), in the PCV and distal L4 and L5. n=4 wings analysed. (B-B'') Control wing showing apical constriction as shown by Cad-GFP (B) and *DSRF* expression (B'), with *DSRF* expression limited to relaxed, intervein cells (merge in B''). (C-D'') Effects of dorsal expression of *Mad dsRNA.* (C-C'') In the dorsal layer, constriction is diminished (C) and *DSRF* expression is expanded as compared to wild type (C'), C''). In the ventral layer, both constriction (D) and *DSRF* expression (D') are wild type. n=5 wings analysed.

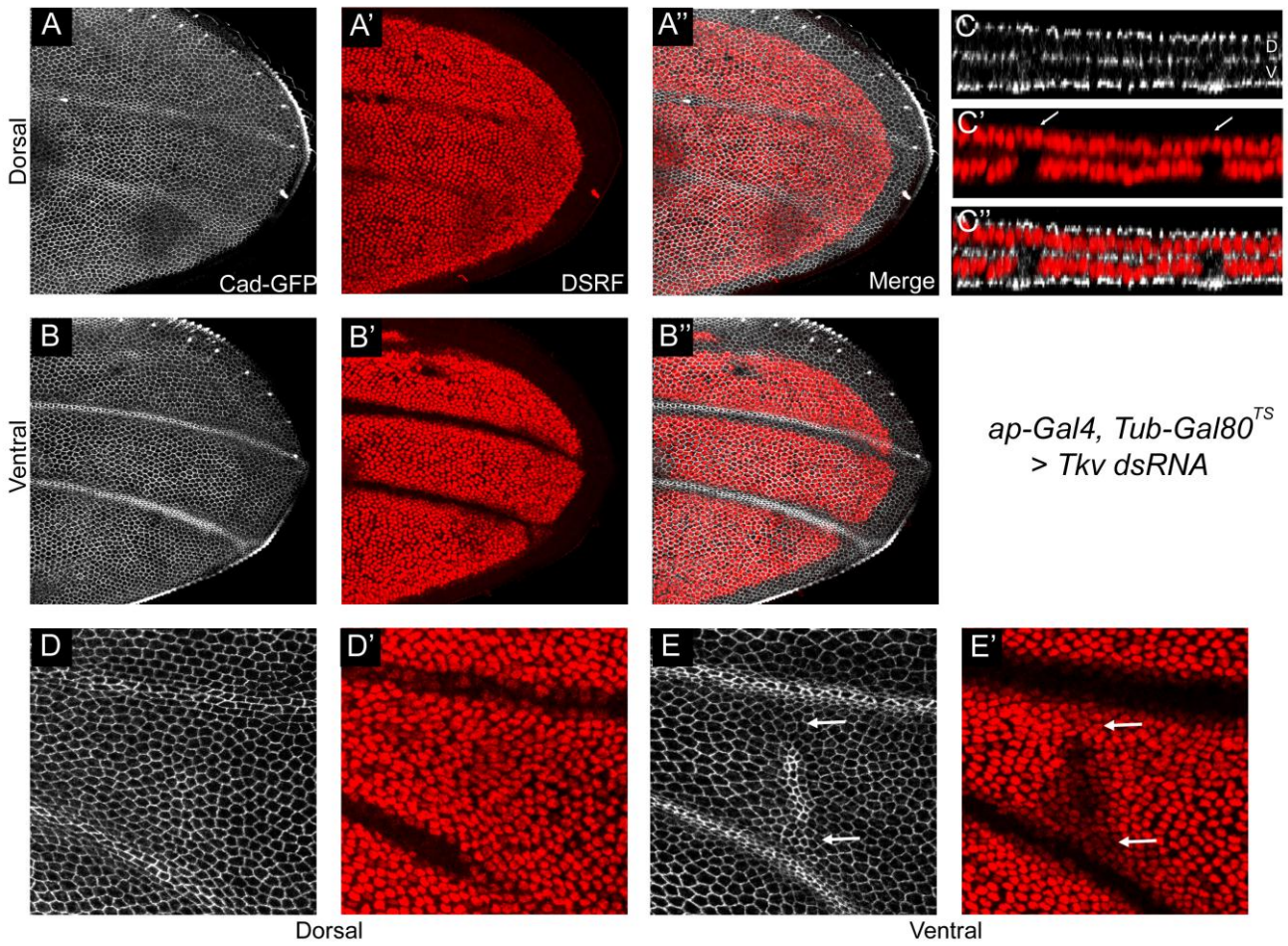

Figure 5.5. Dorsal expression of *tkv dsRNA* causes non-autonomous vein widening and PCV loss. (A-B'') Cad-GFP (A, B) and *DRSF* expression (A', B') in animals of the genotype *ap-Gal4/Ubi-DECad-GFP, UAS-tkv-dsRNA ; TubGal80^{ts}/+* raised at 18ºC until the WPP stage, and shifted to 29ºC until dissection at 32h APF. In the dorsal layer, constriction is diminished (A) and *DSRF* expression extends throughout the distal wing (A', A''). In the ventral layer, vein constriction is broader (B), and *DSRF* expression is confined to intervein regions (B', B''). (C-C') Z section showing autonomous *DSRF* expansion into vein territories in the dorsal (D) layer (arrows). Ventrally (V), *DSRF* is repressed in the vein regions. (D-E') Higher magnification of PCV in wings of the same genotype. (D-D') Dorsal layer shows loss of the PCV and diminishment of L4 and L5. (E-E') Ventral layer, showing loss of PCV in anterior and posterior regions (arrows), and broadening of L4 and L5. n=7 wings analysed.

differentiation in the ventral layer is largely normal, it differs in two respects. Firstly, ventral veins are broadened (e.g. L4 in Fig. 5.5 E), suggesting that loss of *tkv* in one layer interferes with the regulation of vein width in the opposite layer. How could vein loss in one layer be accompanied by vein expansion in the opposing layer? Here we can recall that as well as promoting vein development, Tkv also functions in the provein to antagonise vein development, and loss of *tkv* leads to an expansion of *dpp* expression (de Celis, 1997). If, in addition to the loss of constriction, the provein domain in dorsal cells is lost, this may lead to an expansion of *dpp* expression in dorsal cells (without levels of Tkv necessary to transduce the signal into an expansion of the vein). As a result, Dpp would be able to induce the widening of the vein domain in the opposite layer. This model is supported by experiments using *Notch RNAi*, as detailed below.

Dorsal *tkv RNAi* also affects the development of the ventral PCV: constriction is lost in the anterior and posterior regions of the PCV (arrows in Fig. 5.5 E) leaving a detached island of constriction and a corresponding expansion of *DSRF* expression (arrows in Fig. 5.5 E'). This effect is specific to *tkv*, as PCV loss from dorsal *Mad* (Fig. 5.4) or *Egfr RNAi* (see below) does not affect vein development in the ventral layer. We had previously suggested a model whereby PCV development requires the creation of a sharp distinction between regions of high and low signalling (see Chapter 4). If reducing Tkv function in the dorsal layer leads to an expansion of *dpp* expression, this would in turn induce signalling in the opposing layer, which might abolish the distinction between high and low levels of signalling in the ventral cells. However, this model would predict that the similar expansion of the proveins in *Notch RNAi* would also inhibit ventral vein development; we will show below that it does not. Thus, expansion of the proveins cannot explain PCV loss following dorsal *Tkv RNAi*. A potential mechanism, involving a link with Cv-c (which as discussed above also shows such domineering non-autonomy), is discussed in the Chapter Summary.

Egfr knockdown leads to autonomous vein loss

Both the EGFR and BMP pathways are required for pupal vein development (Yu et al., 1996; Guichard et al., 1999), and we next asked whether knocking down EGFR signal transduction would have the same effect as that of BMP. Expressing *Egfr dsRNA* throughout the posterior compartment with *en-Gal4* leads to a complete loss of L4, the PCV and L5 in the adult wing

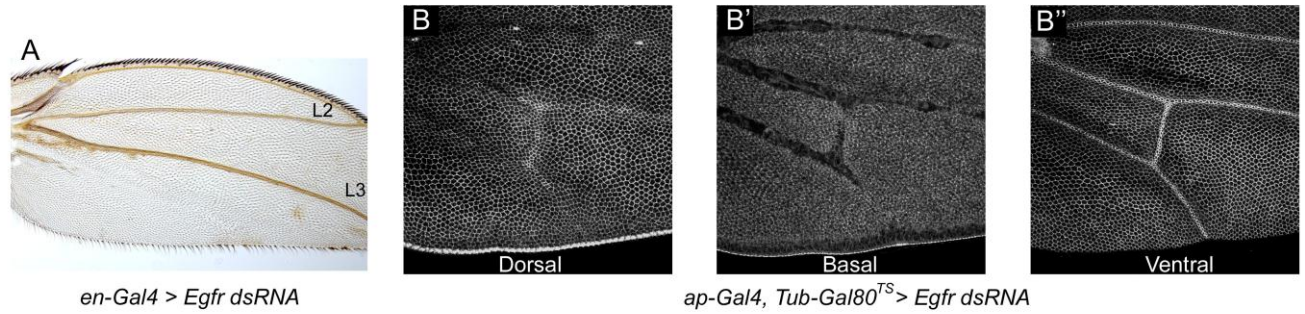

Figure 5.6. Dorsal expression of *Egfr dsRNA* causes autonomous vein loss. (A) *en-Gal4 > UAS-Egfr-dsRNA* animals raised at 25ºC show reductions in size of posterior compartment and complete loss of posterior veins in the adult wing (remaining anterior veins L2 and L3 are labelled). (B-C') Animals of the genotype *Act5C-Gal4/Ubi-DECad-GFP, UAS-Egfr-dsRNA ; Tub-Gal80^{ts}/+* raised at 18ºC until the WPP stage, and shifted to 29ºC until dissection at 32h APF. Dorsal loss of venation in seen in apical sections (B), and basal sections show an expansion of apposition (B'). However, ventral vein differentiation is unaffected (B''). (C-C') High magnification of apical sections in distal L3-L4 region, showing dorsal (C) and ventral (C') layers. n=8 wings analysed

(Fig. 5.6 A), as well as a reduction in compartment size consistent with the requirement for *Egfr* in cell viability (Diaz-Benjumea and Garcia-Bellido, 1990). This shows that, as expected, loss of Egfr function from both layers with *RNAi* leads to vein loss. We next limited RNAi to the dorsal layer of the pupal wing. Such wings show loss of clearly-defined constricted vein stripes in the dorsal layer (Fig. 5.6 B). In basal sections, we observe partial loss of the lumen (Fig. 5.6 B'), which is most evident in distal sections of the wing. In contrast to the dorsal layer, vein constriction occurs as in wild type in the ventral layer (Fig. 5.6 B''). At higher magnification we see the failure of vein differentiation in the dorsal layer (Fig. 5.6 C), and the wild type pattern of ventral vein differentiation (Fig. 5.6 C').

Thus, loss of EGFR signalling in one layer does not affect the development of veins in the other layer, which is consistent with reports that *Egfr* mutant clones appear to have surface-autonomous effects on venation (Diaz-Benjumea and Garcia-Bellido, 1990). This is in contrast to the proposed role for the EGFR pathway activator *rho* in dorsal to ventral induction (Garcia-Bellido, 1977; Guichard et al., 1999). *rho* expression requires the activation of the EGFR pathway (Martin-Blanco et al., 1999), so loss of *Egfr* function in one layer would lead to a concomitant loss in *rho* expression. As veins in the other layer develop normally, there is no requirement for a dorsal EGFR-mediated inductive signal. This is consistent with the above described lack of requirement for a dorsal, BMP-mediated inductive signal in PCV development.

Dorsal knockdown of EGFR pathway activity shows the same effect as the BMP pathway, leading to autonomous loss of vein differentiation. In such cases, dorsal cells are 'deaf' to potential interplanar signals from the opposite layer. Furthermore, apart from the case of Tkv (in which we hypothesise an expansion of interplanar signalling) in these wings ventral differentiation occurs as normal in the absence of dorsal differentiation, highlighting the capacity for autonomous differentiation in each of the component layers of the wing.

Inhibiting provein signalling: non-autonomous induction of vein widening

We have noted how dorsal knockdown of *tkv* leads to ventral vein widening. To further investigate this phenomenon, we antagonised provein development by reducing the activity of Notch. When induced ubiquitously in the pupal wing between 0-32h APF, *N RNAi* leads to the expansion of apical constriction leading to broader veins in both layers (Fig. 5.7 A, A', C-E middle panels). From a normal width of ~3 cells, veins can expand to up to 15 cells wide at

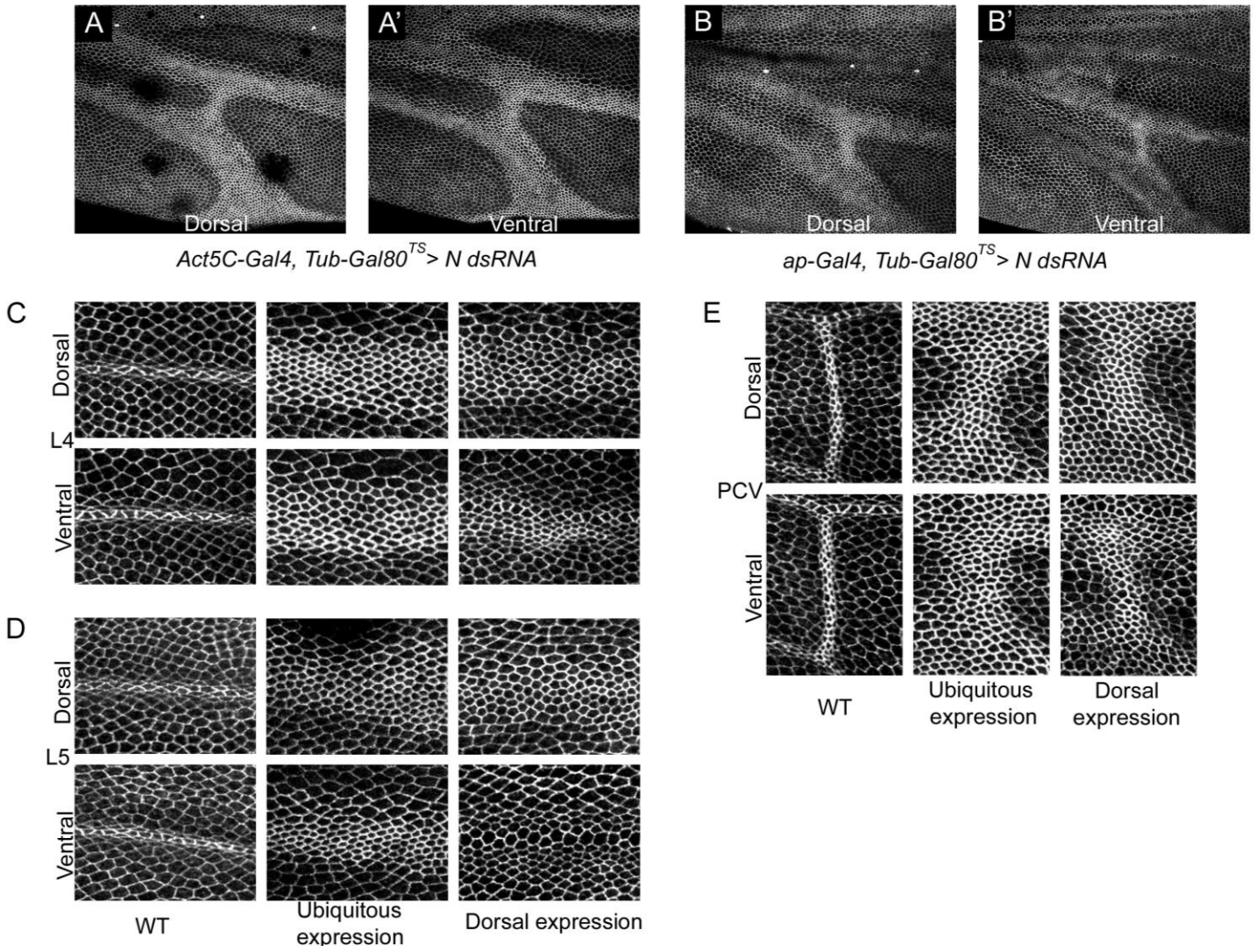

Figure 5.7. Dorsal expression of *Notch dsRNA* causes vein widening in both layers. (A-A') Cad-GFP in animals of the genotype *Act5C-Gal4/Ubi-DECad-GFP, UAS-N-dsRNA ; TubGal80^{ts}/+* raised at 18ºC until the WPP stage, and shifted to 29ºC until dissection at 32h APF. Broadened domains of apical constriction are observed in both dorsal (A) and ventral (A') layers. (B-B') *RNAi* restricted to the dorsal layer with *ap-Gal4* in the same experimental conditions leads to vein broadening in both dorsal (B) and ventral (B') layers. (C-E) Higher magnification of L4 (C), L5 (D) and the PCV (E), comparing wild type (left hand panels), ubiquitous *N dsRNA* expression (middle panels) and dorsal *N dsRNA* expression (right hand panels) between dorsal and ventral apical surfaces. n=9 wings analysed.

their broadest (L5 distally). Dorsal *N RNAi* leads to broader constriction in the dorsal apical surface (Fig. 5.7 B, C-E right top panels), and importantly vein widening is also observed in the wild type ventral surface (Fig. 5.7 B', C-E right bottom panels). These results show that compromising Notch function in one layer leads to broader veins on both surfaces. As with *tkv*, a probable mediator of this effect is Dpp. Loss of Notch activity in the proveins would lead to a reduction in *tkv* expression, which in turn would lead to an expansion of *dpp* expression (de Celis, 1997). Thus, a broader band of *dpp* expression would be capable of inducing similarly broad veins in the opposite layer.

Ubiquitous expression of BMP ligands induces vein fate and shape changes

In both rescue experiments and when antagonising the function of provein genes, extracellular BMP molecules can promote vein development in the interplanar dimension. We introduced above the two potential mechanisms to account for this, namely direct compared to indirect induction. Here, we investigate these hypotheses by asking whether ectopic expression of BMP ligands can activate the pathway in the opposite layer.

As a control, we characterised the effects of ubiquitous expression of BMP ligands in the wing with *Act5C-Gal4*. We used *Gal80^{ts}* to limit expression to the first 24h of the pupal period, and assessed cell fate in the wing based on expression of *DSRF*. In contrast to the wild type wing (Fig. 5.8 A', B'), expression of *dpp* throughout the wing led to near complete loss of *DSRF* expression in both layers of the wing (Fig. 5.8 B-C'). Low-level expression remained in proximal intervein regions (Fig. 5.8 B), and distally in a band of cells in the L3-4 intervein (Fig. 5.8 C). This may reflect the fact that, although seen throughout the wing, *Act5C-Gal4* drives higher levels of expression in the veins compared to intervein (Fig. 3), or that these regions have a higher threshold level for BMP mediated cell fate induction. Ubiquitous expression of *gbb* also led to a reduction in DSRF expression in intervein regions (Fig. 5.8 D-E'), though not to the same extent as *dpp*. Intervein sectors could still be distinguished, and the highest level of *DSRF* expression was seen in the sectors furthest from the veins (Fig. 5.8 E). Thus the intervein regions near the veins appear most sensitive to Gbb mis-expression. This may reflect the fact that only Gbb expressed in vein regions is capable of activating the pathway, which would occur if Gbb could only activate the pathway as a heterodimer with Dpp; this possibility is explored further below.

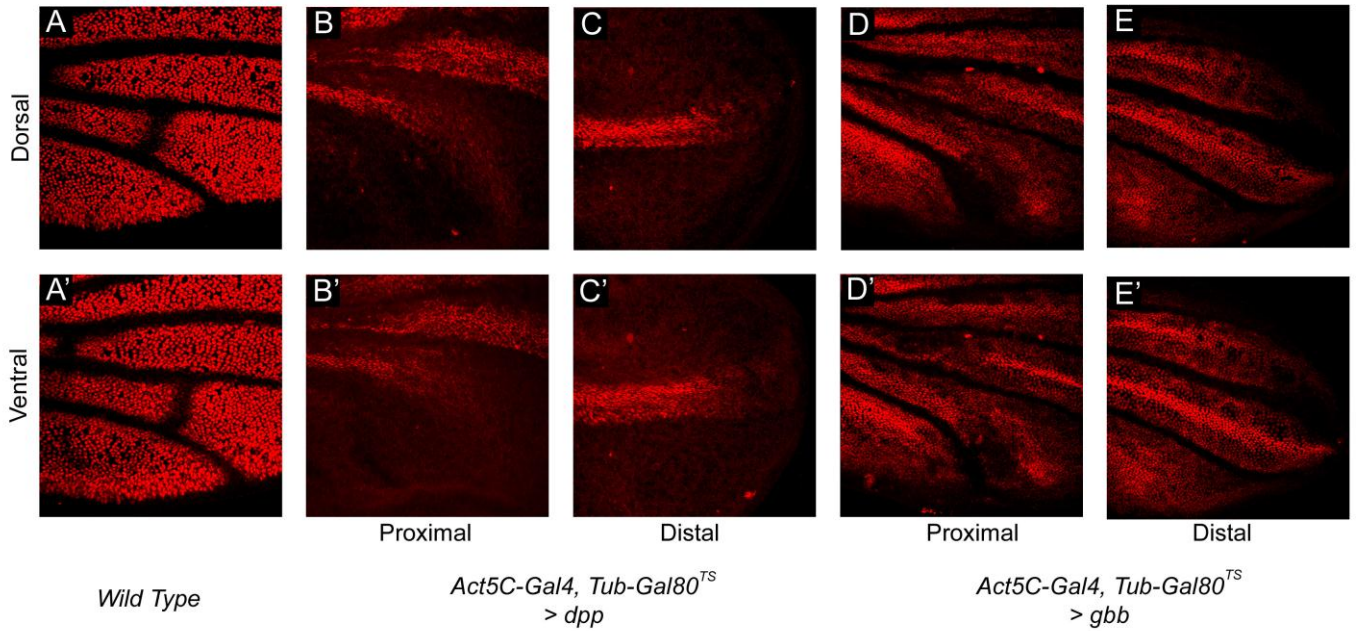

Figure 5.8. Ubiquitous expression of BMP ligands in pupal development: effects on cell fate. (A-B') Wild type pattern of *DSRF* staining in the middle of the wing at 26h APF. *DSRF* is restricted to the intervein regions. (B-C') *DSRF* expression in animals of the genotype *Act5C-Gal4/Ubi-DECad-GFP ; TubGal80^{ts}/UAS-dpp* raised at 18ºC until the WPP stage, and shifted to 29ºC until 26h APF, showing loss of *DSRF* expression in the proximal (B, B') and distal portions of the wing (C, C'). Note the maintenance of expression in a stripe in the middle of the distal portion of the wing (C, C'). n=8 wings analysed. (D-E') *DSRF* expression pattern when *gbb* is expressed ubiquitously as described above, showing down-regulation of *DSRF* expression in proximal (D, D') and distal (E-E') portions of the wing. Note that *DSRF* is most strongly down-regulated near to the veins. n=7 wings analysed.

We next investigated the effect of mis-expression on cell shape. Wild type wings at 32h APF show well defined stripes of apically constricted vein cells (Fig. 5.9 A, A'') overlying sharply demarcated vein lumen which channel through sectors of basally apposed intervein (Fig. 5.9 A'). Expression of Dpp throughout the wing has dramatic effects on these apical and basal profiles. Apically, the distinction between vein and intervein is lost, with large swathes of the wing appearing constricted relative to wild type (Fig. 5.5 B, C). This morphology is seen both dorsally and ventrally (Fig. 5.9 B'', C''), showing that cells in both layers respond the same to the ectopic signal. In basal sections, the pattern of apposition is lost, with large patches of apposed cells and equally large patches of separation (Fig. 5.9 B', C'). The degree of constriction does not always predict the presence or absence of apposition, showing that these two cell behaviours do not always occur together. This phenomenon has also been noted in studies on *DSRF* mutants (Fristrom et al., 1994).

We have previously shown that brief periods of Dpp expression result in ectopic stretches of venation in the adult wing (Fig. 4.5). When mis-expression is restricted to the 8h between separation and reapposition and animals dissected at the definitive stage, ectopically constricted cells snake through the intervein, in a pattern that is the same in both layers (Fig. 5.10). As a result, overlaying projections of the dorsal and ventral apical surface creates clearly distinct intervein and ectopic vein regions (Fig. 5.10 A''). This may reflect a symmetrical sensitivity of intervein regions in either layer to ectopic Dpp. Alternatively, because Dpp is expressed during the separation of the dorsal and ventral layers, it may reflect a process that aligns the ectopic veins between the two layers at reapposition.

Ubiquitous expression of Gbb also induces ectopic apical constriction (Fig. 5.9 D, D''), but in contrast to Dpp the effect is less widespread, and more prominent in cells surrounding the veins. In basal sections, there is expansion of non-apposition, particularly around L3 and anterior to the PCV, and patchy apposition in other wing regions (Fig. 5.9 D'). The less severe effect on cell shape of Gbb as compared to Dpp is consistent with its diminished ability to down-regulate DSRF (see above).

Dorsal expression of BMP ligands induces vein fate and shape in the ventral layer

We next addressed the effects of mis-expressing ligands in the dorsal layer only. Dorsal expression of *dpp* and *gbb* was initiated at the WPP stage and wings dissected after apposition (24h APF) or at the definitive stage (32h APF). Dorsal expression of *dpp* between 0-24h APF led

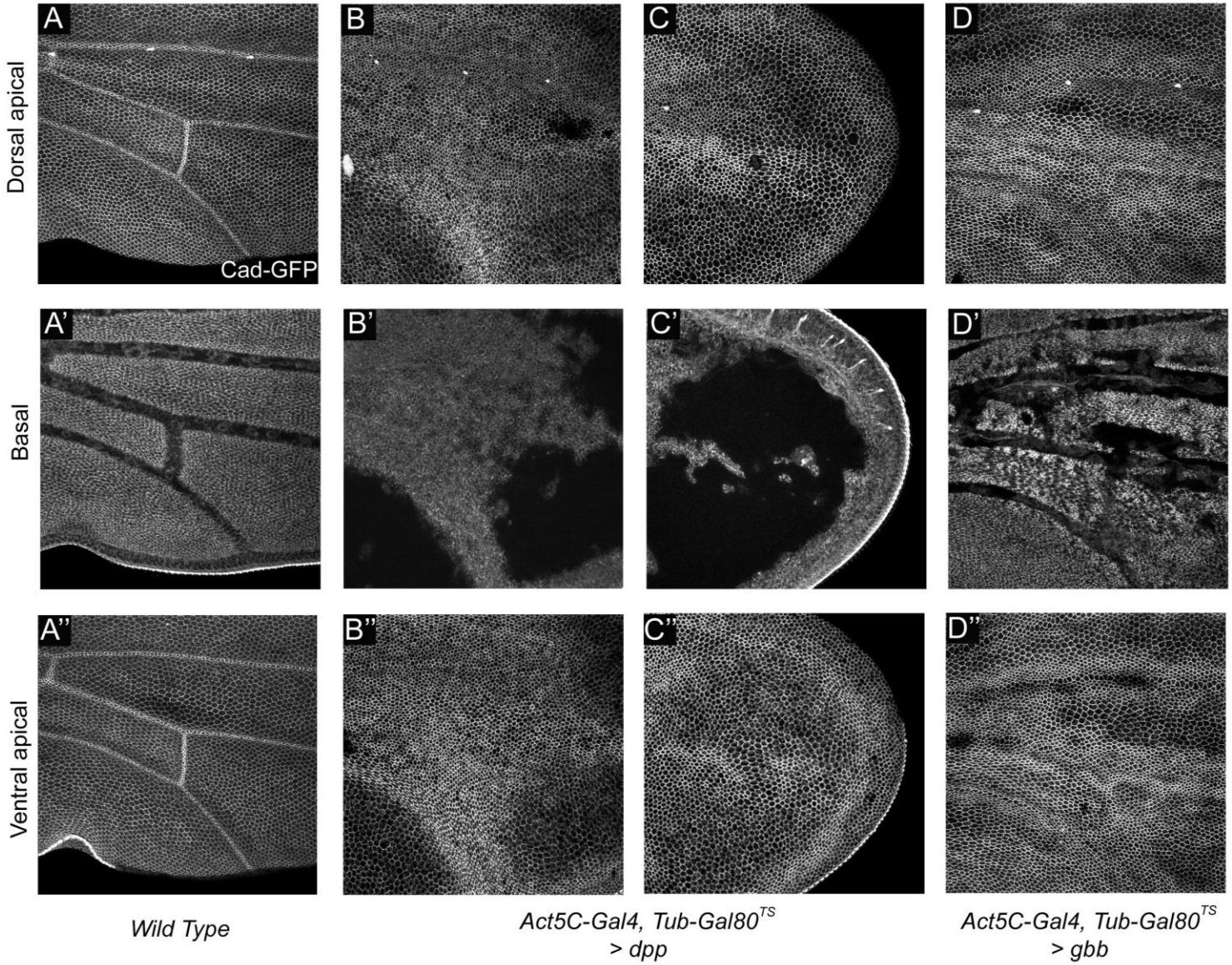

Figure 5.9 Ubiquitous expression of BMP ligands in pupal development: effects on cell shape. (A-A'') Wild type apical (A, A'') and basal (A') profiles in *Ubi-DECad-GFP/+* wings. (B-C'') Cad-GFP in apical and basal profiles in animals of the genotype *Act5C-Gal4/Ubi-DECad-GFP ; TubGal80^{ts}/ UAS-dpp* raised at 18ºC until the WPP stage, and shifted to 29ºC until dissection at 32hAPF, showing middle (B-B'') and distal (C-C'') sections of the wing. Constriction is widespread and apposition is blocked in large portions of the wing. n=5 wings analysed. (D-D'') Effects of expressing *gbb* according to the experimental conditions outlined above. Cells are less severely affected compared to *dpp*. n=5 wings analysed.

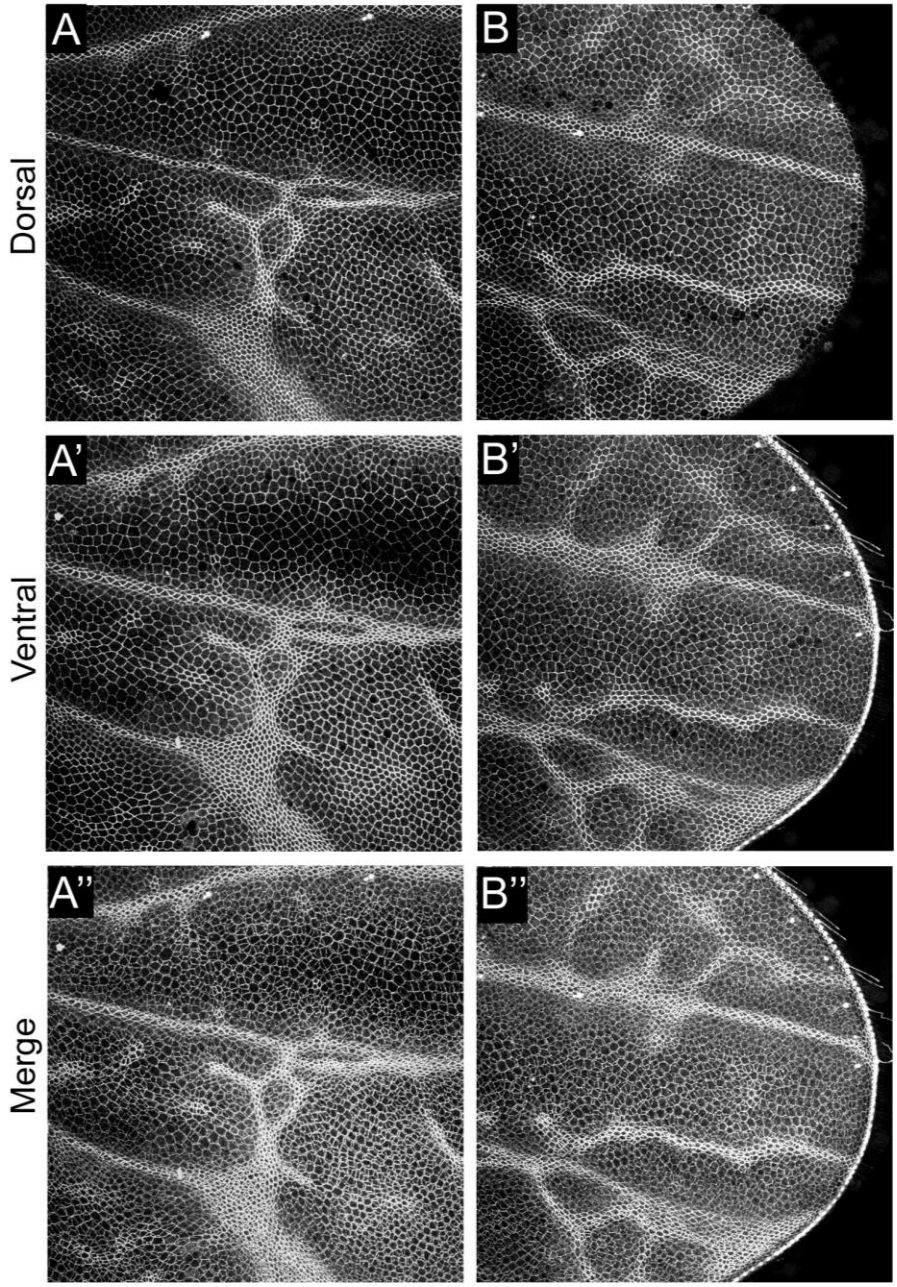

Figure 5.10. Ectopic veins resulting from brief *dpp* mis-expression align between dorsal and ventral layers. Wings from animals of the genotype *Act5C-Gal4/Ubi-DECad-GFP ; TubGal80^{ts}/UAS-dpp* raised at 18ºC until 24h APF, shifted to 29ºC for 8h, and shifted back to 18ºC until dissection 14h hours later. (A, A') Proximal wing, showing ectopic constriction in apical sections of dorsal (A) and ventral (A') layers. (B, B') Distal wing, showing ectopic constriction in apical sections of dorsal (B) and ventral (B') layers. (A'') Overlay of apical sections in (A) and (A''), showing that ectopic constriction aligns. (B'') Distal overlay shows the same alignment. n=4 wings analysed.

to widespread constriction in the dorsal layer, with no clear vein/intervein distinctions (Fig. 5.11 A). Correspondingly, *DSRF* expression was down-regulated (Fig. 5.11 A'), although lower levels of expression remained in the intervein between L3 and L4 (as was seen with ubiquitous expression). In the ventral layer, which does not express *dpp*, we see a similar phenotype: a loss of vein/intervein distinction and the expansion of regions of constriction (Fig. 5.11 B) and *DSRF* down-regulation (Fig. 5.11 B'). Cells in the ventral epithelium are thus induced to adopt vein characteristics by the dorsal expression of *dpp*. In basal sections of such wings, we see a similar failure of apposition to that seen after ubiquitous expression (Fig. 5.11 C), so as well as inducing constriction dorsally expressed *dpp* blocks apposition.

Following dorsal mis-expression of *gbb*, ectopic apical constriction in the dorsal layer was focussed on the veins (Fig. 5.11 D), and *DSRF* down-regulation was correspondingly broader around these regions (Fig. 5.11 D'), particularly at the distal end of L3. In the ventral layer, we see a similar phenotype to the dorsal layer, with *DSRF* expression down-regulated adjacent to the veins, and in distal L3 (Fig. 5.11 E'). Dorsal expression of *gbb* interferes with apposition to a similar extent as with ubiquitous expression (Fig. 5.11 F). Thus dorsal expression of *gbb*, like *dpp*, induces the expansion of vein fates in the ventral epithelium.

Interestingly, when animals were dissected 8h later, at 32h APF, the phenotype is altered as compared to 24h APF. In the case of *dpp*, constriction is seen throughout the dorsal layer (Fig. 5.12 A), and *DSRF* expression is almost completely lost, seen only at low levels in small patches of cells (Fig. 5.12 A'). However, in the ventral layer, even though widespread constriction remains (Fig. 5.12 B), *DSRF* expression is observed in patches of cells throughout the layer (Fig. 5.12 B'). The pattern of *DSRF* expression does not correspond with the degree of constriction: with higher magnification, it can be seen that the expression of *DSRF* does not define cells with larger apical surface areas (Fig. 5.12 E-E''). Furthermore *DSRF* expression is seen in both regions of apposition and separation (compare Fig. 5.12 C with Fig. 5.12 B'), showing that apposition is not a prerequisite for *DSRF* expression. A similar pattern of heightened ventral *DSRF* expression in 32h compared to 24h APF wings was noted following Gbb mis-expression (not shown).

The patchy *DSRF* expression observed between 24 and 32h APF represents a re-emergence of expression, as intervein regions express *DSRF* at the beginning of pupal development prior to induction (Montagne et al., 1996). Because dorsal repression of *DSRF* is increased between 24-32h APF, this does not reflect a reduction in the strength of the Gal4 signal in this period. It could potentially reflect a reduction in the efficiency of interplanar signalling in this period, as

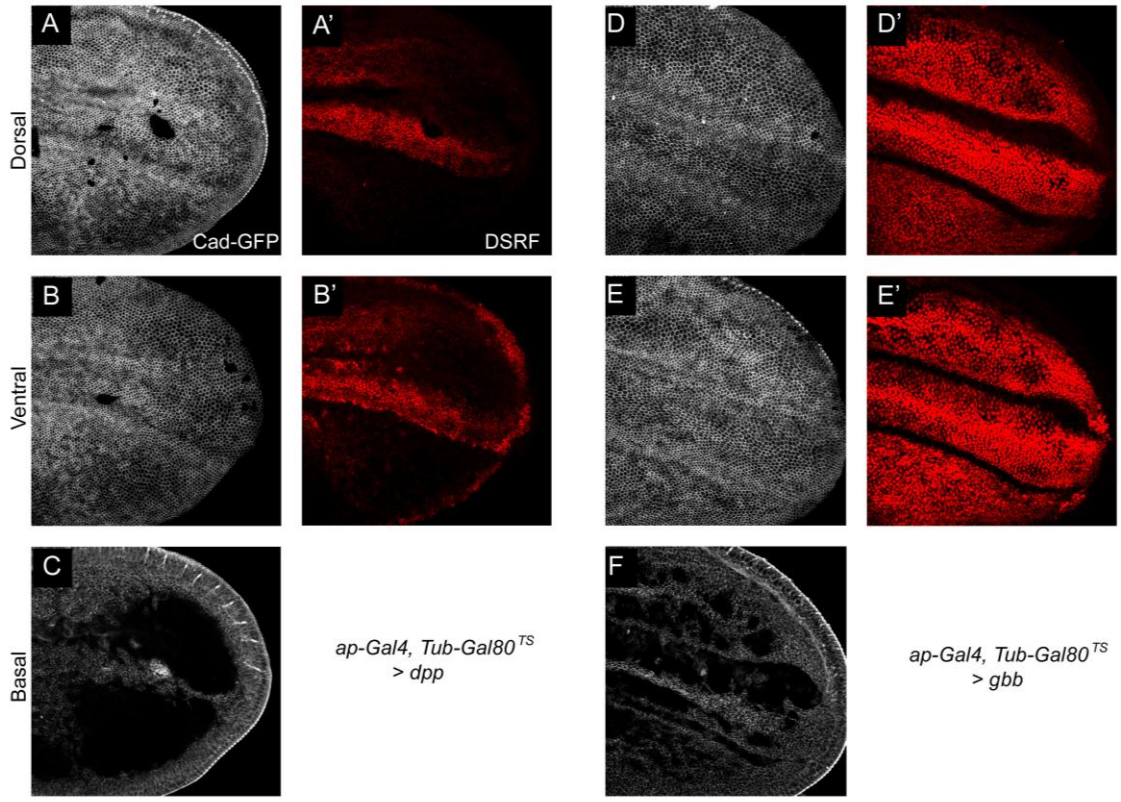

Figure 5.11. Dorsal expression of BMP ligands in pupal development: effects on cell fate shape at 24h. Cad-GFP (A, B, C) and *DRSF* expression (A', B') in animals of the genotype *ap-Gal4/Ubi-DECad-GFP ; TubGal80^{ts}/ UAS-dpp* raised at 18ºC until the WPP stage, and shifted to 29ºC until dissection at 24hAPF. Apical constriction (A, B) and *DSRF* repression (A', B') is seen in both layers. Basal section (C) shows blocking of apposition. n=8 wings analysed. (D-F) Effects of expressing *gbb* according to the experimental conditions outlined above. As with *dpp*, both dorsal and ventral layers are affected. n=7 wings analysed.

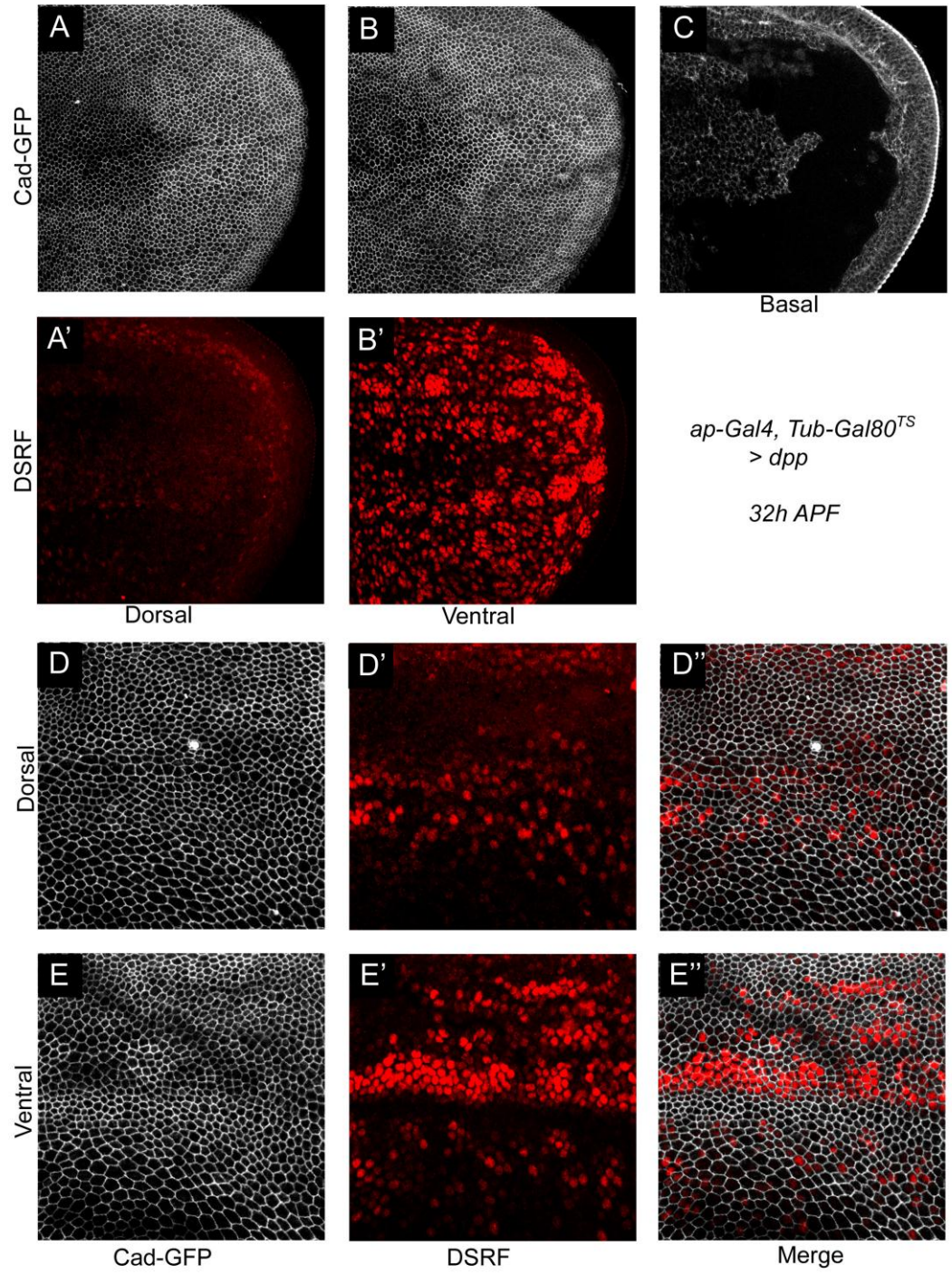

Figure 5.12. Re-emergence of *DSRF* expression between 24-32h APF following dorsal expression of *dpp*. (A-B') Cad-GFP (A, B, C) and *DRSF* expression (A', B') in animals of the genotype *ap-Gal4/Ubi-DECad-GFP ; TubGal80^{ts}/UAS-dpp* raised at 18ºC until the WPP stage, and shifted to 29ºC until dissection at 32hAPF. Note the emergence of patches of cells expressing *DSRF* in the ventral layer (B'). (D-E') Higher magnification in distal sections of the wings, showing the patchy re-emergence of *DSRF* in the ventral layer (E'), which does not strictly correlate with apical cell size (E, E''). n=5 wings analysed.

ventral cells do not continue to receive vein-inhibiting signals. We have previously shown that cells only respond to changes in BMP/EGFR/Notch signalling when induced prior to ~24h APF (see Chapter 4). The re-emergence of DSRF shown here suggests that cells after this period can in fact change their gene expression profiles. However, the re-emergence of *DSRF* is not accompanied by a widespread relaxation of cell apices (compare Fig. 5.12 E to 5.12 D), as would be expected considering the role of DSRF in intervein promotion. This suggests that cell shape and fate have been uncoupled in these cells: ventral cells no longer receive the Dpp mediated signal, and thus express *DSRF*, but are not capable of enacting the 'intervein' cell shape program.

Ubiquitous expression of cell autonomous pathway activators

The above results show that expression of BMP ligands in pupal development can affect cell characteristics both autonomously in expressing cells, and non-autonomously in cells of the opposite layer. In an effort to address whether this reflected direct signalling, we first sought to determine the localisation of ectopically expressed GFP-tagged ligands, but were unable to detect them outside of signalling cells either between or within layers, likely due to technical limitations. Another means of addressing this issue is to use cell autonomous pathway activators. If autonomous pathway activation in one layer leads to the coincident adoption of vein fate in the opposite, non-expressing layer, this would support the 'indirect' hypothesis. However, if the opposite layer developed as wild type, this would support the 'direct' hypothesis, as induction is only be seen with secreted signalling molecules.

As a control, the effects of global expression on cell shape were assessed. To activate the BMP pathway, we utilised tkv^{QD} (Nellen et al., 1996). Ubiquitous expression of tkv^{QD} between 0-32h APF led to a phenotype similar to that observed following *dpp* expression. Constriction is seen in large swathes of the wing in a similar pattern in both layers (Fig. 5.13 B, B''); however, as with *dpp,* not all cells constrict to the same extent (compare distal section in Fig. 5.13 C with proximal section in Fig. 5.13 B). Distinct territories of apposition and vein lumen are lost, with some proximal sections apposed and large sections separated (Fig. 5.13 B', C'). Thus, tkv^{QD} expression induces ectopic apical constriction and basal separation. We also constitutively activated the EGFR pathway with an activated form of Ras, the GTPase which transduces EGFR signals following receptor activation (Shilo, 2005). Compared to tkv^{QD}, expression of Ras^{V12} gives a more severe phenotype. Cell apices are constricted across the wing (Fig. 5.13 D, D''),

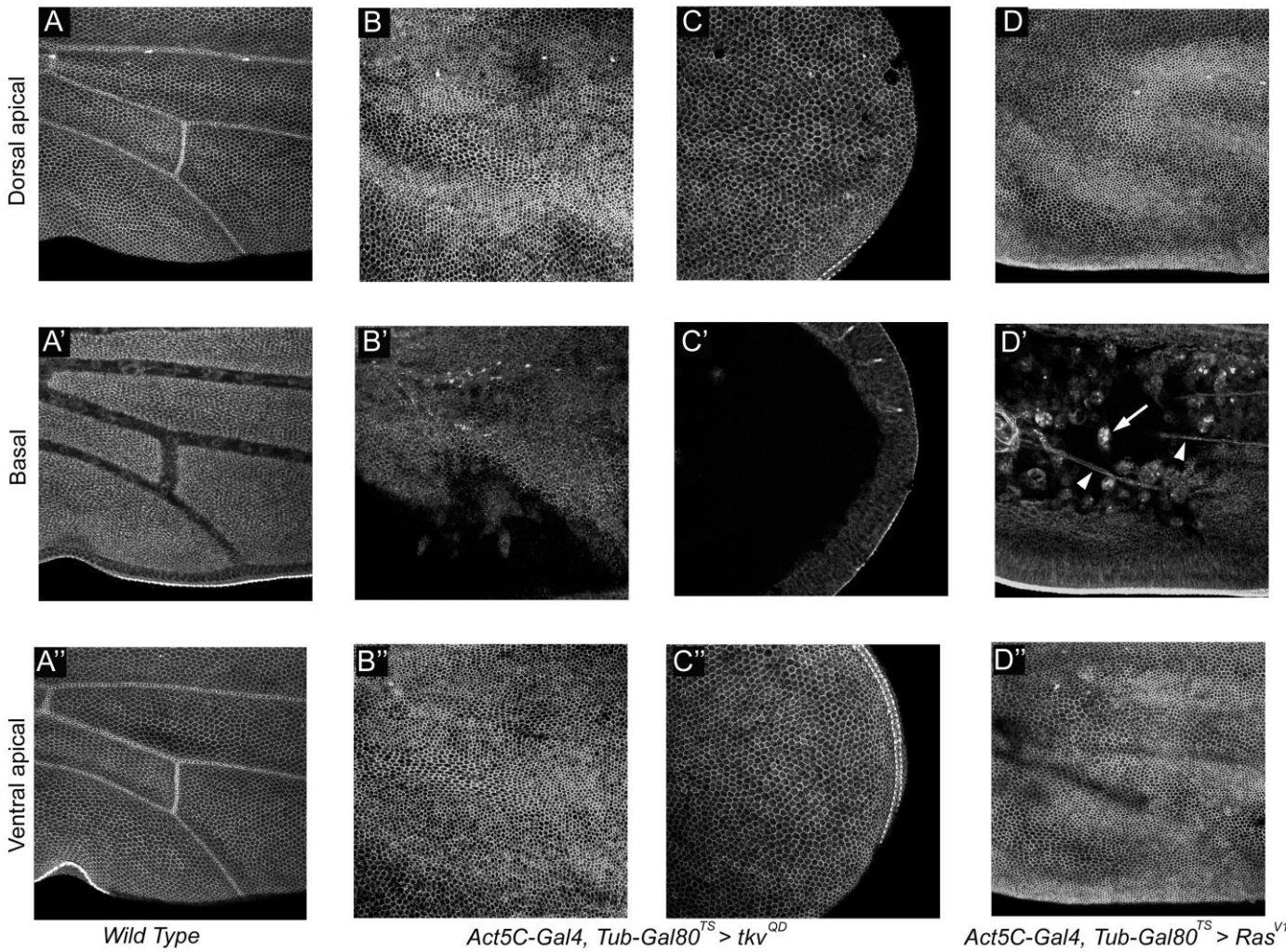

Figure 5.13. Ubiquitous expression of cell autonomous pathway activators: effects on apical cell shape. (A-A'') Wild type apical (A, A'') and basal (A') profiles in *Ubi-DECadGFP / +* wings. (B-C'') Cad-GFP in apical and basal profiles of animals of the genotype *Act5C-Gal4/Ubi-DECad-GFP ; TubGal80^{ts}/UAS-tkv^{QD}* raised at 18ºC until the WPP stage, and shifted to 29ºC until dissection at 32h APF, showing middle (B-B'') and distal (C-C'') sections of the wing. Constriction is widespread and large sectors of the wing do not appose. n=4 wings analysed (D-D'') Effects of expressing *Ras^{V12}* according to the experimental conditions outlined above. In basal section (D'), haemocytes are seen (arrow) as well as putative trachea (arrowheads). n=5 wings analysed

and apposition is inhibited in most of the wing, forming a cavity between the layers in which haemocytes (arrows) and what appear to be trachea (arrowheads) are seen (Fig. 5.13 D'). Thus, activation of the EGFR pathway in both layers of the wing promotes the same cellular phenotypes as BMP pathway activation, albeit in a more severe manner.

Dorsal expression of *tkv^{QD}* does not inhibit ventral intervein development

We next assessed the effects of restricting cell autonomous pathway activation to the dorsal layer. Dorsal expression of *tkv^{QD}* was induced at the WPP stage, and animals dissected at 24h or 32hAPF. At 24h APF, the dorsal layer shows widespread apical constriction, particularly around the veins (Fig. 5.14 A) and an almost complete loss of *DSRF* expression (Fig. 5.14 A'). Thus, most dorsal cells are apically constricted and repress *DSRF* (Fig. 5.14 A''). In contrast, in the ventral layer clear vein/intervein distinctions are seen, both in terms of apical cell shape, with stripes of apically constricted cells and sectors of more relaxed intervein cells (Fig. 5.14 B), and in terms of cell fate, with intervein sectors expressing *DSRF* (Fig. 5.14 B'). Ventral veins are however slightly wider than wild type veins, as assessed with *DSRF* (B'). In Z section, in contrast to wild type wings in which intervein *DSRF* expression is seen in interveins in both layers (Fig. 5.14 C-C''), the autonomous dorsal loss of *DSRF* is seen (Fig. 5.14 D-D'). At 32h APF, this pattern has not altered, although *DSRF* is now completely lost from the dorsal cells (Fig. 5.14 E-E', G-G''). The ventral veins maintain their broadness as compared to wild type (Fig. 5.14 F'', compare to Fig. 5.14 H'). *DSRF* is broader, but interestingly constriction is limited to the middle of the vein (Fig. 5.14 F, F''). Thus, cells flanking the vein show intervein cell shape and vein cell fate. In sum these results show the activation of the BMP pathway in dorsal cells does not transform the ventral layer into vein. This supports the notion that the non-autonomous effects of dorsal ligand expression are a result of direct signalling. An additional implication of the broadly autonomous effect is that the pathway activation provided by Tkv^{QD} does not lead to the induction of *dpp* expression; if *dpp* were expressed we would expect to see the interplanar induction of vein fate.

Aside from broader veins, the ventral layer deviates from wild type in one further respect: the PCV is lost (Fig. 5.15). This is seen both in the absence of apical constriction between L4 and L5 (arrow in Fig. 5.15 B), and in the expansion of *DSRF* expression to fill this region (arrow Fig. 5.15 B'). Thus, PCV development on the ventral layer is inhibited when the dorsal layer expresses *tkv^{QD}*. As other veins appear broader, this non-autonomous inhibition of vein development is specific to the PCV. Furthermore, this loss is specific to Tkv: autonomous

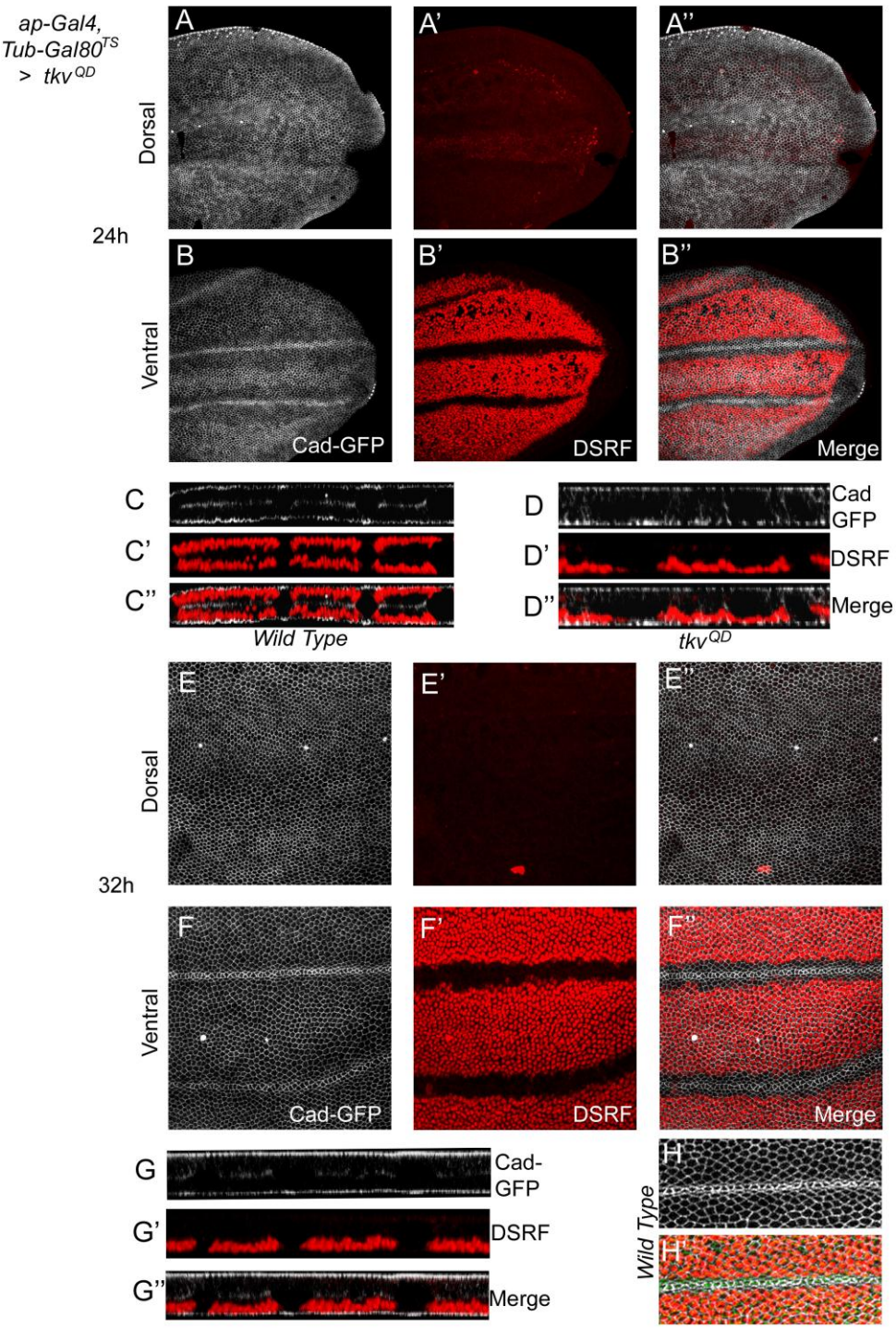

Figure 5.14. Dorsal expression of *tkv^{QD}* causes autonomous intervein loss. (A-D) Cad-GFP (A, B) and *DRSF* expression (A', B') in of animals of the genotype *ap-Gal4/Ubi-DECad-GFP ; TubGal80^{ts}/UAS-tkv^{QD}* raised at 18ºC until the WPP stage, and shifted to 29ºC until dissection at 24h APF. Merge shows constriction and loss of DSRF expression dorsally (A''), whereas ventrally, intervein development is unaffected (B''). (C-C'') Wild type profile of *DSRF* and Cad-GFP in Z section, dorsal is up. (D-D'') Z sections of dorsal *tkv^{QD}* wings: *DSRF* is autonomously lost in dorsal cells. (E-F'') When animals were allowed to develop for 8h more, phenotypes were unchanged. (G-G'') Z section showing autonomous *DSRF* loss in dorsal layer. Note the wider bands of *DSRF* repression in the ventral veins (F', F''), in comparison to wild type (H-H'). n=8 wings analysed.

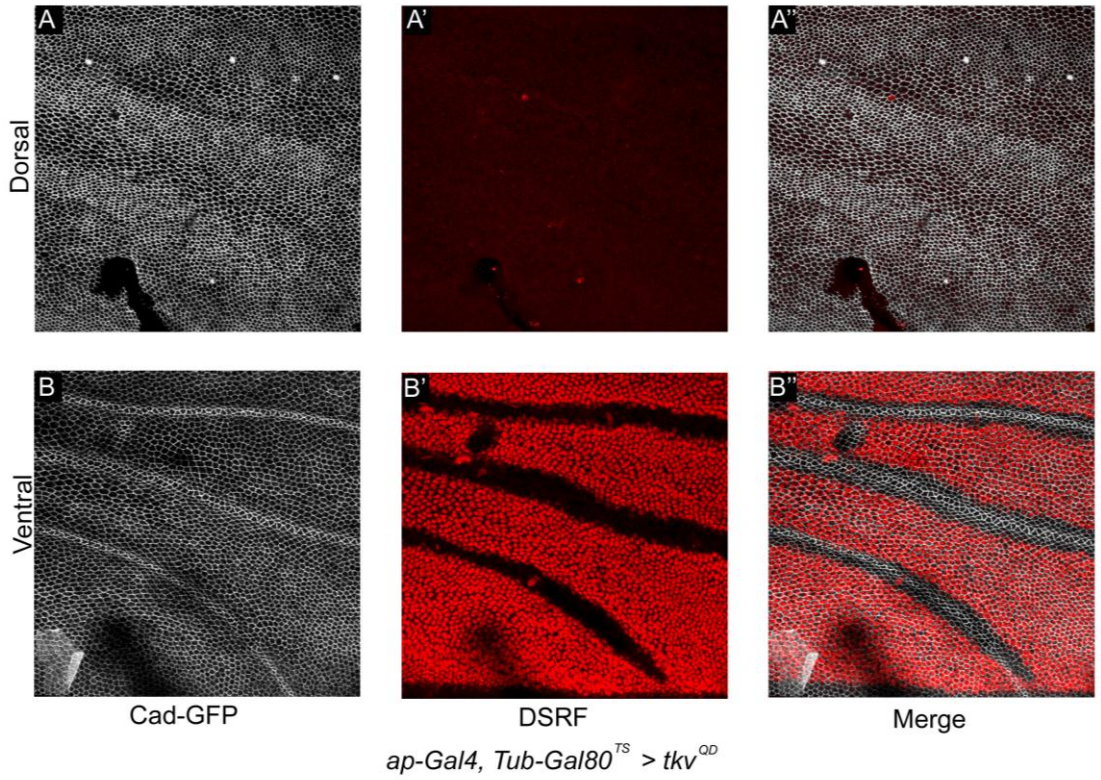

Figure 5.15. Dorsal expression of *tkv*^{QD} causes non-autonomous PCV loss. (A-D) Cad-GFP (A, B) and *DRSF* expression (A', B') in animals of the genotype *ap-Gal4/Ubi-DECad-GFP ; TubGal80*^{ts}*/UAS-tkv*^{QD} raised at 18ºC until the WPP stage, and shifted to 29ºC until dissection at 32h APF. In the dorsal layer, constriction is widespread (A) and *DSRF* is completely repressed (A', A''). In the ventral layer, no constriction (B) or *DSRF* repression (B') is seen in the PCV.

activation of the EGFR pathway does not lead to ventral PCV loss (see below), which shows that the ventral development of the PCV is not inhibited when dorsal cells are converted to vein. We had previously shown that the ventral PCV was also lost when Tkv was dorsally inhibited (Fig. 5.5), showing that the PCV is specifically sensitive to interplanar perturbations in Tkv levels. It is unclear why activating Tkv^{QD} in one layer would achieve this effect, considering this expression shows mainly autonomous effects. A potential reason could relate to the observation in the previous Chapter that brief periods of ubiquitous Dpp also leads to PCV loss. We proposed a model whereby uniformly activating signalling would lead to the loss of the sharp distinction between high and low signalling necessary for PCV development. Tkv^{QD} would presumably also achieve this effect. If the failure to make this distinction led to its failure in the opposing layer, the PCV would be non-autonomously lost.

Continued intervein development does not require apposition

We next addressed the consequences of dorsal activation of the EGFR pathway, by expressing *rho*. Dorsal expression of *rho* leads to widespread apical constriction (Fig. 5.16 A), as would be expected following heightened EGFR pathway activity, and coincident reduction or loss of *DSRF* expression (Fig. 5.16 A'). In contrast, the ventral layer is composed of apically constricted, *DSRF*- vein cells and relaxed, *DSRF*+ intervein cells in a pattern close to wild type (Fig. 5.16 B). As with tkv^{QD}, ventral veins are broader (Fig. 5.16 B'). Additionally towards the distal ends of veins, the vein territory is expanded (Fig. 5.16 B-B'') and at the distal end of the wing ectopic venation is observed (Fig., 5.16 D-D''). These regions correspond to those regions most sensitive to brief bursts of ubiquitous mis-expression (Fig. 4.9). In basal sections, the layers are separated in most of the wing (Fig. 5.16 C), yet non-apposed intervein cells in the ventral layer show expression of *DSRF*.

Following dorsal expression of Ras^{V12}, dorsal cells show widespread constriction (Fig. 5.16 E; (O'Keefe et al., 2007), whereas the ventral layer shows an almost wild type pattern of constricted vein cells and relaxed intervein cells (Fig. 5.16 E'') even though apposition is prevented throughout the wing (Fig. 5.16 E'). As with *rho* and tkv^{QD}, ventral veins are broader and less well-refined. This suggests that apposition and the wild type differentiation of vein/intervein in the opposing layer is required for vein refinement. As intervein cells can develop in the absence of intervein development in the opposite layer, indeed in the absence of basal contacts, this argues against the indirect signalling model. It argues instead that the

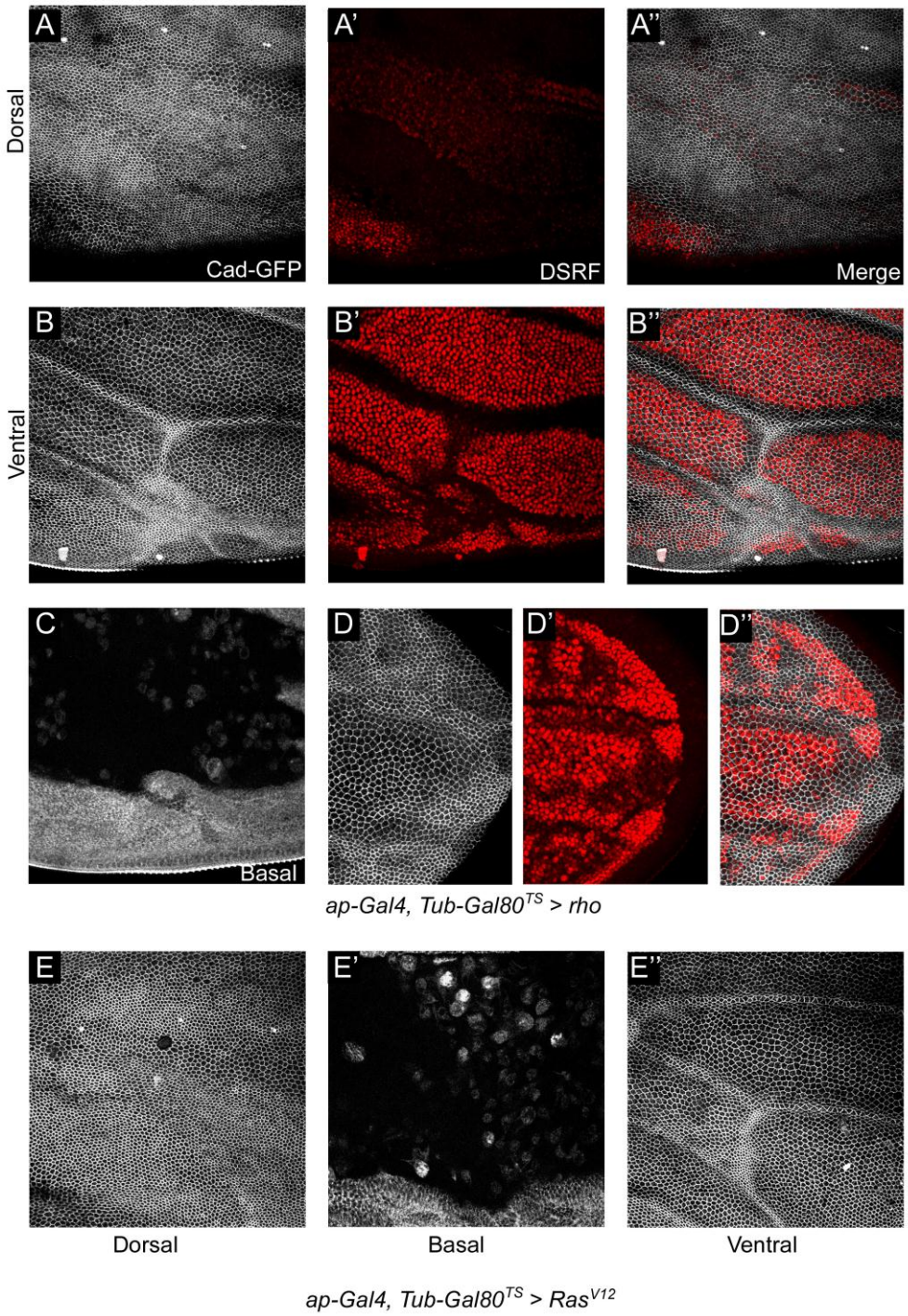

Figure 5.16. Continued intervein development is not dependent on apposition. (A-D) Cad-GFP (A, B, C, D) and *DRSF* expression (A', B', C') in animals of the genotype *ap-Gal4/Ubi-DECad-GFP ; TubGal80^{ts}/UAS-rho* raised at 18ºC until the WPP stage, and shifted to 29ºC until dissection at 32hAPF. In the dorsal layer, constriction is widespread (A) and *DSRF* is repressed (A'), whereas in the ventral layer, intervein cells relax apically (B) and show *DSRF* expression (B'). (C) Basal section, showing failure to appose. (D-D'') Distal section, showing region of ectopic constriction. n=6 wings analysed. (E-F) Effects of expressing *Ras^{V12}* according to the experimental conditions outlined above. In the dorsal layer, constriction is widespread (E), whereas vein/intervein distinctions are clear in the ventral layer (E''). Basal section (E') shows large separated cavity due to the failure of apposition. n=8 wings analysed

adoption of vein fate in ventral cells following dorsal expression of BMP ligands results from a direct signalling event. Furthermore, it reinforces the fact that the distinction between vein and intervein can be made without needing such distinctions in the opposite layer.

Using clones to assess intraplanar signalling

As interplanar BMP ligands can promote vein development in the opposite layer, we next asked whether they could promote signalling in neighbouring cells of the same layer, and if so at what range. Because Gal4/Gal80^{ts} controls mis-expression in the entire epithelium or the entire dorsal layer, we needed another means to restrict ectopic expression to certain cells within the layer. To do this we generated clones of cells expressing BMP pathway components, allowing the effects of restricted ectopic expression in otherwise wild type tissue to be studied. Because the signalling components also play vital roles in the patterning and growth of the larval disc (see Introduction), clones were induced in mid to late third instar larvae, to avoid interfering with these functions. Thus, whereas early induced *dpp*-expressing clones can lead to duplications of the AP axis in the wing (Zecca et al., 1995), late-induced clones do not (see below), and we can assess the effects of restricted mis-expression in the pupal period. Clonal analysis also allows us to assess the effects of restricting ectopic expression to intervein cells, in contrast to Gal4/Gal80^{ts} in which both vein- and intervein-specified cells express the target gene.

In these experiments we compare the effects of BMP components on clone cells and their neighbours, to deduce autonomous (i.e. autocrine) and non-autonomous signalling. Cad-GFP allows us to measure apical area, to see whether target genes can induce apical constriction. We measure the average apical area of clone cells, their first row neighbours (i.e. those cells that share a cell-cell junction with a clone cell) and their second row neighbours (i.e. those cells that share a cell-cell junction with a first row neighbour) (Fig. 5.17 A''). We then compare these average sizes to a clone cell in the same region of the wing (see Materials and Methods). These ratios are then used to determine the effect of a clone on apical cell area in the clone cells and their neighbours. To see if constriction is mediated by pathway activation, we assess *DSRF* expression in these cells.

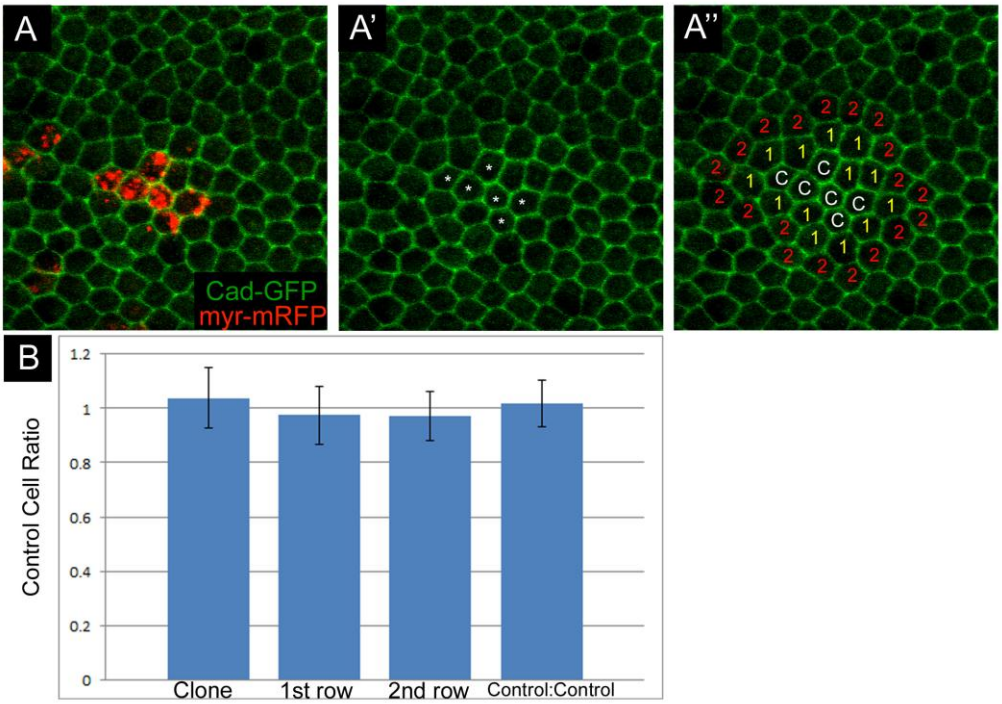

Figure 5.17. Control clones do not affect apical morphology or area. (A-A'') 6-cell *myr-mRFP*-expressing clone in the intervein, with clone cells marked with asterisks in (A'), showing no deviation in apical phenotype. (A'') Designation of clone cells (white 'C'), their 1st row neighbours (yellow '1'), and their 2nd row neighbours (red '2'). (B) Ratio of clone cell : control (stdev = 0.111), 1st row neighbour : control (stdev = 0.107), 2nd row neighbour : control (stdev = 0.092), and control:control (non-clone cells compared to non-clone cells in similar regions of the wing; stdev = 0.087). myr-mRFP expression does not affect apical area, and apical areas in control regions vary on average within a ~10% margin. Control cells were selected from non-clone cells in the same intervein region. n=14 clones in 6 wings, and n=19 clones in 7 wings for control:control ratio. Bars show standard deviation.

Ectopic Gbb is non-functional in the intervein

We previously noted that the regions of intervein most sensitive to Gbb mis-expression are those closest to the veins (Fig. 5.8). This suggests a differential sensitivity of intervein regions to *gbb* expression, so we assessed the effects when mis-expression is restricted to intervein regions. Control clones, which only express the myr-mRFP marker, do not affect cell shape or apical cell area in either labelled cells or their first or second row neighbours (Fig. 5.17 A-B). Similarly, *gbb*-expressing clones in any intervein region do not affect the apical morphology of intervein cells (Fig. 5.18 A-A''). Labelled cells appear the same size as non-labelled cells (asterisks in Fig. 5.18 A'), and even when multiple clones fill intervein region wings appear wild type in apical (Fig. 5.18 B') and basal sections (Fig. 5.18 B, B''). When measuring cell area, clone cells and their neighbours do not differ from control cell apical area (Fig. 5.18 C). Consistent with the absence of cell shape changes, adult wings do not show any ectopic patches of pigmented cuticle (Fig. 5.18 D). We had previously shown that *gbb* expressed throughout the wing could induce *DSRF* repression (Fig. 5.8), but *gbb*-expressing clones in the intervein had no effect on *DSRF* expression: expression is seen at the same level in labelled cells as in the rest of the intervein (Fig. 5.18 E-E''). Thus, the absence of constriction in *gbb* intervein clones coincides with a failure of Gbb to activate the BMP pathway. These results show that in the intervein, Gbb is non-functional, and because mis-expression of Gbb had the greatest effects near the veins (Fig. 5.8, 5.9, 5.10), this suggests that only Gbb expressed in vein regions can elicit pathway activity (see Chapter Summary).

Dpp clones induce vein shape and fate in intervein clone cells and their neighbours

We next asked whether *dpp* was able to affect intervein cells. In contrast to control or *gbb*-expressing clones, *dpp*-expressing clones led to apical constriction in intervein cells. Constriction was observed both in the labelled cells (asterisks in Fig. 5.19 A') and their neighbours (small, RFP- cells in Fig. 5.19 A''), and was accompanied by an increase in the intensity of apical Cad-GFP relative to the surrounding intervein. Apical increases in AJ components such as E-Cad and β-Catenin cells are seen in other developmental contexts involving apical constriction (Kolsch et al., 2007; Kinoshita et al., 2008), and is observed endogenously in the pupal veins (O'Keefe et al., 2007). We next calculated the ratio of clone, first and second row neighbour apical cell area to the area of control cells (Fig. 5.19 D). *dpp*-expressing cells are on average half the size of control cells (x0.499), their first row neighbours

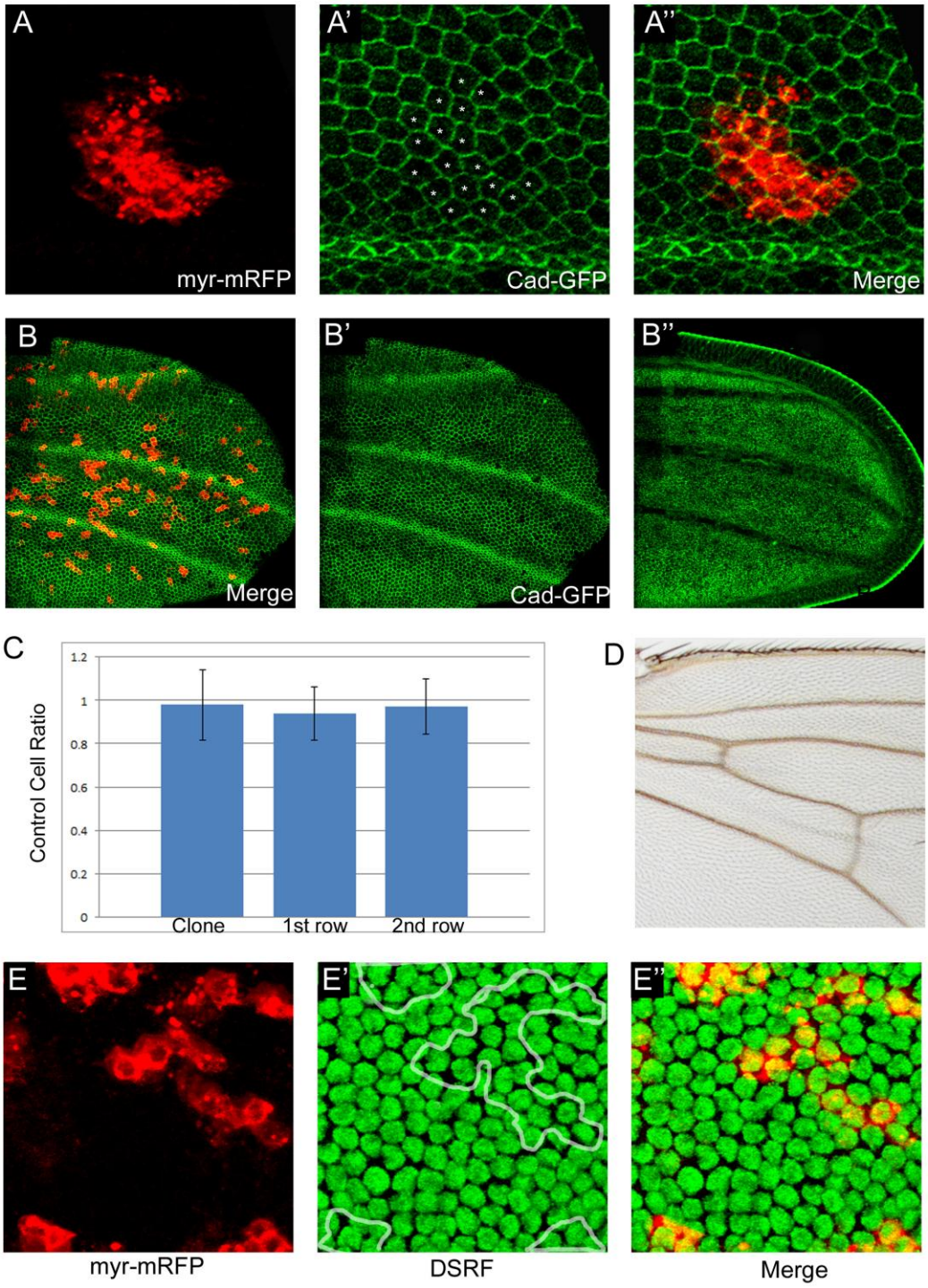

Figure 5.18. Ectopic *gbb* in intervein is non-functional. (A-A'') 18-cell *gbb*-expressing in the intervein does not affect apical morphology (clone cells marked by asterisks in A'). (B-B'') Multiple clones (red) do not induce constriction (B') or ectopic lumens (B'') in intervein cells. (C) Clone cells apical area is unaffected. Control ratios - Clone : control = 0.981 (stdev 0.162), 1st row : control = 0.938 (stdev = 0.124), 2nd row : control = 0.972 (stdev = 0.127). n=36 clones in 10 wings. (D) Adult wings do not show ectopic venation. (E-E'') Effect of *gbb* clones on *DSRF* expression (green), showing no repression of *DSRF* (clones outlined in white in E').

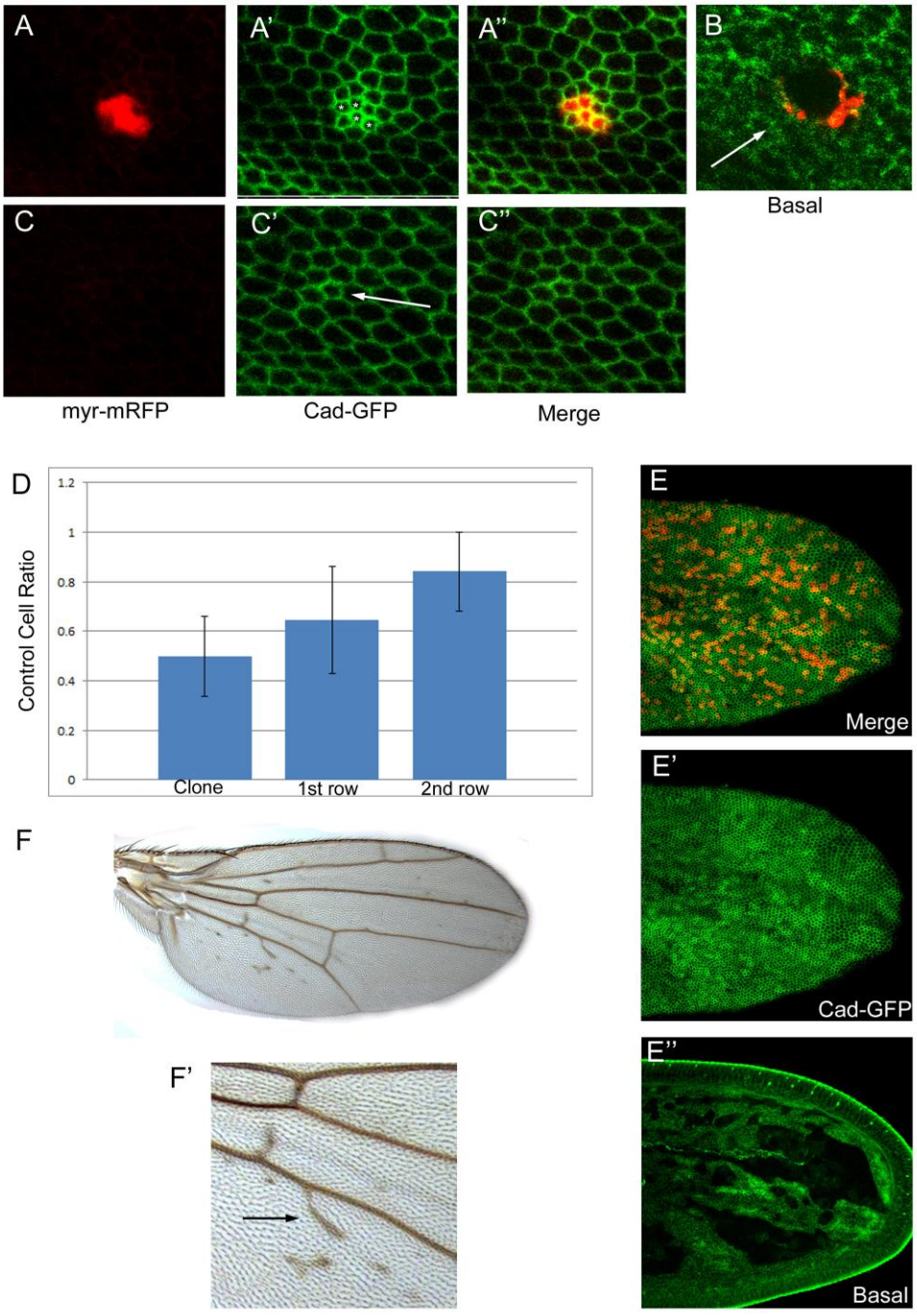

Figure 5.19. *dpp* expression in intervein cells causes apical constriction and ectopic lumen formation. (A-A'') 4-cell clone expressing *dpp* leads to apical constriction and Cad-GFP enrichment in clone cells (asterisks in A') and their neighbours. (B) Basal section of the same clone, showing ectopic lumen formation. (C-C'') In the opposing layer, apical constriction is ectopically induced (C') in wild type tissue (note absence of clones in C). (D) Clone cells and their neighbours constrict relative controls. Control ratios – Clone : control = 0.499 (stdev 0.161), 1st row : control = 0.644 (stdev = 0.215), 2nd row : control = 0.840 (stdev = 0.159). n=20 clones in 12 wings. (E-E'') Mulitple clones generated by extended heatshock cause widespread apical constriction (E') and failure of basal apposition (E''). (F-F') Adult wings differentiate ectopic patches of vein-like cuticle (arrow).

on average x0.664 the size of control cells, and second row neighbours are still slightly smaller than control cells, at x0.840. Thus expression of *dpp* in the intervein leads to constriction in both expressing cells and their neighbours. Clones of four or more cells also commonly led to the basal separation of dorsal and ventral layers, creating an ectopic lumen enclosed within the intervein (Fig. 5.19 B).

We also encountered interplanar effects of *dpp*-expressing clones. In larger clones, constriction was induced both in the clone layer (Fig. 5.19 A'A'') as well as in cells of the opposite layer (arrow in Fig. 5.19 C, C'). Dpp from one layer can thus induce constriction in the opposite, wild type layer. These effects are observed from both dorsal and ventral clones, showing that such signalling can occur in both directions. When duration of heat shock is increased and clone cells make up a large proportion of the wing (Fig. 5.19 E), we see widespread apical constriction leading to a loss of vein/intervein definition (Fig. 5.19 E'), and large regions of basal non-apposition (Fig. 5.19 E''). When heat shocked larvae were raised until eclosion, adult wings showed the differentiation of small patches of ectopic venation, as assessed by pigmented cuticle (Fig. 5.19 F, F'). In summary these results show that expression of *dpp* in intervein regions leads to the induction of vein characteristics both in expressing cells and non-autonomously in neighbouring cells and cells of the opposite layer.

We next asked whether these cell shape changes were the result of BMP pathway activity. If constriction in neighbouring cells is accompanied by *DSRF* down-regulation, this supports the notion that labelled cells signal to adjacent cells and induce constriction. However, if constriction is not accompanied by *DSRF* down-regulation, the effect is indirect. An indirect reduction in apical area may be a consequence of epithelial topology. A typical epithelial cell will share cell-cell junctions with 5-7 neighbours (Gibson and Gibson, 2009; see diagram in Fig 5.26). If one of these neighbours is an autonomously constricting *dpp*-expressing cell, the contact they share with it will reduce in length. If this reduction is not accompanied by an expansion of another cell-cell contact, this will lead to the reduction in overall cell perimeter, and thus a reduction in apical cell area. The reduced area seen in neighbouring cells would thus not arise from BMP-induced apical constriction, but would rather represent a passive response to cell shape changes in the clone cell. A consequence of this model is that if ligands *do* activate signalling in neighbouring cells, the non-autonomous reduction in apical area would result from a combination (i) internally generated apical constriction in response to the Dpp signal, and (ii) a reduction in the length of the cell-cell contact with the cell that provides the signal.

Clones of cells expressing *dpp* in the intervein show loss of *DSRF* expression in labelled cells (asterisks mark clone pair in Fig. 5.20 A). Partial down-regulation is also observed in the first row neighbouring cells (arrow in Fig. 5.20 A), which suggests that pathway-mediated constriction contributes to the reduction in cell area. However, second row neighbours do not show *DSRF* down-regulation (5.20 A). This suggests the slight reduction in apical area of second row neighbours (Fig. 5.19 D) is not a result of BMP pathway activation. Second row neighbours may thus reduce apical area as a result of sharing a cell-cell junction with a constricting first row neighbour. The area of the first row neighbour itself would reduce as a combined result of pathway-mediated apical constriction and from sharing a cell-cell junction with a clone cell.

Larger clones led to *DSRF* repression in cells of the opposite layer (Fig. 5.20 B-C''), in accordance with the constriction seen in cells opposite clones (Fig. 5.19 C), showing that this phenotype coincides with interplanar activation of the BMP pathway. Furthermore these effects are seen in both dorsal and ventral clones, showing that such signalling is bidirectional. A single clone of cells can promote signalling in both adjacent and opposite neighbours, which shows that ligand from the same source is capable of signalling in both dimensions (see Chapter Summary). When multiple clones covered both layers of the wing, large continuous tracts showed repression or down-regulation of *DSRF* (Fig. 5.20 D, D').

Dpp autonomously inhibits and non-autonomously promotes *tkv* expression

The above results show that ectopic Dpp in the intervein is only capable of inducing pathway activity in immediately neighbouring cells. This short range effect is consistent with the endogenous expression pattern of *dpp*, which is limited to regions of pathway activation (i.e. the veins; Yu et al., 1996). One of the proposed ways in which Dpp range is limited is by the heightened expression of *tkv* in the proveins, which may acts as barrier to trap diffusing ligands (Fig. 5.21 A'; de Celis, 1997; Sotillos and de Celis, 2005). However, in the middle of the intervein, where *tkv* expression is minimal (Fig. 5.21 A', A''), there is no endogenous Tkv barrier to Dpp diffusion, yet ectopic Dpp still acts at a short range. We thus tested the effects of ectopic Dpp on the expression of *tkv*. *dpp*-expressing clones in the intervein affect *tkv* expression in two ways: *tkv* expression is down-regulated in clone cells, and up-regulated in a 'halo' of cells surrounding the clone. 'Halos' are induced in intervein regions were *tkv* is usually expressed at a low level (Fig. 5.21 B'). Where clones cover the proveins, *tkv* expression is reduced within the clone (Fig. 5.21 C'). Thus, *dpp* expression can both antagonise and promote

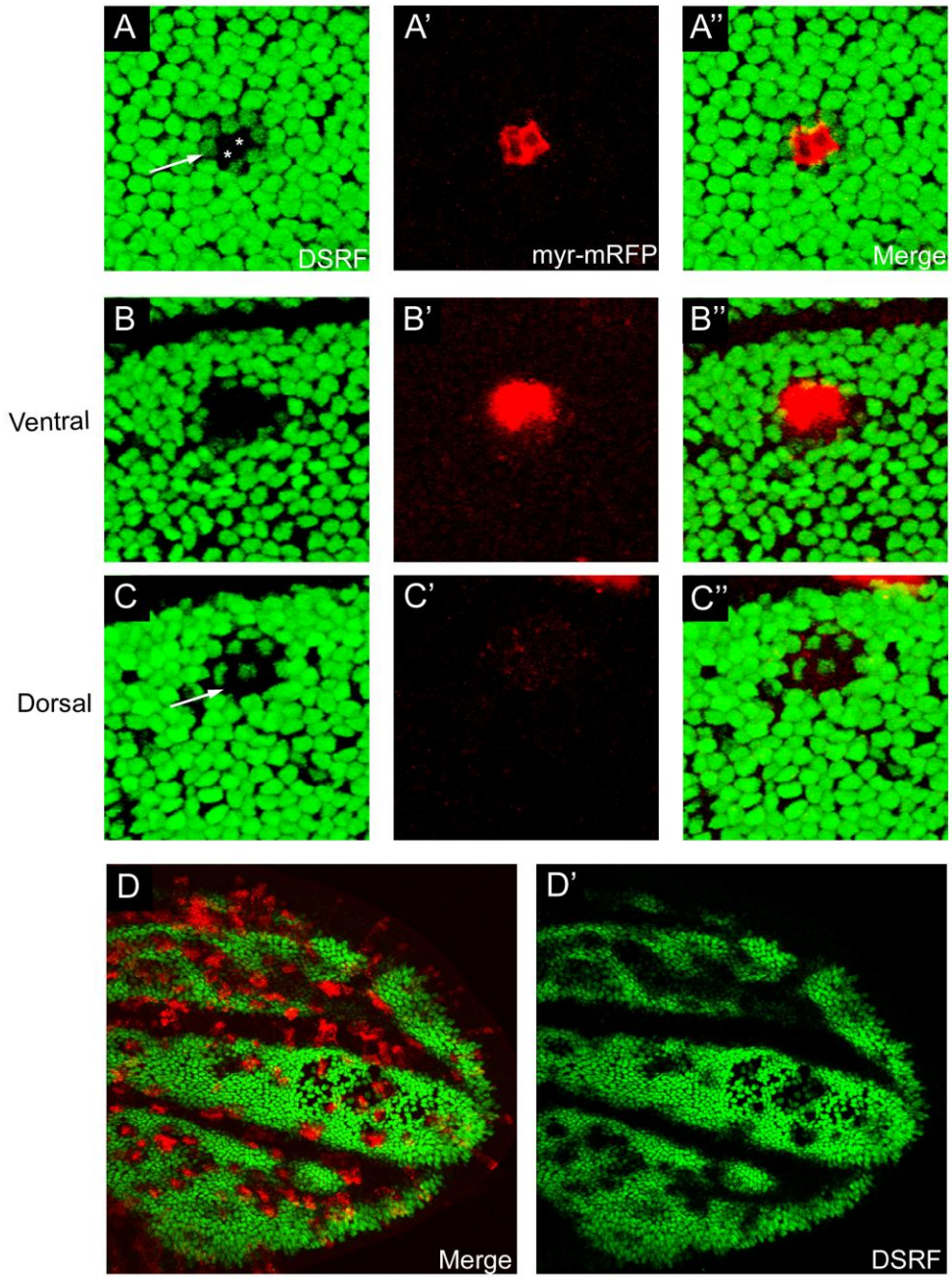

Figure 5.20. *dpp* induces *DSRF* repression at a short range. (A-A'') 2-cell *dpp* clone leads to loss of *DSRF* in clone cells (asterisks in A) as well as partial down-regulation in their neighbours (arrow in A). (B-C'') Non-autonomous inhibition of *DSRF* expression. Ventral clone leads to *DSRF* loss both in the ventral layer (B-B'') and in the dorsal layer (C-C''). Note that no clones are present dorsally (C'). n=14 clones in 6 wings. (D-D') Multiple clones leads to continuous stretches of *DSRF* loss and down-regulation in the intervein.

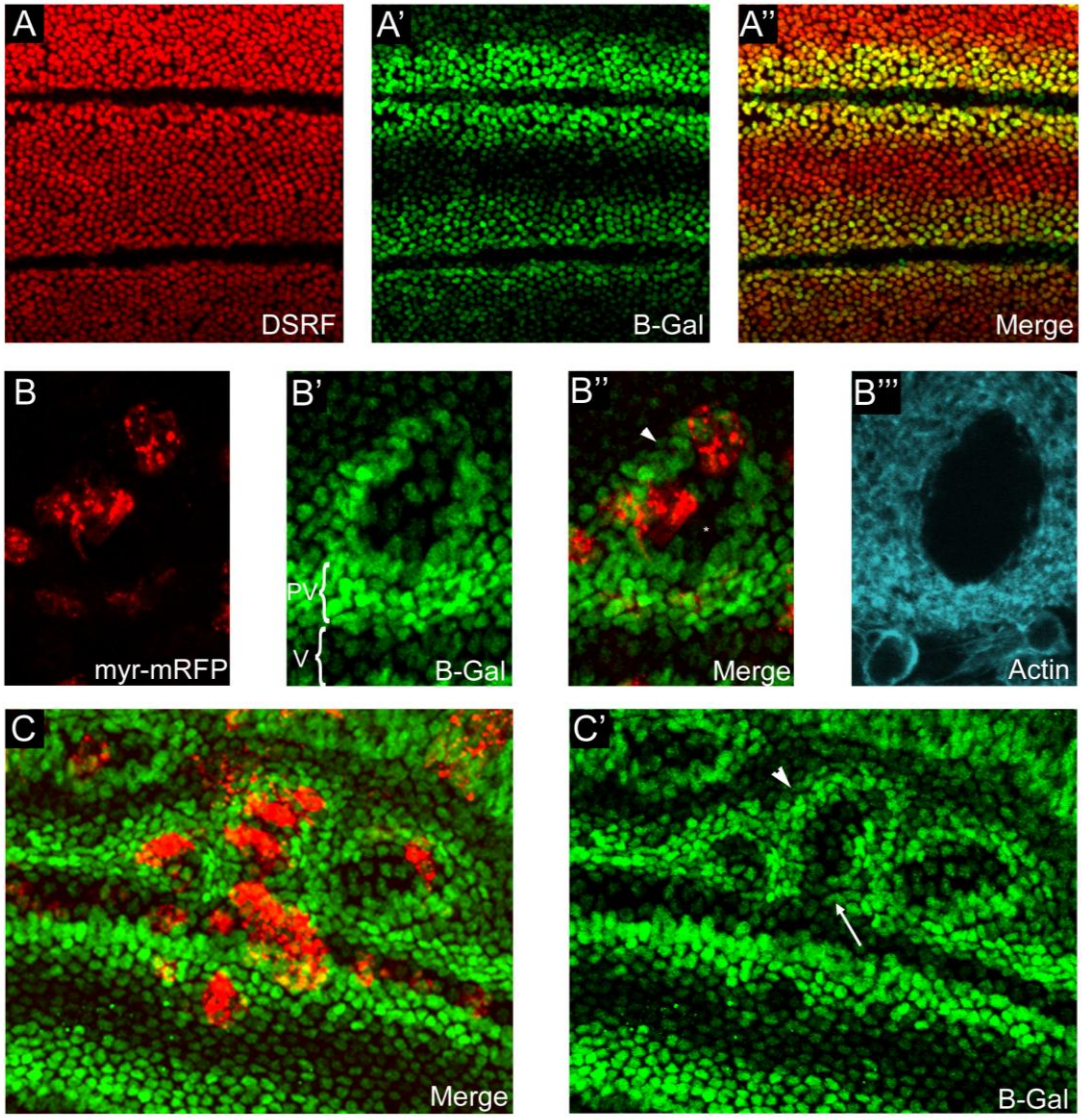

Figure 5.21. *dpp*-expressing clones both inhibit and promote *tkv* expression. (A) *DSRF* expression in wild type. (A') tkv^{LacZ} expression, showing heightened expression in the provein. (A'') Merge, showing co-expression of *DSRF* and *tkv* (yellow cells) in provein. (B-B'') 2 clones of dpp expressing cells anterior to the provein, showing a halo of *tkv* expression around the clones (arrowhead in B'', asterisk shows loss of *tkv* expression due to clone in the opposite layer). Brackets in B' indicate endogenous vein (V) and provein (PV) domains. (B''') Basal section of the clone, stained for Actin, showing failure to appose. (C-C'') Multiple clones show autonomous loss of *tkv* expression (arrow) and halos around the clones (arrowhead). n=32 clones in 7 wings.

the expression of *tkv*, and the latter function is non-autonomous with respect to the expressing cells. The fact that the 'halos' are limited to 1-2 cell thickness around clones is consistent with the short range induction of apical constriction and *DSRF* repression (Figs. 5.19, 5.20).

The difference between *tkv* inhibition and promotion may relate to the strength of the signal, with different thresholds for inhibition and promotion. If ectopic Dpp signalling promotes a high level of pathway activity in expressing cells (i.e. autocrine signalling), then clone cells would inhibit *tkv* expression. Short range signalling to neighbouring cells elicits lower levels of pathway activity, as assessed by *DSRF*, and at this lower threshold *tkv* expression would be promoted. The induction of *tkv* expression provides a potential mechanism for why Dpp has a short range in the pupal wing epithelium. If Tkv limits the diffusion of Dpp by trapping the ligand, then induction of *tkv* expression in adjacent cells would create a barrier for diffusion around the clone. This mechanism has been proposed to act in the disc, where *tkv* receptor levels are highest in the anterior and posterior regions and may limit diffusion (Lecuit and Cohen, 1998), and is not exclusive to the BMP pathway, as the Patched receptor can limit the diffusion of the Hh ligand (Chen and Struhl, 1996). Thus the range of Dpp in the pupal wing may be curtailed by its own induction of Tkv in neighbouring cells. This raises the possibility that, in the absence of the Tkv halo, Dpp would be able to promote signalling at a longer range.

Tkv^{QD} can both promote and inhibit vein differentiation

We next addressed the effects of autonomously activating the BMP pathway in the intervein. Clones of the constitutively activated receptor tkv^{QD} were generated, and we first assessed the effect on cell morphology. Clone cells are apically constricted, and show a substantial increase in the intensity of Cad-GFP at adherens junctions (Fig. 5.22 A, A'). Clone cells were substantially smaller than control cells, and smaller even than *dpp*-expressing clones, averaging x0.286 the size of control cells (Fig. 5.22 B). Their first row neighbours showed larger surface areas, but were still relatively constricted, at x0.685 the size of control cells, and second row neighbours returned to wild type size, at x0.936 the size of control cells. In contrast to *dpp*, tkv^{QD}-expressing clones do not induce the constriction of cells of the opposite layer (Fig. 5.22 A''), consistent with the broadly autonomous effect of dorsal tkv^{QD} expression (Fig. 5.14). In combination with the effects of dorsal mis-expression, this shows that activation of the BMP pathway does not lead to expression of secreted molecules capable of inducing vein in the opposing layer (e.g. Dpp).

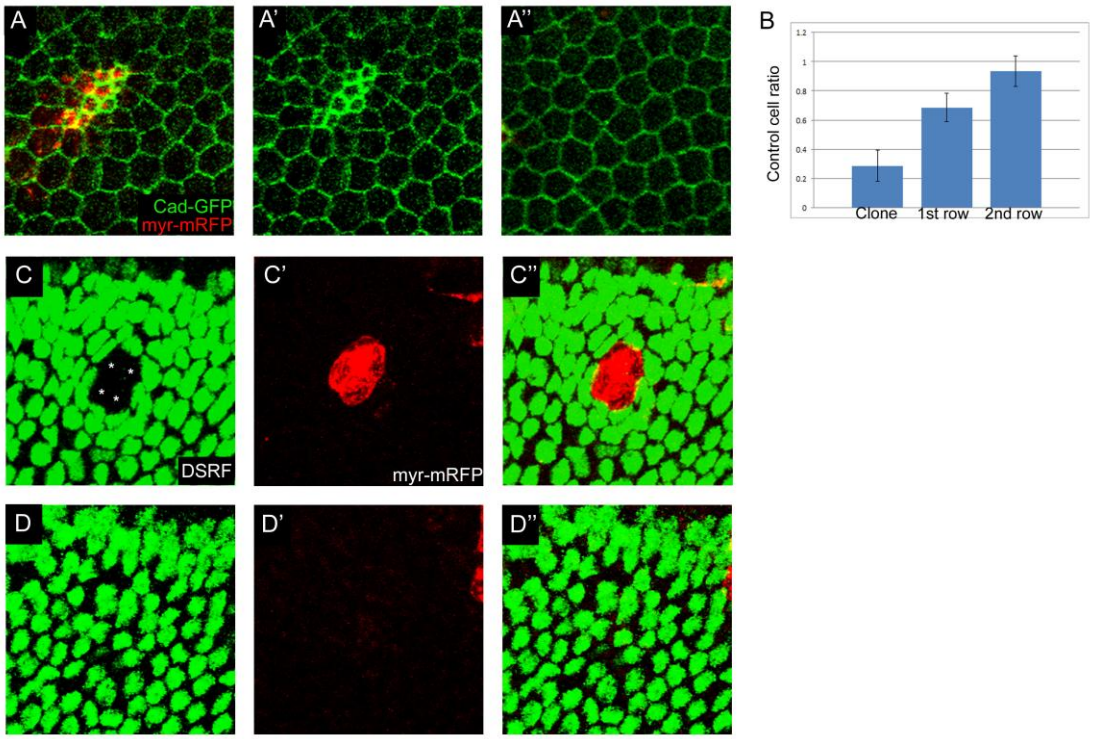

Figure 5.22. *tkv*^{QD}-expressing clones autonomously induce vein fate. (A-A') 8-cell clone expressing *tkv*^{QD} in the intervein, leading to striking apical constriction. (A'') Cell morphology in opposite layer is unaffected. (B) Intervein clone cell apical area is dramatically reduced. Control ratios - Clone : control = 0.286 (stdev 0.107), 1st row : control = 0.685 (stdev = 0.099), 2nd row : control = 0.936 (stdev = 0.104). n=24 clones in 6 wings. (C-C'') 4-cell *tkv*^{QD} expressing clone leads to *DSRF* inhibition in clone cells (asterisks in A) but not in their neighbours. (D-D'') Cells in the opposite layer do not repress *DSRF*.

tkv^{QD} induces apical constriction in intervein cells, and as with *dpp* we see reduced apical area in first row neighbours. We next tested whether this non-autonomous effect was a result of pathway activation in the neighbouring cells. Expression of *tkv*^{QD} in intervein cells leads to the autonomous loss of *DSRF* expression in labelled cells (Fig. 5.22 C, clone cell positions shown by asterisks), but not in the neighbouring cells (Fig. 5.22 C-C''). The constriction seen in first row neighbouring cells is not therefore a result of BMP pathway activation, and the smaller apical surface area may solely be due to the reduced cell-cell junction shared with the clone cell, as described above. In accordance with the lack of interplanar induction of apical constriction, *tkv*^{QD}-expressing clones do not lead to down-regulation of *DSRF* expression in the opposite layer (Fig. 5.22 D-D').

Tkv^{QD} in intervein induces constriction, but intriguingly can also antagonise vein development. When the duration of the heat shock is increased to increase clone number, the wing is covered by spots of apically constricting cells, but the endogenous veins are largely absent, both in terms of apical constriction (Fig. 5.23 A-A'), and the formation of basal lumen (Fig. 5.23 B''). Compared to wild type wings (see Fig. 5.9 A'), apposition is in fact increased in wings containing frequent clones, with lumens mainly restricted to small, non-continuous patches. Vein loss is associated with clones that include vein cells or where the vein should be (arrows in Fig. 5.23 B), and constriction is lost in non-clone, wild type tissue (arrowheads in Fig. 5.23 B'). This dual effect is also revealed with *DSRF*. *DSRF* expression is lost autonomously within the clones, but the continuous stripes of *DSRF* repression typical of veins are absent (Fig. 5.23 C-C'), in contrast to *dpp*-expressing clones (Fig. 5.20 D'). Thus, *DSRF* expression is expanded outside of *tkv*^{QD}-expressing clones, and vein constriction is absent. These two phenomena are seen in the wings of adults, which show both ectopic patches of pigmented cuticle in the intervein (arrows in Fig. 5.23 D, E), and the loss of continuous vein stripes (arrowhead in Fig. 5.23 E). A potential mechanism for the antagonism of veins is via a target of Tkv^{QD} (but not Dpp), as is further discussed in the Chapter Summary.

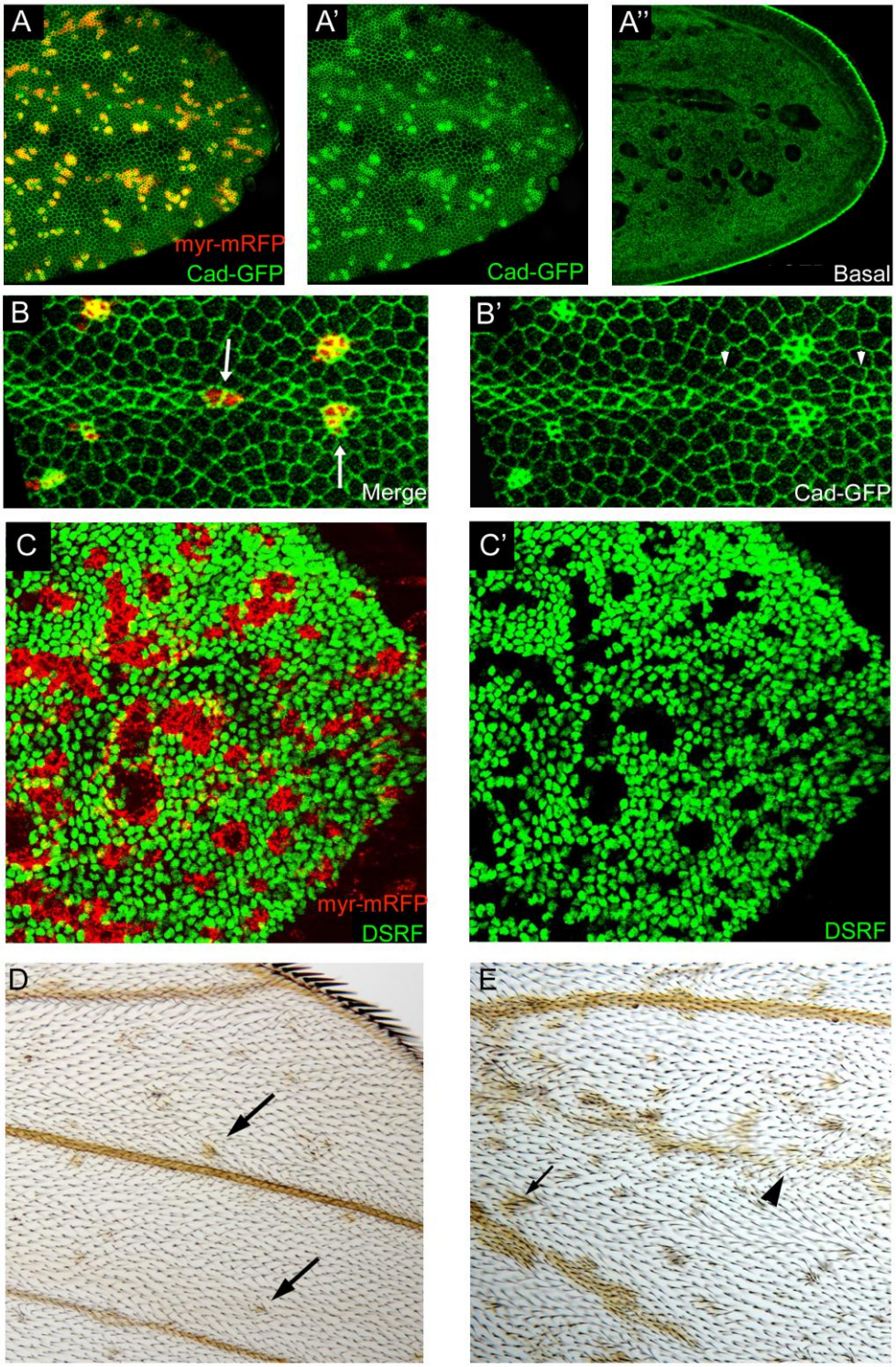

Figure 5.23. *tkv*^{QD} clones non-autonomously inhibit vein development. (A-A'') Multiple *tkv*^{QD}-expressing clones lead to spots of ectopic constriction across the wing but the loss of stripes of apical constriction of the veins (B'), and the loss of coherent vein lumen (A''). (B-B') Close up showing how clones associated with veins (arrows) lead to vein loss non-autonomously (arrowheads). (C, C') Multiple clones lead to autonomous inhibition of *DSRF* in non-continuous patches, and the loss of stripes of vein *DSRF* inhibition, i.e. representing an expansion of *DSRF* into vein territories. (D, E) Adult wings differentiate ectopic spots of vein in the intervein (arrows) and also show vein loss (arrowhead).

IV. Summary

In pupal wing development, intercellular signalling maintains and refines domains of cell fate, and cells in these different fate domains execute distinct cell shape changes. In this Chapter we have investigated the ability of signals to induce fate and shape changes in both dimensions of the pupal wing, and have documented the different behaviours shown by different components of the pathways involved.

Interplanar signalling

By creating asymmetries of gene function specifically in the pupal wing we documented the ability of signals to influence cell behaviour in the opposite layer. The results of the various experimental conditions are shown in Fig. 5.24 and catalogued in Table 5.1. In rescue studies, we showed that extracellular BMP components could promote PCV development in the opposite layer, consistent with previous studies (de Celis, 1997; Ray and Wharton, 2001). Because this rescue occurred in both directions, there is no directional induction of vein differentiation, in contrast to an alternate model (Garcia-Bellido, 1977; Guichard et al., 1999). There are two implications of this 'bidirectional rescue.' The first is that signals can travel in both directions between the veins; that is, there is no inherent directionality to the signalling events. The second is that while interplanar signals can rescue vein formation in mutant tissue, the wild type tissue itself develops as normal in the absence of signals coming from the opposite layer. Thus, *reciprocal* signalling is not required. In such conditions, vein development is promoted in both wild type and mutant tissue (i.e. in both intraplanar and interplanar dimensions), showing that the same signals mediate both events.

The ability of extracellular signals to promote vein development in the opposite layer is also demonstrated by mis-expression experiments. When BMP ligands are expressed throughout the dorsal layer, ventral cells non-autonomously repress *DSRF* and constricted their apices, and large regions of the wing fail to appose. *dpp*-expressing clones show that this effect is also bidirectional. Interplanar signalling also leads to the expansion of ventral veins following dorsal *N* or *Tkv* RNAi. Reductions in *Tkv* or *N* expression would in turn lead to an expansion of *dpp* expression (de Celis, 1997; de Celis et al., 1997), which would then signal to the opposite layer to overcome provein antagonism.

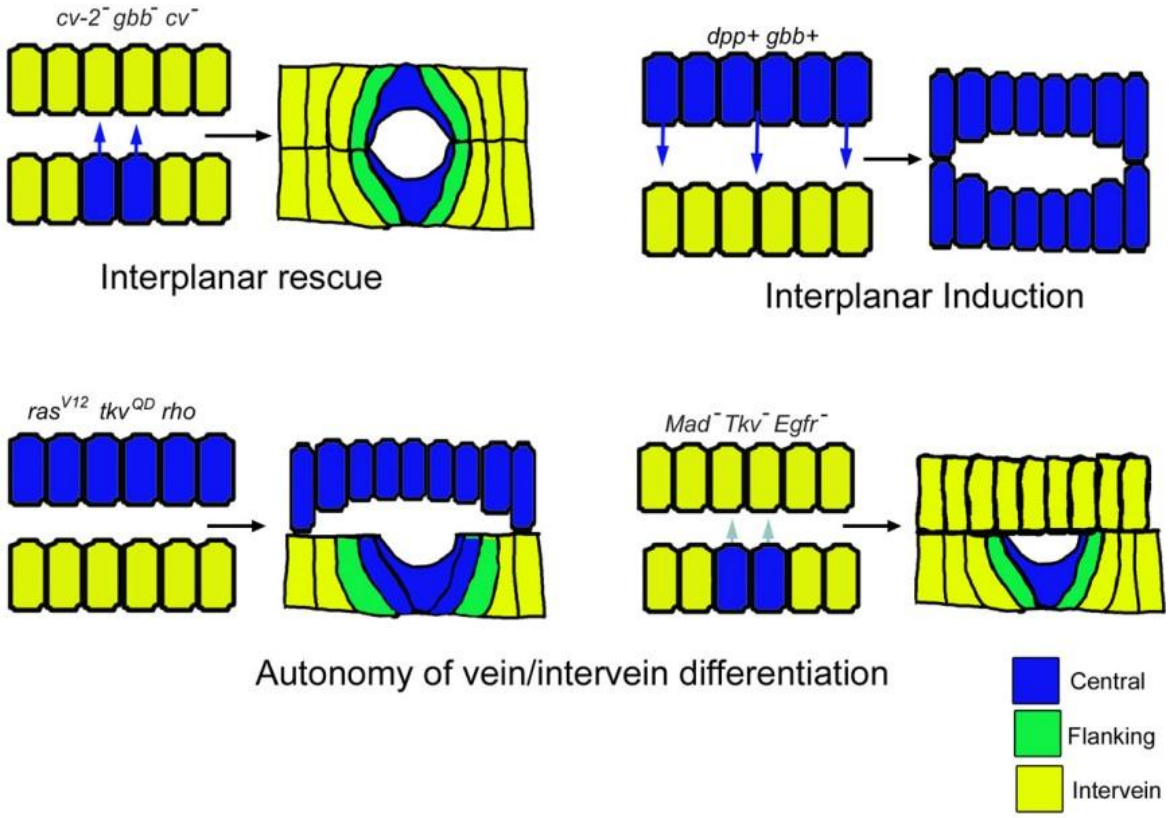

Figure 5.24. Summary of interplanar experiments. Cell types shown in key. Blue arrows indicate induction. Pale blue arrows indicate unsuccessful rescue. See text for details.

	Ubiquitous expression	Dorsal expression
Dpp	Constriction, DSRF repression in both layers. Brief periods = PCV loss.	*Dorsal:* Constriction, DSRF repression *Ventral:* Constriction, DSRF repression
Gbb	Constriction, DSRF repression (primarily near veins) in both layers	*Dorsal:* Constriction, DSRF repression, primarily near the veins *Ventral:* Constriction, DSRF repression, primarily near the veins
Tkv^{QD}	Constriction, DSRF repression in both layers	*Dorsal*: constriction and DSRF repression. *Ventral*: longitudinal veins broader, PCV lost.
Rhomboid	Constriction, DSRF repression in both layers.	*Dorsal*: constriction and DSRF repression. *Ventral*: largely wild type, but veins are broader and some ectopic venation distally.
Ras^{V12}	Constriction in both layers.	*Dorsal*: constriction *Ventral*: largely wild type, veins are broader
Tkv RNAi	-	*Dorsal*: Diminished constriction and DSRF expansion dorsally. *Ventral*: Broader longitudinal veins, PCV partially lost.
Mad RNAi	Diminished constriction and expansion of DSRF in both layers	*Dorsal*: diminished constriction and expansion of DSRF. *Ventral*: wild type.
Egfr RNAi	*en-Gal4* – loss of veins	*Dorsal*: diminished constriction *Ventral*: wild type
N RNAi	Expansion of constriction into provein regions	*Dorsal:* Expansion of constriction into provein regions *Ventral:* Expansion of constriction into provein regions

Table 5.1. Summary of consequences of ubiquitous compared to dorsal expression of pathway activators/inhibitors.

In contrast to ligand expression or provein knockdown, transformation of the entire dorsal layer to vein with non-secreted pathway activators (*tkv*^{QD}*, rho, ras*^{V12}) have only minor effects on opposite intervein cells, which adopted relaxed apical surfaces and showed *DSRF* expression as in wild type. As well as strongly suggesting that the ligand-mediated induction represents a direct signalling event, these results demonstrate that continued intervein development does not require concomitant intervein development in the opposite layer; indeed, does not even require the formation of basal contacts with the opposing layer.

We were also able to show that vein development does not require vein differentiation in the opposite layer, as seen when inducing *Egfr, Tkv* and *Mad RNAi* dorsally. In these cases, dorsal cells are unable to transduce 'vein' signals (whether from intraplanar or interplanar sources), and thus develop as intervein (fail to constrict, express *DSRF*). However, ventral vein cell differentiation occurs as normal, showing that, as was seen for intervein, veins can develop in the absence of vein development in the opposite layer. This is consistent with rescue experiments, which showed normal development in the absence of signals from the opposite layer. Thus, although interplanar signalling can occur, it is not required for cellular differentiation.

If vein/intervein development can occur autonomously, in the absence of interactions (both in physical and signalling terms) with the opposite layer, what is the endogenous role of interplanar signalling in wing development? Although ventral vein differentiation occurs autonomously in the above examples, the pattern was not completely wild type. For example, when the dorsal layer was converted to vein with *tkv*^{QD}, ventral longitudinal vein domains were broader as assessed with DSRF, and dorsally activating the EGFR pathway also lead to broader and less well-defined ventral veins. These results suggest that the refinement of vein domains that occurs after reapposition might rely on interplanar signalling. Thus, whereas intraplanar signalling alone is sufficient for the differentiation of vein/intervein histotype, interplanar signalling may play a key role in correctly refining the vein domains. Incorrectly refined veins would likely affect the structural integrity of the wings, given the importance of the veins to multiple aspects of wing structure including deformability during flight and the prevention of desiccation (Wootton, 1992). If so, interplanar signalling is a key component of the signalling mechanisms that create a flight-ready wing blade.

Another aspect of interplanar non-autonomy was seen for PCV development. The ventral component of the PCV develops as normal when the dorsal component was lost following *Mad* or *Egfr RNAi*. In these cases the PCV shows the same autonomy as the longitudinal veins show.

However, it failed when we expressed *tkv dsRNA* or tkv^{QD} dorsally, and when *cv-c* was lost dorsally. We will show in Chapter 6 how *cv-c* expression is downstream of BMP signalling in the PCV, and that Cv-c inhibits a function for the RhoGTPase Rho1 in promoting intervein development. We will also show that the likely effector of this function (Rho Kinase) is capable of inhibiting crossvein development when hyperactivated in the dorsal layer. Thus, single-sided loss of Cv-c leads to Rho1/Rok hyperactivation, which in turn is capable of dominantly inhibiting vein development in the opposite layer (Fig. 5.25). Rho1 might achieve this if, when hyperactivated, it promoted the extension of basal processes across the lumen, which when contacting vein cells of the opposing layer induce intervein development. This would be an example of cell-cell contact leading to the induction of cell fate.

In this context, loss of BMP ligands from one layer would have no effect, as pathway activation (and hence *cv-c* expression and Rho1 antagonism) would be rescued by interplanar signals from the opposing layer. However, reducing Tkv functionality would lead to a loss of *cv-c* expression and the hyperactivation of Rho1. This would inhibit vein development in both dorsal and ventral layers. Considering this model, we would expect *Mad RNAi* to show a similar phenotype, but it does not. However, if *Mad RNAi* did not reduce pathway activity to the same extent as *Tkv RNAi*, this would leave residual levels of *cv-c* expression in dorsal cells. These levels would lead to partial Rho1 hyperactivation to the extent that constriction was inhibited in dorsal cells, but not to the extent that vein development was dominantly inhibited in ventral cells (Fig. 5.25).

Intraplanar signalling

FLPout clones allowed us to address the ability of signals to travel in the intraplanar dimension. We assessed whether different BMP signalling components could activate the pathway and promote vein differentiation when ectopically expressed in intervein cells, and documented distinctive behaviours by each of the components of the pathway (Fig. 5.26).

We found that clones expressing Gbb cannot activate the BMP pathway and are thus not able to induce apical constriction in intervein cells. *gbb* is required for vein development in the crossveins and distal sections of the longitudinal veins (Ray and Wharton, 2001), and we had shown that its expression throughout the wing layers causes ectopic apical constriction. However, restricted expression in the intervein fails to activate the pathway. A potential cause of this is that Gbb can only signal in the form of a heterodimer with Dpp, as has been

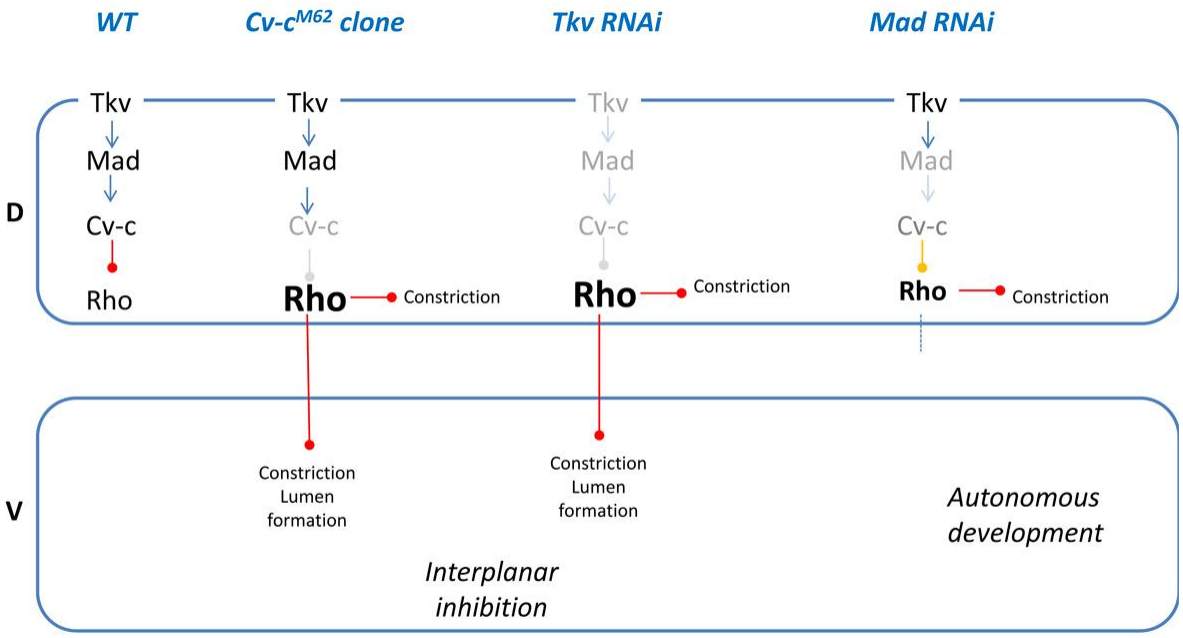

Figure 5.25. Model for domineering non-autonomy of Cv-c and Tkv in PCV development. See text for details.

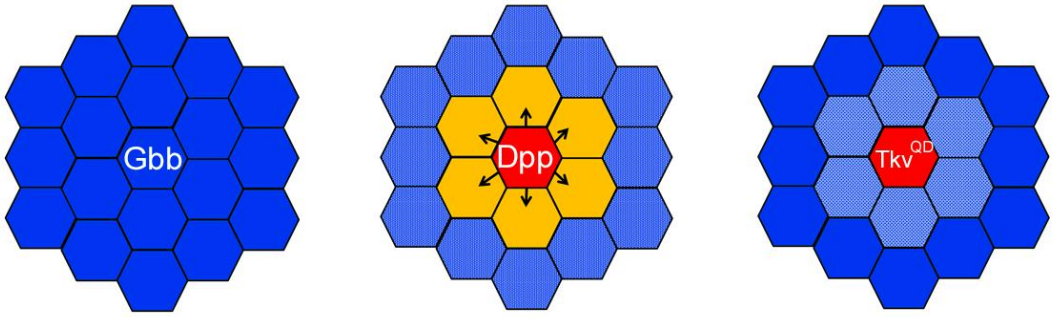

Figure 5.26. Effects of expression of BMP pathway components in intervein cells. Hexagonal array intervein in which one cell at the centre expresses the labelled pathway component. Blue = no effect on apical area. Hatched blue = apical area reduction due to sharing cell-cell contact with clone cell. Orange = apical area reduction and pathway activation. Red = apical constriction due to autocrine signalling.

suggested by previous studies (Ray and Wharton, 2001; Bangi and Wharton, 2006). Tissue-wide expression leads to effects focussed around the veins, i.e. near the regions of *dpp* expression, so this signalling may arise from vein-derived Dpp-Gbb heterodimers. In contrast, clones of cells in the intervein can only lead to inert Gbb-Gbb homodimers. This possibility is further explored in the Discussion (Chapter 7).

Dpp was able induce constriction in the intervein, both in the labelled cells and their neighbours (both adjacent and opposite). The induction of constriction was accompanied by the activation of the pathway, as assessed with *DSRF*. Furthermore, we showed that *tkv* expression was affected by ectopic Dpp in the intervein. Dpp can both inhibit *tkv* expression within clones, and promote it in neighbouring cells, leading to the formation of 'halos' around the clones. Neighbouring cells thus show heightened *tkv* as well as *DSRF* expression. In these halos, Tkv may act as a restriction to diffusion of ectopically expressed Dpp, as it does in the wing disc (Lecuit and Cohen, 1998; Tanimoto et al., 2000). In the pupal wing, *tkv* is expressed in the provein domains, where it presumably plays a similar role (Sotillos and de Celis, 2005). A distinction between ectopic expression and the wild type situation is that whereas *tkv* is induced following pathway activation in the 'halo' cells, in the proveins *tkv* expression is seen where the pathway is not active. Thus, if endogenous Tkv in the provein does act as a ligand trap, it must do so without transducing the Dpp signal.

Like Dpp, expression of Tkv^{QD} led to apical constriction in clone cells and their neighbours, but only led to *DSRF* suppression in the clone cells. Thus, the reduction in cell area in neighbouring cells is not a result of pathway activation, but rather an indirect effect. The reduced length of the shared cell-cell junction may be a contributory factor, which would highlight how the shape of an epithelial cell is strongly influenced by the shape of its neighbour, as we saw in Chapter 3. Furthermore, it would suggest that reduced apical area in the first row neighbours of *dpp*-expressing clones results from a combination of active apical constriction and the passive reduction in the length of the cell-cell junction. This example would serve to reinforce the notion that cell shape changes arise from a combination of intrinsically and extrinsically generated forces (Paluch and Heisenberg, 2009).

As well as inducing constriction in intervein cells, tkv^{QD} can non-autonomously antagonise vein development. This phenotype does not arise from *dpp*-expressing clones, and may reflect the different levels of pathway activation elicited by the two constructs. If Tkv^{QD} activates the pathway to a higher extent, it may lead to the induction of high-threshold targets which Dpp could not induce. One potential target is the Notch ligand *Dl*, which would in turn activate the

Notch pathway in surrounding cells, inhibiting vein formation and leading to the expression of *DSRF*. In this scenario, whereas Dpp directly promotes venation, activating Tkv indirectly leads to vein-inhibition signalling in surrounding cells. Even though these neighbouring cells would show Notch pathway activity, they would still be relatively constricted due to the indirect effect of sharing a junction with a constricting cell.

Chapter 6

The RhoGAP Cv-c controls cell shape downstream of BMP signalling in the PCV

I. Chapter Overview

Cell signalling pathways can control cell shape changes by influencing the activity of cytoskeletal regulators such as the small GTPase Rho1. Rho1 stimulates cytoskeletal alterations by activating effector proteins such as Rho Kinase (Rok), and its activity is precisely controlled within the cell, in part by the RhoGAPs which promote the inactive GDP-bound state. Here we investigate the role of Cv-c, a RhoGAP, in the development of the crossveins in the *Drosophila* wing. We show that *cv-c* is a transcriptional target of BMP signalling, and is required for cell shape changes in PCV development. Cv-c acts to inhibit a hitherto undescribed function for Rho1 in promoting intervein development, and we show that reducing activity of Rho1 or Rok leads to the formation of ectopic crossveins. These results uncover a link between patterning and morphogenesis, whereby BMP signalling inhibits Rho1 activity by the transcriptional upregulation of a RhoGAP.

II. Introduction

The patterning of epithelia by intercellular signalling subdivides a uniform sheet of cells into distinct cell fates. The specification of cell fate, often by the activation of signal transduction pathways, is followed by the appropriate cellular differentiation, often achieved by alterations to the cytoskeleton. The convergence of cell signalling pathways onto regulators of the cytoskeleton, such as the Rho family of small GTPases, is one manner in which patterning can be linked to cellular differentiation.

RhoGTPases are multifunctional proteins that shuttle between active, GTP-bound states and inactive, GDP-bound states (Jaffe and Hall, 2005). This shuttling is controlled by the RhoGEFs, which stimulate the exchange of GDP for GTP thus promoting the active state (Schmidt and Hall, 2002), the RhoGDIs, which sequester GDP-bound Rho in the cytosol (Garcia-Mata et al., 2011), and the RhoGAPs, which increase the intrinsic GTPase activity, thus promoting the inactive state (Bernards and Settleman, 2004). Altering the activity and availability of RhoGEFs/RhoGAPs has emerged as a fundamental aspect of RhoGTPase control. Active RhoGTPases control a multitude of functions in the cell, prominent among which are alterations to the cytoskeleton (Nobes and Hall, 1995). These are mediated via effector proteins such as Rho Kinase (Amano et al., 1996; Mizuno et al., 1999), an effector specific for RhoA (Rho1 in *Drosophila*). A key target of Rok is non-muscle myosin II (Myo-II), which when phosphorylated induces the contraction of Actin filaments. Myo-II driven contractions of Actin filaments are seen in numerous developmental contexts such as cell migration (Ridley et al., 2003), the contractile ring of mitosis (Pollard and Cooper, 2009), and during apical constriction (Sawyer et al., 2010).

Drosophila wing development provides an opportunity to investigate how cell fate specification is linked to differentiation. In contrast to the longitudinal veins, crossvein specification occurs in pupal development, coincident with the reapposition of the dorsal and ventral layers. This is controlled by activation of the BMP pathway, and is independent of EGFR signalling (Conley et al., 2000; Ralston and Blair, 2005). As a result, the crossveins are particularly sensitive to reductions in BMP pathway activity (Ray and Wharton, 2001; O'Connor et al., 2006). The characterisation of certain 'crossveinless' genes has revealed the importance of extracellular regulation of BMP ligands in crossvein patterning. *cv* and *cv-2* encode extracellular proteins which function in ligand transport and ligand availability respectively

(Conley et al., 2000; Shimmi et al., 2005a; Serpe et al., 2008). Pathway activity also requires the Chordin orthologue Sog (Shimmi et al., 2005a) and the metalloprotease Tok (Serpe et al., 2005).

While much is understood of the signalling mechanism upstream of the BMP receptor, what happens downstream is less well understood. The characterisation of two other 'crossveinless' genes has suggested a complex network. *detached* (*det*) was characterised as encoding Dystrophin, which along with Dystroglycan is required for the maintenance of BMP activity after the initial signal (Christoforou et al., 2008). In their absence, signalling is not maintained at the junctions with L4 and L5, resulting in a detached vein fragment in the intervein. *crossveinless-c* (*cv-c*) encodes a RhoGAP (Denholm et al., 2005), and hypomorphic alleles lead to the loss of crossvein material. Elsewhere in *Drosophila* development, *cv-c* functions to orchestrate morphogenetic processes that require co-ordinated changes in cell shape and arrangement, such as tubulogenesis in the trachea and Malpighian tubules (Denholm et al., 2005; Brodu and Casanova, 2006). Its role in the PCV network is however unclear, and the focus of this Chapter.

As Cv-c is a RhoGAP, negative regulation of some aspect of RhoGTPase activity appears to be required for crossvein formation, but RhoGTPases have not yet been described in the crossvein patterning network. Certain *Cdc42* alleles give rise to ectopic crossveins (Genova et al., 2000), but the origin of this phenotype is unclear. Although *Rho1* has been reported to play a role in epithelial shape and adherens junction maintenance in the pupal wing, a role in vein development was not reported (Yan et al., 2009a). However, a Rho1-specific effector, Rho Kinase (Rok), has been reported to suppress crossvein development when ectopically active (Verdier et al., 2006). Characterising the role of Cv-c will help to clarify the putative role for RhoGTPases in crossvein development. Additionally, a mammalian orthologue of *cv-c*, *Dlc-1*, has been identified as a potent tumour suppressor proposed to inhibit RhoA mediated metastatic behaviour (Lahoz and Hall, 2008; Kim et al., 2009), so understanding its function in *Drosophila* development may have relevance for its involvement in cancer metastasis.

III. Results

BMP signalling controls cell shape changes in PCV development

The specification and early development of the PCV between 18-26h APF is known to be controlled by BMP signalling independent of EGFR activity (Ralston and Blair, 2005), but the cell shape changes that accompany this process are not known. We thus observed cell shape during PCV patterning, using Cad-GFP to view apical cell outlines, and *DSRF* repression as a marker for cell fate.

At 18h APF, as the dorsal and ventral layers reappose (see Fig. 3.2), *DSRF* is repressed in stripes corresponding to the presumptive L4 and L5 veins, and expressed throughout the presumptive PCV region (Fig. 6.1 A). At this stage, apical cell shapes and sizes are variable, and the vein is not yet apparent (Fig. 6.1 A'). Vein development is initiated between 18-22h APF, as *DSRF* is down-regulated in a broad band (Fig. 6.1 B). This is accompanied by a corresponding band of apical constriction (Fig. 6.1 B'). By 26h APF, the band of *DSRF* down-regulation has refined (Fig. 6.1 C), and a corresponding refinement of constriction in the crossvein cells is observed (Fig. 6.1 C'). During this 18-26h APF period, the PCV lumen is also formed (Fig. 3.2). Further refinement between 26-32h APF creates a thin stripe of apically constricted cells of the PCV that do not express *DSRF*, bounded by apically relaxed intervein cells that do (Fig. 6.1 D, D'). The specification of the PCV is thus coincident with its cellular differentiation.

To confirm that BMP signalling controls these shape changes, we observed apical constriction in *gbb* mutant wings (Ray and Wharton, 2001). At 22h and 26h APF, *DSRF* expression persists throughout the L4-L5 intervein (Fig. 6.1 E, F), consistent with the loss of the BMP signal. Correspondingly, no apical constriction is seen in this region (Figs. 6.1 E', F'). This shows that apical constriction during early PCV development is dependent on BMP signalling. It had been previously proposed that while BMP signalling maintains vein fate in the pupal wing, cell shape changes are exclusively controlled by EGFR pathway activity (O'Keefe et al., 2007). Considering early PCV development is independent of EGFR activation (Ralston and Blair, 2005), the above results demonstrate an instructive role for BMP signalling in cell shape changes. Therefore, there is not a segregation between 'fate' and 'shape' signal transduction pathways in the pupal wing veins.

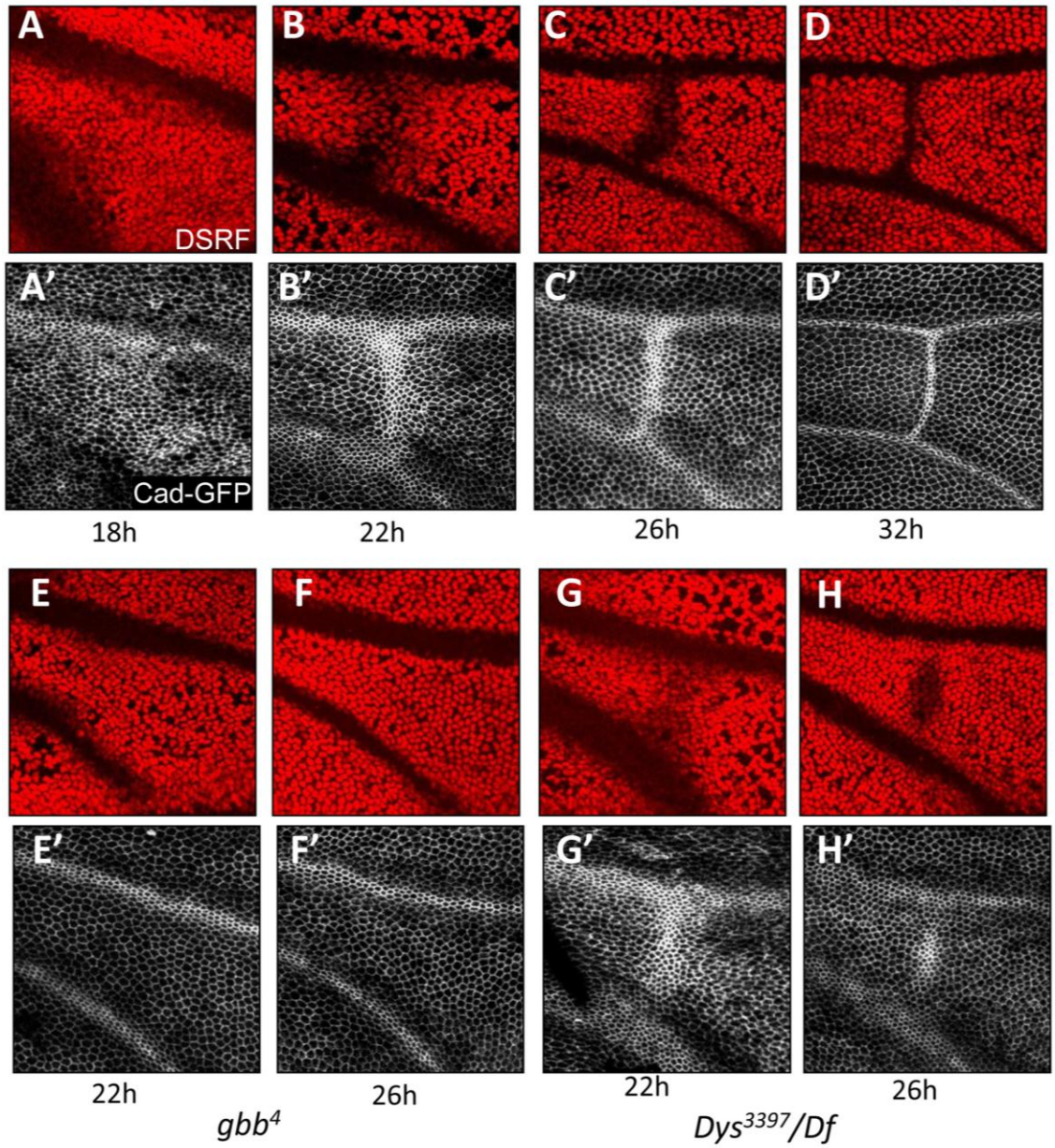

Figure 6.1 Cell fate and shape changes during PCV development. (A-D) *DSRF* expression in *Ubi-DECad-GFP/+* wings focussed on the region of the PCV, at 18h, 22h, 26h and 32h APF. (A'-D') Cad-GFP localisation in the same wings. (E-F) *DSRF* expression in gbb^{4} *DTD48/*gbb^{4} *Ubi-DECad-GFP* wings at 22h and 26hAPF, showing preservation of *DSRF* expression in the PCV region. (E'-F') Cad-GFP localisation in the same wings, showing complete loss of constriction in the PCV region. (G-H) *DSRF* expression in Dys^{3397} *Ubi-DECad-GFP/Df6184* wings, showing repression at 22h APF (G) followed by failure to maintain repression in anterior and posterior regions (H). (G'-H') Cad-GFP localisation in the same wings, showing an initial constriction (G') which is not maintained in those regions which lose pathway activity (H').

Dystrophin (Dys), along with Dystroglycan (Dg), is required for the maintenance of BMP signalling in the junctions of the PCV and the longitudinal veins (Christoforou et al., 2008). In *Dys* mutants, while initial down-regulation of *DSRF* occurs as normal (Fig. 6.1 G), it only persists in the middle of the intervein (Fig. 6.1 H'; Christoforou et al., 2008)). In terms of cell shape changes, an initially broad band of constriction at 22h AFP is only maintained in the centre of the intervein, leaving an island of constricted cells (Fig 6.1 G, H), which presumably give rise to the 'detached' stretch of vein cuticle in the adult wing (Christoforou et al., 2008). Similar phenotypes were seen with *Dg* mutants. This shows that apical constriction during the development of the PCV is dependent on the maintained activation of the BMP pathway after initial specification.

cv-c is required for cell shape changes in PCV development

Various extracellular modulators have been identified that enhance or refine the activity of BMP ligands in PCV development (Conley et al., 2000; Ralston and Blair, 2005; Serpe et al., 2005; Shimmi et al., 2005a; Serpe et al., 2008; Szuperak et al., 2011), but factors downstream of pathway activation that execute cell morphogenesis, the so called 'realisator' genes, are not known. *cv-c* is required in numerous developmental processes which involve co-ordinated changes to cell shape (Denholm et al., 2005; Brodu and Casanova, 2006; Simoes et al., 2006), and as a 'crossveinless' gene it represents a potential candidate. In contrast to wild type wings (Fig. 6.2 A), the hypomorphic allele *cv-c*^{1} results in the loss of most of the PCV in adult wings, although a stretch of venation in the intervein that often runs parallel to L5 remains (Fig. 6.2 B). Incomplete PCV loss is also observed when driving RNAi at high levels in the posterior compartment throughout development using *en-Gal4* (Fig. 6.2 C).

To address the cellular basis of this phenotype, we observed cell shape changes and *DSRF* expression in *cv-c*^{1}/*cv-c*^{6} mutants, a viable hypomorphic allelic combination. At 18h APF, *DSRF* is uniformly expressed and constriction is variable across the region (Fig. 6.2 D, D'), as in wild type (see Fig. 6.1 A, A'). At 22h APF, *DSRF* is down-regulated in a broad band (Fig. 6.2 E). At this stage constriction is variable and often focussed around a patch of cells in the middle of the intervein (Fig. 6.2 E'), in contrast to the coherent broad band of constricting cells seen in wild type. At 26h APF, *DSRF* down-regulation is restricted to a patch of cells in the L4-L5 intervein which tails off distally in the posterior (Fig. 6.2 F). At this stage, constriction is seen only in those cells in which *DSRF* is down-regulated (Fig. 6.2 F, F'), and these cells presumably

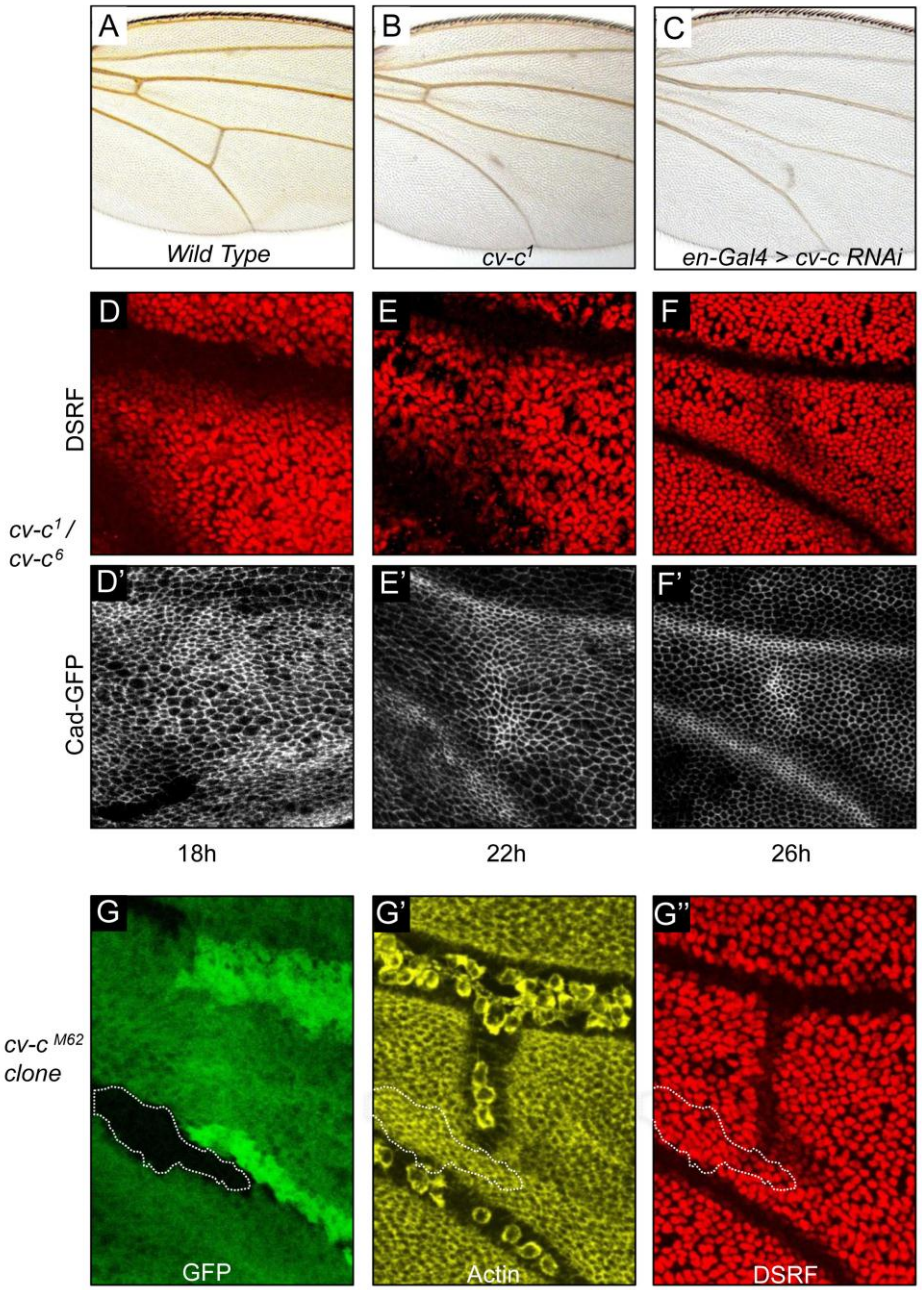

Figure 6.2. *cv-c* is required for cell shape and fate changes in the PCV. (A) Wild type adult wing, showing PCV connecting L4 and L5. (B) *cv-c*^{1} homozygotes lose most of the PCV material. (C) Expression of *cv-c dsRNA* in the posterior compartment with *en-Gal4* throughout development at 29ºC causes a similar phenotype. (D-F) *DSRF* expression in *Ubi-DECadGFP/+ ; cv-c*^{1}*/cv-c*^{M62} wings between at 18h, 22h and 26h APF, showing a weak band of repression at 22h (E), which then refines to a skewed stripe of partial down-regulation at 26h APF (F). (D'-F') Cad-GFP in the same wings, showing constriction warped around a central patch at 22h APF (E'), and subsequently limited to a patch in the middle of the wing by 26h AFP (F'). (G-G'') *cv-c*^{M62} clone, marked by the absence of GFP (G, outlined in white). (G') Basal section of the clone, labelling Actin, showing apposition in the clone region. (G'') *DSRF* expression in clone surface, showing expansion of *DSRF* expression associated with the clone.

correspond to the detached vein fragment seen in adult wings (Fig 6.2 B, C). Thus, partial loss of *cv-c* function leads to a failure of orchestrated apical constriction in the PCV regions, and the failure to down-regulate *DSRF* in those cells that do not constrict.

The above phenotypes arise from incomplete loss of *cv-c* function, and to assess the consequences of complete loss of function on cell morphology we generated clones of the null allele *cv-c*^{M62} (Denholm et al., 2005), using *DSRF* expression and Actin distribution to observe cell fate and shape respectively. Clones did not affect vein morphology when associated with the longitudinal veins, showing that *cv-c* function in the pupal wing is specific to the crossveins. We recovered 7 clones in the PCV region, all of which led the loss of vein cell characteristics. We described in Chapter 5 how such clones lead to the loss of apical enrichment of Actin, both autonomously within the clone and non-autonomously in cells of the opposite layer (Fig. 5.3 G, H). Thus, Cv-c is required for apical constriction in the PCV. These clones also affect the basal morphology of vein cells, with clone cells failing to form a lumen (Fig. 6.2 F, F'). Additionally, clone cells completely fail to down-regulate *DSRF* (Fig. 6.2 G''). Thus, *cv-c* null clones lead to the complete failure of vein shape changes in the PCV and of *DSRF* repression. As we were unable to recover clones that covered the entire vein, we cannot yet attribute an essential role for Cv-c in controlling these phenotypes in *all* cells of the PCV. However, it is noteworthy that vein cell characteristics were always completely lost within the clones, whether they covered the anterior or posterior sections of the PCV.

The requirement for Cv-c in the apical enrichment of Actin is also seen other developmental contexts (Denholm et al., 2005; Brodu and Casanova, 2006), showing it to be a common function of the gene. Furthermore, the failure to form the lumen shows that Cv-c is also required for the basal morphology of PCV cells. An intriguing aspect of the clones, and the hypomorphic mutants, was the failure of *DSRF* repression: in the absence of Cv-c, cells in the PCV region retain an intervein identity. Because of this, it is unclear whether the failure of cell shape changes is due to a direct requirement for Cv-c in directing shape changes (as would be consistent with its role in other developmental contexts), or rather is wholly due to the failure to repress *DSRF*. A final possibility is that Cv-c has both DSRF-dependent and DSRF-independent roles. We further address this problem below when we assess the likely target of Cv-c in PCV development.

cv-c expression arises coincident with *DSRF* repression in the PCV

Considering its functional requirements, we next addressed the expression pattern of *cv-c* in the pupal wing. To do this we used *cv-c*^{06951}, a P element insertion which drives expression of LacZ in a pattern which recapitulates wild type *cv-c* expression (Denholm et al., 2005), and performed α-βGal antibody staining in pupal wings. *cv-c*^{06951} is dynamically expressed during PCV development. At 18h APF, when *DSRF* is expressed throughout the PCV region (Fig. 6.3 A), *cv-c*^{06951} expression is heightened in a small subset of cells in the anterior part of the presumptive PCV (Fig. 6.3 B; expression seen in 4/4 wings). By 22h APF, *cv-c*^{06951} expression is seen in a broad domain in the PCV region (Fig. 6.3 B', B'') which overlaps the region of *DSRF* down-regulation (Fig. 6.3 B, B''). By 26h APF, *cv-c*^{06951} expression has refined and strengthened (Fig. 6.3 C'), but is broader than the band of *DSRF* repression (Fig. 6.3 C). As a result, PCV cells express *cv-c*^{06951}, but not *DSRF*, while the intervein cell flanking the crossvein express both *cv-c*^{06951} and *DSRF* (Fig. 6.3 C''). Expression of *cv-c*^{06951} is thus initiated in the developing PCV at the same time as *DSRF* is down-regulated, and shows a similar pattern of refinement. *cv-c*^{06952} expression is also heightened in other regions of the pupal wing (Fig. 6.3 D-D'''), but these do not correspond to known functions of the gene (see above).

cv-c is downstream of BMP signalling

cv-c^{06951} expression arises at the same time as BMP signalling specifies the PCV (Fig. 6.1), raising the possibility that *cv-c* is a transcriptional target of the BMP pathway. We tested this possibility by observing *cv-c*^{06951} expression in *gbb*^{4} mutants. Although expression of *cv-c*^{06951} in the other regions of the wing is still seen, expression is never observed in the PCV region of these wings, both at 22h (Fig. 6.4 A'') and 26h APF (Fig. 6.4 B''). In the absence of BMP signalling in the PCV, cells do not constrict, down-regulate *DSRF,* or express *cv-c* (Fig 6.4 B''').

As *cv-c* expression in the PCV depends on BMP signalling, we next asked whether ectopic pathway activation in the pupal wing would induce *cv-c* expression. To activate the pathway we generated *dpp*-expressing clones. In intervein regions in which *cv-c*^{06951} is not expressed (Fig. 6.5 A'), ectopic expression of *dpp* led to the induction of *cv-c*^{06951} expression (Fig. 6.5 A-C''), as well as the enrichment of apical Actin (Fig. 6.5 A'''). The induction of *cv-c* expression was seen both in clone cells and their neighbours, which is consistent with the short range action of Dpp demonstrated in the previous Chapter. In contrast to intervein clones, *dpp*-expressing clones that covered longitudinal veins did not induce *cv-c*^{06951} expression (Fig. 6.5 B-B''', arrow in Fig. 6.5 B' shows lack of expression, arrowheads show expression associated with

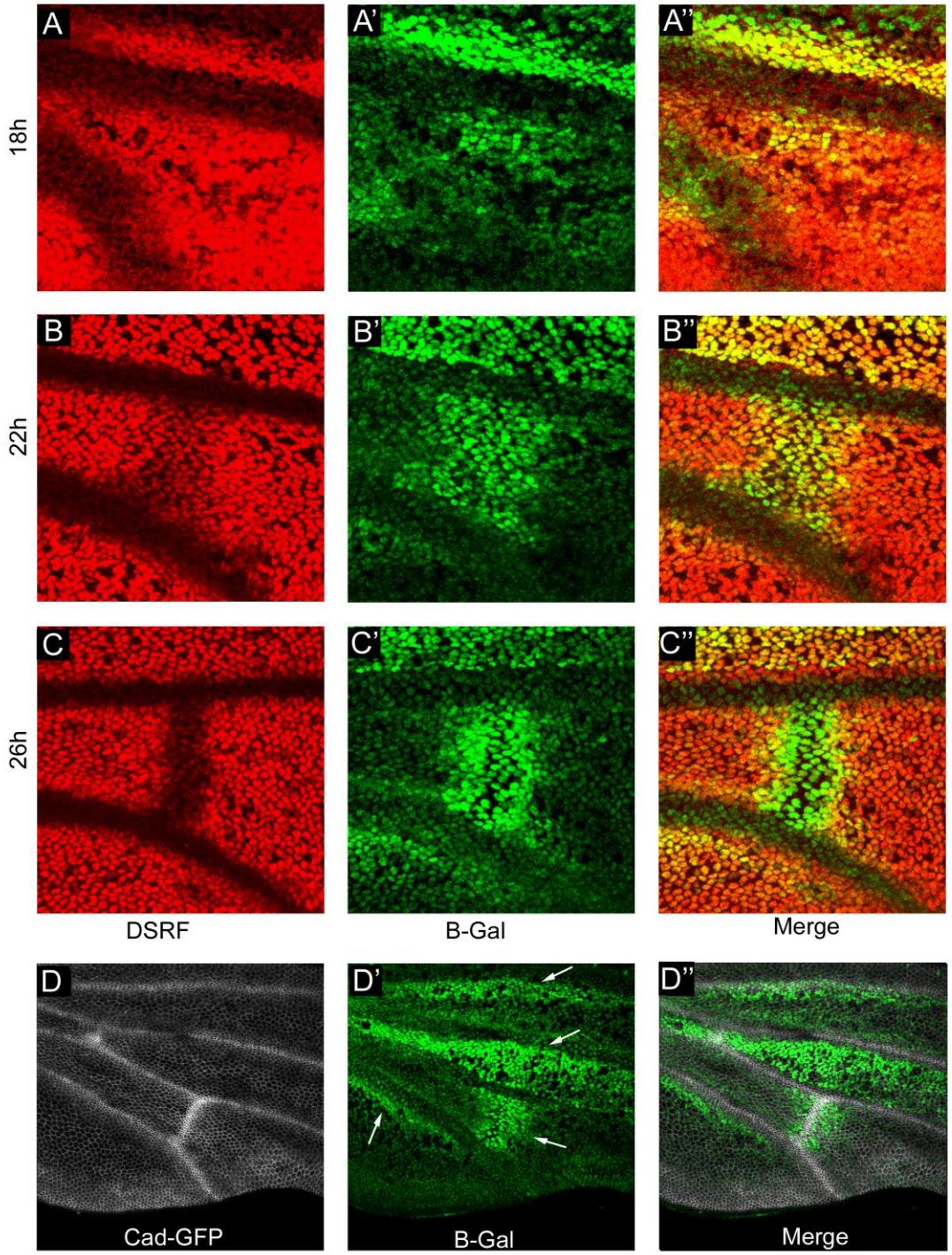

Figure 6.3. *cv-c* expression in the pupal wing. (A-C'') Time course of the PCV region in *cv-c*^{06951}*/+* wings at 18h (A-A''), 22h (B-B'') and 26h APF (C-C'') showing *DSRF* expression (B, C, D) and *cv-c* expression as detected with α-βGal staining (B', C', C''). *cv-c*^{06951} expression is seen in some cells at 18h APF (A'), then in a broad band paralleling that of *DSRF* repression (B'), and then in a refined band by 26h APF (C'), broader than that of *DSRF* repression (yellow cells in D''). (D-D'') 26h APF wing of the genotype *Ubi-DECad-GFP/+ ; cv-c*^{06951}/+, showing 4 regions of heightened expression in the pupal wing: in the L2 vein, the intervein between L3-L4, the PCV and posterior to proximal L5 (arrows).

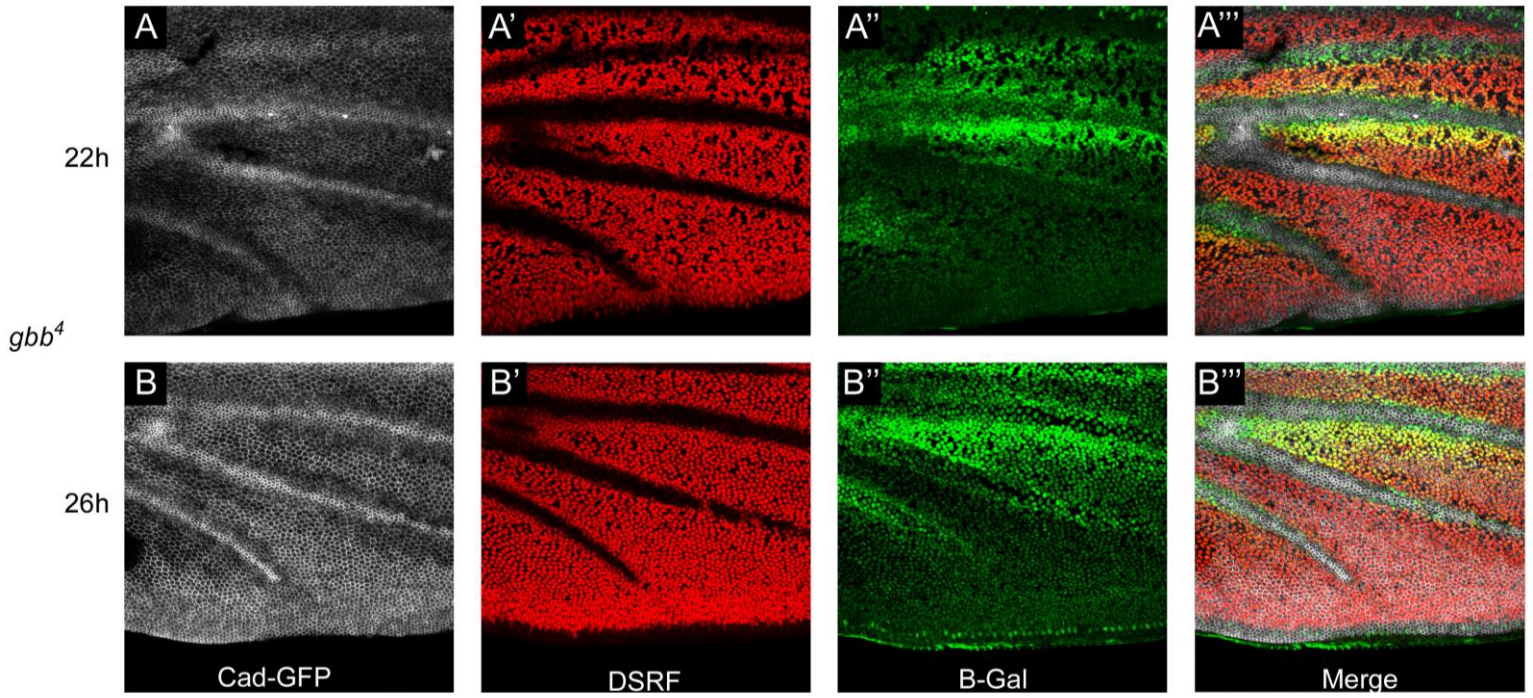

Figure 6.4. *cv-c* expression is downstream of BMP signalling in the PCV. (A-B''') *cv-c* expression in a *gbb* mutant. Wings of the genotype *gbb*^{4}*, DTD48/gbb*^{4}*, Ubi-DECad-GFP ; cv-c*^{06951}*/+*, showing Cad-GFP (white), and stained for *DSRF* (red) and α-βGal (green). *cv-c*^{06951} expression is absent in the PCV region at both 22h APF (A'') and 26h APF (B''), alongside the failure of apical constriction (A, B) and *DRSF* repression (A', B').

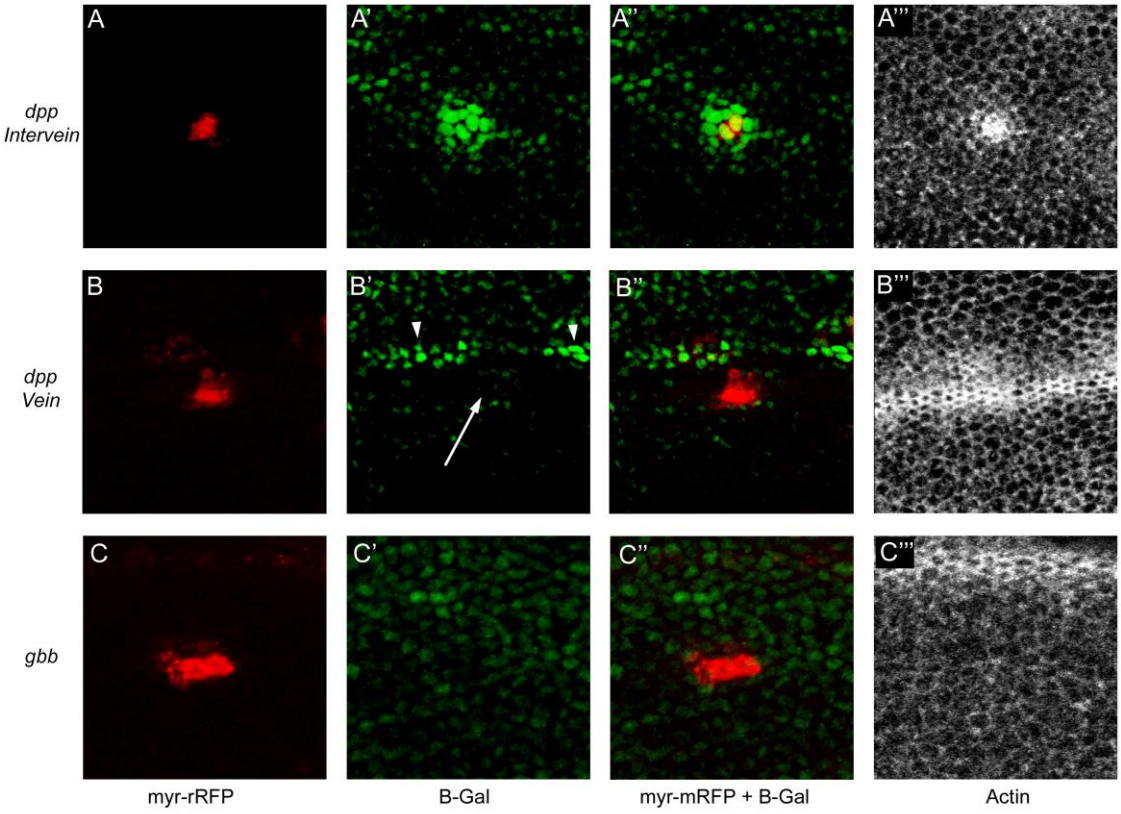

Figure 6.5. Ectopic BMP pathway activation induces *cv-c* expression. (A-A''') 2-cell clone expressing *dpp* in the intervein in a *cv-c*^{06951}*/+* background, leading to induction of *cv-c* expression (A'), in both clone cells and their neighbours (A''). (A''') Apical enrichment of Actin coincides with *cv-c* expression. (B-B''') Clone of cells on L4 (B''') does not lead to induction of *cv-c* expression (arrow in B'; arrowheads show heightened expression associated with two clones in the opposite layer). (C-C''') *gbb*-expressing clone in the intervein in a *cv-c*^{06951}*/+* background does not lead to heightened *cv-c* expression (C'), nor apical Actin enrichment (C''').

intervein clones in the opposite layer). Thus, *dpp* only induces *cv-c* expression in the intervein. Ectopic expression of *gbb*, which as we previously demonstrated does not lead to pathway activation (Fig. 5.19), similarly does not increase expression of *cv-c* (Fig. 6.5 C-C''), and cells do not constrict (Fig. 6.5 C''').

Thus, *cv-c* is downstream of BMP signalling not only in the PCV but when the pathway is ectopically activated elsewhere in the intervein. The fact that ectopic *dpp* could only induce *cv-c* expression when in the intervein suggests either that factors in the intervein co-operate with the BMP pathway to activate *cv-c* expression, or alternatively that factors in the longitudinal veins antagonise *cv-c* expression. The latter possibility is consistent with the absence of *cv-c* expression in the longitudinal veins, where the BMP pathway is active (Yu et al., 1996; Conley et al., 2000).

Dominant cellular phenotypes arising from ectopic *cv-c* expression

cv-c is necessary for vein cell shape changes in PCV development, and its expression is coincident with the apical enrichment of Actin and constriction in *dpp*-expressing intervein clones. We next asked whether ectopic *cv-c* was sufficient for apical constriction. We first used *ap-Gal4, TubGal80^{ts}* to dorsally express *cv-c* between 0-32h APF. This led to a complete and autonomous disintegration of the dorsal layer, such that the remaining wing was composed of a single, ventral layer as assessed with *DSRF* expression and Cad-GFP (Fig. 6.6 A, A'). Z projections show that the ventral layer differentiates vein and intervein in a near wild type manner, although the PCV is broader and less well-defined (Fig. 6.6 A). This shows that in the absence of a dorsal layer, ventral cells can still differentiate vein and intervein (although veins are broader), which corroborates the data presented in Chapter 5. Due to the severity of this phenotype, FLPout clones were generated to restrict expression to small groups of cells in otherwise wild type wings. *cv-c*-expressing clones did not show apical constriction (Fig. 6.7 B, B'). Indeed, clone cells were marginally larger than internal control cells, in the context of increased variation in sizes (see Fig. 6.10 E). In contrast to wild type clones, which stay contiguous (Bryant, 1970), larger clones were often fragmented (Fig. 6.6 C, C'). This fragmentation may arise from the induction of apoptosis certain clone cells, which we infer occurs when *cv-c* is expressed with *ap-Gal4* (Fig. 6.6 A).

To assess the effect of Cv-c on the three dimensional shape of the cells, we utilised GFP-tagged versions of Cv-c (Sato et al., 2010). These cells showed a striking morphology. In apical

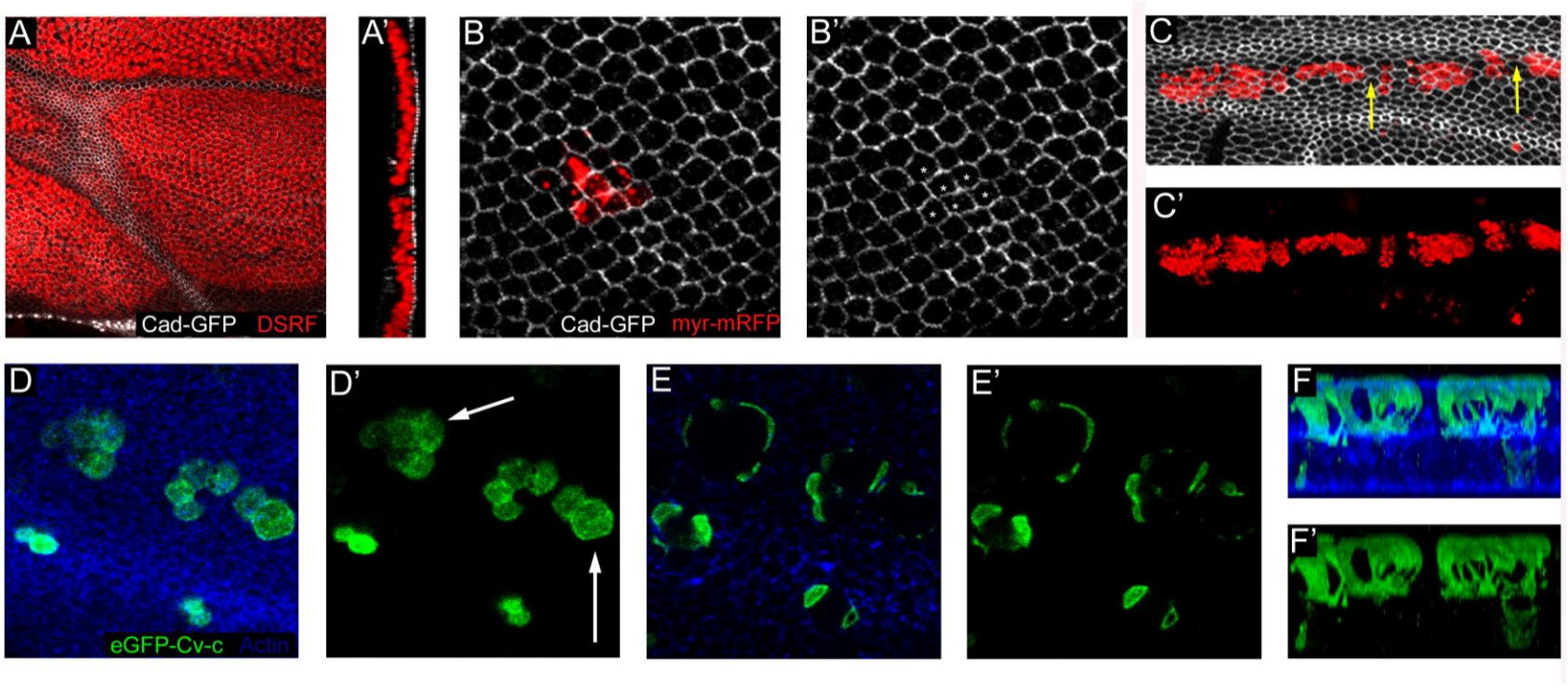

Figure 6.6. Consequences of mis-expressing *cv-c* in the wing. (A-A') Dorsal expression of *cv-c* leads to the loss of the dorsal layer. Animals of the genotype *ap-Gal4, Ubi-DECad-GFP/+ ; TubGal80^{ts}/UAS-cv-c* were raised at 18ºC until the WPP stage, then shifted up to 29ºC for 32h before dissection. (A) Z projection of entire wing, which is composed of a single ventral layer. *DSRF* expression is seen in intervein regions, and the PCV is broader. (A') Z section showing the lack of dorsal nuclei. (B-E') Clones of cells in the intervein expressing *cv-c* do not lead to apical constriction. Clone : control ratio 1.128 (stdev = 0.247), see Fig. 7.10E), n=13 clones in 6 wings. (C-C') Larger clones were often fragmented (arrows), indicating apoptosis or a failure of clone cell adhesion. (D-F'') Clones of cells expressing *cv-c-S-eGFP* (green) stained for Actin (blue). (D-D') Apical sections showing expanded apical surface in certain cells (arrows). (E-E') Basolateral section, showing gaps in the middle of cells and expanded morphology. (F, F') 3D projections of two nearby clones in the same layer, showing extended gaps within the cells.

sections, apical cell shape and area are variable (Fig. 6.6 D), with some cells having an expanded apical surface (arrows in Fig. 6.6 D'). In lateral sections, GFP is fragmented and gaps are seen in the middle of the cells (Fig. 6.6 E, E'). This phenotype is shown in 3D projections, with clone cells showing expanded gaps and the bulk of the cell seen in the apical half of the epithelium (Fig. 6.6 F, F'). In these cells, Cv-c-GFP fills the cell and does not show a particular apical or basal enrichment. Similar results were obtained for a Venus-tagged version of Cv-c (not shown; Cv-c-Venus described in Simoes et al., 2006).

These results show that although ectopic Cv-c is not sufficient for apical constriction, it is capable of dramatically altering cellular morphology. Because cells appear to be very sensitive to the levels of Cv-c, it may only lead to apical constriction at lower levels. Additionally, the control of apical constriction could be dependent on the localisation of Cv-c within the cell. Indeed, Cv-c shows a polarised enrichment within the cell in other developmental processes (Brodu and Casanova, 2006; Simoes et al., 2006). Over-expression in pupal wing cells might lead to a uniform distribution within the cell, affecting cell shape in a dominant fashion that does not reflect its endogenous role. Additionally, the departure from its normal role may reflect a fundamental issue with mis-expression of RhoGAPs: the non-specific inhibition of various RhoGTPase functions, unrelated to the endogenous function of the RhoGAP. For example, the disintegration of the epithelium when dorsally expressing Cv-c could result if Rho1 function in maintaining epithelial integrity is compromised.

The alternate possibility is that Cv-c is not sufficient for apical constriction without additional factors. It is expressed in constricting cells in both the PCV and in *dpp*-expressing clones, but in both cases BMP signalling could be controlling the expression of additional factors that work alongside Cv-c to control cell shape changes.

Rho1 promotes intervein development in the pupal wing

We next turned our attention to the potential target that Cv-c acts upon in PCV development. RhoGAPs stimulate the intrinsic GTP hydrolysis of RhoGTPases, promoting the inactive, GDP-bound state (Bernards and Settleman, 2004), so it is likely that Cv-c promotes PCV development by inhibiting RhoGTPase activity. Cv-c has been predicted to act on different classes of RhoGTPases in different developmental contexts (Denholm et al., 2005; Sato et al., 2010; Pilgram et al., 2011), so we first performed genetic interaction experiments to find its likely target. Mutations in *Rho1* partially suppressed the variable phenotype of *cv-c*

hypomorphs, which range from completely crossveinless ('Cv') to having a gap between the PCV and L4/L5 ('Gap'), leading to more crossvein material when heterozygous for *Rho1* (Fig. 6.7 A). Heterozygosity for an alternate Rho GTPase, *Cdc42*, did not lead to a similar shift of the distribution (Fig. 6.7 B). These results suggest that Rho1 is the primary target of Cv-c in PCV development.

Consistent with a role for Rho1 in the inhibition of crossvein development, knockdown of *Rho1* with *RNAi* (VDRC #12734) throughout the pupal wing led to the formation of ectopic crossveins. These veins are apically constricted (Fig. 6.7 C, D), and form a lumen basally (Fig. 6.7 D'). This leads to the formation of an expanded network of lumens between the layers (Fig. 6.7 C'). As well as showing vein cell morphology, these cells also down-regulate *DSRF* expression (Fig. 6.7 C''). Thus, Rho1 is required to maintain *DSRF* expression in the intervein. An implication of this is that the *DSRF* expression seen in *cv-c* LOF clones (Fig. 6.2 G'') is a result of the failure of Cv-c to inhibit Rho1.

Ectopic crossveins in the pupal wing differentiated pigmented vein cuticle in the adult wing, when *dsRNA* was expressed in the middle of the wing with *sal-Gal4* (Fig. 6.7 F, F') or only in the dorsal layer with *ap-Gal4* (arrow Fig. 6.7 G). As well as ectopic crossveins, the lumens of longitudinal veins were wider, and in the intervein patches of separation were seen (arrow in Fig. 6.7 E), showing that knockdown of Rho1 leads to a reduction of basal apposition across the wing, which had been previously noted (Yan et al., 2009a).

These results demonstrate a function for Rho1 in promoting intervein development in the pupal wing, and suppressing the development of extra crossveins. It is of note that these wings show ectopic crossveins and not just a general increase in venation as is seen with heightened BMP/EGFR activity (see Chapters 4, 5), suggesting that Rho1/Rok function in the interveins is specific to crossvein suppression. Furthermore, the down-regulation of *DSRF* in these cells shows that Rho1 promotes *DSRF* expression, but the means by which this occurs is unclear, although there is a well-established link between RhoA and SRF in vertebrate cells (Olson and Nordheim, 2010; see Discussion). The promotion of *DSRF* expression raises the question of whether the requirements for Rho1 (and by extension Cv-c) in cell shape are solely mediated through the promotion of *DSRF* expression. We address this issue below by investigating the role of Rho1 effectors in the pupal wing.

Activating Rho1 at apposition leads to the failure of vein differentiation

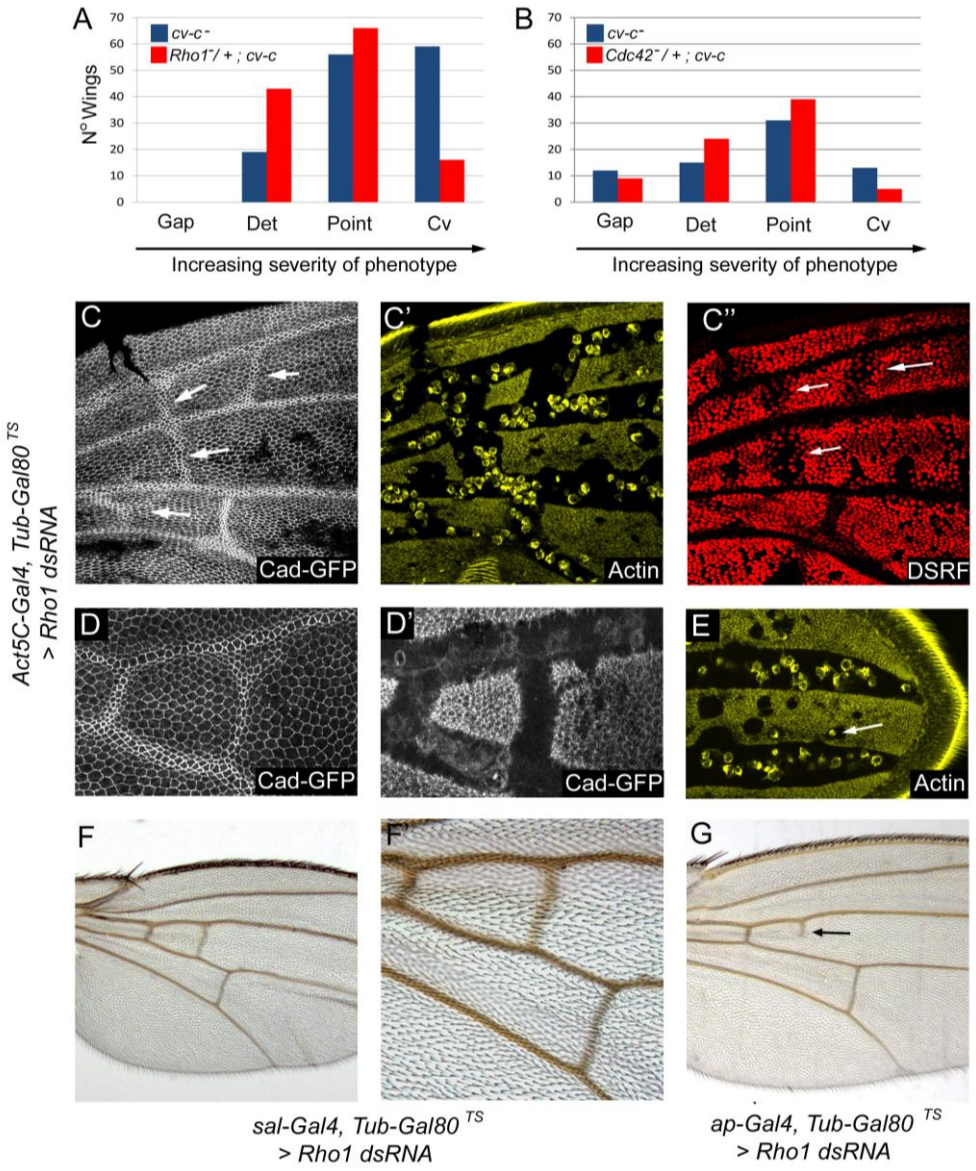

Figure 6.7. Rho1 knockdown in the pupal wing produces ectopic crossveins. (A) *Rho1* heterozygosity in a *cv-c* mutant background leads to a partial suppression of the variable vein loss phenotype ('crossveinless': no vein; 'point': small speck of vein; 'detached': small stretch of vein). Genotypes: control (blue): *If/+ ; cv-c^{1}/cv-c^{1}*; experimental (red): *Rho1^{72R}/+ ; cv-c^{1}/cv-c^{1}*. n=245 wings scored. (B) *Cdc42* heterozygosity in a *cv-c* mutant background does not lead to a similar degree of suppression. Genotypes: control (blue): *y w/FM7h ; ; cv-c^{1}/Df6267*; experimental (red): *Cdc42^{1}/y w ; cv-c^{1}/Df6267*. n=141 wings scored. (C-E) Animals of the genotype *Act5C-Gal4/UAS-Rho1-dsRNA, Ubi-DECad-GFP ; TubGal80^{ts}/+* were raised at 18ºC and shifted to 29ºC at the WPP stage, and dissected at 30h APF. Ectopic crossveins show apical constriction and shown by Cad-GFP (C), form an expanded network of vein lumen as shown with Actin (C'), and show downregulation of *DSRF* expression as shown with *DSRF* (arrows in C''). (D) Apical section of a different wing showing constricted cells of the ectopic crossvein. (D') Basal section showing ectopic lumen. (E) Distal portion of the wing, basal section showing gaps in apposition as shown with Actin, and wider veins. Arrow shows trapped haemocyte in one of the gaps. (F, F') Adult wings of *sal-Gal4, Tub-Gal80^{ts} > UAS-Rho1-dsRNA* flies shifted to 29ºC at various times during pupal development differentiate ectopic crossvein cuticle. (G) Adult wings of *ap-Gal4, Tub-Gal80^{ts} > UAS-Rho-dsRNA* shifted to 29ºC for 8h periods at various points in pupal development differentiate ectopic crossvein segments.

Having investigated Rho1 knockdown, we next activated Rho1 in the pupal wing. If *cv-c* acts to antagonise Rho1, hyperactivation of Rho1 might phenocopy *cv-c* loss. We made use of a UAS inducible form of a constitutively activated Rho1, $Rho1^{V14}$ (Fanto et al., 2000). $Rho1^{V14}$-expressing clones appeared at the centre of rosette-like arrangements of cells (Fig. 6.8 A, A'), and progressive sections from apical to basal reveal the adherens junctions ingress into the epithelium (Fig. 6.8 A''-A''''), suggesting that the cells are being extruded from the epithelium, as happens following Rho1 activation in the wing disc (Speck et al., 2003).

To avoid the problems associated with clones, we induced brief periods of $Rho1^{V14}$ expression in the pupal wing. We limited expression to a 4h period after the reapposition of the two surfaces, using the *en-Gal4* driver to limit expression to the posterior compartment of the wing and leaving the anterior compartment as a control. Hyperactivating Rho1 leads to highly variable cell shapes and the loss of stripes of apical constriction of the veins in the posterior compartment (Fig. 6.8 B, B'). Although the construct does affect the apical morphology of the whole expressing region (Fig. 6.8 B'), this suggests that activated Rho1 is capable of blocking vein constriction in the pupal wing. In basal sections, the lumens in the posterior compartment are lost (Fig. 6.8 C). Lumens were also lost when $Rho1^{V14}$ was expressed in the middle of the wing at reapposition with *sal-Gal4, Tub-Gal80^{ts}* (Fig. 6.8 E). Thus, whereas reducing Rho1 function leads to ectopic lumens, activating Rho1 leads to the loss of vein lumens. As well as the loss of lumens, the intensity Cad-GFP is increased in a patchy pattern through the apposed regions (Fig. 6.8 C). Endogenous E-Cad is enriched basally in intervein cells (O'Keefe et al., 2007), and activating Rho1 thus appears to enhance this enrichment.

Considering the diversity of Rho1 functions in cells (Etienne-Manneville and Hall, 2002), these phenotypes must be interpreted with caution, as they might reflect dominant effects unrelated to the endogenous function of Rho1 in the wing. However, the loss of apical constriction, the loss of lumens, and the enrichment of Cad-GFP are all consistent with a role for Rho1 in promoting intervein development, as was suggested by the knockdown experiments.

The Rho1 effector Rok acts in the intervein-promoting pathway

In addition to their well-characterised effects on the cytoskeleton, RhoGTPases such as Rho1 can affect the transcriptional output of the cell by influencing intracellular signal pathways at multiple levels (Jaffe and Hall, 2005; Olson and Nordheim, 2010). Loss of *cv-c* leads to a failure

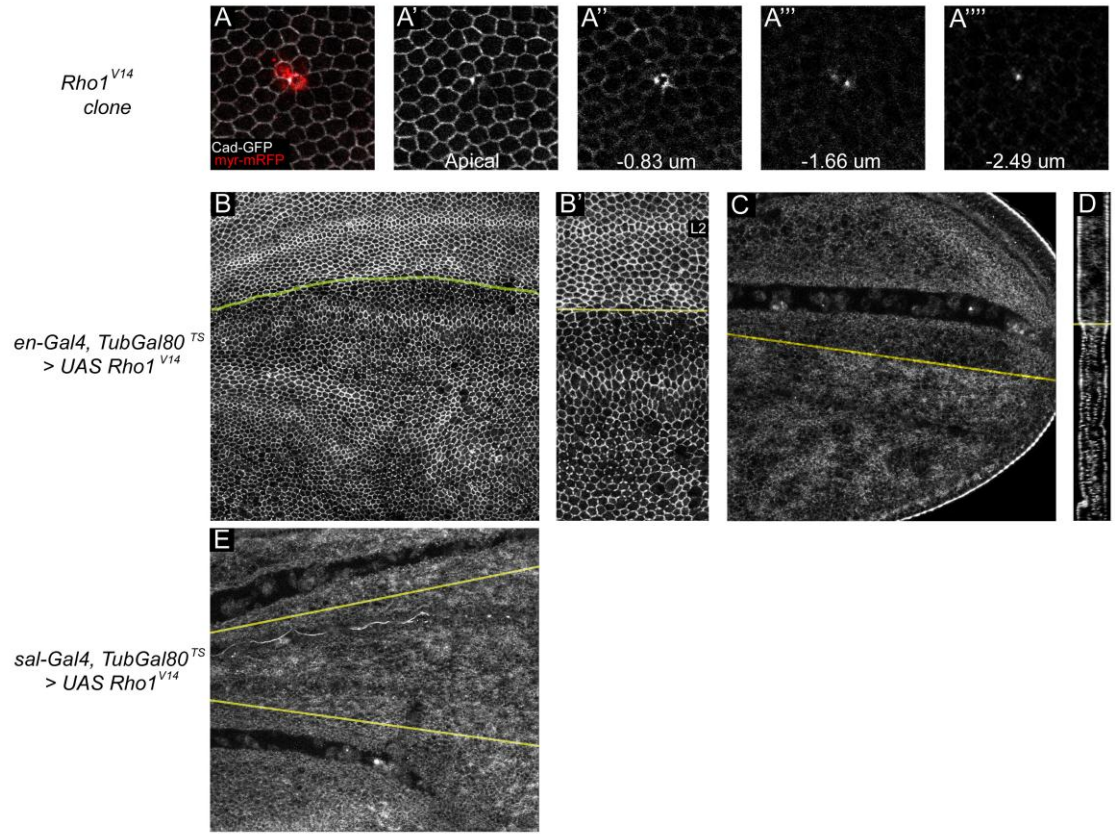

Figure 6.8. The effects of activating Rho1 in the pupal wing. (A-A'''') Clone expressing *Rho1^{V14}* (red) with Cad-GFP (white) showing apical cell outlines. Progressively basal sections show adherens junctions ingressing into the epithelium, suggesting basal extrusion. (B) Animals of the genotype *en-Gal4/UAS-Rho1^{V14}, Ubi-DECad-GFP ; TubGal80^{ts}/+* raised at 18ºC until 40h APF, and shifted to 29ºC for 4h before dissecting. Loss of vein/intervein distinctions is seen in the posterior compartment (yellow line represents anterior boundary of *en* expression). (B') Close up, showing apical disorder and AJ fragmentation in the affected region. (C) Basal section, showing loss of the vein lumen and patchy increase in basal Cad-GFP in the posterior compartment. (D) Z section, showing shorter cells of the posterior compartment. (E) Animals of the genotype *sal-Gal4/UAS-Rho1^{V14}, Ubi-DECad-GFP ; TubGal80^{ts}/+* raised at 18ºC until 40h APF, and shifted to 29ºC for 8h before dissecting. Loss of lumen is observed within the expression domain (marked by yellow line).

of *DSRF* expression in the PCV, and reducing Rho1 activity leads to the loss of *DSRF* expression in the ectopic crossveins. It is thus unclear whether the cell shape phenotypes we observe in the pupal wing are part of the 'transcriptional' output of Rho1 signalling (leading to *DSRF* expression, which in turn would promote intervein cell shapes by currently unknown factors), or are part of the 'cytoskeletal' output. One way of addressing this issue is to ask whether Rho1 effectors with defined functions also have roles in the pupal intervein. A particularly well-characterised pathway involves the Rho1-specific effector Rho Kinase (Rok). Rok links Rho1 signalling to the Actin cytoskeleton via direct or indirect phosphorylation of the regulatory light chain of Myo-II (Mizuno et al., 1999; Winter et al., 2001). It thus represents a canonical 'cytoskeletal' output of Rho1 signalling.

Consistent with Rok being an effector for Rho1 in its role in intervein maintenance, knockdown of *rok* function with RNAi (TRiP #28797) led to the formation of ectopic crossveins. Ectopic crossveins were seen between L2 and L3 when *rok dsRNA* is expressed in the middle of the wing with *sal-Gal* (Fig. 6.9 A), between L3 and L4 when expressed with *dpp-blk-Gal4* (Fig. 6.9 B) and between L4 and L5 when expressed with *en-Gal4* (Fig. 6.9 C). As well as ectopic crossveins, Rok knockdown also led to blistering between the two wing surfaces (Fig. 6.9 D), which commonly results from a failure of apposition between the two layers of the pupal epithelium (Fristrom et al., 1994; Brabant et al., 1996). Considering apposition was incomplete following *Rho1 RNAi* (Fig. 6.7), this suggests that Rho1 acts through Rok to promote basal apposition. Other phenotypes resulting from Rok knockdown included the formation of dark, fluid filled vesicles between the wing surfaces (Fig. 6.9 E), and multiple wing hairs (Fig. 6.9 F) as have been reported for *rok* mutant clones (Winter et al., 2001). Knockdown of another prominent Rho1 effector, the formin Diaphanous (Dia) which nucleates Actin filaments and promotes filament elongation (Homem and Peifer, 2008), did not produce ectopic crossveins (Fig. 6.9 G-I). Phenotypes were restricted to reduced hair density (Fig. 6.9 G) and multiple wing hairs (Fig.7.10 I). As knockdown of Rok phenocopies knockdown of Rho1, these results suggest that Rok is an effector of Rho1 in promoting intervein development, whereas Dia is not.

As has been reported previously, expression of a constitutively active form of Rok (Rok^{CAT}) leads to the loss of crossvein material (Table A.9; Verdier et al., 2006). When independently generated rok^{CAT} constructs (Winter et al., 2001) were expressed generally in the wing with *A9-Gal4*, they led to partial loss of crossvein material (Fig. 6.10 A). When expressed in the middle of the wing with *sal-Gal4*, rok^{CAT} led to autonomous loss of crossvein material within the Gal4 domain (Fig. 6.10 B), as was seen with *cv-c RNAi* (Fig. 5.3 D). In another similarity to *cv-c*, activation of Rok in the dorsal layer only led to crossvein loss in both surfaces of the adult wing

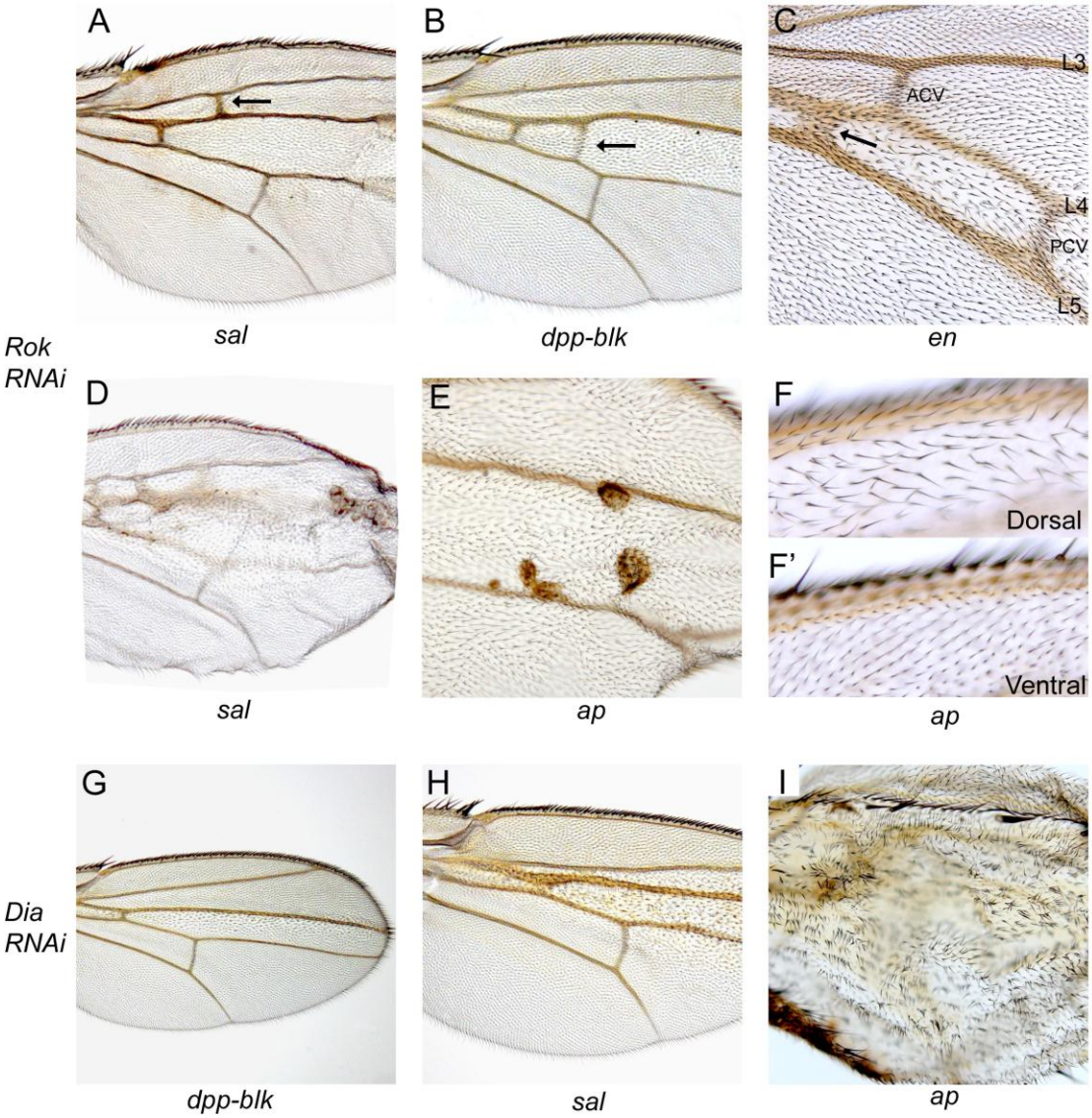

Figure 6.9. Knocking down Rho1 effectors with RNAi. (A-F') Adult wings from flies expressing *Rok dsRNA* with various drivers as indicated at the bottom of the panels. Ectopic crossveins are noted with arrows. Wing blistering (D) and dark, fluid filled vesicles between the surfaces (E) are also observed. (F) shows lower hair density and multiple wing hairs in dorsal surface as compared to control ventral surface (F'). (G-I) Adult wings from flies expressing *Dia dsRNA* with various drivers as indicated at the bottom of the panels. No ectopic crossveins are seen. (I) shows severe multiple wing hair and lower cell density phenotype following dorsal expression.

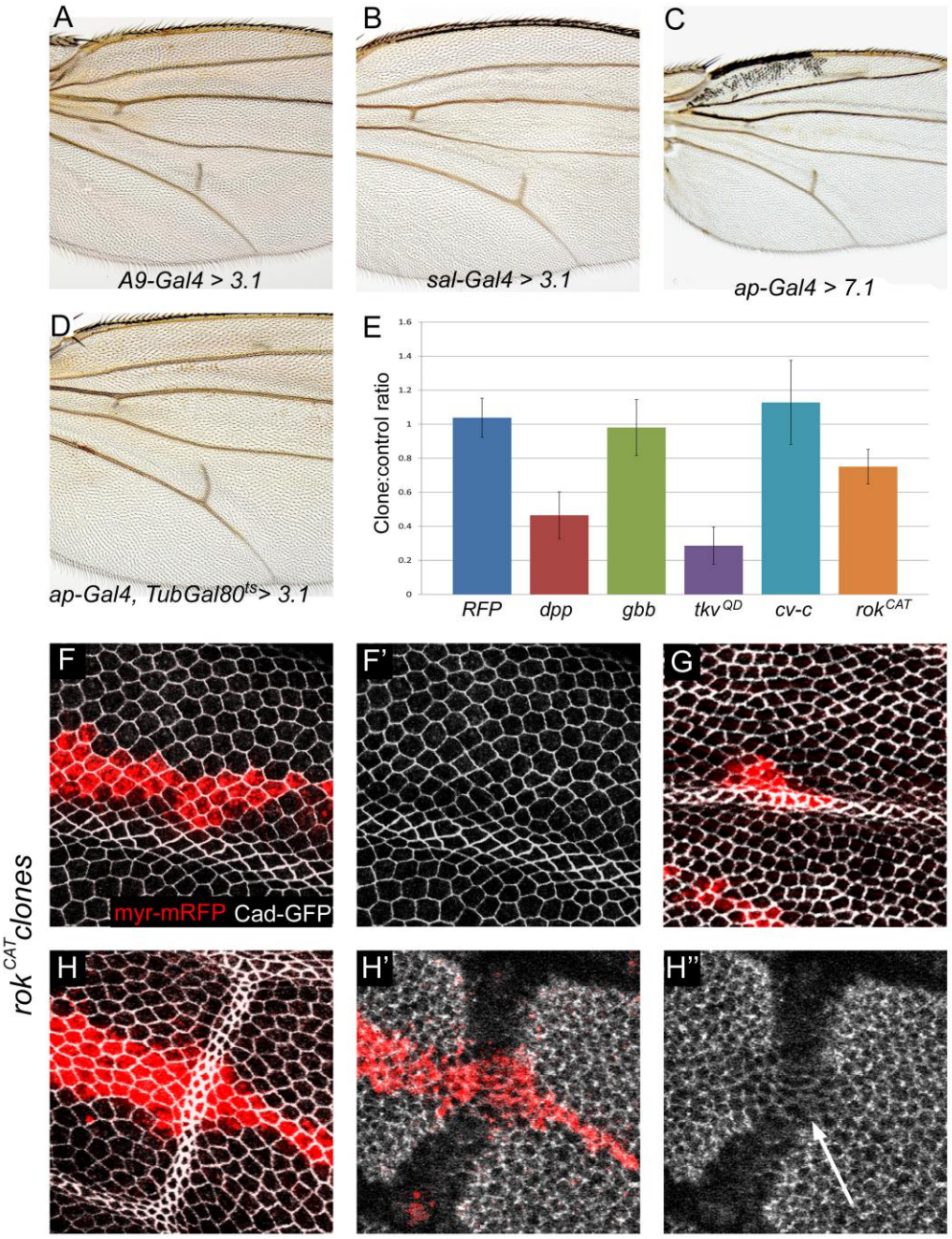

Figure 6.10. Activating Rok in the wing. (A-D) Expression of two *rok*^{CAT} constructs – 3.1 which gives stronger phenotypes, and 7.1 which gives weaker phenotypes - with various drivers as indicated below the panels leads to loss of crossvein material. (C) shows crossvein loss from dorsal expression of *rok*^{CAT} *7.1*, while (D) shows crossvein loss when *rok*^{CAT} *3.1* expression is limited to the dorsal layer in pupal development. (E) Comparison of clone : control ratios of all FLPout clones generated in this thesis, with bars showing standard deviations. (F-F') Clones of cells expressing *rok*^{CAT} *3.1* in the intervein cause reductions in apical area and altered apical morphology (F'). Clone : control ratio = 0.751 (stdev 0.102). n=35 clones in 8 wings. (G-H) Clones crossing veins do not inhibit apical constriction. (H-H') Basal section of the clone in (H): clone interferes with normal apposition, as seen by the pinching in of the lumen (arrow in H'').

(Fig. 6.10 C, D). Thus, activating Rok has the same consequences for PCV development as inhibiting Cv-c, and displays the same effect when restricted to one layer of the wing only, i.e. showing domineering interplanar non-autonomy.

We then generated clones of cells expressing *rok*^{CAT} and assessed cell morphology in the pupal wing. Clones in the intervein adopted more variable shapes than the surrounding non-clone tissue (Fig. 6.10 F, F'), and showed a reduction in apical area (but not to the same extent as *dpp*- or *tkv*^{QD}-expressing clones) with clone cells being x0.75 the size of control cells (Fig. 6.10 E). When clones covered veins, they did not inhibit apical constriction (Fig. 6.10 G, H). These apical phenotypes differ to those of activated Rho1: whereas Rho1^{V14} inhibited vein constriction, Rok^{CAT} did not, and indeed was able to promote it in the intervein. RNAi results suggest that Rho1 activates Rok to promote intervein development, so we would expect activated Rok to show the same phenotype as activated Rho1, which we do not. Other inputs aside from Rho1 can lead to the activation of Rok (Sebbagh et al., 2001), so the effect on apical constriction might reflect a Rho1-independent dominant function (see Discussion).

Whereas the apical consequences of activating Rok differed from Rho1, the basal consequences were the same: *rok*^{CAT}-expressing clones interfered with the formation of a coherent lumen. The basal surfaces of clone cells are seen more basally than those of neighbouring cells (Fig. 6.10 H'-H''), suggesting that the cells are apposing. This was seen both in the PCV and in the longitudinal veins. Such a function is consistent with the incomplete apposition following Rho1 knockdown (Fig. 6.7), the promotion of apposition seen when hyperactivating Rho1 (Fig. 6.8), and the blisters seen in adult *rok RNAi* wings (Fig. 6.9). In this context, the failure of lumen formation seen in *cv-c* null clones (Fig. 6.2) suggests that Cv-c acts specifically in the PCV to inhibit a general function of Rho1/Rok in promoting apposition.

These results demonstrate that Rok is an effector for Rho1 in intervein development. The fact that one of the canonical 'cytoskeletal' outputs of Rho1 signalling plays the same role asRho1 implies that its function in the intervein is not mediated wholly through its promotion of *DSRF* expression.

Apical enrichment of Myo-II in PCV development

Rho1/Rok activity leads to cytoskeletal alterations in numerous systems by the activation of Myo-II, either by direct Rok phosphorylation (Amano et al., 1996), or via the relief of Myosin

Phosphatase-mediated dephosphorylation (Kimura et al., 1996). It has been recently reported that interfering with the function of Myo-II in the wing produces ectopic crossveins and blistering (Franke et al., 2010), phenotypes which we showed result from Rho1/Rok knockdown (Fig. 6.7, 6.9). On the basis of these results a pathway emerges whereby the Rho1/Rok/Myo-II/Actin cassette leads to the promotion of intervein development, mediating basal apposition and the inhibition of apical constriction. Although the localisation of Actin in the wing has been noted – apical enrichment in vein cells, basal enrichment in intervein cells (Fristrom et al., 1993) – it is not known whether Myo-II shows this similar polarisation between the two cell types. We thus addressed the localisation of Myo-II within the pupal wing, using a ubiquitously expressed mCherry-tagged version of the regulatory light chain of Myo-II (Sqh-Cherry). To simultaneously view the localisation of Actin we used SGMCA, a probe comprising GFP fused to the Actin-binding domain of Moesin (Kiehart et al., 2000).

We first took apical sections of wings between 18-26h APF during PCV development. At 18h APF, before co-ordinated constriction is seen, neither SGMCA nor Sqh-Cherry are localised, and the highest signal is seen along the cleavage furrow of dividing cells (arrows in Fig. 6.11, A-A'). At 22h APF, while SGMCA is still uniform (Fig. 6.11 B), Sqh-Cherry, seen as punctate spots in the cell, is enriched along L4 and to a lesser extent in the PCV region (Fig. 6.11 B'). By 26h APF, both SGMCA (Fig. 6.11 C) and Sqh-Cherry (Fig. 6.11 C') show high levels of apical enrichment in the PCV, as well as a lower level in the longitudinal veins. Thus, between 18-26h APF Myo-II and Actin are progressively enriched in the apical surfaces of the PCV cells, coincident with the onset and progressive refinement of apical constriction (see Fig. 6.1). The higher levels of Myo-II and Actin seen in the PCV as compared to the longitudinal veins may underlie the increased constriction of PCV cells (see Fig. 3.4, 3.5). In terms of the basal domain, we used Cad-GFP as a marker for basal apposition (O'Keefe et al., 2007). Although the localisation is not as clear as Cad-GFP (Fig. 6.11 D), we see a line of RFP along the basal surfaces of the intervein cells (Fig. 6.11 D'). This suggests that, like Actin, Myo-II is basally enriched in intervein cells.

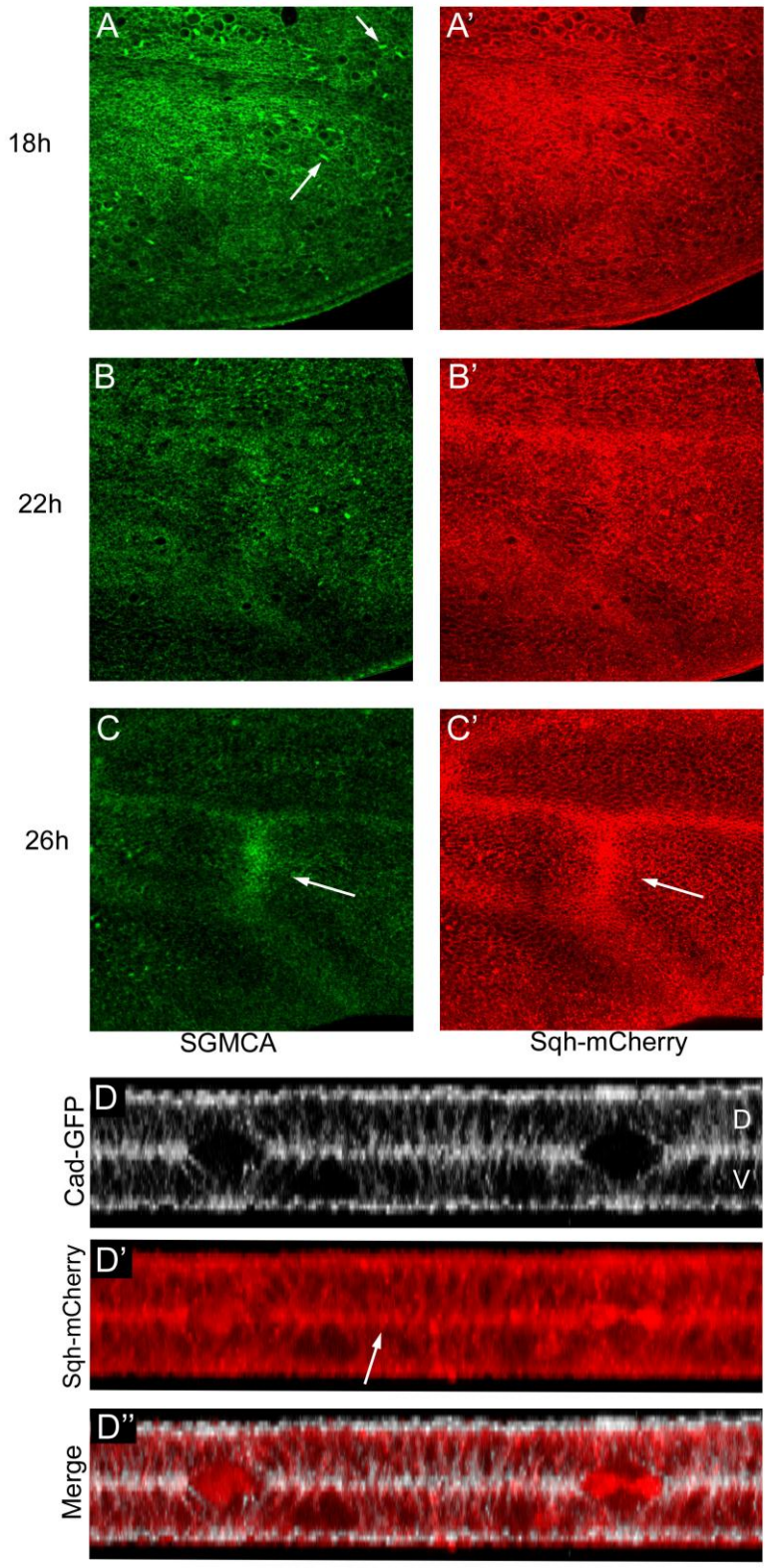

Figure 6.11. Myo-II and Actin in the pupal wing. (A-C') Time course showing apical sections in wings of the genotype *sqh-mCherry/+ ; SGMCA/+* at 18, 22 and 26h APF. Myo-II (red), seen in a punctate distribution, and Actin (green) are progressively enriched in the veins, particularly in PCV cells by 26h APF (arrows). (D-D') Z section wings of the genotype *sqh-mCherry, Ubi-DECad-GFP/+* wings, showing line of basal enrichment in intervein sections (arrow in D').

IV. Summary

The current Chapter has tackled the issue of how the signalling pathways that pattern the wing epithelium achieve cellular differentiation. We have characterised events downstream of BMP signalling in the PCV, showing how the specification of the PCV is coincident with its differentiation. BMP signalling thus instructs vein fate and cell shape changes coincidently. *cv-c* was defined as a transcriptional target of this signalling, the expression of which arises alongside the repression of *DSRF*, and we further showed that loss of Cv-c results in a failure of PCV differentiation. The primary target of Cv-c in the PCV appears to be Rho1. We revealed two outputs for Rho1: the promotion of *DSRF* expression (which explains why *cv-c* loss leads to the failure to repress *DSRF*), and the Rok effector (Fig. 6.12). When Rho1 or Rok function is reduced, ectopic crossveins are formed. Therefore, one of the ways that BMP signalling can inhibit intervein and promote vein development in the PCV is via the inducing the expression of an inhibitor of Rho1, Cv-c.

Cv-c within crossvein patterning

The characterisation of 'crossveinless' genes has revealed a diverse PCV patterning network in which BMP ligands, multiple extracellular BMP modulators, Dystrophin, Dystroglycan, and now Rho1 are involved (Ray and Wharton, 2001; Denholm et al., 2005; O'Connor et al., 2006; Christoforou et al., 2008). The work presented in this Chapter addresses events downstream of BMP pathway activation, and we show that the 'crossveinless' gene *cv-c*, previously characterised as a RhoGAP (Denholm et al., 2005), is a transcriptional target of BMP signalling both in the PCV and when the pathway is ectopically activated in the intervein. In the PCV, Cv-c acts as a link between a fate-determining signalling pathway and cytoskeleton-mediated cell shape changes, and as such is a 'realisator' gene (Garcia-Bellido, 1975). This is similar to its role in other developmental contexts: localised expression of *cv-c* is seen in numerous other tissues undergoing morphogenesis (Denholm et al., 2005), and it contributes to cell shape changes downstream of fate determination genes in both tracheal and posterior spiracle development (Brodu and Casanova, 2006; Lovegrove et al., 2006). Induction of RhoGAP expression may be a general mechanism by which intercellular signalling pathways realise cell shape changes, and Cv-c is a key component of this mechanism throughout *Drosophila* development.

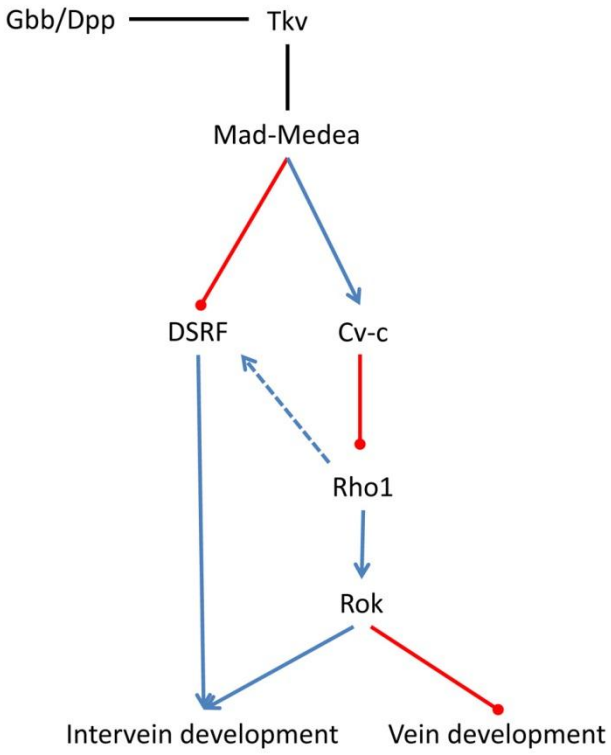

Figure 6.12. Model for the role of Cv-c in PCV development. Red lines indicate repression, blue lines indicate activation. BMP ligands signal through Tkv to promote the regulation of transcription by Mad/Medea. This leads to the inhibition of *DSRF* expression, and the promotion of *cv-c* expression. Cv-c inhibits Rho1, leading to the inhibition of two of its outputs: the promotion of *DSRF* expression, and the promotion of intervein cell differentiation via the effector Rok.

The link between BMP signalling and RhoGTPases

BMP signalling and RhoGTPases are linked in numerous developmental and pathological contexts. BMP and the related TGF-β ligands can induce epithelial-to-mesenchymal transitions by influencing RhoGTPases in ovarian cancer cell lines and mammary epithelial cells (Ozdamar et al., 2005; Theriault et al., 2007). In the former case, rapid degradation of RhoA in response to TGF-β ligands is independent of Smad activation, whereas in the latter case BMP signalling induces the activation of RhoA, Rac and Cdc42 by an as of yet unclear mechanism. A link between BMP signalling and Rho1 has also been reported in *Drosophila*. In the larval wing disc, the elongation of cells in the pouch has been shown to be dependent on BMP pathway activity, and to correlate with the apicolateral enrichment of Rho1 and Actin (Widmann and Dahmann, 2009). However, activation of Rho1 led to shortened cells, suggesting an antagonism between BMP and Rho1 functions similar to what we observe in the pupal wing. In eye development, genetic interaction experiments have suggested that Dpp mediates the morphogenesis of the pupal retina in cooperation with E-Cad and Rho1 (Cordero et al., 2007). A similar relationship was reported for the wing: because *Rho1* mutations enhance the vein thickening phenotype of mutations in the BMP receptor *tkv*, Dpp was proposed to positively act with Rho1 to control vein determination (Cordero et al., 2007). However, as discussed in Chapter 5, *tkv* plays a role in antagonising vein development in the provein domains, and the thickened vein phenotype results from an expansion of Dpp activity (de Celis, 1997). Thus, if both heightened *tkv* and active *Rho1* antagonise vein development, we would expect loss of *Rho1* to enhance the *tkv* phenotype. Whereas a synergism of Rho1 and BMP activity mediates eye morphogenesis, pupal wing development involves the antagonism of Rho1 by BMP signalling.

The inhibitory effect of BMP signalling on Rho1 is mediated by Cv-c in the crossveins. One of the ways in which BMP signalling controls crossvein development is thus via the transcriptional upregulation of this RhoGAP. As *dpp* is expressed in all longitudinal veins at the time of apposition, the inhibition of Rho1 by BMP pathway activity may be general to all veins. As Cv-c function is crossvein-specific, other RhoGAPs, downstream of BMP, would be active in the longitudinal veins. If so, this raises the question of why vein-loss alleles of these genes have not been recovered or characterised. One reason may be due to their pleotropic nature. Cv-c is essential for multiple aspects of embryogenesis, and its function in the wing is only revealed in the viable allele *cv-c*^{1}, which appears to be a regulatory mutation (Rob Ray, pers. comm.).

Alternatively, multiple RhoGAPs might act redundantly to restrict Rho1 activity in the longitudinal veins, such that single alleles would not produce a phenotype. Indeed, the combinatorial action of multiple RhoGAPs on single RhoGTPases has been suggested to be a widespread feature of RhoGAP function (Nir et al., 2010).

Targets of Cv-c in the wing

Both genetic interactions and phenotypic data from knockdowns and mis-expression support the notion that Cv-c function in the pupal wing is mediated through suppression of Rho1. Indeed, a mammalian orthologue of *cv-c*, *Dlc-1*, appears to act primarily through RhoA, and the metastasis that results from *Dlc-1* loss in various cancers has been attributed to RhoA hyperactivation (Lahoz and Hall, 2008; Kim et al., 2009). We have described how knocking down the function of Rho1 or its effector Rok leads to ectopic crossveins, and confirmed that activating Rok phenocopies Cv-c loss, strongly suggesting Cv-c acts to inhibit Rho. However, we cannot rule out the possibility that Cv-c may also act on other RhoGTPases such as Cdc42. Cdc42 is a potential target of Cv-c in other *Drosophila* tissues (Denholm et al., 2005) and Cv-c exhibits GAP activity to Cdc42 in cell-free assays (Sato et al., 2010). Furthermore, *Cdc42* hypomorphic mutations result in ectopic crossveins and occasionally produce blisters in the adult wing which may indicate a failure of basal apposition in the wing epithelium (Genova et al., 2000). The fact that Cdc42 phenocopies Rho1 could suggest a co-operation between these two RhoGTPases in crossvein antagonism, which is also seen for example in their combined roles during growth cone guidance in cultured *Xenopus* spinal neurons (Yuan et al., 2003). Furthermore, if Cv-c acts exclusively through Rho1, this raises the possibility that another RhoGAP may act to suppress Cdc42 activity in PCV development. Crossvein development may thus provide an attractive system to study the interactions between RhoGTPases in development.

Apical constriction in the wing is inhibited by Rho1

In this Chapter we have demonstrated that Rho1, and its effector Rok, is required to prevent the constriction of intervein cells to form ectopic crossveins. This is surprising considering the requirement for Rho1/RhoA and Rok activity in the apical enrichment of Myo-II and Actin, and subsequent apical constriction, in numerous other systems (Escudero et al., 2007; Kolsch et al.,

2007; Kinoshita et al., 2008; Sawyer et al., 2010; Plageman et al., 2011). Here, we have shown that PCV constriction is accompanied by the apical enrichment of Actin and Myo-II, and that in the absence of *cv-c* Actin is not enriched apically and constriction is impeded. Cv-c also controls apical enrichment of Myo-II and Actin in the Malpighian Tubules and tracheal placodes (Denholm et al., 2005; Brodu and Casanova, 2006), showing that this is a common output of Cv-c. Our data suggest that the apical localisation of Actin and Myo-II in the wing is antagonised by Rho-Rok activity, which raises the question as to what promotes it. Other kinases aside from Rok can activate Myo-II (Vicente-Manzanares et al., 2009), raising the possibility that, in the veins, an alternate kinase is responsible for the apical activation of Myo-II that leads to constriction (see Discussion).

As well as enrichment of basal Actin, intervein cells are characterised by basal Integrin-rich focal adhesions that form the mechanical links between the layers. Rho1 is required for the formation of integrin focal adhesions in migrating cells (Ridley and Hall, 1992), so it may play a similar role in the wing, via Rok and NM-Myo-II. Indeed, one of the consequences of *Dlc-1* overexpression is the disassembly of Integrin based focal adhesions (Wong et al., 2008), and the modulation of Rho1 activity by Cv-c may provide a genetically tractable model system to investigate this relationship.

Chapter 7

Discussion

Morphogenesis is controlled by intercellular communication, and executed by cell shape changes. This thesis has investigated the relationship between these two fundamental features of development.

The *Drosophila* wing has long been a model system for investigating the processes that create patterns in developing tissues. Research over the past 40 years has documented the cell signalling networks that establish the venation pattern in the proliferating larval disc, addressing key questions such as the interactions between signalling pathways and the link between patterning and growth (de Celis, 2003; Blair, 2007). Pupal wing development, which involves the formation of the epithelial bilayer, differentiation of cell types and secretion of the adult cuticle, is less well understood. In particular, we lacked an understanding of how cell signalling is translated into different cellular morphologies, and how these morphologies relate to the morphology observed in the adult cuticle.

This thesis has presented investigations into how cell shape changes in the pupal wing are controlled by intercellular signalling. In doing so novel cellular processes and signalling relationships have been uncovered in the developing wing, contributing to a clearer understanding of how the wing is built. Considering the widespread use of the wing as a model system, this work provides necessary insight into the means by which patterning systems are transformed into differentiated tissue structures. Furthermore, the investigations have touched on several fundamental questions in animal development, including how signals travel in tissue, the link between signalling pathways and cell shape, signalling interactions between epithelia, the process of cell fate restriction, and how cells co-ordinate to form tissue structures.

I. BMP signalling in the pupal wing

An intriguing feature of development is how cells signal to one another in the context of a developing tissue (Zhu and Scott, 2004), and how such signalling leads to the specification of cell fate and subsequent differentiation (Barolo and Posakony, 2002). BMP signalling plays multiple key roles in *Drosophila* wing development, from the initial specification of the disc, through its proliferation and patterning in larval stages, to the promotion of vein development in the pupal wing. This latter role was a major focus of the current work. By tackling the pathway at the levels of ligand, receptor and intracellular signal transducer we were able to address multiple aspects of BMP signalling mechanics in the pupal wing.

At the extracellular level, we probed the differential signalling capacities of the two BMP ligands involved in wing development, Dpp and Gbb. When expressed throughout the epithelium, or in all cells of the dorsal layer, both ligands were able to activate the BMP pathway, inducing constriction and blocking apposition. This revealed the cellular basis for the adult wing phenotypes seen with temporally controlled mis-expression, i.e. wing blisters arise from the loss of apposition, and broadened vein cuticle is secreted by the expanded regions of apically constricting cells. *dpp*-expressing clones were able to induce vein cell phenotypes in intervein cells (apical constriction, ectopic lumen formation), but *gbb*-expressing clones were not, and cells retained their intervein characteristics. Whereas Dpp achieved this effect via pathway activation, Gbb in the intervein was unable to activate the pathway. This leads to the question of why ectopic Gbb in the intervein is non-functional, considering expression throughout the epithelium can activate the pathway.

TGF-β superfamily ligands such as Dpp and Gbb signal as dimers, and dimerization occurs prior to secretion, either with the same type of ligands (e.g. Dpp-Dpp or Gbb-Gbb homodimers), or with other ligands of the same family (e.g. Dpp-Gbb heterodimers). Heterodimers are thus dependent on co-expression of the two ligands within the sending cell (Raftery and Sutherland, 1999). The differential signalling capacity of BMP heterodimers as opposed to homodimers has been investigated in a number of cases. Ectopic expression of vertebrate BMP heterodimers induces higher levels of pathway activity than homodimers are able to (Suzuki et al., 1997). In dorsoventral patterning of the zebrafish embryo, although BMP2 and BMP7 can form both form homodimers, only BMP2-7 heterodimers led to pathway activation in rescue conditions (Little and Mullins, 2009). In the *Drosophila* embryo, Dpp and another BMP family ligand,

Screw (Scw; Arora et al., 1994), are required for the specification of dorsal cell fates. Dpp-Scw heterodimers have been proposed to be more efficiently transported by the Sog-Tsg complex, and to elicit higher levels of pathway activation, than Dpp-Dpp homodimers can (Shimmi et al., 2005b). In the wing disc, both Dpp and Gbb are required for the establishment of a long range gradient of pathway activity that patterns the wing (Ray and Wharton, 2001; Bangi and Wharton, 2006), but clonal analysis has shown that *gbb* from the same focus as *dpp* is expressed (i.e. anterior to the AP compartment boundary) is sufficient for long-range patterning. This leads to the possibility that this Gbb function is mediated by Dpp-Gbb heterodimers (Ray and Wharton, 2001; Bangi and Wharton, 2006). Heterodimers thus mediate BMP signalling in numerous developmental contexts, in some cases exclusively so, and often elicit higher levels of pathway activity than homodimers.

In the pupal wing, *dpp* is expressed in vein territories (Yu et al., 1996), whereas *gbb* is expressed throughout the wing (Conley et al., 2000). Our work shows that in the intervein, i.e. where *dpp* is not expressed, ectopic *gbb* is non-functional. This could arise if Gbb function in the pupal wing is entirely mediated through heterodimers with Dpp. *gbb*-expressing clones in the intervein would add to the pool of Gbb already expressed in intervein cells, but because this would not lead to heterodimer formation, no pathway activation would occur. The pathway activation seen when expressing *gbb* throughout the epithelium would plausibly derive from the formation of Dpp-Gbb heterodimers in regions of *dpp* expression (i.e. vein regions). Consistent with this notion, the most sensitive regions of the wing to ectopic *gbb* are those near the veins, the cells closest to the domains of *dpp* expression. A corollary to this model is that the pathway activation caused by *dpp* expression in the intervein may too derive from Dpp-Gbb heterodimers, considering *gbb* is expressed in the intervein. However, in the absence of Gbb, Dpp can promote vein development in most veins (Ray and Wharton, 2001), showing that Dpp homodimers are sufficient for vein development. Thus, BMP signalling in the pupal wing could derive from a mixture of Dpp-Dpp and Dpp-Gbb dimers (Fig. 7.1). The reason for homodimer non-functionality may be due to a reduced receptor affinity as compared to the heterodimers, as has been proposed in vertebrates (Little and Mullins, 2009).

In contrast to Gbb, ectopic Dpp in the intervein induces vein cell phenotypes (apical constriction and the formation of ectopic lumen). The link between Dpp and apical constriction is not unique to the wing: the constriction of amniosereosa cells during dorsal closure is Dpp-dependent (Fernandez et al., 2007), and apical constriction in the morphogenetic furrow of the developing eye requires Dpp along with Hh pathway activity (Escudero et al., 2007). In the eye,

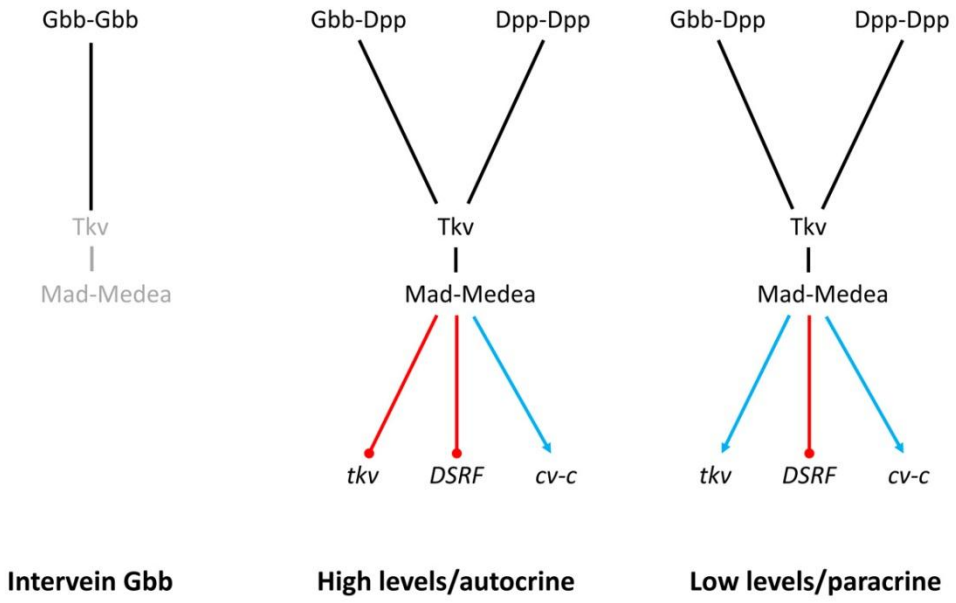

Figure 7.1. BMP signalling in the pupal wing: dimers and outputs. Left: Gbb-Gbb homodimers cannot activate the pathway. Middle and right: a potential mix of Dpp-Dpp and Dpp-Gbb promote signalling in the veins of the pupal wing, acting through Tkv and Mad/Medea to promote or inhibit transcription of target genes. At high levels of signalling (middle), expression of *tkv* and *DSRF* is inhibited, while expression of *cv-c* is promoted. At lower levels of signalling (right), expression of *DSRF* is inhibited (though to a lesser extent), while expression of both *cv-c* and *tkv* are promoted.

as in the wing, one of the ways Dpp appears to control constriction is via the apical enrichment of Actin.

With the use of FLPout clones, we were able to show that while ectopic expression of *dpp* in intervein cells induced apical constriction 1-2 cells away from the source, only the immediate first row neighbours of *dpp*-expressing clones showed reduced *DSRF* expression. This shows that second row neighbours constrict as an indirect result of proximity to a *dpp*-expressing clones (see also below). As well as repression of *DSRF*, Dpp also induces expression of *tkv* and *cv-c* in in a short range non-autonomous fashion (Fig. 7.1).

The short range of ectopic Dpp is consistent with its endogenous activity: pathway activity is confined to the regions where *dpp* is expressed (i.e. the veins). In contrast, in the wing disc a long range concentration gradient of Dpp is formed from a localised source abutting the AP compartment boundary (Affolter and Basler, 2007). This raises the issue of what underlies this shift from short- to long-range action of Dpp in the intraplanar dimension. In the disc, long-range gradient formation requires binding to the cell-surface HSPG Dally (Belenkaya et al., 2004), so the absence of Dally or other HSPG proteins in the pupal wing may play a role. However, the pupal expression pattern or function of HSPGs has not yet been reported. Another potential range-restricting factor is the extracellular environment of the pupal wing. Dpp is found at high levels in the lumenal space between the columnar and peripodial epithelia of the wing disc, and it has been proposed that this lumenal pool of Dpp contributes to the range of the gradient (Gibson et al., 2002). Wing morphogenesis involves the evagination of the wing disc, such that the lumenal facing apical surfaces of the disc evert to face outside the animal. In the pupal wing, we have defined the period during which Dpp signals most efficiently to induce vein characteristics as between separation and the completion of reapposition, and at these stages the pupal wing is loosely enclosed within the pupal cuticle. If intraplanar signalling involves the apical surfaces of the cells, the apical extracellular environment of the pupal wing might not be conducive for the diffusion of the ligand. ECM has been shown to influence the range of Dpp in the embryo and ovaries (Wang et al., 2008), and thus the binding of Dpp by apical ECM components could limit its range. Similarly, if intraplanar signalling is mediated by basally secreted ligands (see below), the basal lumen is filled with ECM components that could affect signalling (Fristrom et al., 1993; Murray et al., 1995).

Another restriction to Dpp diffusion in the wing is provided by the receptor Thickveins. In the wing disc, *tkv* expression is down-regulated in the centre of the disc and expressed at high

levels in its anterior and posterior regions (Brummel et al., 1994), in a pattern inverse to that of pathway activation. High levels of Tkv limit the diffusion of Dpp, thus restricting its range (Lecuit and Cohen, 1998; Tanimoto et al., 2000). In the pupal wing, *tkv* expression is heightened in the provein regions adjacent to the veins (de Celis, 1997) where it limits vein width potentially by limiting Dpp diffusion (Sotillos and de Celis, 2005). If Tkv does serve in the proveins to inhibit Dpp diffusion, ligand binding does not lead to the downstream transduction of the signal, as pMad is limited to vein territories (Conley et al., 2000). Thus, a provein-specific mechanism at the level of the receptor prevents activation of the downstream signalling cascade. This mechanism may involve the Notch pathway, which is activated in the provein.

We demonstrated that *dpp*-expressing clones in the pupal wing have a dual effect on *tkv* expression: clones led to the autonomous repression of *tkv*, and the induction of *tkv* expression in adjacent cells, creating a 'halo' of *tkv* expression around the clone. This correlates with the strength of the signal: whereas cells expressing *dpp* completely repress *DSRF* and constrict to the greatest extent, neighbouring cells only partially repress *DSRF*. The implication is that paracrine signalling activates the pathway to a lesser extent than autocrine signalling. Thus, high *dpp* signalling would inhibit *tkv* expression, as it does in the veins, whereas the lower levels of Dpp received by neighbouring cells would lead to the creation of a new 'provein' region of high *tkv* expression (Fig. 7.1). If the halos of Tkv around *dpp*-expressing clones in the pupal wing similarly act as a ligand trap, binding Dpp and preventing its diffusion, this might underlie its restricted range. This raises the possibility that in the absence of the Tkv trap, Dpp may be able to act at a long range in the intervein. If Tkv is the primary barrier to diffusion, changes to the extracellular environment as discussed above would not play a restricting role. The restriction of ligand diffusion by the induction of receptor expression is also seen in other pathways: in the wing disc, the restricted range of Hh is dependent on the Hh-dependent upregulation of the receptor Patched (Chen and Struhl, 1996).

tkv^{QD}-expressing clones showed two interesting phenotypes. Firstly, they led to apical constriction in first row neighbouring cells. As these cells do not down-regulate *DSRF*, this is an indirect effect of the autonomous pathway activation in the clone cells. We proposed a model whereby this reduction in apical area was an indirect result of sharing a cell-cell junction with a clone cell. Constriction would lead to a reduction in the length of the shared junction, and if this was not accommodated by an increase in length of another of the neighbour's junctions, its apical perimeter would reduce, thus reducing apical cell area. This mechanism could also account for the fact that intervein cells immediately adjacent to the veins show a reduced apical area compared to more distant intervein cells. It serves to reinforce the notion that cell

morphology is often determined by forces exogenous to the cell (Paluch and Heisenberg, 2009), as is additionally highlighted by the 'leaning' morphology of intervein cells near veins. The second interesting aspect of tkv^{QD}-expressing clones was the inhibition of vein development in regions neighbouring the clone. This antagonism of vein development could arise if high levels of pathway activation provided by tkv^{QD} led to the expression of the Notch ligand *Delta*, which would thus induce Notch activation in the cells around the clones. Because Notch antagonises EGFR pathway activity (de Celis et al., 1997), this would inhibit vein development. *dpp* would not be able to induce such high levels of pathway activation, and thus would not induce *Delta* expression.

Assessment of how BMP signalling directs vein development is complicated by the co-activation of the EGFR pathway in vein cells. Both the EGFR and BMP pathways are absolutely and non-redundantly required for pupal vein development, and the two pathways form a positive feedback loop (Yan et al., 2009b). The co-operation of BMP and EGFR signalling is not restricted to the wing: *dpp* and the EGFR ligand *vein* are expressed in the visceral mesoderm from where they co-operatively induce the endoderm (Szuts et al., 1998), and both pathways co-operate to control the expression of *Broad* in follicle cell patterning (Yakoby et al., 2008). The wing offers a further opportunity to address how these two signalling pathways interact to direct cellular differentiation.

On the basis of co-expression of pathway activators or inhibitors, a segregation of the roles of BMP and EGFR in vein development was previously proposed. Whereas EGFR signalling controls vein cell morphogenesis, BMP signalling maintains vein cell fate, and any effect on cell shape is an indirect consequence of activating the EGFR pathway (O'Keefe et al., 2007). By assessing cell shape changes in early PCV development, we have shown that BMP signalling can induce vein cell shape changes, in part by inducing expression of *cv-c*. This process is controlled independently of EGFR (Ralston and Blair, 2005), showing that BMP can control constriction aside from its role in maintaining vein fate. Furthermore, it raises the possibility that the constriction of the longitudinal veins may also be BMP controlled. Indeed, it has been shown that ectopic Dpp can induce vein-like cuticle in rho^{ve} *vn* mutants, which are proposed to lack the ability to activate the EGFR pathway in the pupal wing (de Celis, 1997). The disparity between our results and those of O'Keefe, et al. (2007) may arise from the different cellular phenotypes observed: whereas here we assessed apical constriction and basal apposition, O'Keefe, et al. focussed on the basal relocalisation of E-Cad that precedes the definitive stage. The control of cell morphology by BMP and EGFR activity may indeed be segregated, such that BMP-controlled constriction and lumen formation is followed by EGFR-controlled apical

retention of E-Cad. The positive feedback that exists between the pathways (Yan et al., 2009b) would ensure that the two cellular phenotypes always occur coincidentally.

II. Interplanar and intraplanar signalling

The insect wing is an elegant and simple structure, based on the adherence of two thin cuticular sheets. Wing development involves the creation of a unique epithelial architecture to secrete this structure: an epithelial bilayer with basal surfaces in apposition, and apical surfaces facing outward (Nardi and Ujhelyi, 2001). Because of this architecture, pupal wing development provides an opportunity to study the role of signalling interactions between epithelial layers in development. Inductive interactions between tissues, in which signals from one tissue alter the developmental program of the responding tissue, characterise animal development (Gurdon, 1987; Frasch, 1995; Bienz, 1997). Indeed, it had been previously suggested that inductive signals from the dorsal to the ventral layer are required for ventral vein structures to develop (Garcia-Bellido, 1977), and that in the case of the PCV, BMP signalling mediates this induction (Marcus, 2001). Such a role is not without precedent. Inter-epithelial Dpp is involved in two inductive events in embryonic development: induction of the cardiac and visceral mesoderm by the overlying ectoderm (Frasch, 1995) and of the endoderm by the visceral mesoderm (Bienz, 1997). However, by assessing the dorsal and ventral requirements for BMP ligands and their extracellular modulators it is clear that no such directional induction occurs in PCV development. This is in concert with various other studies showing that ventral veins can develop in the absence of a specific dorsal signal (de Celis, 1997; Milan et al., 1997; O'Keefe and Thomas, 2001; Ray and Wharton, 2001). We were further able to show that ectopic Dpp was capable of inducing vein development in cells of the opposite layer, and that this effect occurs in both directions. There is thus no inherent directionality to interplanar BMP signalling in the pupal wing.

Vein/intervein differentiation is not greatly effected when the corresponding cells in the opposite layer are converted to vein or intervein (or, in the case of Cv-c mis-expression, lost entirely), showing that the process can occur autonomously in the absence of interplanar signalling. Importantly, although ventral veins developed in such cases, they were often broader and less well-refined. Thus, although wing development does not involve an interplanar induction of vein fate, interactions between the layers appear to be required for the refinement of the veins. In addition to a role in vein refinement, interplanar signalling may ensure that the dorsal and ventral components of the vein align on reapposition. An alignment mechanism is suggested by the fact that the ectopic veins that result from brief periods of Dpp expression between separation and reapposition always align between the layers.

Unfortunately, we could not further test this hypothesis by creating an experimental condition wherein only interplanar BMP signalling was affected in an otherwise normally reapposing wing. The loss of vein promoting interplanar signalling might result in misaligned veins, which would have consequences for the mechanical properties and integrity of the wing, considering the contribution of veins to these properties (Wootton, 1992). The unique architecture of the pupal wing necessitates a mechanism to ensure symmetry after apposition, and the ability of BMP ligands to promote signalling in both adjacent and opposite cells fulfils this requirement.

Considering our proposed function of interplanar BMP signalling in the wing, the question arises as to its mechanism. The architecture of the pupal wing dictates that interplanar signalling would occur through the basal surfaces of the cells, a similar scenario to that of mesoderm induction, in which Dpp from the overlying ectoderm induces cell fate changes (Frasch, 1995). Interestingly, Dpp-GFP is observed in both apical and basolateral compartments of the wing disc (Teleman and Cohen, 2000; Gibson et al., 2002), and if the same distribution occurs in the pupal wing, these two pools could mediate intraplanar and interplanar signalling respectively (Fig. 7.2). Basal signalling would also require a basal localisation of the receptors.

As shown in Figure 7.2, interplanar signalling has to be basally mediated, but intraplanar signalling (e.g. between vein and provein cells) could be either apically or basally mediated. We have shown how ectopic expression of *dpp* in intervein clones can promote signalling in both adjacent and opposite cells. BMP signals from the wild type layer can also promote both intra- and interplanar pathway activity in rescue experiments. As the same signal can mediate signalling in both dimensions, it may arise from the same, basal source. In such a scenario the basolateral cell surfaces and the ECM-rich extracellular spaces would become the arena of signalling in the pupal wing. One prediction of the model is that Tkv would be basally enriched in provein cells adjacent to the veins, and the ligand trap would be a basal phenomenon. We can also integrate other signalling pathways into this model. The Notch receptor is apically localised in the wing disc (Fehon et al., 1991), but on the basis of my own preliminary antibody staining, the Delta ligand is found at the basal surface of provein cells in the pupal wing. As Delta activates Notch in these provein cells, this would imply that Notch itself shifts its localisation between apical and basal compartments in the formation of the pupal wing. Pupal wing development may thus offer a model system for the (re-)localisation of signalling on the apical-basal axis of an epithelium.

We can next consider how interplanar ligands would reach the receptor to promote pathway activation. The first option is diffusion of basally secreted proteins through the lumen.

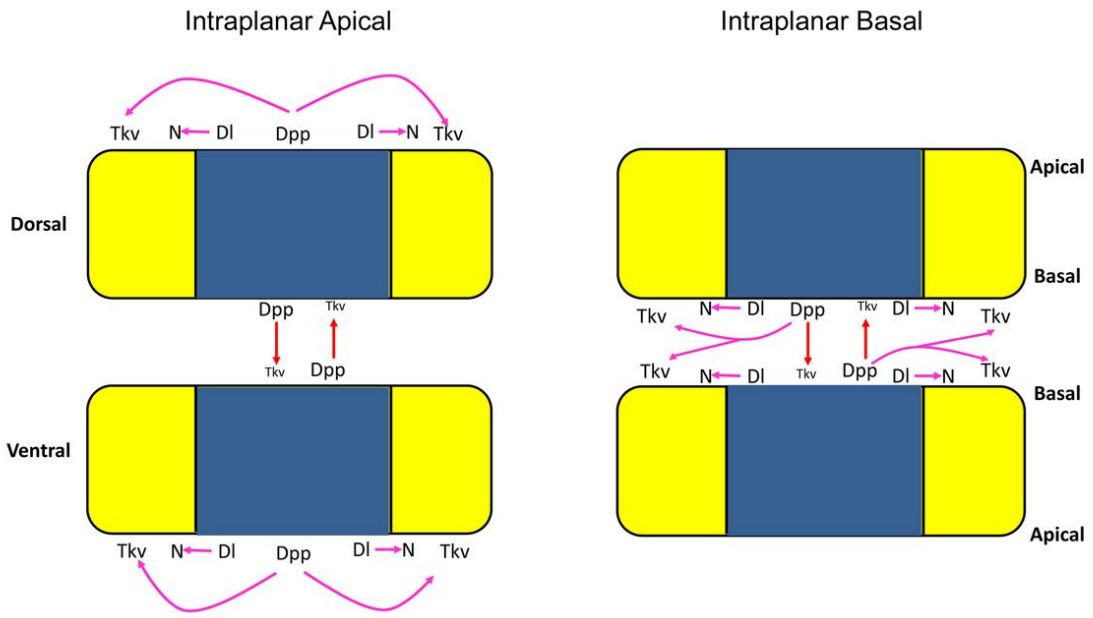

Figure 7.2. Interplanar and intraplanar signalling in the pupal wing. Interplanar signals are shown in red, intraplanar signals are shown in pink. Signals are restricted to the BMP and Notch pathways in the veins (blue domains) and proveins (yellow domains). Left: intraplanar signalling could be mediated by the apical compartment, in which case the two dimensions of signalling are separate. Right: if intraplanar signalling is basally mediated, the same signals could promote pathway activation in adjacent and opposite cells.

Diffusion presents the problem of how to restrict signalling to target cells (i.e. those vein cells in the opposite layer) and prevent diffusion throughout the lumen, which prior to reapposition is formed by all cells in the wing including intervein cells. One means to restrict diffusion is via HSPGs, proteins which bind the ligand and keep it to the cell surface and which are involved in the generation of morphogen gradients in the disc (Belenkaya et al., 2004; Han et al., 2004; Han et al., 2005). However, the cells receiving the interplanar signal in the pupal wing are across the lumen. Whereas HSPGs could influence diffusion within a layer, they could not influence diffusion between layers.

At the time of interplanar signalling, ECM components such as Laminin (Fristrom et al., 1993; Urbano et al., 2009), the Type IV Collagens Cgc25 (Murray et al., 1995) and Viking (this study), and Perlecan (this study) fill the lumen. ECM components play a role in Dpp signalling in other contexts: in the ovaries, loss of Type IV Collagens leads to an expansion of pathway activity, whereas in the embryo, signalling is reduced when Type IV Collagens are lost (Wang et al., 2008). Both effects derive from the ability of Type IV Collagen to bind Dpp, and such binding has also been shown for vertebrate Type IV Collagen and BMPs (Paralkar et al., 1990; Paralkar et al., 1992). ECM-binding regulates the range of the ligand and the efficacy of signalling both positively and negatively. Because ECM components fill the vein lumen, if Dpp is secreted basally, it may bind to Type IV Collagens which would as a result affect its signalling range. Interplanar signalling may provide a further opportunity to explore the means by which ECM effects cell signalling in development.

An alternative signalling mechanism relies on contact between signalling cells. We have shown that both classes of vein cell (central and flanking), make contact with the opposite layer, in the case of central cells by slender cytoplasmic projections. Cellular projections are increasingly seen to play an important role in cell signalling (Rorth, 2003). The paradigm of contact based signalling in development is the juxtacrine signalling of Notch pathway (Bray, 2006), but recent results have shown that cells do not have to be in close proximity for such signalling to occur. Dynamic filopodial extensions emanating from the basal surface of cells in the pupal notum participate in Delta/Notch lateral inhibition, acting over several cell lengths to refine the spacing of bristles in the tissue (Cohen et al., 2010). Cellular extensions are also implicated in Dpp signalling in the disc: long and thin cytoplasmic projections termed cytonemes are seen emitting from cells located at the lateral sides of the disc towards the AP compartment boundary (Ramirez-Weber and Kornberg, 1999). Strikingly, it has recently been shown that cytonemes carry pathway specific receptors towards the source of the signal, for example Tkv is seen on cytonemes projecting to the *dpp* source (Roy et al., 2011). In contrast

to these dynamic projections, the basal projections sent by central cells are stable (as they are seen in fixed sections). However, they may still mediate interplanar BMP signalling in the veins, acting as signalling foci to align the arches and create a complete lumen. If these connections are also required for the integrity of the lumen (see below), basal projections of the central vein cells would serve both structural and signalling functions.

Contact-based signalling during pupal development would negate potential issues arising from the secretion of ligands into the lumen. Firstly, signalling between the veins would not be affected by the ECM of the lumen, which might bind BMP ligands and thus restrict their interactions with receptors in the opposing layer. Second, such signalling would be specific to the cells expressing the ligand (i.e. vein cells), avoiding problems of diffusion of secreted ligands into the lumen (where they could activate signalling in adjacent intervein cells). Signal specificity is a key advantage of contact-based signalling (Rorth, 2003). It should also be noted that our investigations utilised fixed tissue, in which cytonemes are not seen (Ramirez-Weber and Kornberg, 1999), which leaves open the possibility that further and perhaps more extensive contacts occur between the layers.

A final consideration of wing architecture and signalling is that although the pupal wing is grossly symmetrical, our analysis of apical vein morphology revealed that the apical surfaces of veins assume distinct morphologies in the dorsal and ventral layers. These distinctions reflect the future arched/flat pattern, with the future arched surface broader and composed of more cells. This asymmetry originates in the unequal recruitment of cells into the developing vein after apposition, with the future arched surface incorporating more cells into the presumptive vein. This suggests that in the presumptive arched layer, the signal that induces constriction (which we have shown can be provided by the BMP pathway) is stronger or includes more cells. This would not occur at the level of ligand expression, as broader expression in one layer would induce symmetrical signalling in the opposite layer (as is shown when knocking down the activity of the provein). Rather, it could reflect a diminished capacity for the presumptive flat surface to transduce vein-promoting signals, for example if the cells had lower levels of BMP/EGFR receptors. Because the arching alternates on the AP axis, reducing sensitivity within the whole dorsal or ventral compartment would not achieve the pattern; rather the diminished sensitivity would have to alternate between dorsal and ventral sides of the veins. How this is achieved is an intriguing and open question.

III. Cv-c and PCV development

The focus of the discussion thus far has been on the spatiotemporal dynamics of intercellular signalling and the cell shape changes that such signalling controls. We now turn our attention to the relationship between these two developmental processes: how do signalling pathways enact cell shape changes? In this thesis the development of the PCV has been utilised to address this question.

PCV development is characterised by BMP induction of vein fate in the L4-L5 intervein. Because BMP signalling is the master regulator of this process (Ralston and Blair, 2005), it offers an ideal opportunity to investigate how a single signal transduction pathway controls a developmental process. We were able to show that PCV specification is concurrent with cell shape changes of apical constriction and lumen formation, which demonstrates that patterning is coincident with differentiation in the crossveins. This contrasts to the longitudinal veins, in which specification occurs in the wing disc. In the crossveins, the inductive BMP signal controls the expression of multiple target genes, which collectively both define and refine vein fate, and control the necessary cytoskeletal changes (in part through Cv-c, see below). A similar scenario is seen during the progression of the morphogenetic furrow in the developing *Drosophila* eye, where photoreceptor fate specification and cell shape changes derive from the same signals (Escudero et al., 2007).

cv-c was previously characterised as a RhoGAP required for numerous developmental processes in embryogenesis (Denholm et al., 2005), but how it contributed to PCV development was not known. We have identified *cv-c* as a new target of BMP signalling during PCV development. This extends the repertoire of known transcriptional targets of early BMP signalling in the PCV. The feedback factors *cv-2* (Serpe et al., 2008) and *ltl* (Szuperak et al., 2011) are both expressed in response to pathway activity, and the expression of *DSRF*, *tkv* and *sog* are all negatively regulated in response to BMP signalling (Conley et al., 2000; Ralston and Blair, 2005). In Figure 7.3 the various factors in the early PCV patterning network are shown, with established transcriptional targets of BMP signalling in bold. It is of note that Cv-c is the only factor that does not appear to act on the 'patterning level,' i.e. in enhancing or maintaining the initial BMP signal. Although *cv-c* loss does lead to the failure of *DSRF* repression, this is an indirect consequence of the failure to inactivate Rho1 (see below). The Figure serves to highlight how an inductive signal can influence a variety of transcriptional

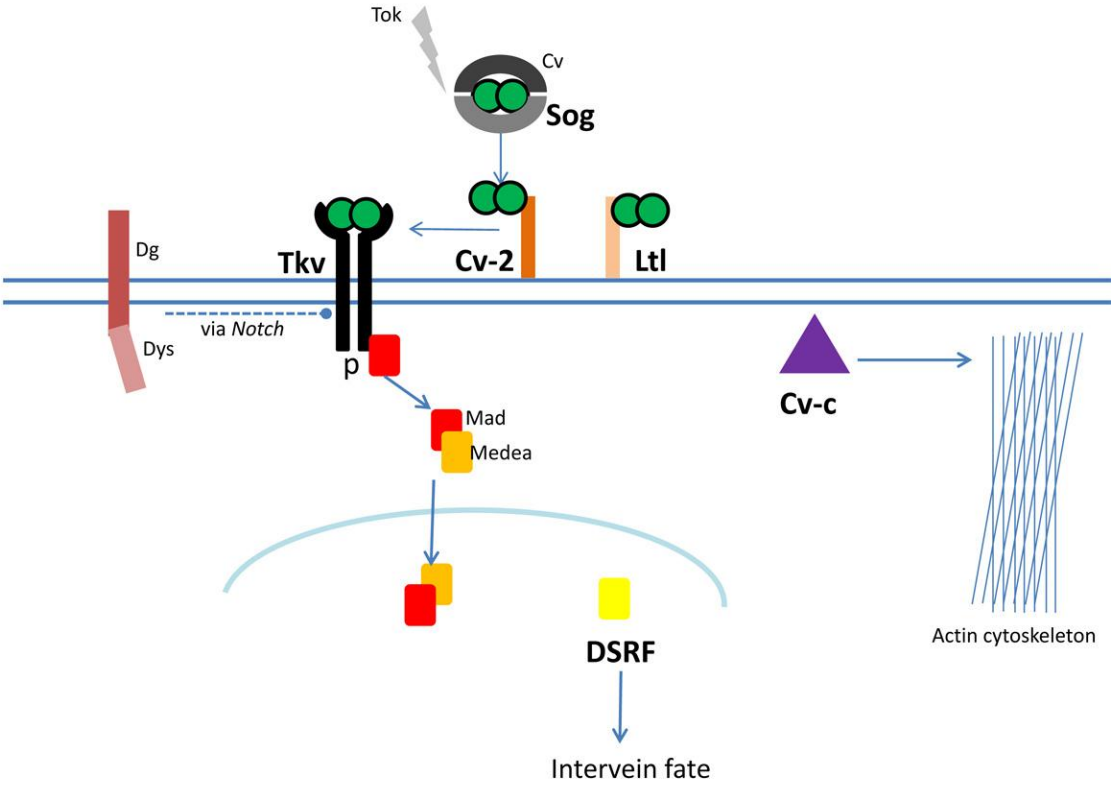

Figure 7.3. Factors involved in early PCV development. Cellular localisation of factors involved in PCV development. Known transcriptional targets of BMP signalling are shown in bold. An extracellular ligand complex formed by Sog, Cv, and BMP ligands is cleaved by Tok to release the ligands. These are in turn presented to Tkv via Cv-2, or sequestered by Ltl. Ligand binding leads to the downstream transcriptional response, which includes these extracellular factors, and, as identified in this study, Cv-c, the only gene that appears to act at the 'morphogenesis' level. Also shown is the putative indirect inhibition of Tkv by Dg/Dys, via Notch inhibition.

targets, which can both enhance pathway activity and reinforce cell fate as well as inducing the appropriate cellular differentiation.

cv-c expression is initiated in the PCV coincident with the repression of *DSRF*, and shows a similar pattern of an initially broad band of expression which then refines. Where the BMP signal is absent, *cv-c* is not expressed, and constriction does not occur. Furthermore, ectopic pathway activation leads to ectopic *cv-c* expression, coincident with vein shape changes, so Cv-c may be contributing to apical constriction in these conditions. It is of note that although *dpp*-expressing clones induce *cv-c* expression when in the intervein, they do not when they cover the veins, which already show high levels of BMP pathway activity. This might reflect the repression of *cv-c* expression in the longitudinal veins. A candidate for this repression is EGFR pathway activity, which is also active in the longitudinal veins (Guichard et al., 1999). If so, BMP signalling is only sufficient for *cv-c* expression in the absence of EGFR activity, i.e. in the interveins.

Diverse inputs control *cv-c* expression in development: it is downstream of the EGFR pathway during tracheal invagination (Brodu and Casanova, 2006), downstream of the Hox gene Abdominal-B (though perhaps indirectly via an Abdominal-B target) in the posterior spiracles (Lovegrove et al., 2006), and downstream of BMP signalling in the PCV (this study). Additionally, it shows localised expression in various other embryonic tissues, such as the head mesoderm, the hindgut, the Malpighian tubules and the peripheral nervous system (Denholm et al., 2005). This suggests a complex regulatory architecture of the *cv-c* gene, which leads to localised expression at specific points in development. In all of these tissues, as in the PCV, *cv-c* expression coincides with tissue morphogenesis, and it is thus a key realisator of multiple developmental events in *Drosophila* development. In response to fate-determining signals, Cv-c orchestrates the morphogenesis that follows.

cv-c function in the pupal wing may also be informed by the role that one of its mammalian orthologues, *Deleted in liver cancer 1* (*Dlc-1)*, plays in cancer metastasis. *Dlc-1* was first isolated as a gene frequently lost in hepatocellular carcinoma cell lines (Yuan et al., 1998), and deletions which include the *Dlc-1* locus are seen in numerous cancers at rates approaching those of the well-established tumour suppressor *p53* (Xue et al., 2008). Its tumour suppressing action is thought to be mediated predominantly through RhoGTPases, in particular RhoA (Lahoz and Hall, 2008). Indeed, reducing RhoA levels in vivo reduces cancer growth in *Dlc-1*$^{-}$ cells (Xue et al., 2008). As well as the family-defining catalytic GAP domain, RhoGAP proteins also contain numerous other protein- or lipid-binding domains which can affect the function

and localisation of the protein in the cells (Bernards and Settleman, 2004). Such domains in Dlc-1 promote the formation of complexes with the focal adhesion associated proteins Talin and Focal Adhesion Kinase, and their abrogation significantly impairs the tumour-suppressing activity of Dlc-1 (Li et al., 2011). In addition, other studies have suggested that a form of Dlc-1 lacking the GAP domain is still capable of inhibiting tumour proliferation (Healy et al., 2008). Both studies raise the possibility that its GAP activity may not be entirely sufficient for its function as a tumour suppressor.

This raises the question of whether there are GAP-independent functions of Cv-c in *Drosophila*. However, in all developmental contexts thus far described its role in morphogenesis is mediated through Rho GTPases (Denholm et al., 2005; Brodu and Casanova, 2006; Simoes et al., 2006; Sato et al., 2010; this study). Furthermore, of the mapped *cv-c* mutations to arise from genetic screens (all of which are embryonic lethal), they truncate the protein before (*cv-c*^{C524}) or within (*cv-c*^{M62}) the GAP domain, or affect a conserved residue within the GAP domain that is required for efficient catalytic activity (*cv-c*^{7}) (Denholm et al., 2005). All these data suggest that Cv-c function in *Drosophila* development is mediated through RhoGTPases.

Dlc-1 localises to focal adhesions (Qian et al., 2007), a prominent site of RhoA function in cell migration (Schoenwaelder and Burridge, 1999). Interestingly, basal apposition, a cellular phenotype which is promoted by Rho1 in the wing (see below), also relies on the formation of Integrin-based focal adhesions (Brabant et al., 1996). If Cv-c, like Dlc-1, is localised at focal adhesions (i.e. basally), this would suggest that its target, Rho1, might also function at these junctions to promote apposition (see below). Unfortunately, we were unable to detect an intracellular enrichment of tagged versions of Cv-c (which were seen throughout the cell but did dramatically alter cell morphology), nor of Rho1 (using either antibodies or a Rho1-GTP specific probe (Simoes et al., 2006)). However, such enrichment may be beyond the resolution of these probes. Intracellular localisation would be consistent with the localised action of RhoGTPases and their regulators within the cell during development (Bement et al., 2006; Simoes et al., 2006).

IV. The roles of Rho1 in the pupal wing

We have presented several lines of evidence to suggest that Cv-c function in the pupal wing is mediated through Rho1. Rho1 plays a multitude of roles in development, but amongst the best characterised is the regulation of the Actin cytoskeleton (Hall, 1998), prominently via its effector Rok (Mizuno et al., 1999). Here we have characterised a function for Rho1 in the promotion of intervein development: knocking down the function of Rho1 or its effector Rok leads to the formation of ectopic crossveins, and a failure of normal basal apposition in intervein sectors. Additionally, we showed that hyperactivation of Rho1/Rok led to a failure of lumen formation. Rho1 is also required for the maintenance of *DSRF* expression in the intervein (see also section VI below). The promotion of *DSRF* expression suggests that Rho1 can promote intervein development both by cytoskeletal (i.e. Rok) and transcriptional (i.e. *DSRF*) outputs. BMP signalling can inhibit these functions in the PCV by inducing expression of the RhoGAP Cv-c.

As Rho1/Rok inhibits apical constriction and promotes basal apposition, the next task is to explain how this activity achieves these cellular phenotypes. It has recently been demonstrated that interfering with *zipper* (*zip,* encoding Myo-II heavy chain) function leads to ectopic crossveins and blister formation (Franke et al., 2010). Considering the well-established role for Rok in activating Myo-II (Vicente-Manzanares et al., 2009), and that Rho1/Rok knockdown also leads to ectopic crossveins and blisters, this strongly suggests that Myo-II is downstream of Rok in the intervein. The involvement of the Rho1/Rok/Myo-II cassette in these cellular phenotypes (apical relaxation, basal apposition) is surprising considering the requirement for the cassette in apical constriction in a number of other developmental contexts (Sawyer et al., 2010). Phosphorylation of the regulatory light chain of Myo-II by Rok (or via Rok inhibition of Myosin Phosphatase) is followed by Myo-II mediated contraction of apical Actin filaments. The contracting network is linked to the adherens junctions and thus pulls the apical perimeter inwards, reducing cell area (Dawes-Hoang et al., 2005; Baum and Georgiou, 2011). In other cases, however, different inputs can converge on to Myo-II. Multiple kinases are capable of phosphorylating Myo-II (Vicente-Manzanares et al., 2009), and in the developing *Drosophila* eye, loss of *rok* does not completely eliminate Myo-II phosphorylation (Corrigall et al., 2007), suggesting redundancy with another kinase. Thus the activation Rho1/Rok is one of many potential paths to Myo-II mediated Actin filament contraction.

Another kinase could act in vein cells to control apical Myo-II activation and hence apical constriction.

The Rho1/Rok/Myo-II cassette is itself utilised in numerous developmental processes aside from apical constriction, and two in particular have relevance for its role in the intervein. In the *Drosophila* ovary, Rho1/Rok/Myo-II activity controls pulsed contractions in the basal surface of follicle cells, leading to the elongation of the egg chamber (He et al., 2010). This shows that the cassette's activity in the basal domain of epithelia can lead to cell shape changes. Secondly, the cassette acts downstream of the planar cell polarity (PCP) pathway to regulate the Actin cytoskeleton during hair morphogenesis in the wing (Winter et al., 2001; Franke et al., 2010). This function is not specific to cell type in the pupal wing, and thus is independent of its role in promoting intervein morphology. Furthermore, Rho1 is required to maintain the integrity of apical adherens junctions in epithelia (Bloor and Kiehart, 2002), including the wing (Yan et al., 2009a), showing an additional function which is independent of vein/intervein differentiation and general to the epithelium.

To address the mechanism by which Rho/Rok/Myo-II functions to promote intervein development and antagonise crossveins, we must additionally consider the apical and basal morphologies of vein and intervein cells. Following apposition, intervein cells relax apically to assume a hexagonal array (Classen et al., 2005), and appose to cells in the opposite layer. Their basal surfaces show enrichment of Integrins, E-Cad, Actin and Myo-II (Fristrom et al., 1993; Fristrom et al., 1994; O'Keefe et al., 2007; this study). In contrast, vein cells constrict apically and form a lumen basally (though, like intervein cells, they make contact with cells of the opposing layer). Vein cells show apical enrichment of E-Cad, Actin and Myo-II (Fristrom et al., 1994; O'Keefe et al., 2007; this study). Thus, Actin and Myo-II display a polarised distribution in the two cell types of the wing: apically enriched in constricting vein cells, and basally enriched in the intervein.

With this polarised cytoskeletal enrichment in mind, we can propose a model of vein/intervein differentiation (Fig 7.4). In intervein cells, Rho1 activity is heightened basally, perhaps by the basal enrichment of a RhoGEF. This leads to Rok phosphorylation and hence Myo-II activation in the basal domain. Myo-II then acts on Actin to promote basal apposition, in a manner that may involve promoting a link between Integrins and the Actin cytoskeleton. Interestingly, the maintenance of Integrin-based focal adhesions in cell culture requires Rho mediated contractility (Chrzanowska-Wodnicka and Burridge, 1996; Schoenwaelder and Burridge, 1999), so a similar scenario may occur in the pupal wing. Basal enrichment of Actin would sequester it

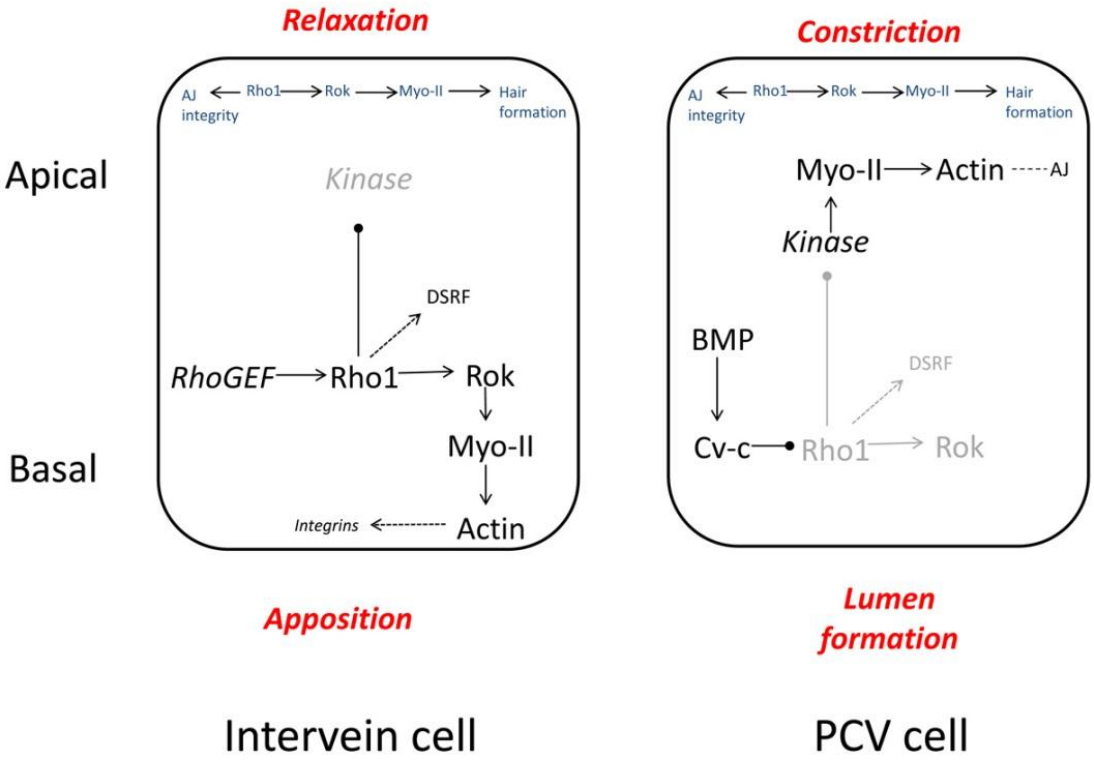

Figure 7.4. Model for Rho1 function in the pupal wing. Details are discussed in the text. Aside from vein/intervein specific functions, blue text shows the requirements for Rho1 in functions general to all wing cells (hair formation, AJ integrity). Arrows: pointed ends indicate promotion, rounded ends indicate inhibition. In italic are predicted factors not yet identified. Grey shows inactive pathways. Red shows associated apical or basal changes.

from the apical compartment, providing a contributory factor to the relaxation of apical area. In vein cells, Rho1 function at the basal membrane is antagonised (in the case of the PCV, by Cv-c), thus inhibiting the activation of Myo-II. Myo-II is in turn activated apically by alternative Kinase, promoting Actin contractility and, via a link to the adherens junctions, apical constriction. Although we did not demonstrate a functional requirement for the apical enrichment of Myo-II in veins, it may be at a higher threshold than that in the intervein. If the activity of the Myo-II activating Kinase in vein cells was antagonised by Rho1, inhibition of Rho1 (e.g. by Cv-c in the PCV) would lead to the relief of this antagonism, such that one input could promote both apical and basal phenotypes.

This model requires the spatial restriction of Rho1 functions within a single cell, and proposes polarised localisation of RhoGAPs and RhoGEFs as a means to achieve this. Such a mechanism is consistent with the restriction of Rho1 activity by polarised enrichment of RhoGAPs/RhoGEFs in other contexts (Bement et al., 2006; Simoes et al., 2006; Kolsch et al., 2007; Plageman et al., 2011). It is important to note the proposed vein/intervein distinctions in Rho1 activity occur alongside the apical functions of Rho1/Rok/Myo-II in hair formation (Winter et al., 2001; Franke et al., 2010), and Rho1 in maintaining AJ integrity (Yan et al., 2009a), both of which occur in all cells of the wing. Thus a baseline level of apical Rho1 activity is required alongside and independent of these cellular morphogenesis functions (Fig. 7.4). It is intriguing to consider how, within a single cell, distinct pools of active RhoGTPases would function to coincidently control different aspects of cellular phenotype.

In the PCV, the RhoGAP Cv-c is the link between cell patterning (i.e. BMP signalling promoting vein fate) and the cytoskeletal regulators that control cell shape changes (i.e. Rho1/Rok/Myo-II). One prediction of the model is that other RhoGAPs, or alternate means of inhibiting Rho1 activity (for example via RhoGDI (Garcia-Mata et al., 2011), which has not yet been ascribed a function in *Drosophila*), act in the longitudinal veins to inhibit Rho1. Because BMP signalling is activated in longitudinal veins too, the BMP-RhoGAP-Rho1 link may not be limited to the crossveins. There are many RhoGAPs in the *Drosophila* genome that have yet to be ascribed a function (Bernards, 2003), and a prediction of our model is that a reverse genetics approach would uncover vein-promoting functions for some of these RhoGAPs. For instance, a RhoGAP RNAi library could be utilised, and RNAi restricted to the pupal wing using the Gal4Gal80^{ts} system as detailed in this thesis. Our model predicts that knocking down certain RhoGAPs would lead to longitudinal vein loss. If redundancy between RhoGAPs was a problem (Nir et al., 2010), double RNAi experiments could surmount this. Finally, as Rho1 activity is required for intervein development, our model predicts that a similar approach for RhoGEFs would uncover

functions in intervein promotion (i.e. leading to an ectopic crossvein phenotype following the failure to basally activate Rho1 in the intervein).

The model predicts that distinct kinases activate Myo-II in vein as compared to intervein cells. Considering the role of Rok in intervein development, we showed that *rok*^{CAT}-expressing clones produce two phenotypes: in intervein, a decrease in apical cell area (though not to the extent of BMP pathway activation), and in vein cells, the promotion of apposition. Whereas the latter phenotype reflects the apparent endogenous function, the former does not. Endogenous Rok activity is dependent on Rho1 (Amano et al., 1996), and thus Rho1 determines its spatial activity within the cell. Catalytically active Rok is not similarly Rho1-dependent, and would thus not be spatially restricted. Apical constriction and basal apposition could thus arise if activated Rok promoted Myo-II activation in both the basal and apical compartments. Myo-II would in turn act on Actin to promote the two phenotypes of apposition and constriction.

The work presented in this thesis provides an example of how cell signalling pathways can cause changes to the cytoskeleton (and hence changes to cell shape) by influencing the transcription of RhoGTPase regulators. There are many more RhoGAPs and RhoGEFs than the RhoGTPases they control (Bernards, 2003), highlighting the importance of RhoGTPase regulation to the success of development. As depicted in Figure 7.4, the next issue is to address how these regulators themselves become spatially localised within the cell to focus RhoGTPase activity. *cv-c* RNA is apically localised in the trachea (Brodu and Casanova, 2006), whereas RhoGEF2 protein appears to be transported to the apical domain of ventral furrow cells via an association with Microtubules (Kolsch et al., 2007). Thus, trafficking of RhoGAPs/RhoGEFs at both RNA and protein levels are potential mechanisms. Pupal wing development offers an opportunity to investigate the polarisation within the cell not only of signalling by conserved signal transduction pathways (see above) but also of their downstream cytoskeletal regulators.

V. Features of crossvein development

The pattern of crossveins varies between insect wings (Wootton, 1992; Stark et al., 1999). This work suggests a mechanism for the addition or loss of crossveins: localised BMP activity in the intervein leads to the induction of *cv-c* expression and thus inhibition of Rho1 activity, so extra crossveins would be produced by new sources of BMP activity. This begs the question of how the BMP signal would become localised to specific regions of intervein in the first place. The mechanism of the positioning of the crossveins at specific points along the proximal-distal axis of the wing is still unclear in *Drosophila* (Blair, 2007), but it is worth noting that the ectopic crossveins following *Rho1/Rok* knockdown are seen in stereotyped positions (e.g. between L3 and L4, half way between the ACV and PCV), suggesting that some regions of the wing are inherently more susceptible than others to the formation of ectopic crossveins. In addition it should be emphasised that *Rho1/Rok* knockdown specifically led to ectopic crossveins and not just gross ectopic venation. This suggests a separation between factors which cause as expansion of vein territories, as seen for example in *DSRF* and *N* mutants, and following *dpp* or *rho* mis-expression, and those that cause ectopic crossveins (*Rho1*, *Rok*). If these two mechanisms are separate, they might offer the insect wing plasticity to alter the number of crossveins while keeping the longitudinal vein pattern unchanged.

We have shown that PCV cells are the most apically constricted in the pupal wing, and also that this constriction coincides with an enrichment of apical Myo-II and Actin, which was markedly higher than that in the longitudinal veins. Thus, higher apical levels of Myo-II and Actin correlate with a smaller apical cell area (i.e. more constriction). Furthermore, PCV cells show higher levels of pMad staining as compared to the longitudinal veins (Conley et al., 2000), suggesting a higher level of BMP pathway activity in these cells. Thus, there is a correspondence between BMP pathway activity, the degree of apical enrichment of Actin and Myo-II accumulation, and the extent of apical constriction in the pupal wing.

The different developmental trajectory of the crossveins culminates in a distinctive cuticular morphology in the adult wing. Rather than being arched/flat, crossvein cuticle is formed of a series of irregular ridges that rise up towards the base of the trichomes, giving an annulated morphology. Owing to the folding of the wing, we were unable to determine whether this morphology arose from distinct apical remodelling in comparison to the longitudinal veins at the time of cuticle secretion. However, it is worth noting that at the definitive stage, PCV cell

shapes are more irregular in comparison to longitudinal veins, so this arrangement may contribute to the irregular cuticle morphology. A similar annulated morphology has been reported in other flies and in locusts, and is proposed to provide the wing with flexibility along its AP axis in flight, in analogy to the way that annulation of a drinking straw or vacuum hose provides flexibility (Wootton, 1992). The functional relevance of crossveins to *Drosophila* flight however has yet to be addressed.

VI. DSRF, Rho1 and intervein development

Uncovering the role of Cv-c defined one way in which BMP signalling directs vein morphogenesis. In terms of the interveins, although the *DSRF* transcription factor is known to direct intervein development (Montagne et al., 1996; Roch et al., 1998), its targets in the wing are poorly understood. A potential mechanism for its function is solely through the inhibition of EGFR and BMP pathway activity, as *DSRF* and *rho* appear to mutually repress each other (Roch et al., 1998). According to this scenario, Rho1 activity would be limited to those regions of the wing which do not show BMP/EGFR activity, i.e. the intervein, and *DSRF* control of intervein development would be via inhibition of vein promoting factors.

DSRF might however play a more direct role in influencing the transcription of 'realisator' genes to promote intervein differentiation. This would be consistent with the behaviour of its mammalian orthologue (*SRF*) which controls the expression of numerous target genes, prominent among which are those involved in the regulation of the cytoskeleton (Sun et al., 2006). Indeed the Actin regulator *Enabled* is downstream of *DSRF* in *Drosophila* tracheal development (Gervais and Casanova, 2010). It has also been shown that *β1-Integrin* is downstream of *SRF* in mammalian cells (Miano et al., 2007), which raises the possibility that *DSRF* promotes Integrin expression in the pupal wing. However, in the wing disc, expression of Integrin genes does not reflect *DSRF* expression in the intervein domains (Brower et al., 1984), and the expression patterns in the pupal wing have not been reported. Although β-PS protein is seen basally in the regions of apposition (Fristrom et al., 1993), our single-cell labelling has revealed that vein cells make basal connections to the opposite layer at the edges of these regions. If Integrins are not excluded from the veins, this raises the possibility that vein-vein contact may too be mediated by Integrins. For example, if the formation of a stable lumen required strong basal contacts, Integrins would fulfil this requirement, and their function would be general to all cells of the wing. Thus, they would not represent an intervein-specific realisator. If Integrin function is not unique to intervein cells, the promotion of intervein development by Rho1 may either be independent of Integrins, or involve a modulation of Integrin function in an intervein-specific manner.

An intriguing aspect of intervein development is the relationship between Rho1 and *DSRF* transcription. Cv-c loss, and hence Rho1 activation, leads to the failure to repress *DSRF*, whereas Rho1 knockdown leads to the loss of *DSRF* in the ectopic crossveins. Thus, Rho1

activity promotes *DSRF* expression. RhoGTPases can affect the transcriptional output of signalling pathways by affecting the signal transduction machinery (Jaffe and Hall, 2005), and one well characterised example involves SRF itself. To activate transcription, SRF binds cofactors, among which are the myocardin-related transcription factors (MRTFs; Posern and Treisman, 2006). MRTFs are Actin binding proteins: when bound to G-Actin, they remain inactive in the cytoplasm, but when G-Actin levels decrease (via polymerisation into Actin filaments), they shuttle to the nucleus and complex with SRF, leading to the regulation of target gene expression (Olson and Nordheim, 2010). Thus, Actin polymerisation, a process controlled in various ways by RhoGTPases (Pollard and Cooper, 2009), leads to SRF-dependent transcription. One of the transcriptional targets of *SRF* is *SRF* itself (Miano et al., 2007), so a consequence of interfering with SRF would be a reduction in *SRF* expression. If a similar scenario occurred in the pupal wing, reductions in Rho1 activity would lead to an increase in net G-Actin, MRTF would be sequestered in the cytoplasm, and *SRF* transcription would be reduced. This model relies on an increased quantity of G-Actin in vein cells as opposed to intervein cells, and such a distribution has not yet been tested. Apical constriction in vein cells is characterised by enrichment of apical F-Actin, but this may still represent a reduced F-Actin content as compared to the intervein, where F-Actin is basally enriched.

VII. Cellular basis of the veins

We return finally to the cellular architecture of the pupal wing epithelium, as revealed by single-cell labelling. The utility of such labelling to uncover epithelial architecture was recently highlighted by the demonstration that the mammalian intestinal epithelium, which was previously thought to be stratified, is actually pseudostratified (labelled cells stretched from the basal surface to the lumen (Grosse et al., 2011)). In the context of the current work, the technique allowed us to define how vein cells construct the lumen. This process was previously hypothesised to be controlled by differential adhesion, such that vein cells do not basally adhere (Hogan and Kolodziej, 2002), or alternatively by the constriction of vein cells on their apical-basal axes (O'Keefe et al., 2007). In contrast, we showed that there are two morphologically distinct vein cell types, both of which make contact with the opposing layer. Central cells form an arch basally and send out thin basal projections to contact the opposite layer, and flanking cells lean in to the midline on either side of the lumen. Thus the vein lumen is composed of a mosaic of these two cell types. The process of lumen formation involves the cellular morphogenesis of two types of vein cell, the arrangement of which is co-ordinated between the two layers of the wing via their basal contacts. This process adds a novel mechanism to the repertoire of how animal tissues construct tubes, as rather than involving cavitation, budding or hollowing (Lubarsky and Krasnow, 2003), it involves the symmetrical adoption of cell morphologies in two apposing epithelial layers.

The two vein cell types also show distinct apical morphologies: central cells are more relaxed, and flanking cells are more constricted (Fig. 7.5). This arrangement is achieved as an initially uniform constriction is followed by relaxation specifically in the central cells. The different behaviour may result from distinct signalling events in the two cell types, considering their cell-cell contacts. Central cells only make contact with other vein cells, but flanking cells make contact with the provein cells, and these connections form the boundary between the vein and intervein domains (Fig. 7.5). If signalling across this boundary were involved in the maintenance of constriction, flanking cells would remain constricted. Central cells would not participate in this signalling, and the failure of feedback to maintain constriction would lead to their relaxation. Juxtacrine signalling by Delta/Notch could underlie this signalling: *Delta* expressed in flanking vein cells activates Notch in adjacent provein cells (de Celis et al., 1997). This signalling could feed back to maintain the vein fate in the *Dl* expressing flanking cells (as occurs in lateral inhibition (Cornell and Eisen, 2005)). Thus the establishment of two cell

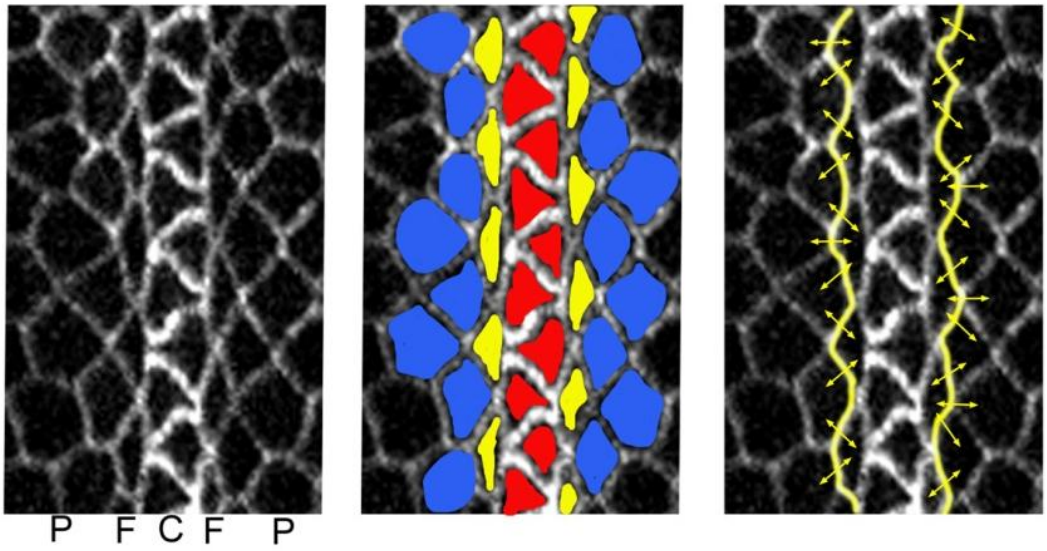

Figure 7.5. Interface signalling model for central cell relaxation. Left: ventral surface of L3, with three cell domains noted below: P = provein, F = flanking vein, C= central vein. Middle: colour coded cell types. Blue = provein, yellow = flanking, red = central. Right: interface between F and P cells shown in yellow, signalling across it shown as mutual arrows.

morphologies could arise from signalling across the boundary of vein and intervein cell types (Fig. 7.5). A potential additional input into the increase in central cell surface area would be the pulling force exerted by the flanking cells constricting on either side of the central cell, pulling the AJs apart. This would serve to reiterate how cell shape in an epithelium is dependent on the combination of internally and externally generated forces.

VIII. Outlook

The emergence of ordered form in developing tissues, a phenomenon of four dimensions that occurs remarkably robustly and repeatedly, is one of the most beguiling and challenging phenomena in biology. The developing fly wing provided us with the means to study this process at multiple levels, particularly with regard to the differentiation of cell types. The work described in this thesis has clarified numerous aspects of pupal wing development, a necessary task considering its widespread use as a model system for how intercellular signalling patterns epithelia, and uncovered novel signalling relationships and shape changes involved in wing construction. The widespread conservation at the levels of genes and proteins, their interactions and pathways, and cell and tissue architecture means that the data presented here are relevant to numerous other processes in animal development. The data presented here give insight into how one of the key components of the animal developmental toolkit, cell shape change, is utilised and controlled during morphogenesis. Furthermore, they provoke numerous questions for further research. For example, many of the models presented here predict the input of additional, as of yet unidentified factors in the process.

Bibliography

Affolter, M. and Basler, K. (2007) 'The Decapentaplegic morphogen gradient: from pattern formation to growth regulation', *Nature Reviews Genetics* 8(9): 663-674.

Aigouy, B., Farhadifar, R., Staple, D., Sagner, A., Roper, J., Julicher, F. and Eaton, S. (2010) 'Cell Flow Reorients the Axis of Planar Polarity in the Wing Epithelium of Drosophila', *Cell* 142(5): 773-786.

Aldaz, S., Escudero, L. and Freeman, M. (2010) 'Live imaging of Drosophila imaginal disc development', *Proceedings of the National Academy of Sciences of the United States of America* 107(32): 14217-14222.

Aman, A. and Piotrowski, T. (2010) 'Cell migration during morphogenesis', *Developmental Biology* 341(1): 20-33.

Amano, M., Ito, M., Kimura, K., Fukata, Y., Chihara, K., Nakano, T., Matsuura, Y. and Kaibuchi, K. (1996) 'Phosphorylation and activation of myosin by Rho-associated kinase (Rho-kinase)', *Journal of Biological Chemistry* 271(34): 20246-20249.

Ambrosio, A. L., Taelman, V. F., Lee, H. X., Metzinger, C. A., Coffinier, C. and De Robertis, E. M. (2008) 'Crossveinless-2 Is a BMP Feedback Inhibitor that Binds Chordin/BMP to Regulate Xenopus Embryonic Patterning', *Developmental Cell* 15(2): 248-260.

Arnold, J. W. (1964) 'Blood circulation in insect wings', *Memoirs of the Entomological Society of Canada* 38: 3-60.

Arora, K., Levine, M. S. and O'Connor, M. B. (1994) 'The screw gene encodes a ubiquitously expressed member of the TGF-Beta family required for specification of dorsal cell fates in the Drosophila embryo', *Genes & Development* 8(21): 2588-2601.

Bainbridge, S. P. and Bownes, M. (1981) 'Staging the Metamorphosis of Drosophila Melanogaster', *Journal of Embryology and Experimental Morphology* 66(DEC): 57-80.

Balemans, W. and Van Hul, W. (2002) 'Extracellular regulation of BMP signaling in vertebrates: A cocktail of modulators', *Developmental Biology* 250(2): 231-250.

Bangi, E. and Wharton, K. (2006) 'Dpp and Gbb exhibit different effective ranges in the establishment of the BMP activity gradient critical for Drosophila wing patterning', *Developmental Biology* 295(1): 178-193.

Barolo, S. and Posakony, J. (2002) 'Three habits of highly effective signaling pathways: principles of transcriptional control by developmental cell signaling', *Genes & Development* 16(10): 1167-1181.

Basler, K. and Struhl, G. (1994) 'Compartment boundaries and the control of Drosopfiffa limb pattern by hedgehog protein', *Nature* 368(6468): 208-214.

Bataille, L., Delon, I., Da Ponte, J., Brown, N. and Jagla, K. (2010) 'Downstream of Identity Genes: Muscle-Type-Specific Regulation of the Fusion Process', *Developmental Cell* 19(2): 317-328.

Baum, B. and Georgiou, M. (2011) 'Dynamics of adherens junctions in epithelial establishment, maintenance, and remodeling', *Journal of Cell Biology* 192(6): 907-917.

Belenkaya, T., Han, C., Yan, D., Opoka, R., Khodoun, M., Liu, H. and Lin, X. (2004) 'Drosophila Dpp morphogen movement is independent of dynamin-mediated endocytosis but regulated by the glypican members of heparan sulfate proteoglycans', *Cell* 119(2): 231-244.

Bement, W., Miller, A. and von Dassow, G. (2006) 'Rho GTPase activity zones and transient contractile arrays', *Bioessays* 28(10): 983-993.

Bernards, A. (2003) 'GAPs galore! A survey of putative Ras superfamily GTPase activating proteins in man and Drosophila', *Biochimica Et Biophysica Acta-Reviews on Cancer* 1603(2): 47-82.

Bernards, A. and Settleman, J. (2004) 'GAP control: regulating the regulators of small GTPases', *Trends in Cell Biology* 14(7): 377-385.

Bertet, C., Sulak, L. and Lecuit, T. (2004) 'Myosin-dependent junction remodelling controls planar cell intercalation and axis elongation', *Nature* 429(6992): 667-671.

Biehs, B., Sturtevant, M. and Bier, E. (1998) 'Boundaries in the Drosophila wing imaginal disc organize vein-specific genetic programs', *Development* 125(21): 4245-4257.

Bienz, M. (1997) 'Endoderm induction in Drosophila: the nuclear targets of the inducing signals - Commentary', *Current Opinion in Genetics & Development* 7(5): 683-688.

Binnerts, M. E., Wen, X., Canté-Barrett, K., Bright, J., Chen, H.-T., Asundi, V., Sattari, P., Tang, T., Boyle, B., Funk, W. et al. (2004) 'Human Crossveinless-2 is a novel inhibitor of bone morphogenetic proteins', *Biochemical and Biophysical Research Communications* 315(2): 272-280.

Blair, S. (2007) 'Wing vein Patterning in Drosophila and the analysis of intercellular signaling', *Annual Review of Cell and Developmental Biology* 23: 293-319.

Blair, S. S. (2003) 'Lineage compartments in Drosophila', *Current Biology* 13(14): R548-R551.

Bloor, J. and Kiehart, D. (2002) 'Drosophila RhoA regulates the cytoskeleton and cell-cell adhesion in the developing epidermis', *Development* 129(13): 3173-3183.

Bokel, C., Prokop, A. and Brown, N. (2005) 'Papillote and Piopio: Drosophila ZP-domain proteins required for cell adhesion to the apical extracellular matrix and microtubule organization', *Journal of Cell Science* 118(3): 633-642.

Brabant, M., Fristrom, D., Bunch, T. and Brower, D. (1996) 'Distinct spatial and temporal functions for PS integrins during Drosophila wing morphogenesis', *Development* 122(10): 3307-3317.

Brabant, M. C. and Brower, D. L. (1993) 'PS2 Integrin Requirements in Drosophila Embryo and Wing Morphogenesis', *Developmental Biology* 157(1): 49-59.

Brand, A. H. and Perrimon, N. (1993) 'Targeted gene expression as a means of altering cell fates and generating dominant phenotypes', *Development* 118(2): 401-415.

Bray, S. (2006) 'Notch signalling: a simple pathway becomes complex', *Nature Reviews Molecular Cell Biology* 7(9): 678-689.

Bridges, C. (1920) 'The mutant crossveinless in Drosophila melanogaster', *Proceedings of the National Academy of Sciences of the United States of America* 6: 660-663.

Brodu, V. and Casanova, J. (2006) 'The RhoGAP crossveinless-c links trachealess and EGFR signaling to cell shape remodeling in Drosophila tracheal invagination', *Genes & Development* 20(13): 1817-1828.

Brook, W. J., DiazBenjumea, F. J. and Cohen, S. M. (1996) 'Organizing spatial pattern in limb development', *Annual Review of Cell and Developmental Biology* 12: 161-180.

Brower, D., Bunch, T., Mukai, L., Adamson, T., Wehrli, M., Lam, S., Friedlander, E. and Roote, C. (1995) 'Nonequivalent requirements for PS1 and PS2 Integrin at cell attachments in Drosophila – genetic analysis of the Alpha(PS1) Integrin subunit', *Development* 121(5): 1311-1320.

Brower, D. and Jaffe, S. (1989) 'Requirement for Integrins during Drosophila wing development', *Nature* 342(6247): 285-287.

Brower, D., Wilcox, M., Piovant, M., Smith, R. and Reger, L. (1984) 'Related cell-surface antigens expressed with positional specificity in Drosophila imaginal disks', *Proceedings of the National Academy of Sciences of the United States of America-Biological Sciences* 81(23): 7485-7489.

Brown, N., Gregory, S. and Martin-Bermudo, Z. (2000) 'Integrins as mediators of morphogenesis in Drosophila', *Developmental Biology* 223(1): 1-16.

Brown, N. H. (2011) 'Extracellular Matrix in Development: Insights from Mechanisms Conserved between Invertebrates and Vertebrates', *Cold Spring Harbor Perspectives in Biology*.

Brummel, T. J., Twombly, V., Marques, G., Wrana, J. L., Newfeld, S. J., Attisano, L., Massague, J., Oconnor, M. B. and Gelbart, W. M. (1994) 'Characterization and relationship of Dpp receptors encoded by the *saxophone* and *thick veins* genes in Drosophila', *Cell* 78(2): 251-261.

Bryant, P. (1970) 'Cell lineage relationships in imaginal wing disc of Drosophila Melanogaster', *Developmental Biology* 22(3): 389-&.

Butler, L., Blanchard, G., Kabla, A., Lawrence, N., Welchman, D., Mahadevan, L., Adams, R. and Sanson, B. (2009) 'Cell shape changes indicate a role for extrinsic tensile forces in Drosophila germ-band extension', *Nature Cell Biology* 11(7): 859-U181.

Cagan, R. (2009) 'Principles of *Drosophila* eye differentiation', *Tissue Remodeling and Epithelial Morphogenesis* 89: 115-135.

Cano, A., Perez-Moreno, M., Rodrigo, I., Locascio, A., Blanco, M., del Barrio, M., Portillo, F. and Nieto, M. (2000) 'The transcription factor Snail controls epithelial-mesenchymal transitions by repressing E-cadherin expression', *Nature Cell Biology* 2(2): 76-83.

Carpenter, A., Jones, T., Lamprecht, M., Clarke, C., Kang, I., Friman, O., Guertin, D., Chang, J., Lindquist, R., Moffat, J. et al. (2006) 'CellProfiler: image analysis software for identifying and quantifying cell phenotypes', *Genome Biology* 7(10): -.

Chen, Y. and Struhl, G. (1996) 'Dual Roles for Patched in Sequestering and Transducing Hedgehog', *Cell* 87(3): 553-563.

Christoforou, C., Greer, C., Challoner, B., Charizanos, D. and Ray, R. (2008) 'The detached locus encodes Drosophila Dystrophin, which acts with other components of the Dystrophin Associated Protein Complex to influence intercellular signalling in developing wing veins', *Developmental Biology* 313(2): 519-532.

Chrzanowska-Wodnicka, M. and Burridge, K. (1996) 'Rho-stimulated contractility drives the formation of stress fibers and focal adhesions', *The Journal of Cell Biology* 133(6): 1403-1415.

Classen, A., Anderson, K., Marois, E. and Eaton, S. (2005) 'Hexagonal packing of Drosophila wing epithelial cells by the planar cell polarity pathway', *Developmental Cell* 9(6): 805-817.

Clifford, R. J. and Schupbach, T. (1989) 'Coordinately and differentially mutable activities of Torpedo, the *Drosophila melanogaster* homolog of the vertebrate EGF receptor gene', *Genetics* 123(4): 771-787.

Cohen, B., Simcox, A. and Cohen, S. (1993) 'Allocation of the thoracic imaginal primordia in the Drosophila embryo', *Development* 117(2): 597-608.

Cohen, M., Georgiou, M., Stevenson, N., Miodownik, M. and Baum, B. (2010) 'Dynamic Filopodia Transmit Intermittent Delta-Notch Signaling to Drive Pattern Refinement during Lateral Inhibition', *Developmental Cell* 19(1): 78-89.

Comstock, J. H. and Needham, J. G. (1899) 'The Wings of Insects.', *The American Naturalist* 33(395): 845-860.

Conley, C., Silburn, R., Singer, M., Ralston, A., Rohwer-Nutter, D., Olson, D., Gelbart, W. and Blair, S. (2000) 'Crossveinless 2 contains cysteine-rich domains and is required for high levels of BMP-like activity during the formation of the cross veins in Drosophila', *Development* 127(18): 3947-3959.

Cordero, J., Larson, D., Craig, C., Hays, R. and Cagan, R. (2007) 'Dynamic Decapentaplegic signaling regulates patterning and adhesion in the Drosophila pupal retina', *Development* 134(10): 1861-1871.

Cornell, R. A. and Eisen, J. S. (2005) 'Notch in the pathway: The roles of Notch signaling in neural crest development', *Seminars in Cell & Developmental Biology* 16(6): 663-672.

Corrigall, D., Walther, R., Rodriguez, L., Fichelson, P. and Pichaud, F. (2007) 'Hedgehog signaling is a principal inducer of myosin-II-driven cell ingression in Drosophila epithelia', *Developmental Cell* 13(5): 730-742.

Costa, M., Wilson, E. and Wieschaus, E. (1994) 'A putative cell signal encoded by the folded gastrulation gene coordinates cell-shape changes during Drosophila gastrulation', *Cell* 76(6): 1075-1089.

Crozatier, M., Glise, B. and Vincent, A. (2004) 'Patterns in evolution: veins of the Drosophila wing', *Trends in Genetics* 20(10): 498-505.

David, D., Tishkina, A. and Harris, T. (2010) 'The PAR complex regulates pulsed actomyosin contractions during amnioserosa apical constriction in Drosophila', *Development* 137(10): 1645-1655.

Dawes-Hoang, R., Parmar, K., Christiansen, A., Phelps, C., Brand, A. and Wieschaus, E. (2005) 'folded gastrulation, cell shape change and the control of myosin localization', *Development* 132(18): 4165-4178.

de Celis, J. (1997) 'Expression and function of decapentaplegic and thick veins during the differentiation of the veins in the Drosophila wing', *Development* 124(5): 1007-1018.

de Celis, J. (2003) 'Pattern formation in the Drosophila wing: the development of the veins', *Bioessays* 25(5): 443-451.

de Celis, J., Bray, S. and Garcia-Bellido, A. (1997) 'Notch signalling regulates veinlet expression and establishes boundaries between veins and interveins in the Drosophila wing', *Development* 124(10): 1919-1928.

del Álamo, D., Rouault, H. and Schweisguth, F. (2011) 'Mechanism and Significance of cis-Inhibition in Notch Signalling', *Current Biology* 21(1): R40-R47.

Delon, I. and Brown, N. (2007) 'Integrins and the actin cytoskeleton', *Current Opinion in Cell Biology* 19(1): 43-50.

Denholm, B., Brown, S., Ray, R., Ruiz-Gomez, M., Skaer, H. and Hombria, J. (2005) 'crossveinless-c is a RhoGAP required for actin reorganisation during morphogenesis', *Development* 132(10): 2389-2400.

Diaz-Benjumea, F. J. and Garcia-Bellido, A. (1990) 'Behaviour of Cells Mutant for an EGF Receptor Homologue of Drosophila in Genetic Mosaics', *Proceedings of The Royal Society B-Biological Sciences* 242(1303): 36-44.

Domingos, P. and Steller, H. (2007) 'Pathways regulating apoptosis during patterning and development', *Current Opinion in Genetics & Development* 17(4): 294-299.

Duffy, J. B. (2002) 'GAL4 system in drosophila: A fly geneticist's swiss army knife', *genesis* 34(1-2): 1-15.

Ehmsen, J., Poon, E. and Davies, K. (2002) 'The dystrophin-associated protein complex', *Journal of Cell Science* 115(14): 2801-2803.

Entchev, E., Schwabedissen, A. and Gonzalez-Gaitan, M. (2000) 'Gradient formation of the TGF-beta homolog Dpp', *Cell* 103(6): 981-991.

Escudero, L., Bischoff, M. and Freeman, M. (2007) 'Myosin II regulates complex cellular arrangement and epithelial architecture in drosophila', *Developmental Cell* 13(5): 717-729.

Etienne-Manneville, S. and Hall, A. (2002) 'Rho GTPases in cell biology', *Nature* 420(6916): 629-635.

Fanto, M., Weber, U., Strutt, D. I. and Mlodzik, M. (2000) 'Nuclear signaling by Rac and Rho GTPases is required in the establishment of epithelial planar polarity in the Drosophila eye', *Current Biology* 10(16): 979-988.

Fehon, R. G., Johansen, K., Rebay, I. and Artavanis-Tsakonas, S. (1991) 'Complex cellular and subcellular regulation of notch expression during embryonic and imaginal development of Drosophila: implications for notch function', *The Journal of Cell Biology* 113(3): 657-669.

Fernandes, I., Chanut-Delalande, H., Ferrer, P., Latapie, Y., Waltzer, L., Affolter, M., Payre, F. and Plaza, S. (2010) 'Zona Pellucida Domain Proteins Remodel the Apical Compartment for Localized Cell Shape Changes', *Developmental Cell* 18(1): 64-76.

Fernandez, B., Arias, A. and Jacinto, A. (2007) 'Dpp signalling orchestrates dorsal closure by regulating cell shape changes both in the amnioserosa and in the epidermis', *Mechanisms of Development* 124(11-12): 884-897.

Finelli, L., Xie, T., Bossie, C., Blackman, R. and Padgett, R. (1995) 'The *tolkin* gene is a Tolloid BMP-1 homolog that is essential for Drosophila development', *Genetics* 141(1): 271-281.

Franke, J., Montague, R. and Kiehart, D. (2010) 'Nonmuscle myosin II is required for cell proliferation, cell sheet adhesion and wing hair morphology during wing morphogenesis', *Developmental Biology* 345(2): 117-132.

Frasch, M. (1995) 'Induction of visceral and cardiac mesoderm by ectodermal Dpp in the early Drosophila embryo', *Nature* 374(6521): 464-467.

Fristrom, D. (1988) 'The cellular basis of epithelial morphogenesis - a review', *Tissue & Cell* 20(5): 645-690.

Fristrom, D. and Fristrom, J. (1993) The metamorphic development of the adult epidermis. in M. Bate and A. Martinez-Ariaz (eds.) *The Development of Drosophila melanogaster*. New York: Cold Spring Harbour Laboratory Press.

Fristrom, D., Gotwals, P., Eaton, S., Kornberg, T., Sturtevant, M., Bier, E. and Fristrom, J. (1994) 'Blistered - a gene required for vein/intervein formation in wings of Drosophila', *Development* 120(9): 2661-2671.

Fristrom, D., Wilcox, M. and Fristrom, J. (1993) 'The distribution of PS Integrins, Laminin-A and F-Actin during key stages in Drosophila wing development', *Development* 117(2): 509-523.

Fritsch, C., Lanfear, R. and Ray, R. (2010) 'Rapid evolution of a novel signalling mechanism by concerted duplication and divergence of a BMP ligand and its extracellular modulators', *Development Genes and Evolution* 220(9-10): 235-250.

Garcia-Bellido, A. (1975) 'Genetic control of wing disc development in *Drosophila*', *Ciba Foundation symposium.* 0: 161-182.

Garcia-Bellido, A. (1977) 'Inductive mechanisms in process of wing vein formation in Drosophila', *Wilhelm Rouxs Archives of Developmental Biology* 182(2): 93-106.

Garcia-Bellido, A. and de Celis, J. (1992) 'Developmental genetics of the venation pattern of Drosophila', *Annual Review of Genetics* 26: 277-304.

Garcia-Bellido, A. and Santamaria, P. (1972) 'Developmental analysis of wing disk in mutant engrailed of Drosophila melanogaster', *Genetics* 72(1): 87-&.

Garcia-Mata, R., Boulter, E. and Burridge, K. (2011) 'The 'invisible hand': regulation of RHO GTPases by RHOGDIs', *Nature Reviews Molecular Cell Biology* 12(8): 493-504.

Genova, J., Jong, S., Camp, J. and Fehon, R. (2000) 'Functional analysis of Cdc42 in actin filament assembly, epithelial morphogenesis, and cell signaling during Drosophila development', *Developmental Biology* 221(1): 181-194.

Gervais, L. and Casanova, J. (2010) 'In Vivo Coupling of Cell Elongation and Lumen Formation in a Single Cell', *Current Biology* 20(4): 359-366.

Ghabrial, A., Levi, B. and Krasnow, M. (2011) 'A Systematic Screen for Tube Morphogenesis and Branching Genes in the Drosophila Tracheal System', *Plos Genetics* 7(7): -.

Gibson, M., Lehman, D. and Schubiger, G. (2002) 'Lumenal transmission of decapentaplegic in Drosophila imaginal discs', *Developmental Cell* 3(3): 451-460.

Gibson, W. and Gibson, M. (2009) 'Cell Topology, Geometry, and Morphogenesis In Proliferating Epithelia.', *Tissue Remodeling and Epithelial Morphogenesis* 89: 87-114.

Gilbert, S. F. (2006) *Developmental biology*, Sunderland, Mass.: Sinauer Associates ; Basingstoke : Palgrave [distributor].

Gonzales-Gaitain, M., Capdevila, M. and Garcia-Bellido, A. (1994) 'Cell proliferation patterns in the wing imaginal disc of Drosophila', *Mechanisms of Development* 46(3): 183-200.

Grosse, A. S., Pressprich, M. F., Curley, L. B., Hamilton, K. L., Margolis, B., Hildebrand, J. D. and Gumucio, D. L. (2011) 'Cell dynamics in fetal intestinal epithelium: implications for intestinal growth and morphogenesis', *Development* 138(20): 4423-4432.

Guichard, A., Biehs, B., Sturtevant, M., Wickline, L., Chacko, J., Howard, K. and Bier, E. (1999) 'rhomboid and Star interact synergistically to promote EGFR MAPK signaling during Drosophila wing vein development', *Development* 126(12): 2663-2676.

Gumbiner, B. (1996) 'Cell adhesion: The molecular basis of tissue architecture and morphogenesis', *Cell* 84(3): 345-357.

Gumbiner, B. (2005) 'Regulation of cadherin-mediated adhesion in morphogenesis', *Nature Reviews Molecular Cell Biology* 6(8): 622-634.

Gurdon, J. (1987) 'Embryonic induction - molecular prospects', *Development* 99(3): 285-306.

Haerry, T. E., Khalsa, O., O'Connor, M. B. and Wharton, K. A. (1998) 'Synergistic signaling by two BMP ligands through the SAX and TKV receptors controls wing growth and patterning in Drosophila', *Development* 125(20): 3977-3987.

Haigo, S., Hildebrand, J., Harland, R. and Wallingford, J. (2003) 'Shroom induces apical constriction and is required for hingepoint formation during neural tube closure', *Current Biology* 13(24): 2125-2137.

Hall, A. (1998) 'Rho GTPases and the actin cytoskeleton', *Science* 279(5350): 509-514.

Han, C., Belenkaya, T., Wang, B. and Lin, X. (2004) 'Drosophila glypicans control the cell-to-cell movement of Hedgehog by a dynamin-independent process', *Development* 131(3): 601-611.

Han, C., Yan, D., Belenkaya, T. and Lin, X. (2005) 'Drosophila glypicans Dally and Dally-like shape the extracellular Wingless morphogen gradient in the wing disc', *Development* 132(4): 667-679.

Hardin, J. and Walston, T. (2004) 'Models of morphogenesis: the mechanisms and mechanics of cell rearrangement', *Current Opinion in Genetics & Development* 14(4): 399-406.

He, L., Wang, X. B., Tang, H. L. and Montell, D. J. (2010) 'Tissue elongation requires oscillating contractions of a basal actomyosin network', *Nature Cell Biology* 12(12): 1133-U40.

Healy, K., Hodgson, L., Kim, T., Shutes, A., Maddileti, S., Juliano, R., Hahn, K., Harden, T., Bang, Y. and Der, C. (2008) 'DLC-1 suppresses non-small cell lung cancer growth and invasion by RhoGAP-dependent and independent mechanisms', *Molecular Carcinogenesis* 47(5): 326-337.

Hildebrand, J. (2005) 'Shroom regulates epithelial cell shape via the apical positioning of an actomyosin network', *Journal of Cell Science* 118(22): 5191-5203.

Hogan, B. and Kolodziej, P. (2002) 'Molecular mechanisms of tubulogenesis', *Nature Reviews Genetics* 3(7): 513-523.

Homem, C. and Peifer, M. (2008) 'Diaphanous regulates myosin and adherens junctions to control cell contractility and protrusive behavior during morphogenesis', *Development* 135(6): 1005-1018.

Huppert, S., Jacobsen, T. and Muskavitch, M. (1997) 'Feedback regulation is central to Delta-Notch signalling required for Drosophila wing vein morphogenesis', *Development* 124(17): 3283-3291.

Hynes, R. (2009) 'The Extracellular Matrix: Not Just Pretty Fibrils', *Science* 326(5957): 1216-1219.

Jaffe, A. B. and Hall, A. (2005) 'RhoGTPases: Biochemistry and Biology', *Annual Review of Cell and Developmental Biology* 21: 247-269.

Johnson, S. and Milner, M. (1987) 'The final stages of wing development in *Drosophila melanogaster*', *Tissue & Cell* 19(4): 505-513.

Kamiya, Y., Miyazono, K. and Miyazawa, K. (2008) 'Specificity of the inhibitory effects of Dad on TGF-beta family type I receptors, Thickveins, Saxophone, and Baboon in Drosophila', *Febs Letters* 582(17): 2496-2500.

Kasza, K. and Zallen, J. (2011) 'Dynamics and regulation of contractile actin-myosin networks in morphogenesis', *Current Opinion in Cell Biology* 23(1): 30-38.

Kiehart, D., Galbraith, C., Edwards, K., Rickoll, W. and Montague, R. (2000) 'Multiple forces contribute to cell sheet morphogenesis for dorsal closure in Drosophila', *Journal of Cell Biology* 149(2): 471-490.

Kim, T., Vigil, D., Der, C. and Juliano, R. (2009) 'Role of DLC-1, a tumor suppressor protein with RhoGAP activity, in regulation of the cytoskeleton and cell motility', *Cancer and Metastasis Reviews* 28(1-2): 77-83.

Kimura, K., Ito, M., Amano, M., Chihara, K., Fukata, Y., Nakafuku, M., Yamamori, B., Feng, J., Nakano, T., Okawa, K. et al. (1996) 'Regulation of myosin phosphatase by Rho and Rho-Associated kinase (Rho-kinase)', *Science* 273(5272): 245-248.

Kinoshita, N., Sasai, N., Misaki, K. and Yonemura, S. (2008) 'Apical accumulation of rho in the neural plate is important for neural plate cell shape change and neural tube formation', *Molecular Biology of the Cell* 19(5): 2289-2299.

Klingenberg, C. (2010) 'Evolution and development of shape: integrating quantitative approaches', *Nature Reviews Genetics* 11(9): 623-635.

Kolsch, V., Seher, T., Fernandez-Ballester, G., Serrano, L. and Leptin, M. (2007) 'Control of Drosophila gastrulation by apical localization of adherens junctions and RhoGEF2', *Science* 315(5810): 384-386.

Lahoz, A. and Hall, A. (2008) 'DLC1: a significant GAP in the cancer genome', *Genes & Development* 22(13): 1724-1730.

Larsen, E. and McLaughlin, H. (1987) 'The morphogenetic alphabet - lessons for simple-minded genes', *Bioessays* 7(3): 130-132.

Lecuit, T. and Cohen, S. (1998) 'Dpp receptor levels contribute to shaping the Dpp morphogen gradient in the Drosophila wing imaginal disc', *Development* 125(24): 4901-4907.

Lecuit, T. and Le Goff, L. (2007) 'Orchestrating size and shape during morphogenesis', *Nature* 450(7167): 189-192.

Lecuit, T. and Lenne, P. (2007) 'Cell surface mechanics and the control of cell shape, tissue patterns and morphogenesis', *Nature Reviews Molecular Cell Biology* 8(8): 633-644.

Lee, J. and Harland, R. (2007) 'Actomyosin contractility and microtubules drive apical constriction in Xenopus bottle cells', *Developmental Biology* 311(1): 40-52.

Levayer, R., Pelissier-Monier, A. and Lecuit, T. (2011) 'Spatial regulation of Dia and Myosin-II by RhoGEF2 controls initiation of E-cadherin endocytosis during epithelial morphogenesis', *Nature Cell Biology* 13(5): 529-U83.

Li, G., Du, X., Vass, W. C., Papageorge, A. G., Lowy, D. R. and Qian, X. (2011) 'Full activity of the deleted in liver cancer 1 (DLC1) tumor suppressor depends on an LD-like motif that binds talin and focal adhesion kinase (FAK)', *Proceedings of the National Academy of Sciences* 108(41): 17129-17134.

Lindsley, D. L. and Zimm, G. G. (1992) *The genome of drosophila melanogaster*: Academic.

Little, S. and Mullins, M. (2009) 'Bone morphogenetic protein heterodimers assemble heteromeric type I receptor complexes to pattern the dorsoventral axis', *Nature Cell Biology* 11(5): 637-U439.

Llimargas, M. and Casanova, J. (2010) 'Apical constriction and invagination: A very self-reliant couple', *Developmental Biology* 344(1): 4-6.

Lovegrove, B., Simoes, S., Rivas, M., SotilloS, S., Johnson, K., Knust, E., Jacinto, A. and Hombria, J. (2006) 'Coordinated control of cell adhesion, polarity, and cytoskeleton underlies Hox-induced organogenesis in Drosophila', *Current Biology* 16(22): 2206-2216.

Lubarsky, B. and Krasnow, M. (2003) 'Tube morphogenesis: Making and shaping biological tubes', *Cell* 112(1): 19-28.

Lunde, K., Biehs, B., Nauber, U. and Bier, E. (1998) 'The knirps and knirps-related genes organize development of the second wing vein in Drosophila', *Development* 125(21): 4145-4154.

Lunde, K., Trimble, J., Guichard, A., Guss, K., Nauber, U. and Bier, E. (2003) 'Activation of the knirps locus links patterning to morphogenesis of the second wing vein in Drosophila', *Development* 130(2): 235-248.

Marcus, J. (2001) 'The development and evolution of crossveins in insect wings', *Journal of Anatomy* 199: 211-216.

Martin, A., Kaschube, M. and Wieschaus, E. (2009) 'Pulsed contractions of an actin-myosin network drive apical constriction', *Nature* 457(7228): 495-U11.

Martin, D., Zusman, S., Li, X., Williams, E., Khare, N., DaRocha, S., Chiquet-Ehrismann, R. and Baumgartner, S. (1999) 'wing blister, a new Drosophila laminin alpha chain required for cell adhesion and migration during embryonic and imaginal development', *Journal of Cell Biology* 145(1): 191-201.

Martin-Blanco, E., Roch, F., Noll, E., Baonza, A., Duffy, J. B. and Perrimon, N. (1999) 'A temporal switch in DER signaling controls the specification and differentiation of veins and interveins in the Drosophila wing', *Development* 126(24): 5739-5747.

Martín, F. A., Herrera, S. C. and Morata, G. (2009) 'Cell competition, growth and size control in the Drosophila wing imaginal disc', *Development* 136(22): 3747-3756.

Massague, J. and Chen, Y. (2000) 'Controlling TGF-beta signaling', *Genes & Development* 14(6): 627-644.

Masucci, J., Miltenberger, R. and Hoffmann, F. (1990) 'Pattern-specific expression of the drosophila *decapentaplegic* gene in imaginal disks is regulated by 3' cis-regulatory elements', *Genes & Development* 4(11): 2011-2023.

McGuire, S. E., Le, P. T., Osborn, A. J., Matsumoto, K. and Davis, R. L. (2003) 'Spatiotemporal Rescue of Memory Dysfunction in Drosophila', *Science* 302(5651): 1765-1768.

Miano, J., Long, X. and Fujiwara, K. (2007) 'Serum response factor: master regulator of the actin cytoskeleton and contractile apparatus', *American Journal of Physiology-Cell Physiology* 292(1): C70-C81.

Milan, M., Baonza, A. and GarciaBellido, A. (1997) 'Wing surface interactions in venation patterning in Drosophila', *Mechanisms of Development* 67(2): 203-213.

Mitchell, H., Roach, J. and Petersen, N. (1983) 'The morphogenesis of cell hairs on Drosophila wings', *Developmental Biology* 95(2): 387-398.

Mizuno, T., Amano, M., Kaibuchi, K. and Nishida, Y. (1999) 'Identification and characterization of Drosophila homolog of Rho-kinase', *Gene* 238(2): 437-444.

Montagne, J., Groppe, J., Guillemin, K., Krasnow, M., Gehring, W. and Affolter, M. (1996) 'The Drosophila Serum Response Factor gene is required for the formation of intervein tissue of the wing and is allelic to blistered', *Development* 122(9): 2589-2597.

Morata, G. and Ripoll, P. (1975) 'Minutes: mutant of *Drosophila* autonomously affecting cell division rate', *Developmental Biology* 42(2): 211-221.

Morin, X., Daneman, R., Zavortink, M. and Chia, W. (2001) 'A protein trap strategy to detect GFP-tagged proteins expressed from their endogenous loci in Drosophila', *Proceedings of the National Academy of Sciences of the United States of America* 98(26): 15050-15055.

Moustakas, A. and Heldin, C. (2005) 'Non-Smad TGF-beta signals', *Journal of Cell Science* 118(16): 3573-3584.

Murray, M., Fessler, L. and Palka, J. (1995) 'Changing distributions of extracellular matrix components during early wing morphogenesis in Drosophila', *Developmental Biology* 168(1): 150-165.

Murray, M., Schubiger, M. and Palka, J. (1984) 'Neuron differentiation and axon growth in the developing wing of *Drosophila melanogaster*', *Developmental Biology* 104(2): 259-273.

Nardi, J. and Ujhelyi, E. (2001) 'Transformations of epithelial monolayers during wing development of Manduca sexta', *Arthropod Structure & Development* 30(2): 145-157.

Nellen, D., Burke, R., Struhl, G. and Basler, K. (1996) 'Direct and long-range action of a DPP morphogen gradient', *Cell* 85(3): 357-368.

Nir, O., Bakal, C., Perrimon, N. and Berger, B. (2010) 'Inference of RhoGAP/GTPase regulation using single-cell morphological data from a combinatorial RNAi screen', *Genome Research* 20(3): 372-380.

Nobes, C. and Hall, A. (1995) 'Rho, Rac, and Cdc42 GTPases regulate the assembly of multimolecular focal complexes associated with Actin stress fibers, lamellipodia, and filopodia', *Cell* 81(1): 53-62.

Nussbaumer, U., Halder, G., Groppe, J., Affolter, M. and Montagne, J. (2000) 'Expression of the blistered/DSRF gene is controlled by different morphogens during Drosophila trachea and wing development', *Mechanisms of Development* 96(1): 27-36.

O'Connor, M., Umulis, D., Othmer, H. and Blair, S. (2006) 'Shaping BMP morphogen gradients in the Drosophila embryo and pupal wing', *Development* 133(2): 183-193.

O'Keefe, D., Prober, D., Moyle, P., Rickoll, W. and Edgar, B. (2007) 'Egfr/Ras signaling regulates DE-cadherin/shotgun localization to control vein morphogenesis in the Drosophila wing', *Developmental Biology* 311(1): 25-39.

O'Keefe, D. and Thomas, J. (2001) 'Drosophila wing development in the absence of dorsal identity', *Development* 128(5): 703-710.

Oda, H. and Tsukita, S. (2001) 'Real-time imaging of cell-cell adherens junctions reveals that Drosophila mesoderm invagination begins with two phases of apical constriction of cells', *Journal of Cell Science* 114(3): 493-501.

Olson, E. and Nordheim, A. (2010) 'Linking actin dynamics and gene transcription to drive cellular motile functions', *Nature Reviews Molecular Cell Biology* 11(5): 353-365.

Ozdamar, B., Bose, R., Barrios-Rodiles, M., Wang, H., Zhang, Y. and Wrana, J. (2005) 'Regulation of the polarity protein Par6 by TGF beta receptors controls epithelial cell plasticity', *Science* 307(5715): 1603-1609.

Pallavi, S. K. and Shashidhara, L. S. (2005) 'Signaling interactions between squamous and columnar epithelia of the Drosophila wing disc', *Journal of Cell Science* 118(15): 3363-3370.

Paluch, E. and Heisenberg, C. (2009) 'Biology and Physics of Cell Shape Changes in Development', *Current Biology* 19(17): R790-R799.

Paralkar, V. M., Nandedkar, A. K., Pointer, R. H., Kleinman, H. K. and Reddi, A. H. (1990) 'Interaction of osteogenin, a heparin binding bone morphogenetic protein, with type IV collagen', *Journal of Biological Chemistry* 265(28): 17281-17284.

Paralkar, V. M., Weeks, B. S., Yu, Y. M., Kleinman, H. K. and Reddi, A. H. (1992) 'Recombinant human bone morphogenetic protein 2B stimulates PC12 cell differentiation: potentiation and binding to type IV collagen', *The Journal of Cell Biology* 119(6): 1721-1728.

Pastor-Pareja, J., Grawe, F., Martin-Blanco, E. and Garcia-Bellido, A. (2004) 'Invasive cell behavior during Drosophila imaginal disc eversion is mediated by the JNK signaling cascade', *Developmental Cell* 7(3): 387-399.

Pastor-Pareja, J. C. and Xu, T. (2011) 'Shaping Cells and Organs in Drosophila by Opposing Roles of Fat Body-Secreted Collagen IV and Perlecan', *Developmental Cell* 21: 245-256.

Phelps, C. B. and Brand, A. H. (1998) 'Ectopic gene expression in Drosophila using GAL4 system', *Methods-a Companion to Methods in Enzymology* 14(4): 367-379.

Piekny, A., Werner, M. and Glotzer, M. (2005) 'Cytokinesis: welcome to the Rho zone', *Trends in Cell Biology* 15(12): 651-658.

Pilgram, G., Potikanond, S., van der Plas, M., Fradkin, L. and Noordermeer, J. (2011) 'The RhoGAP crossveinless-c Interacts with Dystrophin and Is Required for Synaptic Homeostasis at the Drosophila Neuromuscular Junction', *Journal of Neuroscience* 31(2): 492-500.

Plageman, T., Chauhan, B., Yang, C., Jaudon, F., Shang, X., Zheng, Y., Lou, M., Debant, A., Hildebrand, J. and Lang, R. (2011) 'A Trio-RhoA-Shroom3 pathway is required for apical constriction and epithelial invagination', *Development* 138(23): 5177-5188.

Pollard, T. and Cooper, J. (2009) 'Actin, a Central Player in Cell Shape and Movement', *Science* 326(5957): 1208-1212.

Posern, G. and Treisman, R. (2006) 'Actin' together: serum response factor, its cofactors and the link to signal transduction', *Trends in Cell Biology* 16(11): 588-596.

Pradel, J. and White, R. (1998) 'From selectors to realizators', *International Journal of Developmental Biology* 42(3): 417-421.

Prout, M., Damania, Z., Soong, J., Fristrom, D. and Fristrom, J. (1997) 'Autosomal mutations affecting adhesion between wing surfaces in Drosophila melanogaster', *Genetics* 146(1): 275-285.

Qian, X., Li, G., Asmussen, H., Asnaghi, L., Vass, W., Braverman, R., Yamada, K., Popescu, N., Papageorge, A. and Lowy, D. (2007) 'Oncogenic inhibition by a deleted in liver cancer gene requires cooperation between tensin binding and Rho-specific GTPase-activating protein activities', *Proceedings of the National Academy of Sciences of the United States of America* 104(21): 9012-9017.

Raftery, L. A. and Sutherland, D. J. (1999) 'TGF-β Family Signal Transduction in Drosophila Development: From Mad to Smads', *Developmental Biology* 210(2): 251-268.

Ralston, A. and Blair, S. (2005) 'Long-range Dpp signaling is regulated to restrict BMP signaling to a crossvein competent zone', *Developmental Biology* 280(1): 187-200.

Ramirez-Weber, F. and Kornberg, T. (1999) 'Cytonemes: Cellular processes that project to the principal signaling center in Drosophila imaginal discs', *Cell* 97(5): 599-607.

Rauzi, M. and Lenne, P. F. (2011) 'Cortical forces in cell shape changes and tissue morphogenesis', *Forces and Tension in Development* 95: 93-144.

Ray, R. and Wharton, K. (2001) 'Context-dependent relationships between the BMPs gbb and dpp during development of the Drosophila wing imaginal disk', *Development* 128(20): 3913-3925.

Rebay, I., Fehon, R. and Artavanis-Tsakonas, S. (1993) 'Specific truncations of Drosophila Notch define dominant-activated and dominant-negative forms of the receptor', *Cell* 74(2): 319-329.

Ridley, A. (2011) 'Life at the Leading Edge', *Cell* 145(7): 1012-1022.

Ridley, A. and Hall, A. (1992) 'The small GTP-binding protein Rho regulates the assembly of focal adhesions and Actin stress fibers in response to growth-factors', *Cell* 70(3): 389-399.

Ridley, A., Schwartz, M., Burridge, K., Firtel, R., Ginsberg, M., Borisy, G., Parsons, J. and Horwitz, A. (2003) 'Cell migration: Integrating signals from front to back', *Science* 302(5651): 1704-1709.

Roch, F., Alonso, C. and Akam, M. (2003) 'Drosophila miniature and dusky encode ZP proteins required for cytoskeletal reorganisation during wing morphogenesis', *Journal of Cell Science* 116(7): 1199-1207.

Roch, F., Baonza, A., Martin-Blanco, E. and Garcia-Bellido, A. (1998) 'Genetic interactions and cell behaviour in blistered mutants during proliferation and differentiation of the Drosophila wing', *Development* 125(10): 1823-1832.

Rorth, P. (2003) 'Communication by touch: Role of cellular extensions in complex animals', *Cell* 112(5): 595-598.

Ross, J. J., Shimmi, O., Vilmos, P., Petryk, A., Kim, H., Gaudenz, K., Hermanson, S., Ekker, S. C., O'Connor, M. B. and Marsh, J. L. (2001) 'Twisted gastrulation is a conserved extracellular BMP antagonist', *Nature* 410(6827): 479-483.

Roy, S., Hsiung, F. and Kornberg, T. (2011) 'Specificity of Drosophila Cytonemes for Distinct Signaling Pathways', *Science* 332(6027): 354-358.

Rozario, T. and DeSimone, D. (2010) 'The extracellular matrix in development and morphogenesis: A dynamic view', *Developmental Biology* 341(1): 126-140.

Sato, D., Sugimura, K., Satoh, D. and Uemura, T. (2010) 'Crossveinless-c, the Drosophila homolog of tumor suppressor DLC1, regulates directional elongation of dendritic branches via down-regulating Rho1 activity', *Genes To Cells* 15(5): 485-500.

Sawyer, J., Harrell, J., Shemer, G., Sullivan-Brown, J., Roh-Johnson, M. and Goldstein, B. (2010) 'Apical constriction: A cell shape change that can drive morphogenesis', *Developmental Biology* 341(1): 5-19.

Schatz, E. (1951) 'Uber die Formbildung der Flugel bei Hitzenmodifikationen und Mutationen von Drosophila melanogaster', *Biologisches Zentralblatt* 70: 305-353.

Schmidt, A. and Hall, A. (2002) 'Guanine nucleotide exchange factors for Rho GTPases: turning on the switch', *Genes & Development* 16(13): 1587-1609.

Schock, F. and Perrimon, N. (2002) 'Molecular mechanisms of epithelial morphogenesis', *Annual Review of Cell and Developmental Biology* 18: 463-493.

Schoenwaelder, S. M. and Burridge, K. (1999) 'Bidirectional signaling between the cytoskeleton and integrins', *Current Opinion in Cell Biology* 11(2): 274-286.

Schubiger, M. and Palka, J. (1987) 'Changing spatial patterns of DNA replication in the developing wing of Drosophila', *Developmental Biology* 123(1): 145-153.

Sebbagh, M., Renvoize, C., Hamelin, J., Riche, N., Bertoglio, J. and Breard, J. (2001) 'Caspase-3-mediated cleavage of ROCK I induces MLC phosphorylation and apoptotic membrane blebbing', *Nat Cell Biol* 3(4): 346-352.

Serpe, M., Ralston, A., Blair, S. and O'Connor, M. (2005) 'Matching catalytic activity to developmental function: Tolloid-related processes Sog in order to help specify the posterior crossvein in the Drosophila wing', *Development* 132(11): 2645-2656.

Serpe, M., Umulis, D., Ralston, A., Chen, J., Olson, D., Avanesov, A., Othmer, H., O'Connor, M. and Blair, S. (2008) 'The BMP-binding protein Crossveinless 2 is a short-range, concentration-dependent, biphasic modulator of BMP signaling in Drosophila', *Developmental Cell* 14(6): 940-953.

Shellenbarger, D. and Mohler, J. (1978) 'Temperature sensitive periods and autonomy of pleiotropic effects of l(1)N^{ts}1, a conditional Notch lethal in Drosophila', *Developmental Biology* 62(2): 432-446.

Sherrard, K., Robin, F., Lemaire, P. and Munro, E. (2010) 'Sequential Activation of Apical and Basolateral Contractility Drives Ascidian Endoderm Invagination', *Current Biology* 20(17): 1499-1510.

Shevtsova, E., Hansson, C., Janzen, D. and Kjaerandsen, J. (2011) 'Stable structural color patterns displayed on transparent insect wings', *Proceedings of the National Academy of Sciences of the United States of America* 108(2): 668-673.

Shilo, B. (2005) 'Regulating the dynamics of EGF receptor signaling in space and time', *Development* 132(18): 4017-4027.

Shimmi, O., Ralston, A., Blair, S. and O'Connor, M. (2005a) 'The crossveinless gene encodes a new member of the Twisted gastrulation family of BMP-binding proteins which, with Short gastrulation, promotes BMP signaling in the crossveins of the Drosophila wing', *Developmental Biology* 282(1): 70-83.

Shimmi, O., Umulis, D., Othmer, H. and O'Connor, M. (2005b) 'Facilitated transport of a Dpp/Scw heterodimer by Sog/Tsg leads to robust patterning of the Drosophila blastoderm embryo', *Cell* 120(6): 873-886.

Simoes, S., Denholm, B., Azevedo, D., Sotillos, S., Martin, P., Skaer, H., Hombria, J. and Jacinto, A. (2006) 'Compartmentalisation of Rho regulators directs cell invagination during tissue morphogenesis', *Development* 133(21): 4257-4267.

Solon, J., Kaya-Copur, A., Colombelli, J. and Brunner, D. (2009) 'Pulsed Forces Timed by a Ratchet-like Mechanism Drive Directed Tissue Movement during Dorsal Closure', *Cell* 137(7): 1331-1342.

Sotillos, S. and de Celis, J. (2005) 'Interactions between the notch, EGFR, and decapentaplegic signaling pathways regulate vein differentiation during Drosophila pupal wing development', *Developmental Dynamics* 232(3): 738-752.

Speck, O., Hughes, S., Noren, N., Kulikauskas, R. and Fehon, R. (2003) 'Moesin functions antagonistically to the Rho pathway to maintain epithelial integrity', *Nature* 421(6918): 83-87.

Stark, J., Bonacum, J., Remsen, J. and DeSalle, R. (1999) 'The evolution and development of dipteran wing veins: A systematic approach', *Annual Review of Entomology* 44: 97-129.

Stocker, R. (1994) 'The organization of the chemosensory system in Drosophila melanogaster - a review', *Cell and Tissue Research* 275(1): 3-26.

Struhl, G. and Basler, K. (1993) 'Organizing activity of Wingless protein in Drosophila', *Cell* 72(4): 527-540.

Sturtevant, M., Roark, M. and Bier, E. (1993) 'The *Drosophila rhomboid* gene mediates the localized formation of wing veins and interacts genetically with components of the EGF-R signaling pathway', *Genes & Development* 7(6): 961-973.

Sun, Q., Chen, G., Streb, J. W., Long, X. C., Yang, Y. M., Stoeckert, C. J. and Miano, J. M. (2006) 'Defining the mammalian CArGome', *Genome Research* 16(2): 197-207.

Suzuki, A., Kaneko, E., Maeda, J. and Ueno, N. (1997) 'Mesoderm induction by BMP-4 and -7 heterodimers', *Biochemical and Biophysical Research Communications* 232(1): 153-156.

Sweeton, D., Parks, S., Costa, M. and Wieschaus, E. (1991) 'Gastrulation in Drosophila - the formation of the ventral furrow and posterior midgut invaginations', *Development* 112(3): 775-789.

Szuperak, M., Salah, S., Meyer, E., Nagarajan, U., Ikmi, A. and Gibson, M. (2011) 'Feedback regulation of Drosophila BMP signaling by the novel extracellular protein Larval Translucida', *Development* 138(4): 715-724.

Szuts, D., Eresh, S. and Bienz, M. (1998) 'Functional intertwining of Dpp and EGFR signaling during Drosophila endoderm induction', *Genes & Development* 12(13): 2022-2035.

Tanimoto, H., Itoh, S., ten Dijke, P. and Tabata, T. (2000) 'Hedgehog creates a gradient of DPP activity in Drosophila wing imaginal discs', *Molecular Cell* 5(1): 59-71.

Teleman, A. and Cohen, S. (2000) 'Dpp gradient formation in the Drosophila wing imaginal disc', *Cell* 103(6): 971-980.

Tepass, U. and Tanentzapf, G. (2001) 'Epithelial cell polarity and cell junctions in Drosophila', *Annual Review of Genetics* 35: 747-784.

Terracol, R. and Lengyel, J. (1994) 'The *thickveins* gene of Drosophila is required for dorsoventral polarity of the embryo', *Genetics* 138(1): 165-178.

Theriault, B., Shepherd, T., Mujoomdar, M. and Nachtigal, M. (2007) 'BMP4 induces EMT and Rho GTPase activation in human ovarian cancer cells', *Carcinogenesis* 28(6): 1153-1162.

Togel, M., Pass, G. and Paululat, A. (2008) 'The Drosophila wing hearts originate from pericardial cells and are essential for wing maturation', *Developmental Biology* 318(1): 29-37.

Tsuneizumi, K., Nakayama, T., Kamoshida, Y., Kornberg, T., Christian, J. and Tabata, T. (1997) 'Daughters against dpp modulates dpp organizing activity in Drosophila wing development', *Nature* 389(6651): 627-631.

Urban, S., Lee, J. and Freeman, M. (2001) 'Drosophila Rhomboid-1 defines a family of putative intramembrane serine proteases', *Cell* 107(2): 173-182.

Urbano, J., Torgler, C., Molnar, C., Tepass, U., Lopez-Varea, A., Brown, N., de Celis, J. and Martin-Bermudo, M. (2009) 'Drosophila laminins act as key regulators of basement membrane assembly and morphogenesis', *Development* 136(24): 4165-4176.

van der Plas, M. C., Pilgram, G. S. K., de Jong, A. W. M., Bansraj, M. R. K. S., Fradkin, L. G. and Noordermeer, J. N. (2007) 'Drosophila Dystrophin is required for integrity of the musculature', *Mechanisms of Development* 124(7-8): 617-630.

Verdier, V., Guang-Chao-Chen and Settleman, J. (2006) 'Rho-kinase regulates tissue morphogenesis via non-muscle myosin and LIM-kinase during Drosophila development', *Bmc Developmental Biology* 6: -.

Vicente-Manzanares, M., Ma, X., Adelstein, R. and Horwitz, A. (2009) 'Non-muscle myosin II takes centre stage in cell adhesion and migration', *Nature Reviews Molecular Cell Biology* 10(11): 778-790.

Vilmos, P., Sousa-Neves, R., Lukacsovich, T. and Marsh, J. (2005) 'crossveinless defines a new family of Twisted-gastrulation-like modulators of bone morphogenetic protein signalling', *Embo Reports* 6(3): 262-267.

Vivekanand, P. and Rebay, I. (2006) 'Intersection of signal transduction pathways and development', *Annual Review of Genetics* 40: 139-157.

Voigt, A., Pflanz, R., Schäfer, U. and Jäckle, H. (2002) 'Perlecan participates in proliferation activation of quiescent Drosophila neuroblasts', *Developmental Dynamics* 224(4): 403-412.

Waddington, C. H. (1941) 'The genetic control of wing development in Drosophila', *Journal of Genetics* 41: 75-139.

Waddington, C. H. (1957) *The Strategy of the Genes. A Discussion of some Aspects of Theoretical Biology.*, London: Allen and Unwin.

Waldron, I. (1964) 'Courtship sound production in two sympatric sibling Drosophila species', *Science* 144(361): 191-&.

Wang, X., Harris, R., Bayston, L. and Ashe, H. (2008) 'Type IV collagens regulate BMP signalling in Drosophila', *Nature* 455(7209): 72-U49.

Widmann, T. and Dahmann, C. (2009) 'Dpp signaling promotes the cuboidal-to-columnar shape transition of Drosophila wing disc epithelia by regulating Rho1', *Journal of Cell Science* 122(9): 1362-1373.

Winter, C., Wang, B., Ballew, A., Royou, A., Karess, R., Axelrod, J. and Luo, L. (2001) 'Drosophila Rho-associated kinase (Drok) links frizzled-mediated planar cell polarity signaling to the actin cytoskeleton', *Cell* 105(1): 81-91.

Wong, C. C. L., Wong, C. M., Ko, F. C. F., Chan, L. K., Ching, Y. P., Yam, J. W. P. and Ng, I. O. L. (2008) 'Deleted in Liver Cancer 1 (DLC1) Negatively Regulates Rho/ROCK/MLC Pathway in Hepatocellular Carcinoma', *Plos One* 3(7).

Wootton, R. (1992) 'Functional morphology of insect wings', *Annual Review of Entomology* 37: 113-140.

Wright, N. A. and Alison, M. (1984) *The biology of epithelial cell populations*, Oxford: Clarendon.

Xu, T. and Rubin, G. M. (1993) 'Analysis of genetic mosaics in developing and adult *Drosophila* tissues', *Development* 117(4): 1223-1237.

Xue, W., Krasnitz, A., Lucito, R., Sordella, R., VanAelst, L., Cordon-Cardo, C., Singer, S., Kuehnel, F., Wigler, M., Powers, S. et al. (2008) 'DLC1 is a chromosome 8p tumor suppressor whose loss promotes hepatocellular carcinoma', *Genes & Development* 22(11): 1439-1444.

Yakoby, N., Lembong, J., Schupbach, T. and Shvartsman, S. Y. (2008) 'Drosophila eggshell is patterned by sequential action of feedforward and feedback loops', *Development* 135(2): 343-351.

Yan, J., Lu, Q., Fang, X. and Adler, P. (2009a) 'Rho1 has multiple functions in Drosophila wing planar polarity', *Developmental Biology* 333(1): 186-199.

Yan, S., Zartman, J., Zhang, M., Scott, A., Shvartsman, S. and Li, W. (2009b) 'Bistability coordinates activation of the EGFR and DPP pathways in Drosophila vein differentiation', *Molecular Systems Biology* 5: -.

Yasothornsrikul, S., Davis, W. J., Cramer, G., Kimbrell, D. A. and Dearolf, C. R. (1997) 'viking: identification and characterization of a second type IV collagen in Drosophila', *Gene* 198(1-2): 17-25.

Yu, K., Sturtevant, M., Biehs, B., Francois, V., Padgett, R., Blackman, R. and Bier, E. (1996) 'The Drosophila decapentaplegic and short gastrulation genes function antagonistically during adult wing vein development', *Development* 122(12): 4033-4044.

Yuan, B., Miller, M., Keck, C., Zimonjic, D., Thorgeirsson, S. and Popescu, N. (1998) 'Cloning, characterization, and chromosomal localization of a gene frequently deleted in human liver cancer (DLC-1) homologous to rat RhoGAP', *Cancer Research* 58(10): 2196-2199.

Yuan, X., Jin, M., Xu, X., Song, Y., Wu, C., Poo, M. and Duan, S. (2003) 'Signalling and crosstalk of Rho GTPases in mediating axon guidance', *Nature Cell Biology* 5(1): 38-45.

Zecca, M., Basler, K. and Struhl, G. (1995) 'Sequential organizing activities of engrailed, hedgehog and decapentaplegic in the Drosophila wing', *Development* 121(8): 2265-2278.

Zhu, A. J. and Scott, M. P. (2004) 'Incredible journey: how do developmental signals travel through tissue?', *Genes & Development* 18(24): 2985-2997.

Appendix

Table A.1. Stocks used in this thesis

Stock ID	Details	Relevant Reference	Source (if not Bloomington)
General Stocks			
Oregon R	Used as wild type	-	-
y^{1} w^{1118}	Used for confocal autofluorescence in adult wings.	-	-
w ; If/CyO ; MKRS/TM6b	Double balancer stock	-	-
w ; If/CyO, GFP ; MKRS/TM6b	Double balancer stock with CyO-GFP	-	Generated in our lab by Andrew Barrett
Sp Bl L/CyO	Marker stock	-	-
Mutant alleles			
Dp(2;2)DTD48 bw gbb^{4}/SM6a	Hypomorphic allele of *glass bottom boat*, survivability increased by a duplication including the *decapentaplegic* locus	Ray & Wharton, 2001	Generated in our lab by Rob Ray
gbb^{D20}	Amorphic allele of *glass bottom boat*	"	-
w cv^{43}	Null allele of *crossveinless*	Vilmos, et al. 2005.	-
cv-2^{K61}/CyO	Null allele of *crossveinless-2*	-	Generated in our lab by Oliver Robinson
cv-2^{K74}/CyO	Null allele of *crossveinless-2*	-	"
y w ; ; cv-c^{1} sbd	Hypomorphic allele of *crossveinless-c*	-	-
cv-c^{M62}/TM3 Ser	Null allele of *crossveinless-c*	Denholm, et al 2005.	Gift of Barry Denholm, Cambridge.
cv-c^{06951}/TM3 Ser	Strong loss of function allele of *crossveinless-c*. LacZ insertion, heterozygote allows for determination of *cv-c* expression pattern.	"	-
cv-c^{6}	Null allele of *crossveinless-c*	"	Generated in our lab by Rob Ray
w ;; Df(3R)Exel6267/TM6b	Deficiency uncovering the *crossveinless-c* locus	-	-
y w $Cdc42^{1}$/FM6	Strong loss of function allele of *Cdc42*	Genova, et al. 2000	Gift of Rick Fehon, University of Chicago
y w ; $Rho1^{72R}$/CyO	Null allele of the *Rho1*	Strutt, et al. 1997	Gift of David Strutt, University of Sheffield
Dg^{O86}, pr cn/CyO	Null allele of *Dystroglycan*	Christoforou, et al. 2008.	Generated in our lab
Dg^{O43}, pr cn/CyO	"	"	"
Dys^{3397}/TM6b	Allele of *Dystrophin*	"	-
w ;;Df(3R)6184/TM6b	Deficiency uncovering the *Dystrophin* locus	"	-
y w $Fur2^{R4}$ / FM7h	Used for the FM7h balancer	-	Generated by Shona Samarasinghe in our lab
Cell markers			
w ; Ubi-DECad-GFP	Expresses a GFP-tagged Cadherin protein ubiquitously, shows similar localisation to the endogenous protein	Oda and Tsukita, 2001	Gift from Nick Brown (Cambridge)
y w ; UAS-mCD8GFP	UAS controlled membrane-targeted GFP	-	-
w ; UAS-GFP	UAS controlled cytoplasmic GFP	-	-

btl-Gal4 > UAS-GFP	Expressed GFP in the pattern of the *breathless* gene, marking all tracheal cells	-	-
w ; UAS-myr-mRFP	Membrane targeted RFP marker	-	-
w ; sqh-mCherry ; sGMCA/MKRS	mCherry-tagged regulatory light chain of Myo-II and GFP-tagged actin binding protein Moesin, each ubiquitously expressed	Blanchard, et al. 2010	Gift of Nicole Gorfinkel, (University of Cambridge)
y w ; Vkg-GFP	Protein trap line at the *Viking* locus, allowing for assessment of ECM localisation	Morin, et al. 2001	Obtained from the FlyTrap project, Yale
Pcan-GFP	Protein trap line at the *Perlecan* locus, allowing for assessment of ECM localisation	"	"
Clonal analysis			
w hs-FLP; Adv/CyO	Preliminary stock for 2nd chromosome LOF clones	-	-
y w hs-FLP ; ; Dr/TM3	Preliminary stock for 3rd chromosome LOF clones	-	-
y w ; FRT-G13 M(2)53	Used for FLP-FRT clone generation for genes on 2R, with Minute to increase clone size	-	-
FRT82B, Ubi-GFP	Used for FLP-FRT clone generation somatic clones for genes on 3R.	-	-
y w ; FRT-G13 sha gbb^{D20}	Used to generate null *gbb* clones	Ray & Wharton, 2001.	Generated previously in our lab
y w ; FRT-G13 sha cv-2^{K74}	Used to generate null *cv-2* clones	-	Generated previously in our lab
y w ; FRT-G13 sha Dg^{086}	Used to generate null *Dg* clones	Christoforou, et al. 2008.	"
FRT82B cv-c^{M62} / TM3 Ser	Used to generate null *cv-c* clones marked by the absence of GFP	Denholm, et al. 2005.	Gift of Barry Denholm, Cambridge.
w ; UAS-myr-mRFP ; Act5C>CD2>Gal4	Membrane targeted RFP marker and FLPOut Gal4 casette (FLP induces recombination between FRT sites).	-	-
Gal4 and Gal80^{ts}			
w A9-Gal4	See Table 2.1 for expression patterns	-	-
w ; Act5C-Gal4/CyO	"	-	-
w ; ap-Gal4, UAS-GFP/CyO	"	-	-
bs-Gal4	"	-	-
y w ; dpp-blk-Gal4	"	-	-
y w MS1096-Gal4	"	-	-
Sal-Gal4/CyO	"	-	-
ap-Gal4 / CyO, GFP ; TubGal80^{ts}	Allows for temporally controlled dorsal expression of target genes	O'Keefe, et al. 2006.	Gift from Bruce Edgar (ZMBH, Hedielberg)
UAS lines			
w ; ; UAS-dpp^{w}	UAS controlled expression *decapentaplegic*, weaker insertion line	-	-
w ; ; UAS-dpp^{s}	UAS controlled expression of the BMP ligand Dpp, stronger insertion line, poor survival rate. Shows the same degree of non-autonomy as *dpp-w* in intervein clones	-	-
y w ;; UAS-gbb-9.1	UAS controlled expression of *glass bottom boat*.	-	-

w ; ; UAS-tkv^{QD}	UAS controlled expression of an activated form of Thickveins.	Nellen, et al. 1996.	-
y w ; ; UAS-rho-7.1	UAS controlled expression of the EGFR pathway activator *rhomboid*	-	-
w ; ; UAS-N^{ECD} / TM6b	UAS controlled expression of the extracellular domain of the *Notch* receptor, which acts as a dominant negative.	Rebay, et al. 1993.	Gift from Jose Inyaki Pueyo (University of Sussex)
y w ; UAS-Dad	UAS controlled expression of the BMP pathway inhibitor *Daughters against decapentaplegic*	Tsuneizumoi, et al. 2005	Gift from Tetsuya Tabata (University of Tokyo)
w ;; UAS-Ras^{V12} / TM6b	UAS controlled expression of activated Ras, which transduces EGFR pathway signals.	Lee, et al. 1996	-
w ;; UAS-cv-c	UAS controlled expression of *crossveinless-c*	Denholm, et al. 2005	-
w ; UAS-eGFP-cv-c-S/CyO	UAS controlled expression of a GFP tagged version of the short isoform of *crossveinless-c*	Sato, et al. 2010.	Gift of Tadashi Uemura (Kyoto University)
w ; UAS-eGFP-cv-c-L/CyO	UAS controlled expression of a GFP tagged version of the long isoform of *crossveinless-c*	"	"
UAS-Venus-cv-c	UAS controlled expression of a Venus tagged *crossveinless-c*	Simoes, et al. 2005.	Gift of Barry Denholm, Cambridge
UAS-PKNGeGFP/CyO ; Tub-Gal80^{ts}	Allows for temporal control of PKNGeGFP, a probe which binds GTP-bound Rho1	Simoes, et al. 2005.	-
w cv^{43} ; UAS-cv	Allows for expression of *cv* in a mutant background	Vilmos, et al. 2005	Generated in our lab by Claire Greer
w ; UAS-Rho1^{V14}/CyO	Constitutively active Rho1 protein	Fanto, et al. 2000	-
w ; UAS-Rho1^{N19}	Dominant negative Rho1 protein	"	"
RNAi lines:			
w ; ; UAS-Notch-dsRNA	VDRC #1112	Dietzl, et al. 2007.	VDRC, Vienna
w ; UAS-Notch-dsRNA	VDRC # 100002	"	"
w ; UAS-Egfr-dsRNA	VDRC # 43268	"	"
w ; UAS-Egfr-dsRNA	VDRC # 107130	"	"
w ; UAS-Mad-dsRNA	VDRC # 12635	"	"
w ; ; UAS-Medea-dsRNA	VDRC # 19688	"	"
w ; UAS-Medea-dsRNA	VDRC # 19689	"	"
w ; ; UAS-tkv-dsRNA	VDRC # 862	"	"
w ; UAS-tkv-dsRNA	VDRC # 3059	"	"
w ; UAS-cv-dsRNA	VDRC # 9727	"	"
w ; UAS-cv-dsRNA	VDRC # 9729	"	"
w ; UAS-cv-2-dsRNA	VDRC # 2938	"	"
w ; UAS-Rho1- dsRNA	VDRC # 12734	", Yan, et al. 2009a.	"
y v ; ; UAS-rok-dsRNA	TRiP# 28797	http://www.flyrnai.org	Bloomington
y v ; ; UAS-rok-dsRNA	TRiP# 34324	"	"
y v ; ; UAS-Dia-dsRNAi	TRiP# 28541	"	"
y v ; ; UAS-rok-dsRNA	TRiP# 33424	"	"
w ; ; UAS-cvc-dsRNA	-	Denholm, et al. 2005	Gift of Barry Denholm, Cambridge
Miscellaneous			
w ; Dg^{O86}, Ubi-DECad-GFP/CyO, GFP	Allows for assessment of cell shape in *Dg* mutants	-	Generated by Andrew Barrett in

			our lab
w ; Ubi-DECad-GFP/CyO ; Dys^{3397}/TM6b	Allows for assessment of cell shape in *Dys* mutants	-	"

Table A.2. Stocks generated in this thesis	
Stock ID	**Details**
Cad-GFP Recombinant Stocks: Cell Markers	
w ; Ubi-DECad-GFP, sqh-mCherry/(CyO, GFP)	Ubiquitously expressed constructs allow for comparison of Cadherin and Myo-II distribution. Recombinant chromosome
w ; Ubi-DECad-GFP, UAS-myr-mRFP	Allows for detection of Gal4 expression in a Cad-GFP background
Cad-GFP Recombinant Stocks: Overexpression	
w ; Ubi-DECad-GFP / (CyO) ; UAS-dpp^{w} / (TM6b)	Allows for assessment of cell shape when overexpressing *dpp*
w ; Ubi-DECad-GFP / (CyO) ; UAS-gbb$^{9.1}$ / (TM6b)	Allows for assessment of cell shape when overexpressing *gbb*
w ; Ubi-DECad-GFP / (CyO) ; UAS-tkv^{QD} / TM6b	Allows for assessment of cell shape when overexpressing active *tkv*
w ; Ubi-DECad-GFP / (CyO) ; UAS-Ras^{V12} / TM6b	Allows for assessment of cell shape when overexpressing active *Ras*
w ; Ubi-DECad-GFP / (CyO) ; UAS-rho / TM6b	Allows for assessment of cell shape when overexpressing active *rho*
w ; Ubi-DECad-GFP , UAS-Rho1^{V14} / CyO	Allows for assessment of cell shape when hyperactivating *Rho1*
w ; Ubi-DECad-GFP ; UAS-rok$^{CAT 3.1}$/ TM6b	Allows for assessment of cell shape when hyperactivating *rok*
w ; Ubi-DECad-GFP ; UAS-cv-c	Allows for assessment of cell shape when overexpressing *cv-c*
Cad-GFP Recombinant Stocks: RNAi lines	
w ; Ubi-DECad-GFP, UAS-Egfr-dsRNA / (CyO)	Allows for assessment of cell shape when inhibiting EGFR pathway activity (VDRC #107130)
w ; Ubi-DECad-GFP, UAS-Mad-dsRNA	Allows for assessment of cell shape when inhibiting BMP pathway activity(VDRC #12635)
w ; Ubi-DECad-GFP, UAS-tkv-dsRNA	Allows for assessment of cell shape when inhibiting BMP receptor activity (VDRC #3059)
w ; Ubi-DECad-GFP, UAS-N-dsRNA	Allows for assessment of cell shape when inhibiting Notch receptor activity (VDRC #100002)
w ; Ubi-DECad-GFP, UAS-Rho1-dsRNA	Allows for assessment of cell shape when knocking down Rho1 functionality (VDRC #12734)
w ; Ubi-DECad-GFP, UAS-cv-c-dsRNA	Allows for assessment of cell shape when knocking down Cv-c functionality (from Denholm, et al.)
w ; Ubi-DECad-GFP, UAS-rok-dsRNA	Allows for assessment of cell shape when knocking down Rok functionality (TRiP #28797)
Cad-GFP Recombinant Stocks: Mutant lines	
w cv^{43} ; Ubi-DECad-GFP	Allows for assessment of cell shape in a *crossveinless* null background
w ; Ubi-DECad-GFP ; cv-c^{1}	Allows for assessment of cell shape in a *crossveinless-c* mutant background
w ; gbb^{4}, Ubi-DECad-GFP /CyO	Allows for assessment of cell shape in a *gbb* mutant
w ; Ubi-DECadGFP/CyO ; cv-c^{06951}/TM6b Tb	Allows for assessment of *cv-c* expression in a wild type background
w ; gbb^{4} , Ubi-DECad-GFP/CyO ; cv-c^{06951}/TM6b, Tb	Allows for assessment of cell shape and *cv-c* expression in a *gbb* mutant
w ; Dg^{O86} , Ubi-DECad-GFP/CyO ; cv-c^{06951}/TM6b, Tb	Allows for assessment of cell shape and *cv-c* expression in a *Dg* mutant
Gal4/Gal80ts	
w ; Act5C-Gal4 / CyO, GFP ; Tub-Gal80^{ts}	Allows for temporal control of ubiquitous target gene expression

w ; en-Gal4 / (CyO, GFP) ; Tub-Gal80^{ts} / (TM6b, Tb)	Allows for temporal control of target gene expression in the posterior compartment
w ; sal-Gal4 / (CyOGFP) ; Tub-Gal80^{ts} / (TM6b, Tb)	Allows for temporal control of target gene expression in the middle of the wing
A9-Gal4 ; ; Tub-Gal80^{ts}	Allows for temporal control of target gene expression generally in the wing
w ; ap-Gal4, Ubi-DECad-GFP/CyO, GFP ; TubGal80^{ts}	Allows for assessment of cell shape with temporal control of target gene expression in the dorsal compartment
ptc-Gal4/(CyO, GFP) ; TubGal80^{ts}	Allows for temporal control of target gene expression in the a stripe of cells anterior to the AP compartment boundary
w ; ; Tub-Gal80^{ts}	Derived from original *apGal4 TubGal80^{ts}* stock.
Miscellaneous overexpression	
w ; tkv^{LacZ}/CyO ; UAS-dpp^{w} / TM6b	Used to address *tkv* expression following *dpp* overexpression
(w) ; ; UAS-dpp^{w}, cv-c^{06951}	Allows for assessment of *cv-c* expression following *dpp* overexpression
(w) ; ; UAS-gbb$^{9.1}$, cv-c^{06951}	Allows for assessment of *cv-c* expression following *gbb* overexpression
Dorsal rescue	
w ; cv-2^{K74}, ap-Gal4, UAS-GFP/CyO	For cv-2 dorsal rescue experiments
w ; cv-2^{K61}, UAS-cv-2/CyO	"
w ; ap-Gal4/CyO ; cv-c^{1} sbd	For cv-c dorsal rescue experiments
w ; ; cv-c^{1}, UAS-cv-c	"
w ; ; cv-c^{M62}, UAS-cv-c	"
Genetic interactions	
w ; Rho1^{72R}/CyO ; cv-c^{M62}/TM6B	Used to test genetic interactions between Rho1 and Cv-c
w ; Rho1^{72R}/CyO ; cv-c^{1} sbd	"
FLPOut clones	
w hs-FLP ; UAS-myr-mRFP ; Act5C>CD2>Gal4	FLPOut clone stock with a membrane targeted RFP marker to detect clones in the pupal wing
Balancers	
w ; If/CyO	Derived from double balancer stock
w ; ; MKRS/TM6b	"

Table A.3. Lethality arising from progressively induced dorsal expression of BMP/EGFR pathway components

Condition	***Time shifted***	***N° wings analysed****	***Lethality†***
apGal4 TubGal80 > dpp-w	WPP 18° Constant	34	0%
	WPP	22 (from escapers & pharates)	91%
	23h	16	76%
	28h	8	63%
	30h	6	40%
	32h	14	60%
	39h	10	50%
	40h	12	12%
	42h	13	0%
	44h	14 / 40	0%
	46h	14 / 30	0%
	48h	25 / 17	0%
	50h	6	0%
	52h	8	0%
	54h	7	0%
	66h	10	0%
	68h	12	0%
	70h	11	0%
	88h	11	0%
	90h	9	0%
	92h	11	0%
	96h	8	0%
apGal4 TubGal80 > gbb 9.1	WPP	21	58%
	16h	9	54%
	19h	8	14%
	22h	5	0%
	23h	16	0%
	24h	12 / 12	0%
	26h	16	0%
	28h	16 / 16	0%
	30h	12 / 19	0%
	33h	25	0%
	39h	18 / 26	0%
	42h	21	0%
	45h	17	0%
	48h	21	0%
	52h	12	0%
	56h	10	0%
	72h	12	0%
	96h	10	0%
Act5CGal4 TubGal80ts > dpp 8hr burst	WPP	12	0%
	16h	14	
	18h	17 / 13	0%
	20h	20	0%
	24h	31	0%
	38h	14 / 10	0%
	40h	18	0%
	42h	15 / 40	0%
	46h	28 / 14	0%
	48h	15 / 12 / 13	0%

Act5cGal4 TubGal80^{ts} > gbb 16h shifts	24h	34	0%
	28h	34	0%
	32h	30	0%
" 24h shifts	WPP	20	0%
	18h	10	0%
	24h	7	0%
	38h	4	0%
	44h	11	0%
apGal4 TubGal80^{ts} > tkv^{QD}	WPP	1	96%
	23h	0	100%
	26h	0	100%
	30h	13 / 8	46%
	32h	5	75%
	40h	10 / 38	44%
	42h	14	37%
	44h	12 / 16	50%
	46h	26	0%
	48h	28 / 34	0%
	50h	14	0%
	52h	28 / 15	0%
	54h	12	0%
	56h	16	0%
	72h	14	0%
	95h	16	0%
Act5cGal4 TubGal80^{ts} > tkv^{QD} 8hr bursts	WPP	26	14%
	16h	16 / 22	0%
	18h	15 / 23	0%
	20h	23	0%
	22h	28	0%
	24h	22 / 31	0%
	40h	16	63%
	42h	15	44%
	44h	14	80%
	46h	8	0%
	72h	18	0%
	92h	10	0%
	96	28	0%
apGal4 TubGal80^{ts} > rho	WPP	0	100%
	15h	6 / 9	67%
	17h	7	63%
	20h	4 / 6	0%
	24h	6 / 23	
	26h	9	0%
	28h	14	0%
	30h	5	0%
	32h	12	0%
	40h	20	0%
	44h	16	0%
	48h	14 / 11	0%
	50h	8	0%
	52h	7	0%
	56h	11	0%
	64h	9	0%
	70h	21	0%

	88h	10	0%
	96h	10	0%
Act5cGal4 TubGal80^{ts} > rho 8hr bursts	WPP	14	0%
	16h	8	0%
	18h	14	0%
	20h	11	0%
	22h	17	0%
	24h	18	0%
	38h	13	0%
	40h	12	0%
	44h	15	0%
	48h	12	0%

* Where duplicate experiments were performed, indicated by '/'

† Lethality calculated as 1-(total escapers / total balancer progeny)x100.

Table A.4. Lethality and phenotypes from *N* and *Egfr RNAi* lines.

RNAi line	Driver	Balancer Class	Active Class*	Lethality†	Comments
N VDRC: 1112	*A9*	N/A	16 ♀ escapers 243 filled pupal cases	>94%	Female escapers have smaller, almond shaped wings with margin defects, blistering, and bristle abnormalities. Highly lethal
	Act5C	159	0	100%	No filled pupal cases or dead wallcrawlers: indicates pre-L3 lethality
	ap	149	0 escapers ~120 filled pupal cases	100%	Lethality in pupal phase and possibly earlier
	bs	N/A	250	0%	Thicker veins, some notching/thickened posterior margin. Infrequent blistering
	dpp-blk	N/A	0 escapers 190 filled pupal cases	100%	Lethality in pupal phase, and possibly earlier
	en	N/a	0 escapers 160 filled cases	100%	Lethality in pupal phase, and possibly earlier
	MS1096	N/A	3 ♀ escapers 36 filled cases	>74%	Small, dark wings, bristle pattern defects
	sal	358	0 escapers 122 filled pupal cases	100%	Pupal and pre-pupal lethality
	Tub	292	0 escapers 0 filled pupal cases	100%	Pre-pupal lethality
Egfr VDRC: 107130	*A9*	N/A	297	0%	♀Wings extremely curled on A-P axis (with A and P margins folding inwards), no obvious alterations to venation ♂Wings small and dark, do not expand
	Act5C	115	0 escapers 0 filled cases	100%	Pre-pupal lethality
	ap	276	38	86%	Small, dark and blistered wings
	bs	N/A	296	0%	Wild type wings

	dpp-blk	N/A	43	0%	ACV loss, L3 partial loss
	en	N/A	42 escapers 65 filled cases	>60%	Reduced size and complete vein loss in P compartment, Ectopic bristles on posterior margin.
	MS1096	N/A	275	0%	Small, folded, curled wings with vein loss visible where the cuticle is flatter.
	sal	268	142	47%	Rounder wings, loss of L3 and L4 distally, L2 slight thickening.
	Tub	103	0 escapers 16 filled cases	100%	Pupal and pre-pupal lethality

*Where balancer class is available, calculated as 1-(total escapers / total balancer progeny)x100. Where no balancer class is available, calculated as total escapers / (total escapers + filled pupal cases)x100, to get a lower bound in the estimate of lethality.

† 'Filled cases' are pupal cases which have failed to eclose, hence showing lethality in the pupal period.

Table A.5. *cv RNAi* phenotypes when driven with a wing general driver *A9Gal4* as compared to the dorsal specific driver *apGal4*

***cv RNAi* line**	**Driver**	**Balancer class**	**Active class**	**Phenotype**
VDRC#9727	*ap*	61	65	Ectopic venation around tips of LVs, PCV wild type in all wings 108/108 scored wings.
	ap 29°C	58	49	Wings crumpled and some ectopic venation, but wild type PCV in 73/73 scored wings.
VDRC#9729	*A9*	N/A	69	♀ 5/40 showed anterior gap, 35/40 showed wild type PCV, ♂ 31/35 showed complete PCV loss, 4/35 showed remaining fragment in intervein*
	A9 29°C	N/A	52	♀ 26/46 scored wings showed some PCV loss, 20/46 were wild type. ♂ 40/40 scored wings showed complete crossvein loss
	ap	53	49	Ectopic venation around tips of LVs, PCV wild type in 96/96 scored wings
	ap 29°C	197	64	68% lethality; wings crumpled and some ectopic venation, but wild type PCV in 94/94 scored wings.

* Disparity in phenotype between the sexes is due to *A9Gal4* being an X-chromosome insertion, and thus more highly expressed in males as compared to females.

Table A.6. Expression of *dsRNA* targeting components of the BMP signal transduction machinery

NAi line	Driver	Balancer class	Active Class	Lethality*	Phenotype
tkv VDRC # 862	*A9*	N/A	101	-	Broad wings with a combination wing blistering, thickened an ectopic veins, and vein loss
	ap	88	1	98.86%	Blistered, dark and minuscule wings and severely cleft thorax
tkv VDRC # 3052	*A9*	N/A	46	-	More severe than #862
	ap	54	0	100%	-
	dpp-blk	N/A	All flies remain stuck to their cases, even though wings expand	-	Expanded anterior compartment, loss of L3 and duplication of L2, consistent with an anterior expansion of Dpp signalling in the disc
Mad VDRC # 12635	*A9*	N/A	27	-	Blistered and crumpled wings lacking obvious venation
	ap	142	0	100%	-
	ap	134	0	100%	-
Medea VDRC # 19688	*ap*	134	0	100%	-
Medea VDRC # 19689	*A9*	N/A	43	-	Loss of distal LVs and partial loss of ACV and PCV
	ap	67	4	92%	Blistered, dark and minuscule wings and severely cleft thorax
	dpp-blk	N/A	77	-	Loss of L3, and expansion of intervein between L2 and L4.

* Calculated by 1-(active class/balancer class) x 100

Table A.7. Effects of inducing *Dys RNAi* with multiple Gal4 lines in development.

Dys RNAi line	Driver	Balancer Class	Active Class	Lethality†	Phenotype
X2	*A9*	70*	15	78.57%	Thin and curled wings, PCV+
	Act5C	123	0	100%	Lethal
	Ap	119	0	100%	Lethal
	En	N/A	0	-	Lethal
	MS1096	N/A	15	-	Severely curled wings, PCV cannot be scored
	Sal	92	0	100%	Lethal
COOH	*A9*	80*	107	0%	Mostly wild type, commonly gapped/detached
	Act5C	203	185	0%	PCV^-, mostly detached
	Ap	141	215	0%	Wild type
	En	N/A	0	-	Lethal
	MS1096	20*	32	0%	PCV^-, most are detached/point.
	Sal	127	146	0%	PCV^-: all show anterior gaps
Ex4	*A9*	71*	80	0%	Wild type
	Act5C	46	102	0%	PCV^-, generally detached/gapped
	Ap	92	85	0%	Wild Type
	En	N/A	65	-	Mostly wild type, occasional gapping
	MS1096	36*	33	0%	PCV^- range of loss.
	Sal	73	76	0%	PCV^-, most gapped

*As Gal4/Y males were used for the parental cross, controls are +/Y ; *UAS-Dys-dsRNA* males from the same cross.

† If percentage was within <10%, classed as 0% lethality as within the expected range of variability between two equally surviving classes.

Table A.8. Progeny ratios from *cv-c* dorsal rescue experiment.

(Derived from cross *ap-Gal4 / If ; cv-c^{1} /MKRS* X *cv-c^{M62}, UAS-cv-c / TM6b, Tb)*

	Class	Genotype	Number	% of expected*
25°C	***Experimental*** Dorsal expression of cv-c in a mutant background	*apGal 4 / + ; cv-c^{1} / cv-c^{M62}, UAS-cv-c*	0	0
	Control 1 Gal4>UAS in a heterozygous background	*apGal 4 / + ; MKRS / cv-c^{M62}, UAS-cv-c*	0	0
	Control 2 cv-c mutant, no apGal4, silent UAS	*If / + ; cv-c^{1} / cv-c^{M62}, UAS-cv-c*	175 *Most wings show PCV phenotypes*	167%
	Remaining compiled	*Various*	661	129%†
18°C	***Experimental*** Dorsal expression of cv-c in a mutant background	*apGal 4 / + ; cv-c^{1} / cv-c^{M62}, UAS-cv-c*	21	25%
	Control 1 Gal4>UAS in a heterozygous background	*apGal 4 / + ; MKRS / cv-c^{M62}, UAS-cv-c*	28	34%
	Control 2 cv-c mutant, no apGal4, silent UAS	*If / + ; cv-c^{1} / cv-c^{M62}, UAS-cv-c*	113 *Most wings show PCV phenotypes*	138%
	Remaining compiled	*Various*	492	120.37%†

*Calculated by dividing total number of progeny by 8 to give the expected Mendelian proportions of the parental cross, then dividing each class by that number to give observed/expected.

† Average % of expected of the remaining 5 classes.

Table A.9. Effects of expressing two *rok*^{CAT} constructs.

	Driver	Balancer Class	Active Class	Lethality	Phenotype
rok^{CAT} 3.1	*A9*	NA	23♂ 86♀	-	Crossvein loss and loss of definition, serrated margin.
	ap	78	0	100%	Lethal
	bs	NA	121	0%	Wild type wings
	ptc	NA	13	-	All survivors are ACV^{-}
	sal	68	44	64%	PCV loss within the *sal* domain, and wing serrating
rok^{CAT} 7.1	*A9*	NA	51♂ 74♀	-	Wild type
	ap	112	155	0%	Mostly wild type, some PCV gaps
	bs	NA	87	-	Wild type
	dpp-blk	NA	203	-	Wild type
	MS1096	NA	67	-	Wild type
	ptc	NA	93	-	Wings are slightly curled on A-P axis, infrequent ACV partial loss
	sal	169	156	0%	Wild type